

---

# Investigation of AML-specific *FLT3* mutations – from next generation diagnostics to combined targeted therapy

---

Dissertation der Fakultät für Biologie  
der Ludwig-Maximilians-Universität München



Katrin Schranz  
München 2019





# Dissertation

zur Erlangung des Doktorgrades der Naturwissenschaften  
Doctor rerum naturalium (Dr.rer.nat.)  
an der Fakultät für Biologie  
der Ludwig-Maximilians-Universität München

vorgelegt von  
Katrín Susanne Schranz  
geboren in Salzburg, Österreich



Diese Dissertation wurde angefertigt  
unter der Leitung von Prof. Dr. Heinrich Leonhardt  
im Bereich von Department Biologie II  
an der Ludwig-Maximilians-Universität München

Erstgutachter: Prof. Dr. Heinrich Leonhardt

Zweitgutachter: Prof. Dr. Dirk Eick

Tag der Abgabe: 28.06.2018

Tag der mündlichen Prüfung: 22.03.2019



## **Erklärung**

Ich versichere hiermit an Eides statt, dass meine Dissertation mit dem Titel:

“Investigation of AML-specific *FLT3* mutations – from next generation diagnostics to combined targeted therapy”

selbständig und ohne unerlaubte Hilfsmittel angefertigt worden ist.

Die vorliegende Dissertation wurde weder ganz, noch teilweise bei einer anderen Prüfungskommission vorgelegt.

Ich habe noch zu keinem früheren Zeitpunkt versucht, eine Dissertation einzureichen oder an einer Doktorprüfung teilzunehmen.

München, den 28.06.2018

Katrin Schranz, M.Sc.



# Table of content

<b>1</b>	<b>Summary</b>	<b>i</b>
<b>2</b>	<b>Zusammenfassung</b>	<b>iii</b>
<b>3</b>	<b>Introduction</b>	<b>1</b>
3.1	Acute myeloid leukemia	1
3.1.1	Epidemiology and incidence of AML	1
3.1.2	Pathogenesis of AML	2
3.1.3	Diagnostic classification of AML subtypes	5
3.1.4	Prognostic risk stratification and survival rates amongst AML patients	8
3.1.5	AML therapy	10
3.2	The receptor tyrosine kinase FLT3	13
3.2.1	Expression and function of FLT3 in the normal hematopoiesis	14
3.2.2	Aberrant expression and signalling activation of FLT3 in AML	16
3.2.3	Diagnostic identification and prognostic implication of <i>FLT3</i> mutations	20
3.2.4	FLT3-targeted therapy approaches	22
3.3	Rationale of this study	27
3.3.1	The applicability of a NGS-based <i>FLT3</i> -ITD detection tool compared to standard routine assays	28
3.3.2	The relevance of a new and recurrent <i>FLT3</i> deletion mutation in AML	28
3.3.3	TKI-mediated effects on FLT3 and the potential for a combination with FLT3-directed immunotherapy in AML	28
<b>4</b>	<b>Results</b>	<b>31</b>
4.1	Clonal heterogeneity of FLT3-ITD detected by high-throughput amplicon sequencing correlates with adverse prognosis in acute myeloid leukemia	31
4.2	The new and recurrent FLT3 juxtamembrane deletion mutation shows a dominant negative effect on the wild-type FLT3 receptor	95
4.3	Tyrosine kinase inhibition increases the cell surface localization of FLT3-ITD and enhances FLT3-directed immunotherapy of acute myeloid leukemia	107
<b>5</b>	<b>Discussion</b>	<b>135</b>
5.1	The applicability of NGS-based <i>FLT3</i> -ITD detection compared to standard routine assays	135
5.1.1	Challenges in <i>FLT3</i> -ITD detection based on NGS applications	135
5.1.2	Clinical relevance of <i>FLT3</i> -ITD detection with high sensitivity	138
5.1.3	NGS compared to other sensitive <i>FLT3</i> -ITD detection strategies	140

5.1.4	The impact of the sample material on <i>FLT3</i> -ITD detection sensitivity	141
5.1.5	Prospective NGS-application in future <i>FLT3</i> -ITD routine diagnostics	142
5.2	The relevance of new and recurrent <i>FLT3</i> deletion mutations in AML	143
5.2.1	Deciphering the biological consequences of <i>FLT3</i> p.Q569Vfs*2	143
5.2.2	Consequences of truncations in other receptors associated with AML	145
5.3	TKI-mediated effects on FLT3 and the potential for a combination with FLT3-directed immunotherapy in AML	146
5.3.1	The role of the <i>FLT3</i> -genotype on TKI response	147
5.3.2	Biological mechanisms behind the increase in surface FLT3	151
5.3.3	Clinical applicability of combining TKIs with FLT3-directed immunotherapy	153
5.3.4	Other TKI drug combinations to evade therapy-resistance	158
<b>6</b>	<b>Conclusion</b>	<b>161</b>
<b>7</b>	<b>Annex</b>	<b>162</b>
7.1	References	162
7.2	Abbreviations	193
7.3	Contribution	196
7.4	Acknowledgements	198
7.5	Curriculum vitae	199

# 1 Summary

Despite high initial response rates for acute myeloid leukemia (AML) patients, fit enough to receive intensive chemotherapy, relapse remains common, underlying the fatal nature of the disease. Activating mutations in the fibroblast-macrophage stimulating factor like tyrosine kinase receptor 3 (*FLT3*) are frequent amongst AML patients. Most prevalent and associated with an unfavorable prognosis are in-frame internal tandem duplications (ITDs) in *FLT3*. Point mutations in *FLT3* are capable of mediating tyrosine kinase inhibitor (TKI) therapy-resistance. Therefore, an accurate measurement of *FLT3*-ITDs and an early detection of relapse for clinical intervention are essential. This might be achieved by the higher sensitivity of next generation sequencing (NGS) applications. For *FLT3*-ITD detection this doctoral work proved the accuracy of NGS-based *FLT3*-ITD detection by high throughput amplicon sequencing (HTAS). The benefit of this tool was based on ITD detection with high sensitivity. A high ITD clonal heterogeneity by HTAS correlated with adverse prognosis. On the other hand, some challenges in ITD detection were revealed that require further improvement before implementation into routine diagnostics. In the context of relapse prediction, new and recurrent mutations in *FLT3* require elucidation regarding their potential to drive disease progression and therapy-resistance. The role of the new and recurrent *FLT3* mutation p.Q569Vfs\*2 was therefore investigated. The mutation resulted in a truncated receptor lacking essential parts for autophosphorylation. A dominant-negative effect of *FLT3*-p.Q569Vfs\*2 on *FLT3*-WT was demonstrated in cells expressing both receptor variants. With regards to AML therapy, novel therapeutic approaches are needed to combat highly aggressive types of AML with high relapse rates, including leukemia driven by *FLT3*-ITD. Since differential TKI-responses were observed for AML patients, this doctoral work focused on investigation of AML cells regarding their TKI response based on their *FLT3* genotype. A TKI-driven increase of the *FLT3* surface localization was encountered in *FLT3*-mutated cells, which inversely correlated with proliferation. The TKI-mediated *FLT3* surface expression was *N*-linked glycosylation dependent and correlated with the *FLT3*-ITD mRNA levels prior treatment. As response of AML patients to single agent TKI treatment is often temporary, our finding provided a rationale to combine TKIs with *FLT3*-directed immunotherapy. Proof-of-principle experiments confirmed a synergistic effect of a combined treatment with Quizartinib and a bispecific *FLT3*×CD3 antibody in *FLT3*-ITD positive AML cells. Thus, this doctoral work provided several interesting biological findings with clinical relevance for the diagnosis and therapy of *FLT3*-mutated AML.





## 2 Zusammenfassung

Patienten mit einer Akuten Myeloischen Leukämie (AML) sprechen zu Beginn einer Chemotherapie gut auf die Behandlung an. Trotzdem kommt es aufgrund der Natur dieser Erkrankung häufig zu einem Rezidiv. Aktivierende Mutationen im Fibroblasten-Makrophagen-stimulierenden Faktor ähnlichen Tyrosinkinase-Rezeptor 3 (*FLT3*) werden oft bei AML Patienten nachgewiesen. Interne Tandem Duplikationen (ITDs) in *FLT3* kommen am Häufigsten vor und sind mit einer ungünstigen Prognose assoziiert. Punktmutationen in *FLT3* hingegen können eine Therapieresistenz gegenüber Tyrosinkinase-Inhibitoren (TKIs) vermitteln. Deshalb ist eine akkurate Messung von *FLT3*-ITDs sowie die Früherkennung eines Rezidivs enorm wichtig, um gegebenenfalls klinisch intervenieren zu können. Die hohe Sensitivität der Sequenzierungsanwendungen der nächsten Generation (NGS) könnte dazu maßgeblich beitragen. In dieser Doktorarbeit wurde die Genauigkeit des NGS-basierten *FLT3*-ITD Nachweises mittels Hochdurchsatz-Amplikon-Sequenzierung (HTAS) ermittelt. Ein großer Vorteil dieser Methode ist die ITD-Erkennung mit hoher Sensitivität. Die hohe klonale Heterogenität an ITDs gemessen durch HTAS korrelierte mit einer ungünstigen Prognose. Jedoch wurden auch ITD Detektionsschwierigkeiten dieser Methode aufgedeckt, welche behoben werden müssen bevor diese Methode in die Routinediagnostik implementiert werden kann. Um das Rezidiv-Risiko für Patienten mit neuen rekurrenten *FLT3*-Mutationen abschätzen zu können ist die funktionelle Untersuchung notwendig. Dadurch soll deren Beitrag zur Krankheitsprogression und Therapieresistenz ermittelt werden. Daher wurde die Rolle der neuen rekurrenten *FLT3* Mutation p.Q569Vfs\*2 untersucht. Diese Mutation führte zu einem verkürzten *FLT3* Rezeptor, dem wesentliche Teile für die Autophosphorylierung fehlen. Ein dominant-negativer Effekt von *FLT3*-p.Q569Vfs\*2 auf *FLT3*-WT wurde in Zellen gezeigt, die beide Rezeptorvarianten exprimierten. Um hoch aggressive Arten der AML, einschließlich *FLT3*-ITD positiver Leukämien, mit hohen Rezidiv-Raten zu bekämpfen, sind neue therapeutische Ansätze erforderlich. Da AML-Patienten ein unterschiedliches Ansprechen auf eine TKI-Therapie aufzeigen, wurden in dieser Doktorarbeit zudem AML-Zellen hinsichtlich ihres TKI-Ansprechens, basierend auf dem *FLT3*-Genotyp untersucht. Ein TKI-basierter Anstieg der *FLT3* Oberflächenexpression wurde in *FLT3*-mutierten Zellen gezeigt, welcher invers mit der Proliferation korrelierte. Die TKI-vermittelte *FLT3*-Oberflächenexpression war abhängig von der *N*-Glykosylierung und korrelierte mit dem *FLT3*-ITD mRNA Level vor der Behandlung. Da das TKI-Therapieansprechen bei AML-Patienten nur von kurzer Dauer ist, lieferte diese Beobachtung eine rationelle Grundlage für eine Kombination von TKIs mit *FLT3*-gerichteter Immuntherapie. Unsere Experimente bestätigten eine synergistische Wirkung der kombinierten Behandlung mit Quizartinib und einem bispezifischen *FLT3*×*CD3* Antikörper in *FLT3*-ITD positiven AML-Zellen. Somit lieferte diese Doktorarbeit einige interessante biologische Ergebnisse mit klinischer Relevanz für die Diagnostik und Therapie von *FLT3*-mutierter AML.



### 3 Introduction

Cancer is one of the leading disease-related causes of death worldwide. Amongst all cancer-related deaths, approximately 7% are due to hematological malignancies, including lymphoma, leukemia and myeloma. Leukemia represents up to 2.6% of all cancer incidences worldwide. It is the second-most common type of hematological malignancy. [1, 2] In high income countries leukemia occurs 1.92-fold more frequent, with Germany in the upper third according to rates across Europe. [1-3] Despite rather low incidence rates, leukemia demonstrates a disproportional high mortality rate - irrespective of country-specific industrialization-state. After initial diagnosis, the relative five years survival rate for leukemia in Germany is 57-58%. [1, 2]

Clinically, there are four major types of leukemia: acute myeloid leukemia (AML), acute lymphoid leukemia (ALL), chronic myeloid leukemia (CML) and chronic lymphoid leukemia (CLL). Depending on the onset of the disease leukemia clusters into an “acute” or “chronic” type. The chronic form evolves slowly over months and even years, with infrequent symptoms. The acute form is highly aggressive and progresses quickly, requiring immediate treatment. On a cytomorphological level, leukemia is furthermore classified into “lymphoid” and “myeloid” entities. Each refers to the respective disrupted hematopoietic lineage, microscopic features and expression of phenotypic markers. [4-6]

In adults AML is the most common acute leukemia, with lowest survival rates. [7, 8] Mutations in the fibroblast-macrophage stimulating factor (FMS)-like tyrosine kinase receptor 3 (FLT3) occur in up to 30% of AML patients. Length mutations of FLT3 are known to confer a poor prognosis and these patients have a high relapse-risk. [9-13] Although research has led to better understand *FLT3*-mutated AML during the past years, treatment of *FLT3*-mutated AML remains challenging. Thus, it is important to translate the biological findings of mutated AML into new therapeutic approaches to overcome disease progression and novel diagnostic tools to accurately identify patients of this high-risk AML sub-group.

## 3.1 Acute myeloid leukemia

### 3.1.1 Epidemiology and incidence of AML

AML accounts for 34% of all leukemia cases. Incidence dramatically increases with age. Per year 1.3 cases per 100,000 individuals are below 65 years, whereas 12.2 cases per 100,000 individuals are above 65 years. The incidence in childhood or adolescence is lower. Of all pediatric leukemias, AML accounts for about 18%. [5, 7, 8, 14, 15] In Germany, every year 4 out of 100,000 people are diagnosed with AML, with a median of 4,030 AML cases. Of those 3,950 are assigned to adults and 80 to children. Slightly higher rates are observed in men. [2, 7]

Corresponding to the etiology, only a few environmental and personal factors have been elucidated to be associated with the development of the disease. Apart from a steady increase of incidence with age, modifiable aspects such as exposure to benzene, radiation and chemotherapeutics are known contributors. On a genetic level, chromosomal alterations such as trisomy 21, causing Down syndrome, predispose to AML. Inherited syndromes, including Li-Fraumeni syndrome and Fanconi anemia, are known risk factors for pediatric AML. Furthermore, polymorphic variants in genes responsible for metabolizing carcinogens or others known to effect genomic stability increase the risk of developing AML. [5, 14, 16, 17] Also a myelosarcoma, which is an extramedullar tumor of undifferentiated myeloic cells that frequently affect the skin, lymph nodes, liver, spleen or testis, can lead to AML within 5 to 12 months when untreated. [18, 19] In the elderly, AML occasionally evolves from a concomitant hematopoietic neoplasia, such as myelodysplastic syndrome (MDS), or another malignancy treated 5 to 10 years earlier. Up to 30% of AML cases are assigned to this category, which is termed secondary and therapy-related AML respectively (s-AML; t-AML). Cases without an identifiable leukemic cause evolve “de-novo”. [5, 17, 20]

### 3.1.2 Pathogenesis of AML

In human adults, mature blood cells are constantly produced, with rates of more than one million cells per second. Specific functional cells originate from a self-renewing hematopoietic stem cell (HSC) population. In the normal hematopoiesis self-renewal and differentiation of the HSC compartment is tightly regulated by transcription factors and cytokines. They mediate signal transduction via specific receptors. These mechanisms are altered in AML (Figure 1; upper panel). [21-23]

AML develops by a multistep process through a transformation of an HSC, multipotent progenitor (MPP) or common myeloid progenitor (CMP) cell in the bone marrow (BM). These cells accumulate epigenetic and genetic changes in different genomic loci. This leads to a block of differentiation and increased proliferation. [5, 14, 23] The so called leukemic stem cells (LSCs) can remain in a quiescent state of G<sub>0</sub>/G<sub>1</sub> phase while sustaining their self-renewing capacity. LSCs can also give rise to several propagating clonogenic leukemic progenitor cells. Immature abnormal hematopoietic cells, so-called leukemic blasts, consequently outgrow in an uncontrolled manner. At the same time the number of mature blood cells decreases, since they are predominantly short-lived (Figure 1; lower panel). The permanent accumulation of blasts in the BM subsequently leads to their washout into the peripheral blood (PB) and infiltration of other organs, including the spleen, liver and lymph nodes. Thus, leukemia is clinically characterized by hematopoietic insufficiency of all lineages, resulting in anemia, thrombocytopenia and immunodeficiency. [21, 22, 24]

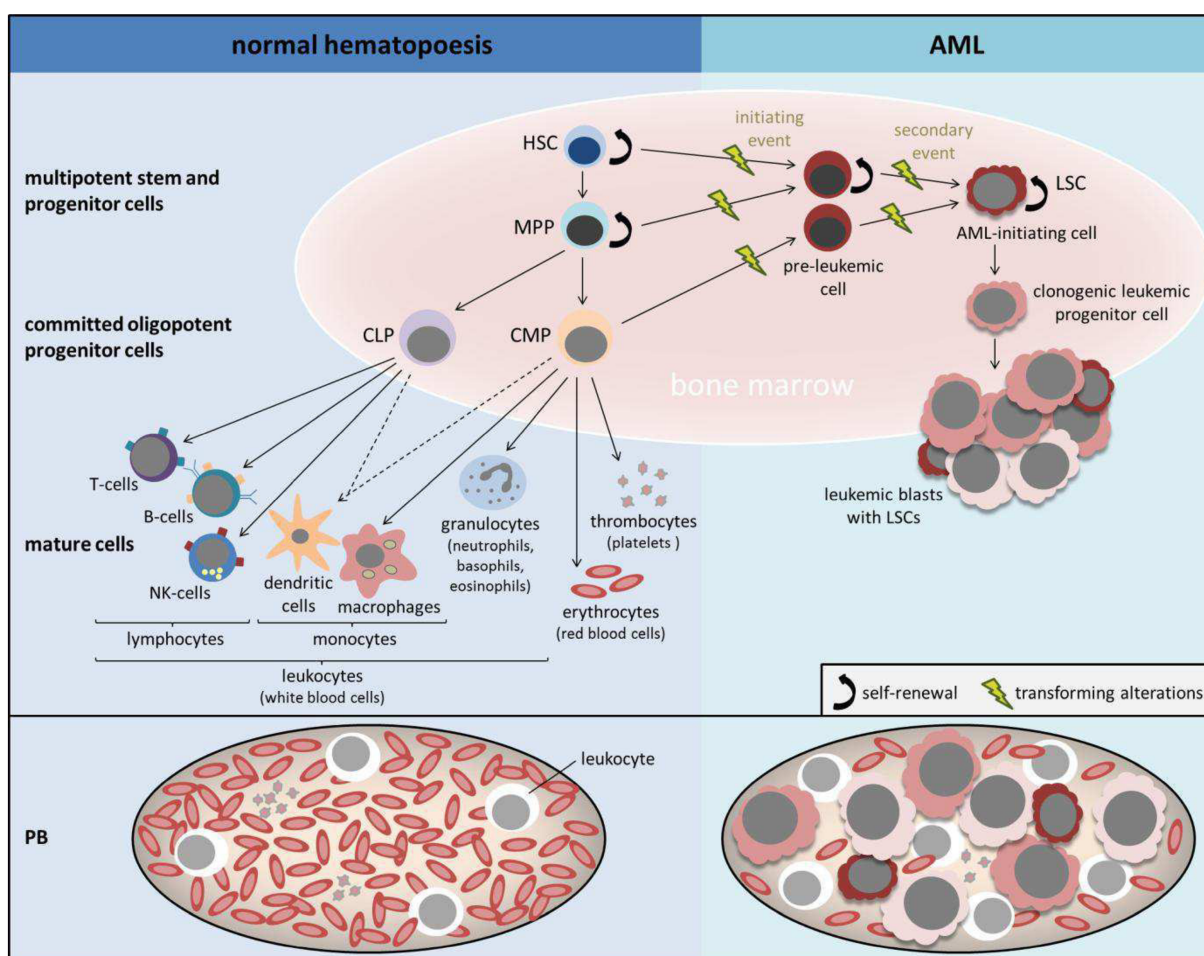


**Figure 1: Schematic illustration of the normal hematopoiesis compared to the development of AML with respective blood counts.**

Upper panel: In normal hematopoiesis a self-renewing and multipotent hematopoietic stem cell (HSC) in the bone marrow generate multipotent progenitor (MPP) cells. MMPs give rise to oligo-potent common lymphoid or myeloid progenitor cells (CLP and CMP respectively), which differentiate into functional hematopoietic cells. In AML, the maturation of an HSC, MMP or CMP is impaired, while altered self-renewing capacities are acquired. This leads to an initiating leukemic stem cell (LSC), progressing to leukemia progenitors. These immature transformed cells clonally expand and are called leukemic blasts (modified from Tan 2006, Siveen 2017, Uribealga 2011 and Krönke 2013). [22, 25-27] Lower panel: Normal hematopoiesis generates an erythrocytes-dominant peripheral blood (PB) count. In AML an imbalanced cellular composition is present. The altered cellular composition of the PB was already observed and described in the 19<sup>th</sup> century. The observed “white blood” termed the disease leukemia (adapted from Kampen 2012). [28]

On a genetic level, the combination of at least two major genetic events in a single cell is necessary to induce AML. These alterations disturb gene sequences or whole chromosomal regions crucial for cellular mechanisms such as the cell cycle control, nucleic acid metabolism and DNA repair. Typically activating mutations in receptor tyrosine kinase genes, involved in signalling pathways (class V mutations), cooperate with genomic rearrangements affecting myeloid transcription factors (class I and VII mutations). Only together these alterations lead to a block of differentiation, increased leukemic cell proliferation and survival – cooperatively inducing a leukemic phenotype. As an example length-mutated *FLT3* has been shown to

interplay with the runt-related transcription factor 1 - RUNX1 translocation partner 1 (*RUNX1-RUNX1T1*) fusion, in leukemogenesis. [5, 23, 29]

Depending on the dimension of DNA copy number alterations, either few gains or losses of whole chromosomes (for example monosomy 5 or trisomy 8), clustered high-level DNA amplifications or translocations generating fusion-genes, are involved. In up to 80% of cases, AML blasts comprise a complex interplay of multiple genetic changes (class I – IX mutations; Figure 2). [5, 23, 29, 30] On average 13 acquired, so-called “somatic” mutations in protein coding regions can be detected per AML patient. Several are found to collaborate with each other or interfere with other genes. Already at the pre-leukemic stage, an extensive genetic evolution can exist. During early leukemogenesis, especially mutations in epigenetic regulators occur (class IV and VI mutations), which frequently persist during AML therapy. [23, 27, 29-33] Epigenetic alterations include histone modifications as well as methylation of cytosine (C) bases in genome-areas, rich in CpG dinucleotides (“CpG islands”). Since the DNA-methylation state determines if the promotor region of a gene is accessible for the transcription machinery, gene expression in AML is modified in a tumor-supportive manner. Local hypermethylation for example occurs in areas of tumor-suppressors, while global hypomethylation results in genomic instability. [34] Incidences of alterations increase with genomic instability and dynamics in clonal evolution of transformed cells. Hence a high molecular complexity is present especially in s-AML, elderly patients and at relapse. [27, 30, 32, 33]

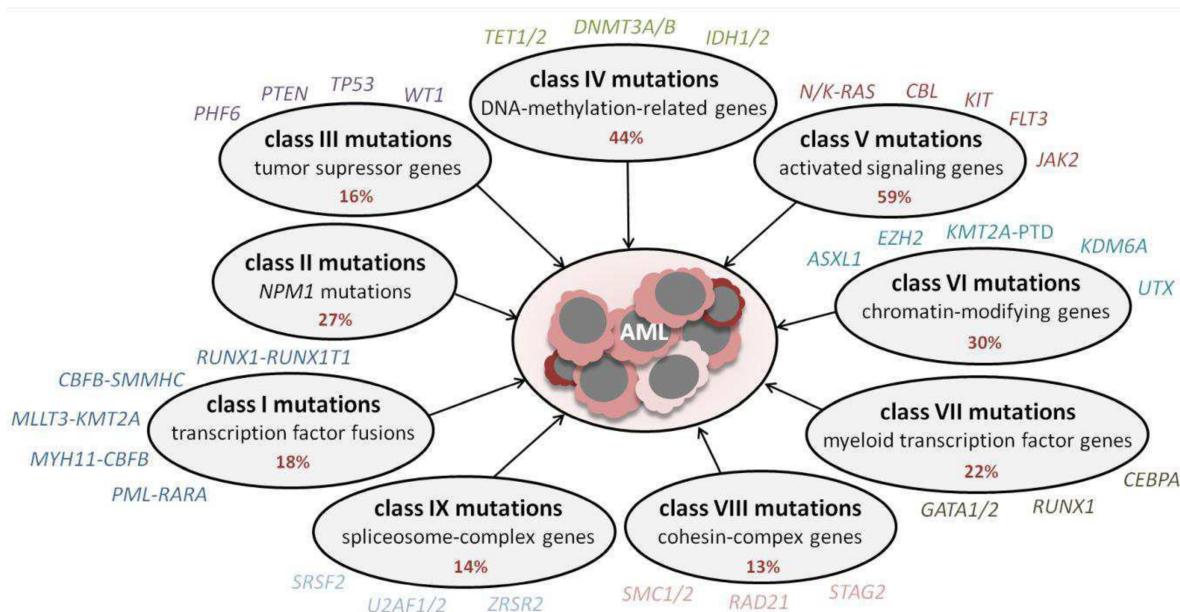


**Figure 2: Mutational classes in AML.**

Many genetic and epigenetic modifications interplay during leukemogenesis. The most frequently affected genes (tumor suppressor- and oncogenes) as well as fusion genes are shown. They are classified according to their relevant biological function. Class I and VII mutations induce a block of differentiation by modified transcription factors. Class II mutations cover mutations in *NPM1*. Class III mutations affect tumor-suppressor genes. Class IV and VI mutations are epigenetic modifications, implying altered DNA methylation and chromatin modification to modulate gene expression. Class V mutations involve activated cell signalling inducing increased proliferation, inhibition of apoptosis and cell survival. Class VIII mutations include cohesion-complex genes, which stabilize the chromatin structure. Class IX mutations include spliceosome-complex genes,

required for the removal of introns from a transcribed pre-mRNA. Both class VIII and IX are thus implicated in proper gene expression (modified from Thiede 2012 and Chen 2013). [31, 33, 35-37]

### 3.1.3 Diagnostic classification of AML subtypes

The molecular and clinical heterogeneity of AML is reflected by its complex sub-classification. AML subtypes are distinguished by cytomorphologic and cytogenetic analyses of PB and BM specimens at diagnosis. [7, 38]

On a cytomorphological level, AML is classified into eight sub-groups, according to cell type and differentiation status as defined by the French-American-British (FAB) cooperative groups (Table 1). [39-41]

**Table 1: FAB-classification of AML according to cellular morphology, including associated molecular markers defined by the WHO.**

defined by the WHO:

FAB type	morphology			molecular marker
M0	myeloblastic	with	minimal	differentiation from ALL by immunophenotypic determination (CD13, CD14, CD15, CD33), frequently <i>RUNX1</i> and <i>ASXL1</i> mutated
M1	myeloblastic without maturation			frequently <i>NPM1</i> and <i>CEBPA</i> mutated, <i>FLT3</i> -ITD
M2	myeloblastic with maturation			t(8;21)(q22;q22) <i>RUNX1-RUNX1T1</i> fusion in one-third of cases, frequently <i>ASXL1</i> mutated
M3*	promyelocytic (hypergranular)			t(15;17)(q22;q21) <i>PML-RARA</i> or other <i>RARA</i> -fusions e.g.
M3v	promyelocytic (hypogranular)			t(11;17)(q23;q21) and t(5;17)(q13;q21) <i>PLZF-RARA</i> and <i>NuMA-RARA</i> respectively, frequently <i>FLT3</i> -ITD or <i>FLT3</i> -TKD mutated
M4	myelomonocytic			frequently <i>NPM1</i> , <i>DNMT3A</i> , <i>NRAS</i> and <i>FLT3</i> -TKD mutated
M4eo	myelomonocytic with abnormal eosinophils			frequently inv(16)(p13.1q22) <i>CBFB-MYH11</i> fusion, frequently <i>NRAS</i> mutated
M5	monocytic			11q23 rearrangements, frequently <i>NPM1</i> mutated
M5a	monoblastic			t(9;11)(p22;q23) <i>MLLT3-KMT2A</i> fusion, t(6;11)(q27;q23) <i>KMT2A-AFDN</i> fusion, t(8;16)(p11;p13) <i>KAT6A-CREBBP</i> fusion, frequently <i>ASXL1</i> mutated
M5b	monocytic			frequently <i>DNMT3A</i> mutated
M6	erythroid			frequently <i>TP53</i> mutated
M7	megakaryocytic			diagnostic proof by immunophenotypic determination (CD13, CD33, CD34, CD41, CD42, CD61)

\*referred to as acute promyelocytic leukemia (APL) due to a promyelocytic pattern induced by inhibition of apoptosis and granulopoietic differentiation [42-44]; FAB (French-American-British) cooperative groups; WHO (world health organization); CD (cluster of differentiation); t (translocation); inv (inversion); (adapted from Bennett 1976, 1985, Rose 2014 and Ladines-Castro 2015). [39-41, 45]

Cytogenetic changes in AML allow the sub-classification of patients into three groups, namely patients with a cytogenetically normal (CN), aberrant or complex karyotype. [38] Cytogenetic analysis is performed on BM cells in inter- or metaphase. Staining of chromosomes is performed on dividing cells in metaphase. This enables to identify each chromosome by its specific banding

pattern, size and centromere length. Specific genetic regions are visualized utilizing fluorescently-labeled DNA probes. Fluorescent in-situ hybridization (FISH), allows the detection of chromosomal alterations. This includes the detection of deletions of chromosomal regions, loss of a chromosome (monosomy), amplifications as well as structural chromosomal changes and rearrangements (translocations). [46-49] Using flow cytometry AML cells are investigated for their antigen expression profile (immunophenotype), aiding lineage classification. In addition, PCR or RT-PCR based methods, including capillary gel electrophoresis and sequencing, are performed to detect molecular alterations in known driver genes such as mutations in *nucleophosmin 1 (NPM1)* and *FLT3*. [50, 51]

About half of all AML patients show a normal karyotype, frequently harboring mutations in *NPM1*, *isocitrat-dehydrogenase 1 and 2 (IDH1/2)*, *DNA-methyltransferase (DNMT3A)* and *FLT3*. An aberrant karyotype implies balanced or unbalanced chromosomal translocations. These translocations lead to fusion genes, producing chimeric proteins. [31, 52, 53] Balanced translocations appear in approximately 20% of AML patients, with higher incidences in elderly. In addition, activating mutations in common driver genes, including *KIT proto-oncogene receptor tyrosine kinase (KIT)*, *Janus kinase 2 (JAK2)* and *FLT3* are frequent. [54, 55] A complex karyotype is present in 10 to 15% of de-novo AML as well as 25 to 27% of s- and t-AML respectively. It is characterized by at least three cytogenetic alterations in one AML clone. [52, 56-60] Frequently, translocations of chromosome 11 are implicated, involving the *lysine methyltransferase 2A (KMT2A)* gene (known as *myeloid/lymphoid or mixed-lineage leukemia (MLL)*). *KMT2A*-rearrangements lead to fusion genes deregulating several homeobox (HOX) genes, which are responsible for governing stemness. [59, 61-63] Prevalently deletions of 17p13 occur, involving the tumor suppressor gene *tumor protein p53 (TP53)*. [57]

Based on combined information about the morphologic, cytogenetic, immunophenotypic and mutational profile as well as clinically relevant patient-derived factors, AML is categorized into four main groups according to the world health organization (WHO) (Table 2). [64-66]



**Table 2: WHO-classification of AML, based on cytogenetics, morphology and clinically relevant patient-derived factors.**

WHO type				sub-type according to molecular marker or morphologic pattern
AML with recurrent genetic abnormalities				t(8;21)(q22;q22) <i>RUNX1-RUNX1T1</i> fusion
				inv(16)(p13.1q22) <i>CBFB-MYH11</i> fusion
				t(15;17)(q22;q21) <i>PML-RARA</i> fusion (APL)
				t(9;11)(p22;q23) <i>MLLT3-KMT2A</i> fusion
				t(6;9)(p23;q34) <i>DEK-NUP214</i> (one-third displays <i>FLT3</i> -ITD)
				inv(3)(q21q26.2) <i>RPN1-MECOM</i> , <i>GATA2</i> mutated
				t(1;22)(p13;q13) <i>RBM15-MKL1</i> (megakaryoblastic)
				t(9;22)(q34;q11.2) <i>BCR-ABL1</i> *
				<i>NPM1</i> mutated
				<i>CEBPA</i> mutated (bi-allelic)
				<i>RUNX1</i> mutated*
AML with myelodysplasia-related changes**				n.a.
Therapy-related myeloid neoplasms*** (t-AML, t-APL, t-MDS)				n.a.
AML not otherwise specified (based on morphology; FAB-classification)				with minimal differentiation
				without maturation
				with maturation
				myelomonocytic
				monoblastic and monocytic
				erythroid (pure erythroid and mixed erythroid-myeloid)
				megakaryoblastic
				basophilic
				panmyelosis with myelofibrosis

\*\* MDS according to medical history or complex karyotype ( $\geq 3$  chromosomal alterations); involving the following unbalanced and balanced alterations and none of which are included in the "AML with recurrent genetic abnormalities" sub-type:

unbalanced:

-7 or del(7q)

-5 or del(5q)

i(17q) or t(17p)

-13 or del(13q)

del(11q)

del(12p) or t(12p)

del(9q)

idic(X)(q13)

balanced:

t(11;16)(q23;p13.3) *KMT2A-CREBBP* fusion

t(3;21)(q26.2;q22.1) *RUNX1-MECOM* fusion

t(1;3)(q36.3;q21.1)

t(2;11)(p21;q23) translocation without *KMT2A*-rearrangement

t(5;12)(q33;p12)

t(5;7)(q33;q11.2) *HIP1-PDGFRB* fusion

t(15;17)(q33;p13)

t(5;10)(q33;q21) *CCDC6-PDGFRB* fusion

t(3;5)(q25;q34) *NPM1-MLF1* fusion

\*\*\*frequently complex karyotype (-7 or del(7q), -5 or del(5q), *TP53* deletion, t(9;11)(p22;q23) *MLLT3-KMT2A*, inv(16)(p13.1q22) *CBFB-MYH11*, t(8;21)(q22;q22) *RUNX1-RUNX1T1*, t(15;17)(q22;q21) *PML-RARA*). Of note t-APL and CBF-translocated t-AML display a better therapy response than other t-AMLs.

\*provisional entity; n.a. (not applicable); WHO (World Health Organization); AML (acute myeloid leukemia); t-AML (therapy related AML); MDS (myelodysplastic syndrome); t (translocation); inv (inversion); del (deletion); i (isochromosome); idic (isodicentric); (adapted from Vardiman 2009 and De Kouchkovsky 2016). [8, 64]

Whilst a blast count above 30% in BM or PB is defined as AML according to FAB, above 20% is sufficient to distinguish AML from MDS according to WHO. In certain cases, genetic abnormalities enable to diagnose an AML below a blast count of 20%. These include the translocations t(15;17), which leads to a *promyelocytic leukemia - retinoic acid receptor alpha* (*PML-RARA*) fusion, t(8;21) encoding a *RUNX1-RUNX1T1* fusion and inv(16) which leads to a *core-binding factor beta subunit - myosin heavy chain 11* (*CBFB-MYH11*) fusion. [64, 67]

Since AML progresses quickly and symptoms appear at rather late stages, the disease is commonly first diagnosed when the leukemia is already fully established. Therefore a rapid risk-stratification and therapy decision is essential. [50]

### 3.1.4 Prognostic risk stratification and survival rates amongst AML patients

Within the major types of leukemia, AML displays lowest survival rates. AML is lethal within weeks, if left untreated. After five years post-diagnosis, more than half of adult patients are deceased. Depending on the subtype and age, the survival rate ranges from 13 to 60%. [7, 68, 69] To choose the appropriate therapy, evaluating the probable response to treatment and prognosis of outcome, firm risk stratification criteria have been established by the European Leukemia Net (ELN) and Medical Research Council (MRC). They divide AML into three risk-groups: favorable, intermediate and adverse. [38, 50, 52, 70, 71]

According to MRC AML is classified based on the patients' cytogenetics and karyotype respectively. These parameters display strongest prognostic impact on induction therapy response and outcome (Table 3). [52, 70-72]

**Table 3: MRC risk stratification of AML patients based on cytogenetics.**

MRC risk-group	cytogenetics
<b>favorable</b>	t(15;17)(q22;q21) <i>PML-RARA</i> fusion t(8;21)(q22;q22) <i>RUNX1-RUNX1T1</i> fusion inv(16)(p13q22) or t(16;16)(p13;q22) <i>CBFB-MYH11</i> fusion
<b>intermediate</b>	normal karyotype, other alterations neither specified as favourable nor as unfavourable
<b>adverse</b>	abnl(3q) except t(3;5)(q21~25;q31~35) <i>NPM1-MLF1</i> fusion inv(3)(q21q26) or t(3;3)(q21;q26) <i>RPN1-MECOM</i> fusion add(5q), del(5q) or -5 add(7q), del(7q) or -7 (except those with a favourable karyotype) t(6;11)(q27;q23) <i>KMT2A-AFDN</i> fusion t(10;11)(p11~13;q23) <i>KMT2A-ABI1</i> fusion t(11q23) <i>KMT2A</i> -rearrangements, except t(9;11)(q21~22;q23) <i>KMT2A-MLLT3</i> fusion or t(11;19)(q23;p13) <i>KMT2A-ELL</i> or <i>KMT2A-ENL</i> fusion t(9;22)(q34;q11) <i>BCR-ABL1</i> fusion -17/abnl(17q) complex alterations (≥4 independent abnormalities)

Of note, classification is based on patients younger than 60 years. t (translocation), inv (inversion), abnl (abnormal), add (additional), del (deletion), MRC (Medical Research Council); (adapted from Grimwade 2010). [70]

Since almost half of all AML patients show a normal karyotype, the ELN-classification further risk-stratify patients. This is based on incorporating prognostically relevant gene mutations, associated with a high risk of relapse (Table 4). [38, 50, 73]

**Table 4: ELN risk stratification of AML patients based on cytogenetics and relevant gene mutations.**

ELN risk-group	cytogenetic and molecular markers
<b>favorable</b>	t(8;21)(q22;q22) <i>RUNX1-RUNX1T1</i> fusion inv(16)(p13.1;q22) or t(16;16)(p13.1;q22) <i>CBFB-MYH11</i> fusion mutated <i>NPM1</i> without <i>FLT3</i> -ITD or with <i>FLT3</i> -ITD <sup>low</sup> * (normal karyotype) bi-allelic mutated <i>CEBPA</i> (normal karyotype)
<b>intermediate</b>	mutated <i>NPM1</i> with <i>FLT3</i> -ITD <sup>high</sup> * (normal karyotype**) wild-type <i>NPM1</i> without <i>FLT3</i> -ITD or with <i>FLT3</i> -ITD <sup>low</sup> * (normal karyotype**) t(9;11)(p22;q23) <i>KMT2A-MLLT3</i> fusion cytogenetic abnormalities not classified as favorable or adverse
<b>adverse</b>	inv(3)(q21q26.2) or t(3;3)(q21;q26.2) <i>GATA2, MECOM</i> -rearrangements t(6;9)(p23;34) <i>DEK-NUP214</i> fusion t(v;11)(v;q23) <i>KMT2A</i> -rearrangements t(9;22)(q34.1;q11.2) <i>BCR-ABL1</i> fusion del(5q) or -5; -7; abn(17q) or -17 complex or monosomal karyotype*** wild-type <i>NPM1</i> and <i>FLT3</i> -ITD <sup>high</sup> * mutated <i>RUNX1</i> mutated <i>ASXL1</i> mutated <i>TP53</i>

\*low allelic ratio (<0.50) determined by semi-qualitative assessment of *FLT3*-ITD allelic ratio by DNA fragment analysis; \*\*other alterations not specified as adverse; \*\*\*≥3 different chromosomal alterations, in absence of one of the WHO designated recurring abnormalities including: t(15;17), t(8;21), inv(16) or t(16;16), t(9;11), t(v;11)(v;q23), t(6;9), inv(3) or t(3;3), t(9;22)(q34.1;q11.2) – a worse prognosis display monosomal karyotypes implying: a monosomy (e.g. -7, -5, -17, -18) in association with ≥1 additional monosomy or structural chromosome abnormality (excluding CBF-AML). t (translocation), inv (inversion), del (deletion), abn (abnormal), v (variable), ELN (European Leukemia Net); (adapted from Döhner 2017). [50, 74, 75]

Commonly, the prognostic impact of genetic markers is context-dependent. The most prominent example is the interplay between an *NPM1* mutation and *FLT3*-ITD. Mutated *NPM1* is associated with a good prognosis, however only if *FLT3*-ITD is absent or expressed at low levels. Likewise, *TP53* mutations are associated with a complex and monosomal karyotype as well as a neoploidies of chromosome 5, 7 or 17. Both confer poor outcome, but in combination, outcome is even worse. Thus, cooperating mutations should be tightly monitored during treatment and beyond. [50, 73]

Despite cytogenetic and molecular factors, risk stratification and therapy decision is based on the white blood cell (WBC) count, the immunophenotype and other factors, including the physiological condition (defined as performance status), concomitant diseases (e.g. infections) as well as the age and family history of the patient. [38, 50, 70] A low performance index is the major risk driver for the treatment-related mortality, which is defined as death before or within achieving complete remission (CR; commonly within 30 days of treatment). Key players for relapse are therapy-resistance mediating alterations, cytogenetic aberrations and mutations in

known driver genes including *FLT3*. [76] The distribution and rates for CR, relapse and overall survival (OS) of AML patients according to the ELN risk-profile is shown in Figure 3 and Table 5. Notably, s-AML and t-AML patients display an unfavorable prognosis with decreased therapy response and shorter OS. This is due to their high frequency of unfavorable cytogenetic abnormalities, including a complex and monosomal karyotype. [77-79]

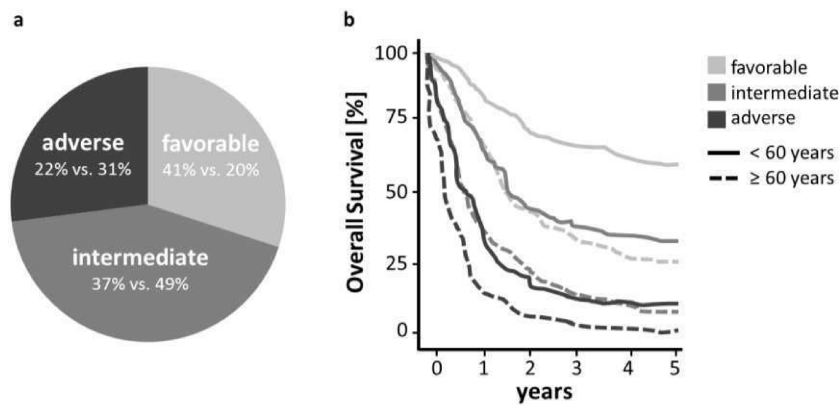


**Figure 3: Distribution and clinical outcome of AML patients according to ELN risk stratification.**

**a)** Distribution of the European Leukemia Net (ELN) risk-groups in younger versus (vs.) elderly AML patients (adapted from Estey 2016). **b)** Schematic representation of the overall survival of AML patients assigned to the three risk-stratification groups (modified from Estey 2016). [76]

**Table 5: Rates for CR, relapse and 10-year OS of AML patients who received standard treatment.**

ELN risk-group	CR [%]	relapse [%]	OS [%]
<b>favorable</b>	90	35-40	55-81
<b>intermediate</b>	50-80	80	22-39
<b>adverse</b>	<30*	≤90	≤10

\*Patients older than 60 years achieve remission rates of 5 to 15% within this group. CR (clinical remission), OS (overall survival). [38, 76, 80]

### 3.1.5 AML therapy

Despite being very heterogeneous, AML therapy is quite uniform. Patients either receive standard chemotherapy or palliative and supportive treatment, depending on the occurrence of targetable markers, assessed risk of relapse and predicted treatment-related mortality rate (Figure 4). Standard chemotherapy and palliative treatment each may be combined with targeted investigational therapy if applicable. [38, 76, 81-83]

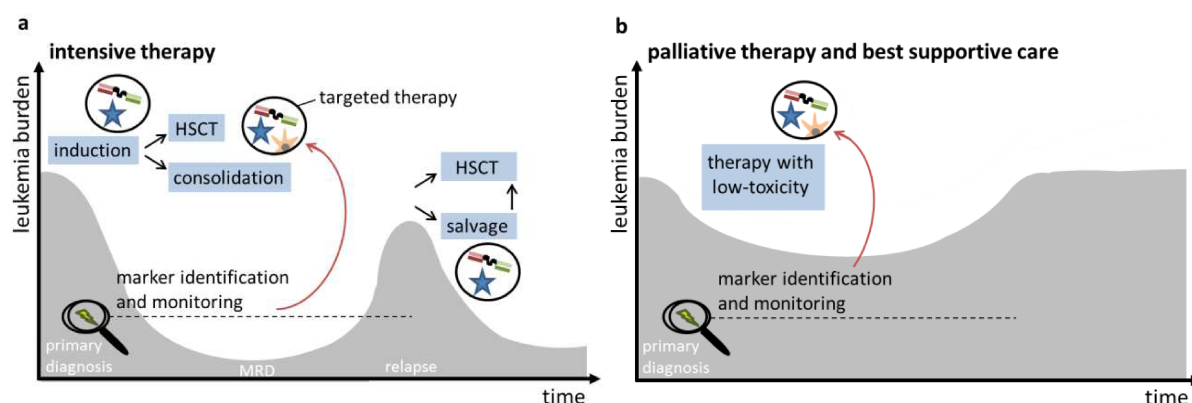


**Figure 4: Treatment model of AML.**

**a)** Standard intensive therapy implies an initial induction therapy, followed by consolidation therapy or hematopoietic stem cell transplantation (HSCT). In case of relapse salvage therapy is applied first or HSCT is performed directly. **b)** In contrast palliative therapy implies low-toxicity treatment, solely reducing the leukemic burden without a curative intent. At primary diagnosis prognostic markers are identified and used for targeted therapies in both therapy options, if applicable. Targeted therapies imply dendritic cell vaccination, tyrosine kinase inhibitors, T-cell engaging antibody constructs and chimeric antigen receptor (CAR) T-cells respectively (modified from Lichtenegger 2015). [84]

Standard chemotherapy implies an initial treatment, so-called “induction therapy”. Induction therapy consists of a combination of the nucleoside analogue drug Cytarabine (cytosine arabinoside) and an anthracycline such as Daunorubicin. These agents interfere with DNA replication and repair in dividing cells, inducing apoptosis. The combined treatment during induction is termed “7+3 regimen”, which consists of several repetitive cycles (7 days Cytarabine with 3 days Daunorubicin, beginning on day 3). [22, 38, 76, 81, 85, 86] Only for the morphologic AML subtype M3 (APL) a different standard therapy with all-trans retinoic acid (AraC, ATRA) and arsenitrioxid (ATO) is applied. [44, 87, 88] By induction therapy a curative intent reaching CR is aimed. The leukemic burden is reduced to less than 5% blasts in the BM, with no extramedullary detectable blasts. If successful, in up to 60 to 70% of patients between 15 and 60 years, the normal hematopoiesis recovers within 3 to 6 weeks. [38, 76, 81, 85, 86, 89] Treatment response is monitored closely, following minimal residual disease (MRD) if a respective genetic marker has been identified at initial diagnosis. Thereby, MRD monitoring detects the molecular disease long before hematologic signs are visible. [50, 76, 90, 91] In certain cases chemotherapy may also be combined with targeted therapy. [92, 93]

If reaching CR, a post remission treatment, so-called “consolidation therapy” follows. In consolidation therapy, cycles of Cytarabine or AraC are administered over several months. Thereby, residual leukemic cells should be eliminated to prevent a relapse and to increase relapse-free survival (RFS) and OS. Consolidation therapy is adapted to the risk of relapse, based on prognostic risk factors and on the therapy-associated probability of death according to ELN. [50, 76, 81, 94, 95] Infrequently, after consolidation “maintenance therapy” is performed. This intends to further reduce the risk of relapse. [96] In contrast, patients displaying poor prognostic markers indicating a high risk of a relapse (such as s-AML patients or patients within the intermediate and adverse risk-group) as well as patients with inadequate initial blast reduction after the first cycles of induction therapy (>10% leukemic cells in the BM) are considered for an

allogeneic hematopoietic stem cell transplantation (HSCT). For an HSCT patients have to demonstrate an adequate performance index and appropriate donor cells have to be available. If this is the case, patients first undergo a conditioning therapy. [50, 76, 81, 91, 97, 98] Conditioning therapy consists of chemotherapy and total body irradiation. This should eradicate leukemic blasts and remaining hematopoietic cells of the HSCT recipient. In HSCT, immunocompromised patients receive donor cells by an intravenous transfusion. Donor cells thereafter start to home in the recipients' BM. In the BM donor cells generate new functional hematopoietic cells and initiate a graft versus leukemia effect. If donor cells of the other gender were used, engraftment and subsequent persistence of donor cells is monitored closely. This is performed by chimerism analysis performing FISH. A HSCT in first CR reduces the risk of relapse down to 25%, despite implying a 5-fold increased therapy-associated mortality rate. [38, 76, 97, 99-101] If however, a resistant clone arises and grows out or leukemic stem cell (LSC) within the BM survives the anti-leukemic treatment and subsequently self-renew and proliferate, a relapse may arise. In case of a relapse so called "salvage" therapy is performed to reduce the leukemic burden and if possibly to bridge towards an HSCT. Alternatively individualized therapies may be applied. [12, 84, 102-107]

Although treatment results of younger adults have improved, the prognosis of medically unfit patients above 60 years remains poor. Despite CR rates between 40 and 65%, the median 2-year survival rate is 6%. The poor outcome is mainly due to therapy-resistance, related to a complex karyotype, treatment-related toxicity and mortality. In addition, elderly are frequently not eligible for cytotoxic therapies due to reduced tolerability (e.g. conditioned by substantial comorbidities, including cardiovascular distress, metabolic disease as well as reduced liver and kidney function). Thus, only about 30% of medically-unfit patients above 60 years receive standard chemotherapy. Same applies to an HSCT, since preceding intensive conditioning therapy is a requirement, plus elderly patients have a higher risk of treatment-related complications (including serious to fatal graft-versus-host disease). [5, 7, 68, 69, 81, 108-111] Instead elderly AML patients receive a reduced-intensity conditioning, so-called "palliative treatment". Palliative treatment consists of low-dose Cytarabine chemotherapy with hydroxyurea or a targeted therapy if applicable - or the combination of both. [81, 86, 110]

Individualized treatments are mostly investigational therapy trials. They are mostly less toxic than standard chemotherapy and have the intent to reduce the leukemic burden. In few cases leukemia cells are reduced towards a CR enabling a trial-based HSCT. [76, 82, 110] For palliative treatment hypomethylating agents are an attractive targeted therapy, since they have relatively low side effects. Hypomethylating agents, such as Azacitidine and Decitabine, may counteract epigenetic changes due to mutations of *IDH1/2* or *DNMT3A*. Azacitidine has been already approved for elderly AML patients with 20 to 30% leukemic burden. However, if no targeted therapy is applicable and patients do not tolerate palliative therapy, supportive treatment is the remaining therapeutic option. [34, 38, 82, 110] Supportive treatment in form of "best supportive care" intends to impede disease progression by stabilizing the disease. Symptoms are monitored and alleviated, to sustain the patient's quality of life by prophylaxes reducing complications such as infections (using anti-bacterial and anti-fungal agents). Supportive treatment prolongs the patient's life for a certain time period (11-20 weeks). [76, 83, 86, 112]

As with hypomethylating agents, individualized investigational therapies are selected based on AML-specific cell markers. Thereby, distinct biological features of leukemic cells are targeted. In clinical trials, many other treatments are currently under investigation. Immunotherapeutic agents for instance target proteins structures, so called “antigens” that are highly expressed on leukemic cells, preferably in a leukemia-specific manner. In this context, it has been shown that cytogenetically favourable patients, who display a high cluster of differentiation 33 (CD33) expression, profit from a combined therapy with a toxin-coupled CD33 antibody. Furthermore CD33/CD3-bispecific T-cell engaging antibodies are under investigation. They aid in cancer cell eradication by activating the patients’ own immune system. [113, 114] Another promising candidate for targeted therapy is FLT3. It is the most mutated mitogenic receptor in AML, with high aberrant expression in leukemic blasts and LSCs, while being rarely detectable in normally differentiated cells. [115, 116] Since length mutated FLT3 as well as certain activating FLT3-TKD mutants are associated with poor disease-free survival, there is high clinical interest in targeting FLT3. [9, 10, 12, 13]

## 3.2 The receptor tyrosine kinase FLT3

FLT3, also known as fetal liver kinase 2 (FLK2), stem cell kinase 1 (STK1) and CD135, belongs to the receptor tyrosine kinase (RTK) family III. The RTK family III is one out of about 20 RTK protein families, including 58 genes in the human genome. Besides FLT3, the family III comprises other transmembrane cytokine receptors namely the stem cell growth factor receptor (SCFR, also known as KIT), the platelet-derived growth factor receptor (PDGFR)  $\alpha/\beta$ , and the colony-stimulating factor 1 receptor (CSF1R). [117-120]

The *FLT3* gene is located on chromosome 13(q12-q13). *FLT3* spans a genomic region of approximately 100 kilobases and comprises 24 exons (Figure 5a). [116, 118, 121, 122] It encodes a receptor, consisting of 993 amino acids. [116, 123] During protein processing, two differentially-glycosylated FLT3 forms are generated - an immature (~130 kDa) and a fully-glycosylated form (~160 kDa). While the immature FLT3 merely localizes in the cytoplasm, the fully-glycosylated FLT3 is shuttled to the cell membrane. [124] Like all RTK family III members, FLT3 acts as a membrane-spanning signal transduction protein. It consists of five extracellular immunoglobulin-like globes (Ig1-5), a lipophilic helical transmembrane domain (TM), followed by an intracellular juxtamembrane domain (JMD), a hinge region and two cytoplasmic tyrosine kinase domains (TKD1 and TKD2), which are separated by a hydrophobic kinase insert (Figure 5b). While the extracellular part is responsible for ligand binding, the JMD and TKD region collectively mediate receptor activation and signalling. [123-126] Since the TKD region is key in the interaction with downstream signalling molecules, this region is highly conserved amongst tyrosine kinase receptors. [126, 127]

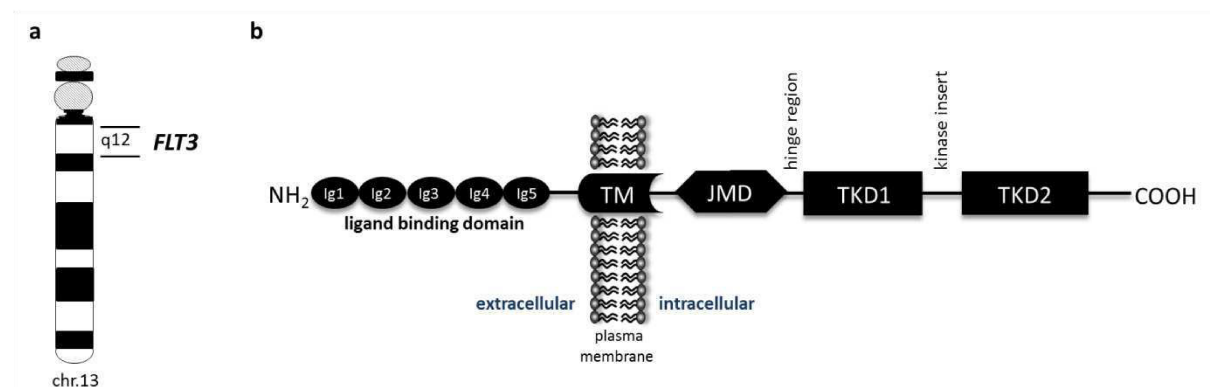


**Figure 5: Schematic chromosomal banding pattern of chromosome 13, indicating *FLT3* localization, which encodes the growth factor receptor *FLT3*.**

**a)** G-banding ideogram of chromosome 13 and location of the gene *FLT3*. Performing G-banding, proteins stabilizing the three-dimensional structures of the DNA are degraded (e.g. using Trypsin). Subsequent staining of the DNA is performed utilizing a DNA-binding dye (Giemsa). As a result actively transcribed regions with a less condensed chromatin are lightly stained compared to dark stained areas, which refer to heterochromatic DNA regions. A normal karyotype consists of a diploid set of chromosomes (modified from Shaughnessy 2000, Whitman 2001 and Spinner 2016). [128-130] **b)** Illustration of the growth factor receptor *FLT3* with its functional domains: the extracellular N-terminal ligand binding domain (consisting of five immunoglobulin-like lobes (Ig1-5)), the intracellular juxtamembrane domain (JMD) as well as two tyrosine kinase domains (TKDs). The transmembrane domain (TM) attaches the receptor to the plasma membrane of the cell (modified from Opatz 2013). [131]

### 3.2.1 Expression and function of *FLT3* in the normal hematopoiesis

*FLT3* and its ligand play an essential role in normal haematopoiesis and in the development of the immune system. Their interaction is important for the maintenance and propagation of multipotent HSCs and early stage hematopoietic progenitors in the BM. Furthermore, *FLT3* is implicated in the differentiation of hematopoietic cells, including dendritic cells (DCs) - which are responsible for the recognition and presentation of antigens. During normal hematopoiesis, *FLT3* expression decreases with increasing cellular differentiation - being undetectable in fully differentiated hematopoietic cells. Therefore, *FLT3* can be found on approximately 50% of normal HSC and partially on DCs, but largely not on peripheral lymphocytes. The transcription of *FLT3* is thereby regulated by transcription factors, including *HOXA9*, *MEIS1*, *CEBPA* and *MYB*. Besides being expressed on immature cells in the BM, PB, lymph nodes, thymus and spleen, *FLT3* can be selectively found in cells of other organs, including the gonadal system as well as the central nervous system. [116, 125, 132-142]

Under normal conditions, *FLT3* receptor activation is tightly regulated by phosphorylation and concomitant protein conformational changes. Protein conformational changes are induced by binding of its ligand to the external receptor domain. The *FLT3* ligand (FL) is widely expressed in almost every cell type. Unstimulated *FLT3* remains in an auto-inhibited state. This is governed by three distinct parts of the JMD: a binding, a switch and a zipper motif. They maintain the activation loop within the two TKDs in an inaccessible state (Figure 6; structure model). [116, 143-145] The conformational state of the activation loop in turn determines kinase activation, hence it



encases the adenine-triphosphate (ATP) binding site. A key regulatory element within the TKD region that controls confirmation of the activation loop is the catalytic loop. Upon ligand stimulation, FLT3 receptors dimerize. Thereby, several distinct intracellular amino acid residues are trans-phosphorylated, causing an unfolding of the binding pockets within the TKDs. [143, 146-149] Leaving the activation loop in an open state, the encased tyrosine residues are then accessible for phosphorylation by transfer of an ATP derived  $\gamma$ -phosphate (Figure 6). Together with three to six adjacent amino acids, phosphorylated tyrosine residues form high-affinity sites for cytoplasmic signalling proteins, which contain either a phosphotyrosine binding (PTB) or Src-homology 2 (SH2) domain. Activation of these relay molecules subsequently induces downstream signalling cascades, which mediate cell proliferation, apoptosis and differentiation. [116, 120, 148, 150-153]

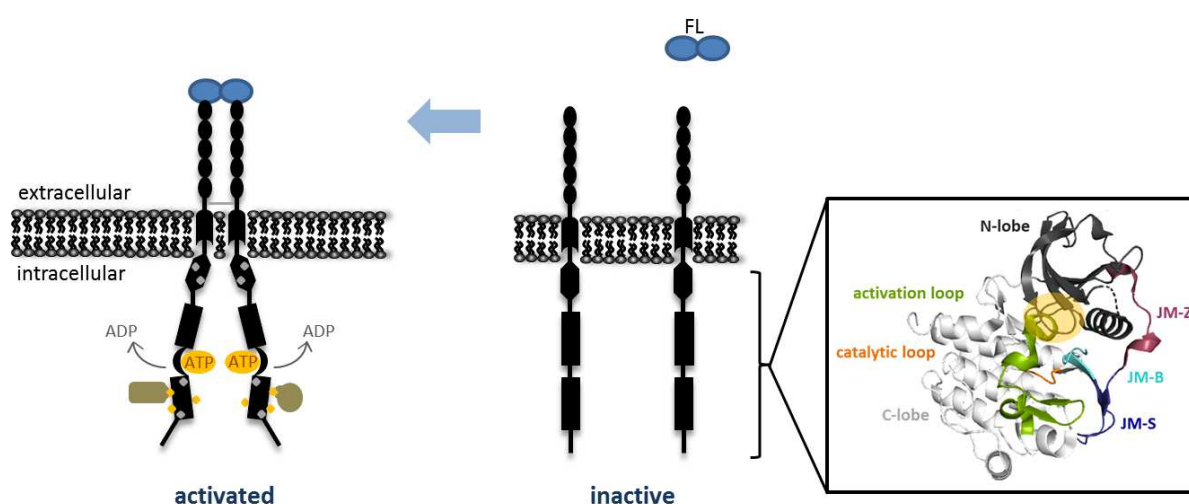


**Figure 6: Inactive and ligand-activated FLT3 receptor.**

FLT3 receptors dimerize upon binding of its ligand. This results in conformational changes and activation of the kinase domains, including trans-phosphorylation of cytoplasmic tyrosine residues (grey squares). The ATP-binding pocket is subsequently in an accessible state. Its accessibility enables the transfer of an ATP derived  $\gamma$ -phosphate to tyrosine residues in the tyrosine kinase domain (TKD). Phosphorylated tyrosine residues in the TKD build high-affinity binding pockets (orange squares) for a variety of signalling proteins (green), which show compatible domains for docking. In a phosphorylated state they in turn mediate intracellular downstream signalling (modified from Swords 2012, Grafone 2012, Matrone 2017). [127, 148, 153-156] In the 3D-model the structure of the intracellular FLT3 domains are shown (inactive state), which mediate receptor activation. Within the JMD the binding motif (JM-B; turquoise) maintains the rotation of the two beta-sheets away from the C-terminus. Correct position of the C-terminus is regulated by the switch motif (JM-S; blue). Important tyrosine residues responsible for receptor activation are located within the switch and zipper motif (JM-Z; magenta) at amino acid position 589, 591 and 599. [116, 135, 143-145, 157] A key tyrosine residue in mediating the switch from a closed to an open activation loop (green) confirmation is Y842, which interacts with the catalytic loop (orange). The unfolding of the activation loop generates ATP-binding pockets (yellow sphere highlights the ATP binding region) within the TKDs. The structural model was generated utilizing the PyMOL software (PDB-code: 1RJB; Griffith 2004, Kiyoi 2015 and Lagunas-Rangel 2017). [143, 158-160]

Through de-phosphorylation of the tyrosine residues in the JMD by tyrosine-phosphatases, such as the Src-homology 2 domain-containing phosphatase 2 (SHP2), FLT3 returns in its inactive state. [143, 161] A negative regulator of FLT3 activation and signalling is casitas B-lineage lymphoma (CBL). CBL is an E3-ubiquitin ligase, which competes with other compatible signalling

proteins for phosphorylated tyrosine residues, to ubiquitinate them. Upon ubiquitination, CBL mediates the internalization and proteasomal degradation of FLT3. Non-ubiquitinated receptors or those from which ubiquitin has been removed by deubiquitinases are recycled. [162-167] The half-life of FLT3 wild-type (WT) receptor is approximately two to three hours, decreasing to approximately half an hour upon stimulation. [167, 168]

While in normal cells FLT3 expression and activation is tightly regulated, aberrant expression of *FLT3* frequently leads to proto-oncogenic activation in hematopoietic malignancies, including MDS, ALL and AML. [55, 116, 169-172]

### 3.2.2 Aberrant expression and signalling activation of FLT3 in AML

In approximately 90% of AML cases FLT3 is aberrantly overexpressed or activated. [123, 148, 173-175] Increased FLT3 signalling is mediated either by enhanced transcriptional upregulation, *FLT3* gene mutations or increased ligand stimulation. Commonly, these factors collaboratively mediate an oncogenic transformation. [137, 145, 176-181]

A high level of *FLT3* mRNA expression is associated with an unfavourable prognosis in adult AML patients. In the case of FAB M5 subtype and cases with *KMT2A* rearrangements OS is impacted negatively by elevated *FLT3* mRNA levels, both in pediatric and adult AML patients. Of note, similar FLT3 surface expression levels are found on FLT3-positive bulk and leukemic stem cells - irrespective of *FLT3* mutational state. [115, 177, 181-183] Subsequent receptor activation occurs by exogenous FL or intrinsically produced FL, hence BM stromal cells as well as several primary leukemic cells and cell lines express FL. Based on this, most AML blast are capable of activating the receptor in an autocrine, paracrine or intracrine way. [115, 178] On the other hand, FLT3 can be constitutively activated by specific genetic alterations, belonging to “class V” activating mutations in leukemogenesis. Mutations of the *FLT3* gene affect up to 40% of newly diagnosed AML patients – up to 28% of *de-novo* and 19% of t/s-AML cases. Consequently, FLT3 is the most recurrently mutated receptor in AML. [33, 115, 116, 184-187]

There are two major types of FLT3 mutations. In-frame insertions of variable *FLT3* nucleotide sequences so called “internal tandem duplications” (ITDs) and point mutations (PMs). Furthermore, however less frequent, in-frame deletions of a few nucleotides can occur. [116, 184, 185, 188] Of all *FLT3* mutations, *FLT3*-ITDs represent the most common type. *FLT3*-ITDs are most prominent in patients with a normal karyotype (CN-AML), in patients with the cytogenetic setting of a t(6;9)(p23;q34) *DEK-NUP214* translocation and in APL patients positive for the translocation t(15;17)(q22;q21), which generates the *PML-RARA* fusion. In *core-binding factor* (*CBF*) AML or AML with a complex karyotype they are rather uncommon. [11, 53, 185, 186, 189, 190]. Incidences of *FLT3*-ITDs increase with disease progression and genetic instability, since they occur relatively late in leukemogenesis. They affect prevalently elderly and relapsed AML patients – showing a 2-fold higher rate in adult compared to pediatric AML patients. [115, 116, 145, 179, 191, 192] While always resulting in an in-frame transcript, *FLT3*-ITDs vary in length (between three to over 400 nucleotides) and sequence [11, 53, 145, 185, 193-195].

Predominately nucleotide insertions are located in exon 14 and 15, affecting the functional domains in the juxtamembrane and the tyrosine-kinase 1 region of the FLT3 receptor (Figure 7). Moreover, also in exon 20, encoding the functional domain TKD2, ITDs are detectable. Besides of tandem repeats, ITD mutants frequently imply additional nucleotide insertions or deletions [11, 53, 160, 188, 193, 196-198]. Activating *FLT3*-PMs and amino acid substitutions accordingly, are found in up to 10% of adult as well as pediatric AML patients. They frequently affect the JMD and both TKD regions (exon 13 – 20). The most common residues of the JMD are at amino acid position V579, F590, Y591, V592 and F594. In the TKD, they frequently affect amino acid residue N676 as well as the catalytic residues D835, I836 and Y842 in the activation loop (Figure 6). [11, 115, 131, 149, 157, 199-202] In-frame deletions, implicated in the onset of AML are less frequent (<1%) or coupled with an ITD, implying up to 18 nucleotides. By a deletion commonly affected residues within the JMD are for example the phosphorylation sites F594-Y597 in the zipper motif. [125, 188, 203]

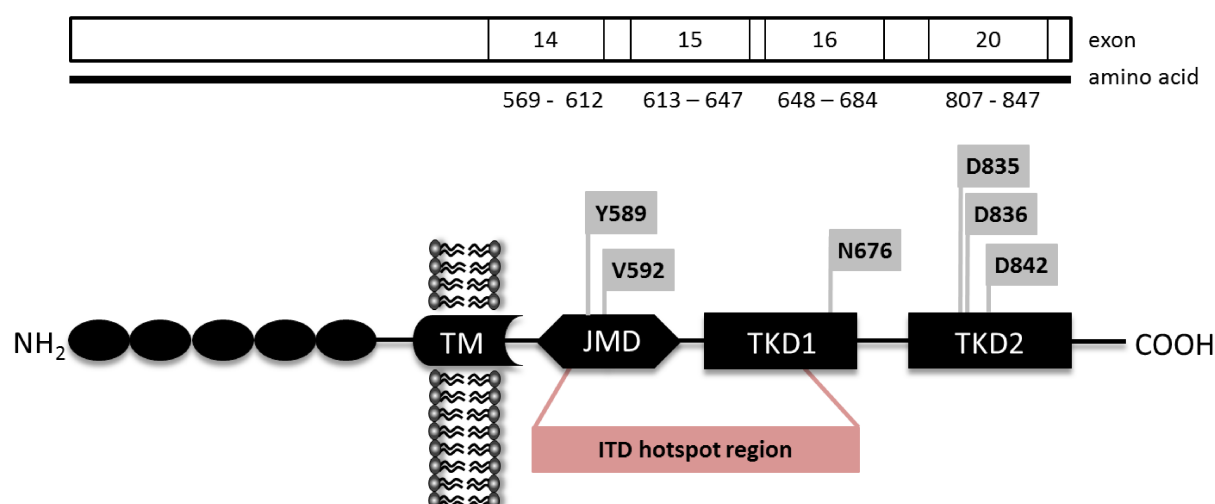


**Figure 7: Mutational hotspot regions of AML-specific FLT3-mutations (ITDs and PMs).**

*FLT3*-ITDs are predominantly located within exon 14 and 15, encoding the JMD and TKD1 of the receptor. *FLT3*-PM are found across the intracellular domains of FLT3, affecting the JMD as well as the two TKDs. The residues most frequently affected by PMs are indicated. [11, 131, 149, 157, 193, 200] (modified from Opatz 2013) [131]

On a biological level, these oncogenic FLT3 mutants lead to a ligand independent FLT3 receptor dimerization and constitutive activation, with subsequent downstream target phosphorylation. [115, 147, 157, 193, 200, 203]

ITDs and in-frame deletions change the sequence and length of receptor domains. This results in an abnormal receptor conformation, interrupting the auto-inhibited state, while the activation loop residues become accessible. [143, 184] Subsequently, interaction partners are constantly influenced. Besides activating the phosphoinositide-3-kinase (PI3K) - serine/threonine-kinase or protein kinase B (AKT) and V-Ki-ras2 Kirsten rat sarcoma viral oncogene homolog (RAS) - extracellular signal-regulated kinase (ERK) pathways, ITDs are capable of massively phosphorylating the signal transducer and activator of transcription 5 (STAT5); unlike the WT receptor (Figure 8). This probably accounts for their mere cytoplasmic localization, hence being ER-retained, remaining in an immature, underglycosylated but constitutively phosphorylated

form. [148, 184, 204-209] When activating STAT5 its subsequent dimerization leads to accessing the nucleus. Within the nucleus it activates the transcription of genes implied in cell proliferation, including *cyclin D1* (*CCND1*) and *MYC* as well as of anti-apoptotic genes, including *BCL-XL*, *MCL1* and of the gene encoding the serine/threonine kinases PIM1/2. Of note, PIM1 provides a positive feedback loop in phosphorylating and stabilizing the immature FLT3 receptor. Thereby, the half-life of immature FLT3 is increased up to three hours, despite phosphorylation. Stabilized, phosphorylated cytoplasmic FLT3 in turn promotes aberrant STAT5 signalling. Moreover, activated STAT5 signalling increases the production of reactive oxygen species (ROS). ROS induce DNA double-strand breaks and DNA repair deficiency, causing genomic instability. [155, 205, 207, 208, 210-220]

A second feedback loop governing a proliferative advantage is mediated by mutant FLT3 in increasing the expression of the receptor Frizzled-4 (encoded by *FZD4*; responsive to Wnt-type (Wnt) ligands) and  $\beta$ -catenin (encoded by *CTNNB1*). Activation of Frizzled-4 leads to stability of  $\beta$ -catenin.  $\beta$ -catenin then translocates to the nucleus and acts as a transcriptional co-activator for the transcription of *MYC* and *CCND1*. Activation of apoptosis is furthermore inhibited by preventing FOXO3-mediated transcription of *BIM*. [221] In addition, oncogenic FLT3 mutants contribute to leukemic progression by repression of myeloid transcription factors, including CCAAT-enhancer-binding protein alpha (CEBPA) and PU.1 (encoded by the gene *SPI1*). Targeting PU.1 is mediated by micro RNA 155 (miR-155), whose expression is upregulated by STAT5 and nuclear factor kappa B (NF $\kappa$ B) signalling. Repression of CEBPA and PU.1 enforces a block of differentiation. Other transcription factors, including RUNX1 and forkhead box 1 (FOXO1) are found upregulated in *FLT3*-ITD positive AML. They selectively mediate target gene expression increasing cell survival. For example, RUNX1 regulates the expression of the apoptotic regulator *BCL2* (Figure 8). [137, 212, 215, 222-226]

In case of small deletions and *FLT3*-PMs, the auto-inhibitory function of the JMD is destabilized and catalytic domains are activated. Therefore, they have higher constitutive dimerization rates than the WT receptor in the absence of FL, being able to constitutively phosphorylate downstream targets. *FLT3*-PMs induce a strong activation of PI3K/AKT and RAS/ERK signalling cascades. Expression of negative mediators of activated signalling cascades in turn is down-regulated. This implies for instance sprouty RTK signalling antagonist 3 (SPRY3), which acts negatively on RAS/ERK signalling. [157, 188, 203, 206, 227, 228] Depending on the affected residue and its function, *FLT3*-PMs show stronger or weaker transforming potential. *FLT3*-PMs affecting residues in the catalytic domain are more oncogenic. Activating PMs in the catalytic domain as well as *FLT3*-ITDs are furthermore associated with high *FLT3* expression levels and faster intracellular turn-around times. Besides the oncogenic mutational variants mentioned, several other *FLT3*-PMs are detectable in AML patients. Of these not all may confer a transforming potential. [9, 11, 115, 157, 167, 177, 213, 229]

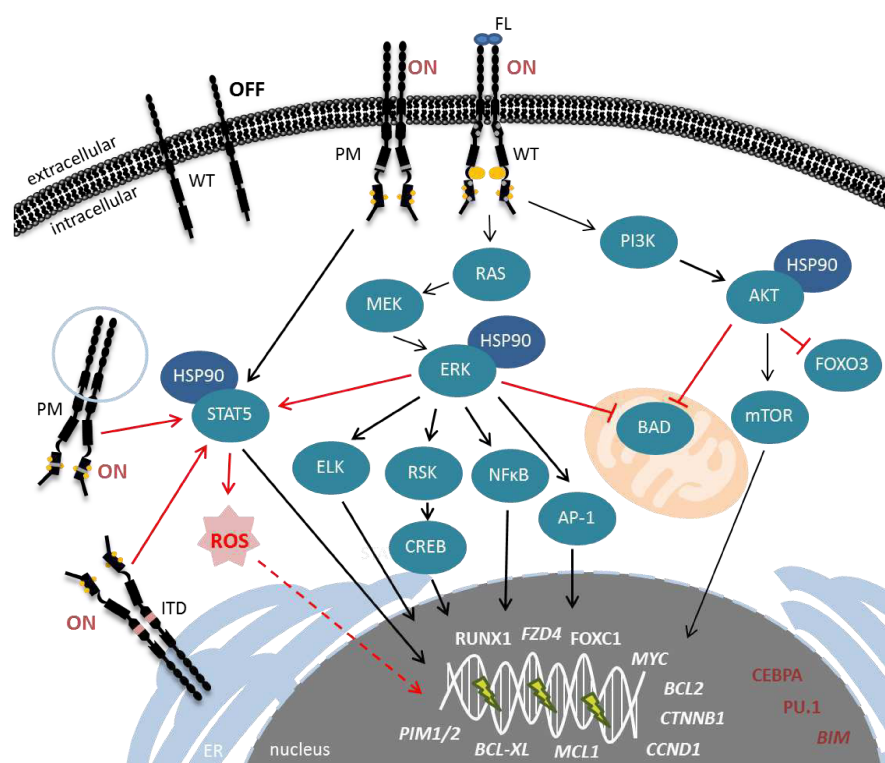


**Figure 8: Schematic summary of the main aberrantly activated signalling cascades by FLT3 mutants, compared to normal FL-induced signal transduction by wild-type FLT3.**

FLT3 wild-type (WT) only exerts its signalling cascade upon ligand binding. In contrast, mutant FLT3 receptors, although remaining FL-sensitive, are auto-activated. They are able to dimerize and subsequently phosphorylate signalling molecules without requiring an external signal. In addition to normal FLT3-signalling cascades (thin black arrows), including PI3K- and RAS-signalling, mutant FLT3 can activate signalling pathways more excessively (bold black arrows) or activate and inhibit additional regulatory mediators (red arrows / bars). Activated mediators furthermore interact more excessively with heat shock protein 90 (HSP90), which protects from inactivation and degradation. Gene expression signatures are also altered by mutant FLT3, showing specific upregulation of pro-survival mediators (white) and down-regulation of apoptotic and differentiation factors (red) in the nucleus (modified from Chan 2011, Choudhary 2009, Swords 2012 and Grafone 2012). [154, 155, 207, 213]

In summary, activating *FLT3* aberrations are capable of inducing a myeloproliferative phenotype in murine models by mediating anti-apoptotic and proliferative advantages. [55, 116, 169, 171, 172, 230-232] *FLT3*-PMs though show a weaker transforming potential compared to ITDs, while both display a gain-of-function phenotype. [9, 11, 115, 157, 229] Clinically, activating *FLT3* mutations are associated with increased leucocyte and blast counts in the PB and BM. [145, 233]

However, aberrant *FLT3* alone is not sufficient to induce AML. But in leukemogenesis and disease progression, aberrant *FLT3* highly cooperates with “class I and VII” mutations e.g. *RUNX1/RUNX1T1* as well as “class IV and VI” mutations e.g. *DNMT3A*. [55, 116, 169, 171, 230, 234] With respect to mediating relapse, *FLT3*-ITD is associated with high expression of CXCR-4. CXCR-4 is a G-protein coupled receptor that plays an essential role in hematopoietic homing and engraftment. Apoptosome inhibition, inducing chemotherapy-resistance, can also be mediated by mutated *FLT3*. This is accomplished by inhibition of apoptotic peptidase activating factor 1 (Apaf-1) / caspase-9 apoptosome activity, which induces mitochondrial-related programmed cell

death. In *FLT3*-ITD positive AML cells, moreover a downregulation of the equilibrative nucleoside transporter 1 (ENT1), responsible for Ara-C cellular uptake, has been noted. Additionally, in many AML cells increased FL levels are observed. [212, 235, 236] As *FLT3* mutations appear with many other alterations, AML with aberrant *FLT3* is not assigned as independent stratification group. Nonetheless, since affecting crucial cellular mechanisms being highly oncogenic, both *FLT3*-ITDs and activating *FLT3*-PMs imply prognostic relevance. [9, 11, 31, 115, 157, 229]

### 3.2.3 Diagnostic identification and prognostic implication of *FLT3* mutations

Mutations in the *FLT3* gene are routinely assessed at initial diagnosis of AML using standardized methods. Alterations affecting the size of *FLT3*, including *FLT3*-ITDs or deletions in *FLT3* are detectable by fragment analysis or genescan analysis, respectively. Thereby, PCR amplification of exon 14 and 15 using either gDNA or cDNA samples as well as fluorescently-tagged primers is performed, followed by PCR product sizing using capillary electrophoresis (Figure 9a). To detect specific point mutations within *FLT3*, PCR amplification is followed by Sanger sequencing (Figure 9b). TKD-PMs at codon D835, D836 and D839 can be further revealed by restriction endonuclease digestion of the PCR amplicon of exon 20, with subsequent polyacrylamide or agarose gel electrophoresis (Figure 9c). [38, 50, 51, 195, 237-241] *FLT3* mutations are detectable in both leukemic blasts as well as LSCs. [242]

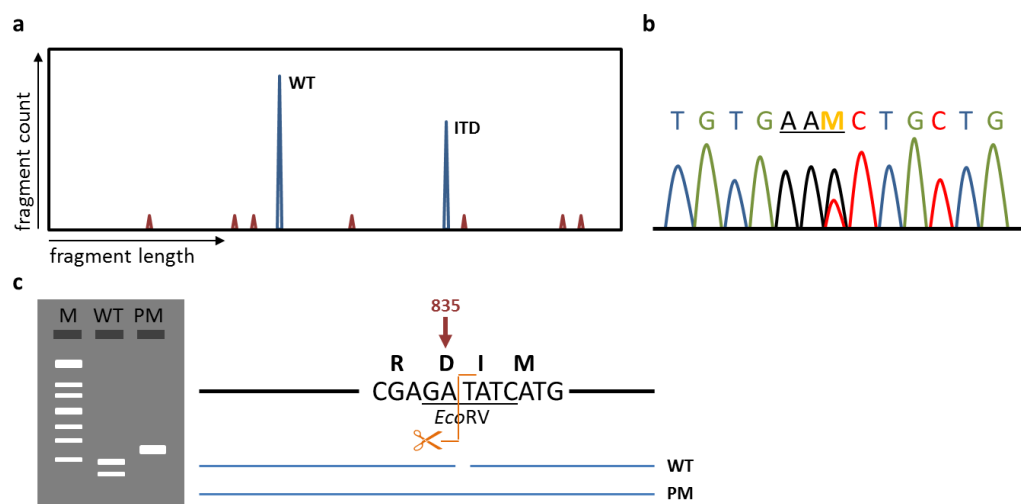


**Figure 9: Schematic illustration of *FLT3* mutation detection.**

**a)** Electropherogram of a fragment analysis of *FLT3*-ITD using denaturing capillary electrophoresis and fluorescence detection. PCR-fragment length is represented by number of base pairs, while the fragment count represents relative fluorescence intensity. In the presented case, two differently sized *FLT3* fragments are detected (blue peaks): WT and a larger variant, representing a heterozygous ITD, with a lower fragment count for the ITD than for WT. Red peaks represent an internal size standard. Depending on the length of the PCR amplicon normal WT size fragments are distinguishable from smaller fragments (referring to deletions) and larger fragments (showing *FLT3*-ITDs). Absence of WT indicates loss of heterozygosity (LOH). LOH is commonly due to deletion of one allele. Another mechanism is copy-number-neutral LOH through recombination. Based on the fragment specific area under the curve the ratio of WT to ITD can be calculated semi-qualitatively, enabling estimation of the mutational load of a *FLT3*-ITD clone. **b)** Chromatogram showing two nucleotide variants at cDNA position NM\_004119.2:c.2028 (C>A, represented by the nucleotide ambiguity code “M”; the

three nucleotides representing the codon are underscored). This variant refers to a heterozygous *FLT3*-TKD-PM (p.N676K). **c)** Exemplary detection of a TKD-PM by restriction enzyme digestion. *FLT3*-amplicon of exon 20 is digested with *EcoRV* endonuclease. While *FLT3*-WT is digested into 3 bands by *EcoRV*, point mutations either at location D835 or I836 disrupt the *EcoRV* site, resulting in slower migrating undigested fragments using agarose gel electrophoresis. For the detection of point mutations at location D839, a digestion with the restriction enzyme *HinfI* can be performed. Marker (M); (adapted from Yamamoto 2001, Thiede 2002, Mills 2005, Best 2012 and Opatz 2013). [11, 131, 200, 238, 241]

Although the number, size, position and mutational load of a *FLT3*-ITD can vary amongst patients, the presence of a *FLT3*-ITD itself negatively impacts on prognosis (except for APL patients). Harboursing a *FLT3*-ITD is associated with an unfavourable prognosis due to reduced chemotherapy-treatment response and a decreased duration of CR, shorter RFS and OS. In adult as well as in pediatric AML patients, a *FLT3*-ITD is associated with a high risk of relapse. [12, 95, 145, 160, 185, 189, 194, 197, 233, 243-248] The ITD mutational load or mutant to WT allelic ratio, respectively, adds prognostic strength. A high allelic burden is associated with a very poor prognosis (shorter OS, RFS), with worse outcome for patients with loss of *FLT3*-WT during disease progression. By multivariate analysis the *FLT3*-ITD mutational load showed to be the second most-relevant prognostic factor besides cytogenetics. [11, 130, 145, 160, 185, 189, 193, 237, 239, 249] Depending on the *FLT3*-ITD insertion site and respective functional domain, differential outcome and response to treatment with conventional chemotherapy, as well as tyrosine kinase inhibitors (TKIs) have been observed. Especially *FLT3*-ITDs outside of the JMD have been shown to be associated with an inferior outcome (RFS and OS) and resistance to TKIs (*in vitro* and *in vivo*) - however not in every cohort. [160, 196, 250-254] Similarly, the relation of ITD size and therapy outcome is discussed controversially. [160, 185, 194, 255-257]

In comparison, *FLT3*-ITD predisposes to a worse outcome with lower survival rates than activating *FLT3*-PM. However, activating *FLT3*-PMs confer worse outcome compared to patients with *FLT3*-WT. [9, 115, 258] Of note, TKD-PM (especially D835 and I836), have been shown to play a role in resistance to standard and especially targeted therapies. These TKD-PMs mediate relapse and imply on RFS. Their impact, however, seems to depend on the presence of other mutations - as seen in conjunction with a *FLT3*-ITD, t(15;17) *PML-RARA* fusion or *KMT2A*- partial tandem duplication (PTD). [9, 202, 229, 243, 253, 259-267]

During disease progression, *FLT3* remains a rather diverse and changing marker, implying mutational shifts between diagnosis and relapse. In up to 20% of cases, mutational changes of *FLT3* occur; frequently with increases in the mutational ITD load. In some cases, patients show a conversion of a heterozygous state at diagnosis to a homozygous state at relapse. In other cases subclonal ITDs detected at diagnosis are lost during disease progression, while others are gained or grow out at relapse. [27, 80, 268-276] Mutational shifts in *FLT3* and a gain of new variants (ITD and/or activating TKD-PM) are associated with worse RFS for both, conventional or *FLT3*-targeted therapies, compared to stability of *FLT3* mutations during the course of the disease. [130, 264, 266, 269, 277, 278] When detected at initial diagnosis *FLT3* mutations may therefore be followed up during disease progression and therapy as MRD marker. Several studies have pointed out the potential of quantitative RT-PCR, digital droplet PCR and next-generation sequencing (NGS) based approaches for molecular *FLT3*-ITD MRD assessment over conventional

diagnostic applications with regards to sensitivity of subclonal ITD detection. [80, 249, 259, 268, 270, 279-286] For example, monitoring deep molecular response rates after treatment with a TKI, high responders (ITD level during treatment  $\leq 10^{-2}$ ) amongst *FLT3*-ITD positive AML patients can be identified, who show a better prognosis implying longer OS. [287] Another important surrogate marker for initial response rates to TKIs is the reduction of phosphorylated *FLT3* (p*FLT3*), determined by a plasma inhibitory activity assay. Rates of above 85% of reduction in p*FLT3* are being survival supportive. [288, 289]

Since correlated with poor outcome, *FLT3*-ITDs as well as resistance-mediating *FLT3*-TKD-PM mutations have gained increased importance in AML therapy evaluation. Thus, the development and evaluation of *FLT3*-targeted therapy approaches are of high interest. [50, 80, 135]

### 3.2.4 *FLT3*-targeted therapy approaches

*FLT3*-targeted therapy is based on either interference with *FLT3* activation and subsequent receptor signalling utilizing TKIs or *FLT3* antigen identification and subsequent receptor blocking or cytolysis by *FLT3*-directed immunotherapy. [154, 290]

TKIs are small molecules, preventing RTKs from activating signalling cascades. Up to date, there are many different TKIs available, with ongoing investigations concerning their inhibitory profile, pharmacodynamics, -kinetics and -vigilance as well as effective therapeutic use in clinical trials. First generation TKIs, such as Midostaurin (PKC-412, type I TKI), Sunitinib (SU11248, type I TKI), Lestauritinib (CEP-701, type I TKI) and Sorafenib (BAY43-9006, type II TKI), are multi-kinase inhibitors, showing a broad spectrum of kinase interactions. In contrast, next-generation TKIs, including Crenolanib (CP-868596, type I TKI), Gilteritinib (ASP-2215, type I TKI), Quizartinib (AC220, type II TKI), Cabozantinib (XL184, type II TKI) and Tandutinib (MLN-518, type III TKI), act more specifically against only a few RTKs. [291-297] Regarding their inhibitory mode of action, type I TKIs are ATP-competitive inhibitors, targeting the ATP-binding site of activated receptors. Both type II and III are so-called allosteric inhibitors, inducing a conformational change towards a kinase inactive state to inhibit kinase activity (Figure 10). [156, 298, 299]



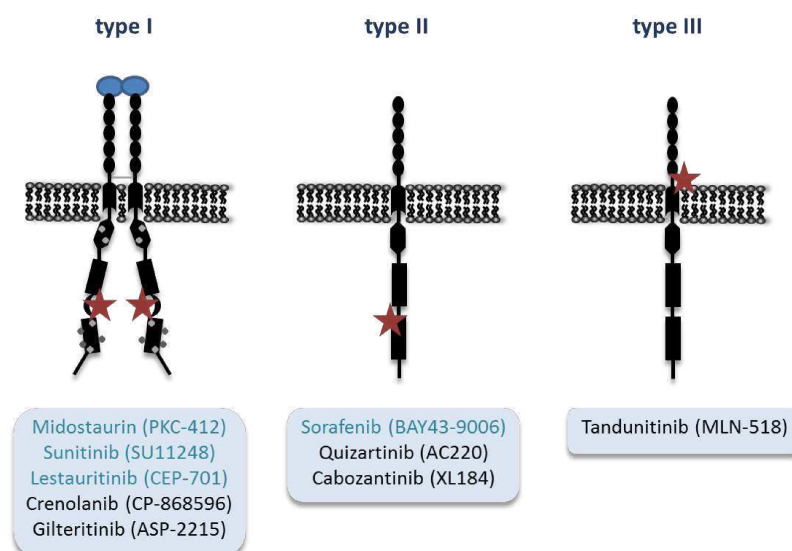


**Figure 10: Schematic illustration of the binding sites of type I to III TKIs.**

Type I TKIs recognize the active conformation and compete with high levels of intracellular ATP to bind reversibly to the ATP-binding site. Since the ATP-binding pocket is highly-conserved and homologous amongst RTKs, type I TKIs are not very selective. Type II TKIs indirectly compete with ATP by occupying the hydrophobic pocket, adjacent to the ATP-binding site, making activation energetically unfavorable. Thus type II TKIs target inactive receptors in a more specific manner. Either ways, the enzymatic capacity (phosphorylation) and thus downstream pathway activation of the receptor is blocked. In contrast, type III TKIs bind covalently to cysteines at specific sites of the kinase, outside of the ATP-binding region (variably located). Thereby, they modify the structural conformation of the receptor, preventing receptor dimerization while inducing the closed receptor conformation, whereof ATP binding is inhibited. Both type II and III bind independent of receptor activation. The TKI binding site is depicted with a red star. First generation TKIs are shown in turquoise (modified from Matrone 2017). [156, 300]

In many *in vitro* studies, TKIs have shown their potential to inhibit aberrant FLT3 receptor phosphorylation and signalling. Thereby, they block AML cell proliferation and mediate cytotoxicity. Besides FLT3-WT, TKIs have shown to effectively target mutant FLT3 (ITD and TKD-PM), however with variable sensitivity depending on the type of TKI and on the target cells.[291, 295, 301-307] Several trials investigate the clinical impact of TKIs. Administration of first generation TKIs Lestauritinib, Sorafenib or Midostaurin as single agent is well-tolerated by AML patients. Initial response rates show an effective reduction of peripheral blasts for patients with WT and mutant FLT3 (ITD and TKD). However efficacy in prolonging CR rates and OS is limited due to incomplete eradication of AML blasts in the BM and rapidly evolving resistance mechanisms driving relapse. In relapsed *FLT3*-ITD positive AML patients, Sorafenib induced sustained remission when combined with HSCT. [154, 289, 308-314] Next-generation TKIs, Quizartinib and Gilteritinib show a beneficial impact as mono- and bridging therapy in relapsed and refractory *FLT3*-ITD positive AML patients in phase I and II clinical trials. In contrast to the first generation TKIs, they are very potent and selective against FLT3, especially mutant FLT3 (ITD and TKD). After several weeks of treatment, they may induce a BM blast cell clearance. However, also with Quizartinib and Gilteritinib treatment resistance mechanisms were encountered, posing limits in long term eradication of leukemia cells. [154, 291, 306, 308, 315-324] The type III inhibitor Tandutinib has not exceeded study phase II so far. Tandutinib shows low anti-leukemic

activity and unfavorable pharmacokinetics with slow plasma level clearance, thus limiting its clinical utility for the treatment of AML. [154, 294, 325, 326] Thus, resistance to TKIs remains a challenging phenomenon.

Resistance to TKI treatment is mediated by the acquisition of varying secondary *FLT3*-PMs (e.g. E608K, D835H/V/Y, Y842C/H and F691L), as well as intrinsic mechanisms mediated by mutant *FLT3* as indicated in Figure 8. In the BM niche, stromal cells additionally govern protection against TKIs, enabling LSCs to survive this treatment. [222, 253, 260, 263-265, 306, 308, 327-331] To maintain the eradication of leukemic cells, combinatorial approaches of TKIs with chemotherapy have been investigated. In these studies TKIs were added to induction and consolidation therapy and subsequently administered as maintenance therapy. In newly diagnosed and relapsed / refractory AML patients younger than 60 years, Sorafenib and Midostaurin but not Lestauritinib, have proven their benefit in significantly increasing RFS. In the case of Midostaurin also OS has been prolonged. In elderly AML patients, however, higher toxicities and mortality rates for combinations of Sorafenib and chemotherapy were observed, thus lacking an improvement in survival. [93, 96, 308, 332-340] The benefit of a combination of Sunitinib, Crenolanib or Gilteritinib with chemotherapy is still under investigation in clinical studies. [13, 341, 342] Nonetheless, a recent major breakthrough was the FDA-approval of the TKI Midostaurin for *FLT3*-mutated AML in combination with induction chemotherapy. [92, 343]

Another therapeutic approach to specifically target *FLT3*-expressing cells is antigen-directed immunotherapy. Up to date, *FLT3*-targeted immunotherapeutic approaches are either mediated by anti-*FLT3* antibodies or *FLT3*-directed chimeric antigen receptor (CAR) T-cells. [154, 155, 186]

So far three types of therapeutic antibodies have been constructed to target *FLT3*. First, antibodies that directly bind to *FLT3*, competing with FL for receptor docking (Figure 11a; purple background). They inhibit FL-induced signalling activation by receptor coupling and subsequent internalization. Monoclonal humanized antibodies bear an Fc-receptor compatible part that can recruit and activate Fc-receptor-bearing effector cells, including natural killer (NK) cells. [344-348] Up to date, a number of fully human immunoglobulin anti-*FLT3* monoclonal antibodies have been developed. They are derived from fragments, originally isolated from naïve human monovalent antibody fragment phage display libraries. *In vitro* anti-*FLT3* antibodies show target specificity and anti-leukemic activity. [345, 347-349] Investigations with the humanized monoclonal *FLT3*-antibody LY30122218 (IMC-EB10) showed inhibition of receptor signalling and effectiveness in eradicating AML cells *in vitro*, however only moderately for *FLT3*-mutated cells (*FLT3*-ITD and *FLT3*-TKD). Nevertheless, engraftment of cells with either *FLT3*-genotype was reduced in mice by antibody administration. [346, 347, 350, 351] An initial phase I study is assessing the Fc-optimized anti-*FLT3* antibody FLYSYN as monotherapy in adult MRD-positive AML patients (clinical trial identifier: NCT02789254). [352]

Secondly, antibodies comprising two antigen recognition sites – one targeting *FLT3* and the other one directed against CD3, for specifically recruiting and activating T-cells (Figure 11a; blue background). Hence, they are called “bispecific” antibodies. *FLT3*xCD3 antibodies are available in either a Fabsc or tandem double single chain variable fragment format (scFv and bssc,

respectively; Figure 11b). The latter is also known as bispecific T-cell engager (BiTE). [344-346, 348, 350, 351, 353, 354] An initial phase I clinical trial has investigated the monoclonal bispecific FLT3-antibody LY30122218 (IMC-EB10) for the treatment of relapsed and refractory AML (26% *FLT3*-mutated; clinical trial identifier: NCT00887926). Although LY30122218 demonstrated to be safe, the antibody failed to show clinical activity as single agent and therefore the study was abrogated. [355] Optimized monoclonal bispecific antibodies BV10-SDIEM (BV10xUCHT1 in Fabsc-format) and 4G8-SDIEM (4G8xUCHT1 in Fabsc- and bssc-format), showed efficient antibody-dependent cytotoxicities in *in vitro* studies. *In vivo* assays in patient-derived xenograft (PDX) mice and non-human primates confirmed efficient anti-tumor activity. A more than 2-fold extended survival was revealed when treated with an optimized FLT3 BiTE. However, their clinical efficacy has not been evaluated so far. [182, 353, 354, 356]

Thirdly, antibodies that carry cytotoxic cargos release their toxic payload after receptor internalization when bound to the target (Figure 11a; brown background). [344-347] Cytotoxine-coupled anti-FLT3 antibodies, such as the anti-FLT3 antibody drug conjugate (ADC) AGS62P1, showed pre-clinical anti-tumor efficacy against FLT3-expressing AML cells (*FLT3*-ITD and non-ITD) *in vitro*. *In vivo* anti-FLT3 AGS62P1 impaired engraftment and outgrowth of primary AML cells in PDX mice. [357] ADCs mediate tumor cell killing by specifically delivering linker-conjugated high potent cytotoxic agents to FLT3-expressing cells, while stably remaining in the plasma. ADCs induce internalization upon cell surface binding to allow maximum delivery of conjugated agent into the intracellular compartment, where the cytotoxic agent is subsequently released by the cell endosomes or lysosomes. Cytotoxic payloads may be chemotherapeutics like Daunorubicin. Novel agents include microtubuline inhibitors such as auristatins. Auristatins interfere with the polymerization of  $\alpha$ -tubulin. Thereby, they prevent the formation of the mitotic apparatus causing G2/M-phase cell cycle arrest. Furthermore, DNA-damaging drugs can be attached to antibodies. They have the benefit of being active during different cell cycle phases. There are DNA-alkylating bacteria-derived agents such as calicheamicin or duocarmycin. These agents bind to the minor groove of DNA, inducing DNA double-strand breaks. On the other hand, there are mushroom-derived toxins such as  $\alpha$ -amanitin. A-amanitin inhibits the RNA polymerase II enzyme, thus inhibiting mRNA synthesis. Alternatively to a linker-conjugated drug, a potent DNA cross-linker can be incorporated into the structure of the antibody by conjugation with cysteine residues. Upon specific antibody-binding, the molecule is internalized, leading to cell cycle arrest and induction of apoptosis. [347, 358-360]

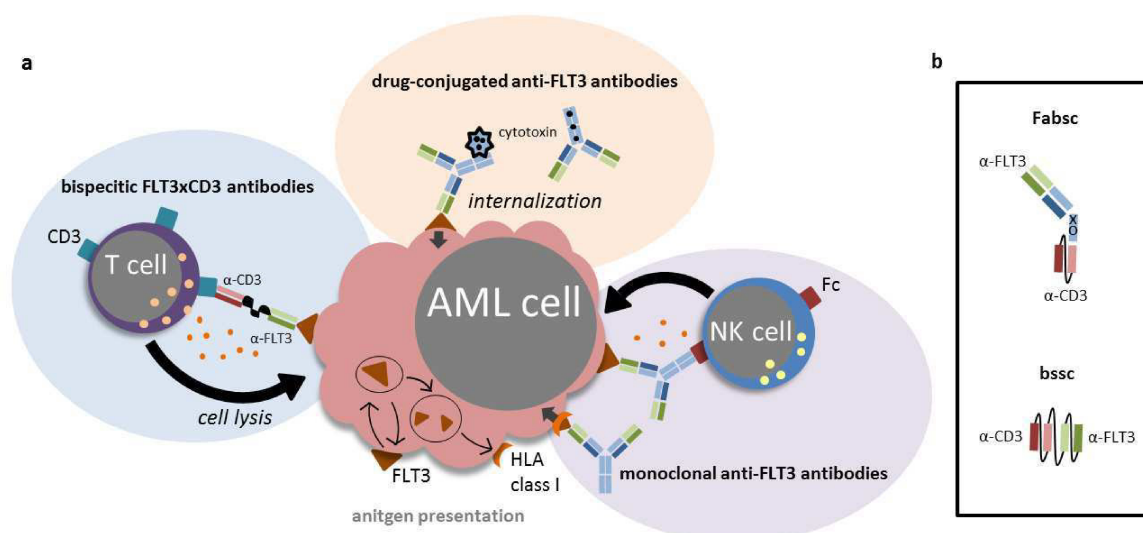


**Figure 11: Illustration of therapeutic FLT3-targeted antibodies and their antigen interaction on target cells.**

**a)** Humanized anti-FLT3 antibodies target antigens presented on the AML cell surface - either FLT3 receptor itself or specific immunogenic FLT3-peptides presented by major histocompatibility complex (MHC) molecules. Monoclonal humanized anti-FLT3 antibodies block ligand-mediated receptor activation and induce down-regulation of receptor surface expression, enabling receptor degradation. In addition, they can recruit Fc-receptor expressing effector immune cells (e.g. natural killer (NK) cells) with high affinity. Effector immune cells subsequently induce cell-mediated cytotoxicity, which in turn stimulates further immune responses (purple background). Drug-conjugated antibodies (entire antibodies or single chain variable fragments) or modified antibodies comprising DNA-cross linkers specifically bind FLT3. Upon binding, they are internalized and release their cytotoxic agents intracellularly. A high affinity rate is essential for proper cytotoxicity (brown background). While single chain antibody fragments (scFv) comprise one individual antigen recognition site, bispecific antibodies target two different antigens or epitopes. Thereby, they specifically target FLT3 while recruiting T-cells to induce cytotoxicity through their activation via CD3 (blue background; modified from Gasiorowski 2014 and Grosso 2015). **b)** Schematic representation of the two bispecific antibody formats. The Fabsc-format consists of an N-terminal FLT3-specific Fab part linked to a C-terminal single chain (sc) binding CD3 antibody. The inserted linker CH2 domain separates the two specificities to hinder undesired interactions between them. To prevent homodimerization and binding to Fc-receptors, cysteines in the hinge region (x) and amino acid residues in the CH2 domain (o) are frequently modified. In contrast, the bispecific single chain (bssc)-format and bispecific T-cell engager (BiTE), respectively, consist of two single chains – one directed against FLT3 and the other against CD3. The anti-FLT3 and anti-CD3 are connected by a glycine-serine linker, while the single-chains themselves are linked by the sequence derived from the elbow fragment of human IgG1. Regardless of antibody specificity and efficient T-cell activation, BiTE antibodies show a higher tendency to form aggregates and a reduced serum half-life compared to Fabsc-format antibodies (adapted from Durben 2015). [346, 347, 353, 358, 360, 361]

Investigations on CAR T-cells targeting FLT3 have just recently begun. Anti-FLT3 CAR T-cells are modified T-cells primed to detect and eradicate FLT3-positive cells (Figure 12a). They are generated from primary T-cells of healthy donors (HDs), transduced with FLT3-CAR constructs (anti-FLT3-scFv-CD28-CD3 $\zeta$  or BV10-scFv-IgG4hinge-CD28-CD3 $\zeta$ - EGFRt; EGFR (epidermal growth factor receptor), t (transduction marker); Figure 12b). Modified T-cells are subsequently capable of MHC-unrestricted activation when binding the target antigen via the antibody fragment. They mediate cytotoxicity by secretion of cytokines, including interferon gamma (INF- $\gamma$ ) and interleukin 2 (IL-2). In pre-clinical studies, FLT3-targeting CAR T-cells showed cytotoxicity

exclusively against FLT3-expressing AML cell lines and patient samples (WT and ITD) *in vitro*. *In vivo* they demonstrated significant anti-leukemic activity with prolongation of survival rates of up to 100% in PDX mice. HSC engraftment and differentiation was not impaired by the FLT3-CAR construct anti-FLT3-scFv-CD28-CD3 $\zeta$  *in vivo*, hence the quality and proportion of human CD34+ cells, differentiated mature lymphocytes (e.g. NK and B-cells) and myeloid cells (e.g. DCs) was maintained. In contrast, the other FLT3-CAR construct, BV10-scFv-IgG4hinge-CD28-CD3 $\zeta$ -EGFRt, recognized normal HSCs and interfered with hematopoiesis in colony forming cell (CFC) assays *in vitro*. Thus, its therapeutic window is limited prior to HSCT, following FLT3-CAR T-cell depletion to enable hematopoietic reconstitution. [136, 360, 362]

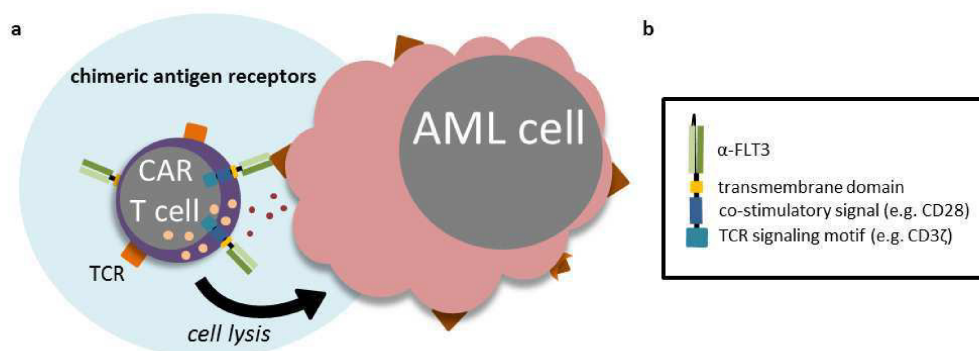


**Figure 12: Illustration of therapeutic FLT3-directed CAR T-cells and their antigen interaction on target cells.**

**a)** Genetically modified T-cells are primed to detect FLT3 by expressing chimeric antigen receptors (CARs), which enable direct targeting of FLT3-positive AML cells. Upon target binding, CAR T-cells are self-activated by their intracellular receptor signalling parts, inducing the release of cytokines. T-cell receptors (TCR) are capable of recognizing immunogenic FLT3-peptides presented by major histocompatibility complex (MHC) molecules signalling (modified from Grosso 2015 and Lim 2017). **b)** FLT3-CAR constructs are cell-membrane bound receptors designed to link the binding part of a high-affinity single-chain antibody fragment (scFv) specific against FLT3, with T-cell signalling parts, such as CD3 $\zeta$ . Thereby, CARs mediate an MHC-independent antigen-specific recognition with subsequent T-cell activation. In case of next generation CARs co-stimulatory parts such as CD28 are added for enhanced T-cell responsiveness. In some CARs a hinge region is implemented for optimal distancing between binding and signalling components increasing T-cell activation. An optional EGFRt transduction and depletion marker attached to CARs enables a selection for transduced T-cells as well as a rapid and complete removal of CAR T-cells by an anti-EGFR antibody to protect engrafting normal HSCs and reverse CAR T-cell induced systemic toxicity (modified from Jackson 2016, Lim 2017 and Whilding 2015). [360, 363-366]

### 3.3 Rationale of this study

Since AML, especially with activating *FLT3*-mutations, is an aggressive and heterogeneous disease with an unfavourable outcome and high relapse-rates [9, 10, 12, 145, 160, 185, 233], sensitive detection methods for an early identification as well as patient-tailored therapeutic approaches are highly warranted. Furthermore, the clinical assessment of novel and recurrent FLT3 variants remains essential to advance AML diagnostics and therapy. [229, 259] Thus within this doctoral work the biology and translational aspects of *FLT3*-mutated AML regarding

diagnostic and therapeutic application as well as the biological role of a new and recurrent *FLT3*-PM in the setting of AML was addressed and investigated.

### **3.3.1 The applicability of a NGS-based *FLT3*-ITD detection tool compared to standard routine assays**

In the first project, a new diagnostic approach to detect *FLT3*-ITDs with high sensitivity was established and assayed for its applicability and impact on *FLT3* diagnostics. To this means we developed an amplicon-based high-throughput next generation sequencing (NGS) method for the detection of *FLT3*-ITDs. Sequencing of 267 AML samples from patients treated on trial was compared to the routine diagnostics, with regards to its accuracy and sensitivity. To this aim, barcode-primer combinations were used to enable sequencing of up to 96 amplicons at once. For validation purpose *FLT3*-targeted genomic sequencing and fragment analysis of *FLT3*-amplified gDNA was used to evaluate data discrepancies of standard assays compared to the new method. While fragment analysis is still referred to as gold-standard it has limited sensitivity and does not provide any information about the altered *FLT3*-ITD sequence, including the insertion position. Both are of interest with regards to subclonal *FLT3* mutations, which may mediate therapy-resistance and outcome. Moreover, ITD characteristics were evaluated regarding their impact on RFS and OS and compared between both methods to determine potential differences in data quality relevant for prognostics. Hence high-throughput sequencing costs decline and the hands-on-time is comparable, NGS-techniques applied to diagnostics may provide an attractive and feasible alternative to current standard methods.

### **3.3.2 The relevance of a new and recurrent *FLT3* deletion mutation in AML**

Moreover, high throughput sequencing approaches led to the discovery of several new *FLT3* mutations of which some likely are passenger mutations, not showing a transforming or therapy resistance-mediating potential [229]. Thus, the identification of their biological impact remains essential. To this aim, within the second project we investigated the biological relevance of a new and recurrent *FLT3* mutation, detected by routine diagnostics in a relapsed AML patient. To functionally characterize the novel *FLT3* mutation, pathway signalling activation, protein localization, ligand stimulation and cell proliferation was evaluated.

### **3.3.3 TKI-mediated effects on *FLT3* and the potential for a combination with *FLT3*-directed immunotherapy in AML**

Since risk factor research further aims for practical interventions, in the third project the influence of TKIs on different *FLT3* genotypes was investigated systematically, hence variable responses have been reported in AML patients. [289] To this means, the impact of TKIs on the cellular localization and glycosylation of *FLT3*-WT and several mutants, including resistance-mediating PMs, was investigated and correlated with inhibition of proliferation. To decipher the

impact of the *FLT3* genotype on TKI response, we investigated different *FLT3* genotypes in variable biological settings. Furthermore, the potency and kinetics of the TKI-mediated FLT3 surface expression was investigated, comparing type I and type II TKIs. A TKI-mediated surface expression might also open up avenues for targeting FLT3 by immunotherapeutic approaches, especially for *FLT3*-ITD positive patients. Therefore, the hypothesis of a combinatorial therapeutic approach using TKIs and immunotherapy evolved. This has important clinical implications, since combinatorial approaches seem required in light of the unsatisfying results of TKI monotherapy with regards to RFS and OS due to resistance mechanisms. [13, 154, 308, 352, 367] Proof-of-principle experiments were performed to assess the efficacy of a combined treatment using a TKI and a FLT3xCD3 antibody. In particular, the combinatorial effectiveness in eradicating FLT3-positive AML cells and the impact of the TKI AC220 on T-cell function were assessed.





## 4 Results

---

### 4.1 Clonal heterogeneity of FLT3-ITD detected by high-throughput amplicon sequencing correlates with adverse prognosis in acute myeloid leukemia

---

*Accepted: June 19, 2018 - Oncotarget*

**Clonal heterogeneity of *FLT3*-ITD detected by high-throughput amplicon sequencing correlates with adverse prognosis in acute myeloid leukemia**

Katrin Schranz<sup>1,2,3,4\*</sup>, Max Hubmann<sup>2\*</sup>, Egor Harin<sup>2</sup>, Sebastian Vosberg<sup>1,2,3,4</sup>, Tobias Herold<sup>2,3,4</sup>, Klaus H. Metzeler<sup>1,2,3,4</sup>, Maja Rothenberg-Thurley<sup>2,3,4</sup>, Hanna Janke<sup>2</sup>, Kathrin Bräundl<sup>2,3,4</sup>, Bianka Ksienzyk<sup>2</sup>, Aarif M. N. Batcha<sup>5</sup>, Sebastian Schaaf<sup>5</sup>, Stephanie Schneider<sup>2,6</sup>, Stefan K. Bohlander<sup>7</sup>, Dennis Görlich<sup>8</sup>, Wolfgang E. Berdel<sup>9</sup>, Bernhard J. Wörmann<sup>10</sup>, Jan Braess<sup>11</sup>, Stefan Krebs<sup>12</sup>, Wolfgang Hiddemann<sup>1,2,3,4</sup>, Ulrich Mansmann<sup>5</sup>, Karsten Spiekermann<sup>1,2,3,4</sup>, Philipp A. Greif<sup>1,2,3,4</sup>

1 Experimental Leukemia and Lymphoma Research, Department of Medicine III, University Hospital, LMU Munich, Munich, Germany

2 Laboratory for Leukemia Diagnostics, Department of Medicine III, University Hospital, LMU Munich, Munich, Germany

3 German Cancer Consortium (DKTK), partner site Munich, Germany

4 German Cancer Research Center (DKFZ), Heidelberg, Germany

5 Department of Medical Data Processing, Biometrie and Epidemiology (IBE), LMU Munich, Munich, Germany

6 Institute of Human Genetics, University Hospital, LMU Munich, Munich, Germany

7 Leukaemia and Blood Cancer Research Unit, Department of Molecular Medicine and Pathology, Faculty of Medical and Health Sciences, University of Auckland, Auckland, New Zealand

8 Institute of Biostatistics and Clinical Research, University of Münster, Münster, Germany

9 Department of Medicine A, Hematology and Oncology, University of Münster, Münster, Germany

10 German Society of Hematology and Oncology, Berlin, Germany

11 Department of Hematology and Oncology, Barmherzige Brüder Hospital, Regensburg, Germany

12 Laboratory for Functional Genome Analysis, Gene Center, LMU Munich, Munich, Germany

\*These authors contributed equally.

Correspondence:

Philipp A. Greif

Max-Lebsche-Platz 30

81377 Munich, Germany

Phone: +49 89 4400 43982

FAX: +49 89 4400 43970

Philipp.Greif@med.uni-muenchen.de; p.greif@dkfz-heidelberg.de

Key Words: acute myeloid leukemia (AML), fms-related tyrosine kinase 3 (*FLT3*), internal tandem duplication (ITD), next generation sequencing (NGS), fragment analysis

Conflicts of Interest: The authors have no conflict of interest to declare.

Total number of figures and tables: 12

## ABSTRACT

In acute myeloid leukemia (AML), internal tandem duplications (ITDs) of *FLT3* are frequent mutations associated with unfavorable prognosis. At diagnosis, the *FLT3*-ITD status is routinely assessed by fragment analysis, providing information about the length but not the position and sequence of the ITD. To overcome this limitation, we performed cDNA-based high-throughput amplicon sequencing (HTAS) in 250 *FLT3*-ITD positive AML patients, treated on German AML Cooperative Group (AMLCG) trials. *FLT3*-ITD status determined by routine diagnostics was confirmed by HTAS in 242 out of 250 patients (97%). The total number of ITDs detected by HTAS was higher than in routine diagnostics (n=312 vs. n=274). In particular, HTAS detected a higher number of ITDs per patient compared to fragment analysis, indicating higher sensitivity for subclonal ITDs. Patients with more than one ITD according to HTAS had a significantly shorter overall and relapse free survival. There was a close correlation between *FLT3*-ITD mRNA levels in fragment analysis and variant allele frequency in HTAS. However, the abundance of long ITDs ( $\geq 75$ nt) was underestimated by HTAS, as the size of the ITD affected the mappability of the corresponding sequence reads. In summary, this study demonstrates that HTAS is a feasible approach for *FLT3*-ITD detection in AML patients, delivering length, position, sequence and mutational burden of this alteration in a single assay with high sensitivity. Our findings provide insights into the clonal architecture of *FLT3*-ITD positive AML and have clinical implications.

## INTRODUCTION

Mutations in the fms-related tyrosine kinase 3 (*FLT3*) gene are prevalent in newly diagnosed acute myeloid leukemia (AML) cases, affecting up to 39% patients. Internal tandem duplications (ITDs) represent the most common type of *FLT3* mutation, being most frequent in patients with normal karyotype (cytogenetically normal AML, CN-AML) and in patients positive for the translocation t(6;9)(p23;q34) or t(15;17)(q22;q21) [1-4]. *FLT3*-ITD is associated with an unfavorable prognosis due to reduced duration of complete remission (CR), shorter event free survival (EFS) and shorter overall survival (OS) [1, 5-7]. The European Leukemia Net included the *FLT3*-ITD mutation as prognostic risk factor into a clinical risk-stratification that may guide physicians in therapy decisions [8, 9]. Patients carrying *FLT3*-ITD mutations with high allelic ratio benefit from a more intensive consolidation treatment such as allogeneic stem cell transplantation [7, 10-12]. Since the recent approval of the tyrosine kinase inhibitor (TKI) Midostaurin in combination with induction chemotherapy, *FLT3*-mutated patients may profit from this targeted treatment. [13-15] *FLT3*-ITDs are predominately located in exon 14 and 15, affecting the juxtamembrane domain (JM) and tyrosine kinase domain 1 (TKD1) of the *FLT3* receptor [16]. Depending on the *FLT3*-ITD insertion site and respective functional domain, differential outcome and response to treatment with conventional chemotherapy as well as TKIs were observed; especially non-JM ITDs displayed a resistance to TKIs [10, 16-21]. Although always leading to an in-frame transcript, *FLT3*-ITDs vary in length (between three to over 400 nucleotides (nt)) and sequence [1, 2, 4, 6, 17, 22, 23]. Whether the ITD length has an impact on outcome remains controversial [1, 22, 24, 25]. However, a prognostic relevance was observed for the mutant to wild-type (WT) allelic ratio which corresponds to the size of the clone(s) with the *FLT3*-ITD. A high allelic burden is associated with poor prognosis (shorter OS, EFS), and outcome is even worse for patients with a loss of WT *FLT3* [1, 4, 6, 16, 17, 26-29]. Additionally, up to five distinct clones with different *FLT3*-ITDs were observed per patient [16]. In light of these findings, the assessment of *FLT3*-ITD characteristics is of important

prognostic value. In routine diagnostics, the *FLT3*-ITD status is assessed by capillary electrophoresis of PCR-amplified cDNA (hereafter referred to as ‘fragment analysis’) [26]. However, this assay only provides the length but not the position and the sequence of the insertion. Therefore, it is attractive to overcome these methodological limitations by the use of high-throughput amplicon sequencing (HTAS) as an alternative strategy for *FLT3*-ITD detection. Techniques based on next generation sequencing (NGS) have the potential to assess multiple parameters simultaneously with scalable sensitivity [27, 30-32]. Previous studies already highlighted the potential of *FLT3*-ITD detection by NGS, especially with regards to diagnosis and disease monitoring, e.g. minimal residual disease (MRD) detection, as evaluation of treatment response and early detection of relapse [16, 17, 27, 30-34]. Establishment of NGS assays in diagnostic routine requires high sensitivity at low costs as well as fast turn around time and reliable results. To evaluate the applicability and accuracy of NGS-based *FLT3*-ITD detection for routine diagnostics, we compared *FLT3*-ITD detection by HTAS and fragment analysis in 250 adult *FLT3*-ITD positive AML patients.

## RESULTS

### HTAS reliably identifies *FLT3*-ITD subclones of prognostic relevance

For our comparative analysis we selected 250 AML patient samples obtained at initial diagnosis, all *FLT3*-ITD positive according to routine diagnostics (Figure 1), as well as 17 *FLT3*-ITD negative AML samples. All patients were treated on AMLCG trials (AMLCG 1999 [35], AMLCG 2004 [36] or AMLCG 2008 (ClinicalTrials.gov identifier: NCT01382147)) and received an intensive, high-dose cytarabine based induction therapy. The study cohort included patients with all cytogenetic aberrations and was not restricted to patients under the age of 60 years (Table 1). Performing HTAS, we sequenced the same *FLT3*-ITD mutational hot-spot region as covered by cDNA fragment analysis using identical primer sites in both assays (Figure 2 and Table 2). The output of both methods is shown by an exemplary patient in Figure 3. Overall, HTAS detected a total of 312 *FLT3*-ITDs in 242 of 250 *FLT3*-ITD positive patients (97%), compared to 274 ITDs detected by fragment analysis (Supplementary Table S1). The median length of ITD measured by HTAS was 51 nt (range: 12-175 nt) at a median allele frequency of 12.2% (range: 0.5-91.1%). By fragment analysis, the median ITD length was 54 nt (range: 15-153 nt) at a median *FLT3*-ITD mRNA level of 0.40 (range: 0.01 – 0.96). In 11 patients, we observed differences in length between HTAS and routine assays (fragment analysis or Sanger sequencing using cDNA template) with a median variation in length of 6 nt (range: 1-45 nt; median ITD size: 66 nt, range: 12-90 nt; n=11/242; 5%). Validation of the insertion length on the genomic level by targeted sequencing and/or fragment analysis of amplified gDNA confirmed either the results from HTAS or diagnostic routine, each in about half of the cases (Supplementary Table S2). In paired samples (HTAS and Sanger sequencing, n=182), we found identical insertion sites of the dominant ITD in all patients. The highest number of *FLT3*-ITDs was detected in the zipper motif of the JM, followed by the  $\beta$ 1-sheet of the TKD1 and then the hinge region of the JM (Figure 4). Neither the insertion site nor the length of ITDs showed any significant correlations with clinical outcome (OS, RFS, and CR rate; Supplementary Table S3 and S4). In contrast to other

studies [16, 37], patients with ITDs in the TKD1 did not show worse clinical outcome compared to patients with ITDs in the JM domain (Supplementary Figure S1). Using HTAS, one ITD was detected in 190 (78.5%) patients, two ITDs were detected in 40 patients (16.5%), three ITDs were detected in nine patients (3.75%) and four ITDs were detected in three patients (1.2%; Figure 5a). In eight patients, who were tested *FLT3*-ITD positive in diagnostic routine, no ITD was detected by HTAS at a VAF above the detection limit (0.5%). However, in four of these eight patients, HTAS detected an ITD consistent with routine results regarding length and position at a VAF below the cut-off. According to routine, another two of these eight patients had each a deletion (three and ten nucleotides) neighbouring or within the ITD. For the remaining two patients, no information about the *FLT3*-ITD mutational burden (*FLT3*-ITD mRNA level) was available from routine diagnostics. Furthermore, HTAS missed eight subclonal ITDs each in one patient reported by routine diagnostics, including three with a length >75 nt (median *FLT3*-ITD mRNA level: 0.09, range: 0.06-0.25), while 46 additional subclonal ITDs were detected in 34 patients by HTAS only (median VAF: 1.79%, range: 0.50-19.21%; median ITD-supporting reads: 1759, range: 460-23878). The distribution of ITDs over *FLT3* domains was the same in HTAS and Sanger sequencing with regards to the dominant clone (Supplementary Figure S2). Out of the 46 additional *FLT3*-ITD clones by HTAS 38 (83%) were validated, ten of which displayed differences in length compared to the genomic level (targeted sequencing and / or fragment analysis with gDNA template; Supplementary Table S5). Overall, HTAS detected more ITDs per patient (mean: 1.27, range: 1-4) compared to fragment analysis (mean: 1.14, range: 1-3; Figure 5b). In contrast to fragment analysis, HTAS revealed a significantly shorter OS and RFS for patients with more than one ITD (HTAS: p-value (OS): 0.038 , p-value (RFS): 0.042; fragment analysis: p-value (OS): 0.230, p-value (RFS): 0.157; compare Figure 6 a and b versus c and d). However, the CR rate did not show any obvious correlation with the number of detected ITDs (data not shown). A multivariate analysis, including *NPM1* mutation status, karyotype and number of *FLT3*-ITD mutations per patient (single versus multiple), did not show significant correlations with clinical outcome (Supplementary Table S6). However,

there was a trend for longer RFS associated with single *FLT3*-ITD mutations detected by HTAS (p-value: 0.057). A serial dilution of cDNA derived from the heterozygous *FLT3*-ITD positive cell line MOLM-13 in cDNA derived from the *FLT3*-WT cell line HL60 analysed by both methods confirmed higher sensitivity of HTAS ( $10^{-3}$ , ITD-supporting reads: 58-73 with a coverage of 79,376x to 93,019x) in a 96 sample-setting as compared to fragment analysis ( $10^{-1}$ , Figure 7). Out of 17 control patients which were *FLT3*-ITD negative according to routine diagnostics, HTAS detected a very small subclonal ITD (VAF: 0.58%) in one patient (UPN C-1; Supplementary Table S1). This subclone could not be validated by gDNA-based fragment analysis (Supplementary Table S5).

#### **HTAS reliably detects small and intermediate insertions but underestimates the mutational burden of long *FLT3*-ITDs**

The VAF in HTAS showed a strong correlation with the mutational burden detected by fragment analysis (Pearson: 0.758, p-value: 0.001, n=220; Figure 8). Consistent with previous reports [26, 38], high *FLT3*-ITD mRNA levels (>0.5) measured by fragment analysis showed a significant correlation with shorter relapse-free survival (RFS) and overall survival (OS) (Supplementary Figures S3a and S3b). This correlation could also be observed for *FLT3*-ITD levels by HTAS for RFS and as trend for OS (Supplementary Figures S3c and S3d). Given that the *FLT3*-ITD/*FLT3*-WT ratio based on the sum of all ITD clones is recommended by the ELN for standard of care [8], we calculated the total *FLT3*-ITD mutational burden per patient. Adding the mutational *FLT3*-ITD burden of ITD subclones increased the significance of the correlations between ITD load and outcome (Supplementary Figures S4a-c). This was also evident in multivariate analysis (Supplementary Table S6). A total *FLT3*-ITD mRNA load below 50% was an independent favorable prognostic factor for outcome measured by fragment analysis for both RFS (p-value: 0.005) and OS (p-value: 0.020). For HTAS a low ITD mutation load correlated significantly with longer RFS in multivariate analysis (p-value: 0.025).



193 The VAF levels of *FLT3*-ITD measured by HTAS were up to 5-times lower than the *FLT3*-ITD  
194 mRNA level measured by fragment analysis. Interestingly, the difference in mutational  
195 burden between HTAS and fragment analysis increased with ITD length irrespective of clonal  
196 dominance (Spearman: 0.530, p-value: 0.001, n=220; Supplementary Figures S5a and S5b).  
197 Using HTAS, long ITDs were detected on average with lower VAF compared to short ITDs  
198 (Supplementary Figure S5c, Spearman: -0.249, p-value: 0.001, n=312), while fragment  
199 analysis measured *FLT3-ITD* mRNA levels more accurately, regardless of ITD length, with  
200 only a minor decrease for long ITDs (Supplementary Figure S5d; Spearman: -0.054, p-value:  
201 0.418, n=228). In HTAS, the number of ITD-supporting reads was negatively correlated with  
202 ITD length, while the total number of reads was similar in short and long ITDs (Pearson:  
203 0.309, p-value: 0.001, n=242). This correlation is likely due to the fact that long ITDs were  
204 more difficult to map to the reference sequence. Samples harbouring ITDs with a length <75  
205 nt showed significantly fewer unmapped reads compared to samples harbouring ITDs with a  
206 length >75 nt (Mann-Whitney-U test, p-value: <0.001; Figure 9). The ITD position was also  
207 related to the difference in mutational burden between HTAS and fragment analysis  
208 (Supplementary Figure S6), with longer insertions at cDNA nucleotide positions encoding C-  
209 terminal domains of *FLT3* (Spearman: 0.536, p-value: 0.001, n=312; Supplementary Figure  
210 S7). Validation of ITDs using gDNA in 43 patient samples furthermore revealed differences in  
211 the *FLT3*-ITD levels from those measured using cDNA in several cases. Besides the  
212 underestimation of the mutational burden for long ITDs by HTAS, discrepancies might be  
213 attributed to transcriptional imbalance favouring either the WT or the ITD allele. Overall and  
214 in line with published data [23, 39], *FLT3*-ITD levels measured by HTAS with cDNA template  
215 showed a strong correlation with the genomic levels measured by fragment analysis  
216 (Spearman: 0.846, p-value: <0.001, n=86 ITDs; Supplementary Figure S8a) and targeted  
217 haloplex sequencing (Spearman: 0.752, p-value: <0.001, n=41 ITDs, Supplementary Figure  
218 S8b). Comparison of genomic and transcriptional *FLT3*-ITD levels measured by fragment  
219 analysis excluded gross methodological differences. However, the distribution pointed  
220 towards a transcriptional imbalance in favour of the ITD allele, consistent with a moderate

correlation (Spearman: 0.554, p-value: <0.001, n=40 ITDs, Supplementary Figure S8c). Internal cell line controls were sequenced in each of the four instrument runs. The *FLT3*-ITD positive cell line MOLM-13 displayed the expected *FLT3*-ITD (size: 21 nt; cDNA position: 1774) [40]. Comparison of the mutational burden in the heterozygous *FLT3*-ITD positive cell line MOLM-13 between instrument runs revealed a lower experimental variance in HTAS (0.17%, mean VAF  $\pm$  standard deviation:  $49.24 \pm 0.36$ ) compared to fragment analysis (4.92%, mean *FLT3*-ITD mRNA level  $\pm$  standard deviation:  $0.49 \pm 0.02$ ; Supplementary Figure S9), indicating high inter-run reproducibility and accuracy of HTAS.

### ***FLT3*-ITD detection by HTAS requires controls to exclude ITD artifacts**

We detected ITD artifacts, which were present in the negative control cell line HL60 and the *FLT3*-ITD negative patient samples, at VAF levels below our cut-off of 0.5% (Supplementary Table S7). By manual inspection, these two ITD artifacts were therefore excluded from the analysis, even if occurring in patient samples at VAFs above the cut-off of 0.5%. This applied for the artifact ITD at cDNA position 1712 in 148 (61%) of analysed samples (median VAF: 0.99%; range: 0.5 – 4.71%). Furthermore, we identified and excluded a second ITD artifact within the primer region (cDNA position: 1831-1848), occurring at reference cDNA position 1837 exclusively. This ITD artifact occurred as subclone in 36 patients (15%), at a median VAF of 0.93% (range: 0.5-3.71%) and a median size of 68 nt (range: 35-107 nt). These ITD artifacts showed high sequence similarity to the ITD of the predominant clone, however, they were one nt shorter and displayed 1/20 of the VAF of the original *FLT3*-ITD (median length: 69 nt, range: 36-108 nt; median VAF: 20.57%, range: 6.38-79.49%, example shown in Supplementary Table S7). Thus, this points towards a PCR-based mispriming event, similar to those reported for false-positive calls in multiplex PCR-based NGS approaches [41].

### **Mutations in other genes do not correlate with ITD position, length or clonality**

Individual patients were evaluated for mutations in *NPM1*, *CEBPA*, *KIT*, *IDH1/2* and *KMT2A*-PTD. One hundred nineteen of 182 patients (65%) were positive for an *NPM1* mutation, nine

out of 112 patients (8%) were positive for a *CEBPA* mutation (three *CEBPA*-double positive), two out of 164 (1%) were positive for a *KIT* mutation, 14 out of 75 (19%) were positive for a *IDH1/2* mutation, 19 out of 233 patients (8%) were positive for a *KMT2A*-PTD mutation. A point mutation in the TKD of *FLT3* was found in six out of 208 patients (3%). Other mutations, in amongst others *NRAS* and *RUNX1*, occurred in up to four patients per affected gene. There was no correlation of *FLT3*-ITD clonality with other co-occurring mutations (Supplementary Figure S10). Mutations were equally distributed between the patients when clustered according to *FLT3* domains (Table 3). Neither length nor position of *FLT3*-ITD correlated with the co-occurrence of other mutations. In agreement with published results [42], *NPM1* mutations correlated with better clinical outcome in our study cohort (Supplementary Figure S11). Patients positive for *FLT3*-ITD and *NPM1* mutation had a significantly increased RFS compared to *FLT3*-ITD positive and *NPM1* negative patients (p-value: 0.049). For OS, a similar trend with borderline significance was observed. In line with published results [35, 43-45], an *NPM1* mutation remained an independent favorable prognostic factor in multivariate analysis (Supplementary Table S6). In contrast, the other evaluated mutations did not show any correlations with clinical outcome in our *FLT3*-ITD positive study cohort.

## DISCUSSION

In this study, we report the comparison of two different methods to detect *FLT3*-ITD mutations in 250 adult *FLT3*-ITD positive AML patients. Since *FLT3*-ITD parameters, including position and mutational burden, are of clinical relevance for risk stratification and therapy decision [1, 6, 9, 10, 16, 26, 46], a fast and reliable detection method for routine diagnostics is essential. Therefore, we established a high-throughput *FLT3*-ITD amplicon sequencing assay to gain information complementary to the results from routine fragment analysis. Although HTAS identified nearly all dominant ITD clones that were detected by routine diagnostics, we encountered technical limitations consistent with previous studies investigating smaller cohorts [47, 48]. In particular, we found methodological differences between HTAS and fragment analysis with respect to ITD length and the quantification of the *FLT3*-ITD mutational burden. In 5% of our patients the ITD length differed when comparing HTAS and fragment analysis results. In contrast to other studies with lower patient numbers [16, 22, 29], the ITD length and position did not correlate with clinical outcome in our study. Concordant with other reports [16, 17, 49, 50], the presence of ITDs with high mutational burden correlated with worse prognosis. In multivariate analysis, the *FLT3*-ITD level below 50% was an independent favorable prognostic factor. In our study, HTAS revealed more subclonal ITDs compared to fragment analysis and the additional clonal complexity uncovered by HTAS correlated with adverse clinical outcome. In line with our findings, it was recently shown that the number of driver mutations has prognostic relevance in MDS and AML [3, 51, 52]. It has already been suggested by others to consider the number of *FLT3*-ITD clones per patient for prognostic stratification [38, 49, 53]. Whereas in our analysis the *FLT3*-ITD clonality (single versus multiple) did not reach statistical significance in multivariate analysis, we observed a trend for better outcome associated with single alterations when evaluated by HTAS. Although the scalable sensitivity of NGS approaches based on read depth seems attractive, the sensitivity might be limited by false-positive variant calls as observed in the present study. Therefore, the implementation of appropriate negative

controls is essential. Moreover, NGS data has to be analyzed carefully to identify and to exclude ITD artifacts as detected at cDNA position 1837 in more than 15% of our patients.

Besides clonality, another important prognostic parameter is the *FLT3*-ITD mutational burden. Although there was a significant correlation between *FLT3*-ITD mRNA level detected by fragment analysis and variant allele frequency by HTAS, the prognostic relevance of *FLT3*-ITD mutational burden was more pronounced when considering the results from fragment analysis. Of note, in fragment analysis the *FLT3*-ITD mRNA levels were up to five-fold higher for patient samples compared to the VAF determined by HTAS. Consistent with results from a study utilizing Pindel software as well as a custom de-novo assembly approach for *FLT3*-ITD detection [54], we found that HTAS underestimated the *FLT3*-ITD mRNA levels of long ITDs, which are less likely to be mapped correctly compared to shorter ITDs. In our study, ITDs with a length of more than 75 nt showed inappropriate mapping to the reference sequence. Interestingly, ITD detection by Pindel was recently shown to be dependent on the length and on the relative position of the amplicon [47]. Thus, algorithms for read mapping and variant detection are currently limiting the detection of long ITDs. This limitation might be overcome with increasing read length, as in the present study 2x250 bp paired-end reads did not provide sufficient bi-directional coverage of long ITDs. Since the *FLT3*-ITD/*FLT3*-WT ratio, which is of prognostic value [4, 26, 28, 38, 49, 55], is currently measured more accurately by fragment analysis, ITD quantification by HTAS needs to be further optimized. On the other hand, detection of ITD subclones by NGS-based approaches with increased sensitivity contributes to the total *FLT3*-ITD mutational burden and thus increases the *FLT3*-ITD/*FLT3*-WT ratio. Superior sensitivity of NGS is also relevant for MRD monitoring in leukemia patients. In our serial dilution, HTAS reached a sensitivity of  $10^{-3}$  for the heterozygous *FLT3*-ITD positive cell line MOLM-13, in a multi-sample sequencing setting of 96 samples per run, being superior to fragment analysis. Since sensitivity and coverage is scalable, depending on the number of samples per run, a higher sensitivity can be achieved, if required, as shown by others [30]. Although *FLT3*-ITD is a rather variable marker during

therapy and disease progression, with mutational plasticity between diagnosis and relapse [56-59], several studies [27, 30, 33] have pointed out the advantages of NGS approaches for *FLT3*-ITD MRD assessment over conventional diagnostic applications. Especially, the recently approved TKI treatment with Midostaurin in combination with induction chemotherapy for *FLT3*-mutated AML [13] requires the reliable reveillance of *FLT3* mutations for initial risk assessment, monitoring and therapeutic intervention. In a recent study, *FLT3*-mutation positive relapsed or refractory AML CHRYSALIS Phase I/II study patients were analysed for their TKI-response to Gilteritinib (ASP2215; clinical trail number: NCT02014558 [60]). Interestingly, the clinical response correlated with the post-treatment *FLT3*-ITD MRD levels, evaluated by NGS [61]. In addition, the identification of the ITD position by NGS approaches might be of prognostic relevance considering the impact of *FLT3*-ITD insertion site on therapy resistance and outcome – for conventional chemotherapy as well as for TKI treatment [10, 16-21]. However, the clinical relevance of ITD position still remains controversial [22, 24, 25, 38]. Furthermore, newly arising *FLT3* point mutations during clonal evolution, as for example D835Y and D835G, have prognostic impact as being capable of mediating TKI resistance [33]. Thus, reads spanning the *FLT3* regions JM to TKD2 should be used in future approaches as sequence read length steadily increases. With multiple parameters obtained from a single assay and hands-on time for sample preparation and analysis similar to *FLT3*-ITD fragment analysis or Sanger sequencing, NGS techniques become more and more attractive for diagnostic laboratories. Down-scaling of our 96-sample setting according to the needs in diagnostic routine is feasible when using recently introduced scalable sequencing instruments and reagents. HTAS may enable more precise therapy decisions based on the detection of small ITD clones and has a strong pontential for monitoring of *FLT3*-directed interventions.

In summary, our study demonstrates the feasibility of HTAS for *FLT3*-ITD detection in AML. We show that the sensitive *FLT3*-ITD subclone detection by HTAS is of prognostic relevance and has the potential to shed light on the clonal architecture of AML. However, the detection

346 of long ITDs and the detection of ITDs in combination with deletions remain challenging.  
347 Increasing read length as well as improving variant detection algorithms will likely help to  
348 overcome these limitations. After methodological improvement, HTAS may serve as a robust  
349 and sensitive tool that could be implemented in future diagnostic routines, essential for a  
350 rapid risk stratification and therapeutic intervention.

## MATERIALS AND METHODS

**Patient samples.** This study included 267 newly diagnosed patients with AML, of which 250 were *FLT3*-ITD positive according to routine diagnostics (median age: 59, range: 18–80 years; Figure 1). All patients were treated intensively according to the German Acute Myeloid Leukemia Cooperative Group (AMLCG) clinical trial study protocols with curative intent (AMLCG 1999 (ClinicalTrials.gov identifier: NCT00266136) and 2004 as published [35, 36], AMLCG 2008 (n= 38, ClinicalTrials.gov identifier: NCT01382147)), which were approved by the institutional review boards of the participating centers. Patients with acute promyelocytic leukemia (FAB M3) were not treated on these trials, and therefore not analysed in our study. Informed written consent was obtained from all patients in accordance with the Declaration of Helsinki. According to the ELN-classification [9] patients clustered into the following groups: intermediate I (70%), intermediate II (21%) or adverse (9%). A normal karyotype was observed in 70%, while 30% had a complex aberrant karyotype. After intensive induction chemotherapy, 142 (56.8%) patients achieved CR, 16 (6.6%) patients achieved CRi, while 34 (13.6%) patients had refractory disease, 35 (14.0%) patients died during induction therapy, and for 23 (9.1%) patients no remission status was available. Hematopoietic stem cell transplantation in first CR was performed in 36 (14.4%) patients. After a median follow-up of 50 months (range: 0–136), 97 (68.3%) patients that had reached CR eventually relapsed and 187 (74.8%) of all patients died. The median RFS and OS observed were seven and nine months, respectively. The two-year rates of RFS and OS were 20.0% and 25.2%, respectively. Samples were collected at the University Hospital LMU Munich at the time point of first diagnosis. Mononuclear cells were isolated from bone marrow aspirates or peripheral blood and subjected to routine diagnostics for conventional cytogenetic and routine mutational analysis of known molecular markers, including *NPM1*, *CEBPA* and *FLT3*-ITD, according to standard protocols [2, 26, 35, 62]. Patient characteristics and clinical parameters are provided in Table 1.



**Cell lines.** All cell lines were purchased from the German Collection of Microorganisms and Cell Culture (DSMZ, Braunschweig, Germany), with certified cell authentication using karyotyping and fluorescent in-situ hybridization, immunophenotyping, and testing of cancer-type specific mutations using RT-PCR analyses [63, 64]. AML cell lines positive for *FLT3*-ITD (MOLM-13, ACC-554) and negative for *FLT3*-ITD (HL60, ACC-3) were cultivated according to the supplier's recommendations. Cell lines were tested for a mycoplasma contamination on a regular basis (MycoAlert Mycoplasma Detection Kit, Lonza Rockland Inc., Rockland, ME, USA).

**DNA and RNA isolation.** Extraction of DNA and RNA was performed using standard procedures. Per sample five million cells were used for DNA or RNA isolation each. gDNA and total RNA were extracted using the QIAamp DNA Mini Kit (51106, Qiagen) or RNeasy Mini Kit (74106, Qiagen, Hilden, Germany), respectively, utilizing a QIAcube (Qiagen) according to the suppliers' recommendations. Purity of isolated RNA and DNA was verified by absorbance measurements (260/280 ratios) with a Nanodrop instrument (PepLab Biotechnology, Erlangen, Germany).

**cDNA synthesis.** cDNA synthesis was performed by reverse transcription (RT) using total RNA extracted out of five million cells, the Superscript II Reverse Transcriptase and corresponding buffer (18064071, Invitrogen – ThermoFisher Scientific, Munich, Germany), 100 mM dNTPs Set (10297-117, Invitrogen – ThermoFisher Scientific), 25  $\mu$ M Random Primer p(ND)6 (1034731, Roche Diagnostics, Penzberg, Germany) and RNase Inhibitor (N2615, Promega, Mannheim, Germany). Reactions were performed on a thermocycler (PepLab Biotechnology), according to the technical protocol of the Superscript II Reverse Transcriptase (70°C 10 min, 37°C 120 min and 90°C 5 min, 1 cycle each).

***FLT3*-ITD fragment analysis.** For fragment analysis, PCR (amplification for 28 cycles –1 min 95°C, 1 min 60°C, 1 min 72°C) with 1  $\mu$ L patient or cell line cDNA or gDNA (10 ng/ $\mu$ L) template, respectively, was performed in a 25  $\mu$ L reaction volume to amplify *FLT3*, utilizing

fluorescently-labelled primers (10 pmol each, Table 2, Metabion, Planegg, Germany) as published [65, 66] and the *Taq* PCR Master Mix (201445, Qiagen). Thereafter, 0.5  $\mu$ L fragment-length standard (GeneScan (500) ROX Size Standard, 401734, Applied Biosystems, Foster City CA, USA) and 13.5  $\mu$ L PCR-grade water were added to 1  $\mu$ L PCR-product. After initial denaturation of this mixture at 95°C, size-separation by capillary electrophoresis was performed on a Genetic Analyzer 3500xl (Applied Biosystems) using the separation matrix POP-6 polymer (4316357, Applied Biosystems). Data analysis was performed using the Gene-Mapper software (Version 3.5, Thermo Fisher Scientific). *FLT3*-ITD mutational burden (*FLT3*-ITD mRNA level respectively) was calculated based on the WT to ITD ratio equation as previously published [26]. Comparative analysis of detected ITDs was based on cDNA fragment analysis, whilst gDNA fragment analysis, referred to as g(F), was performed as validation.

***FLT3* amplification and Sanger sequencing.** For Sanger sequencing PCR (amplification for 35 cycles – 1 min 95°C, 1 min 60°C, 1 min 72°C) with 1  $\mu$ L patient cDNA template was performed in a 25  $\mu$ L reaction volume to amplify *FLT3*, using the *FLT3* primers 11F and 12R (10 pmol each, sequence as described [65]) and *Taq* PCR Master Mix (201445, Qiagen). After PCR-product purification with the Qiaquick PCR Purification Kit (28106, Qiagen), bidirectional sequencing was performed with a second round of amplification using the Big Dye Terminator v1.1 kit (4337451, Life Technologies) and the *FLT3* primer 11F and 12R (10 pmol each, sequence as described [65]). Samples were purified using the CentriSep 8 solution and Columns (CS-912, Princeton Separations) and subsequently sequenced using a Genetic Analyzer 3500xl (Applied Biosystems) according to the manufacturers' instructions. Chromatograms were analyzed using Sequencher Software 5.1 (Gene Codes Cooperation, MI, USA) and the *FLT3* cDNA reference sequence (NM\_004119.2).

**High-throughput *FLT3*-ITD amplicon sequencing (HTAS) and genomic targeted sequencing.** In case of HTAS, *FLT3* amplicons were generated performing PCR (TD58, amplification for 30 cycles – 30 sec 95°C, 30 sec 58°C, 1 min 72°C) with 1  $\mu$ L cDNA template

in a 25  $\mu$ L reaction volume, using the *Taq* PCR Master Mix Kit (201445, Qiagen) and custom-designed *FLT3* cDNA primers (10 pmol each, Table 2). The *FLT3* cDNA primers, spanning the mutational hotspot region (spanning 366 base-pairs (bp)), included a barcode and Illumina-specific adapter-sequences (Supplementary Table S8), enabling a one-step PCR-protocol for barcoded *FLT3*-targeted amplification and multiplex-sequencing. As controls, cDNA from *FLT3*-ITD positive (MOLM-13) and negative (HL60) human cell lines were amplified. Correct amplicon fragment size was verified by agarose gel-electrophoresis. The PCR-product was purified utilizing NucleoFast 96 PCR clean-up plates (743100, Machery-Nagel, Düren, Germany) according to the manufacturers' instructions. DNA concentration was measured using the Quant-iT dsDNA Broad Range High Sensitivity Kit (Q33120, Thermo Fisher Scientific) in compliance with the manufacturer's protocol, following dilution to a final concentration of 4 nM (4 fmol/ $\mu$ L). Library preparation was performed according to the manufacturers' instructions using the MiSeq Kit v2 500 cycles (MS-102-2003, Illumina, San Diego CA, USA), while adding PhiX control (PhiX Control v3 Kit, FC-110-3001, Illumina) in a ratio 4:1 (800  $\mu$ L library, 200  $\mu$ L PhiX control). Per library, up to 96 samples were pooled, adding 10  $\mu$ L of each 4 nM sample. The cell lines HL60 and MOLM-13 were included in every instrument run, serving as inter-run *FLT3*-WT and *FLT3*-ITD control. Sequencing (2x 250 bp paired end) was performed on a MiSeq Personal Sequencer instrument (Illumina, San Diego CA, USA) in four independent runs, yielding a median of 79,110 reads per amplicon (range: 31,996–259,783). For validation purposes genomic targeted sequencing data, was obtained from a previous study, generated by utilization of an HaloPlex target enrichment system (Agilent Technologies, Santa Clara, USA) as described previously [3].

**Next generation sequencing data analysis.** Raw sequence reads were aligned to the *FLT3* cDNA reference sequence (NM\_004119.2) using BWA [67]. Parameters were adjusted in order to allow the incorporation of long insertions, i.e. minimized gap open and gap extension penalties, maximum number of gap extensions. Analysis of NGS-data was performed using the Galaxy platform [68, 69]. Tandem duplications were called using Pindel

(version 0.2.5a7) [70] with a minimum size of 6 bp and a minimum of 10 supporting reads. Pindel reports left-aligned positions of variants, which is the leftmost possible position of an alteration. As tandem repeats are two identical and consecutive sequences, Pindel reports the starting position of the first sequence (i.e. the 5'-template) by default. In order to indicate the position of the inserted sequence (i.e. the 3'-duplicate), we added the length of the ITD to the position reported by Pindel. Furthermore, the 5'-UTR region (82 nucleotides), included in the *FLT3* cDNA reference sequence, were subtracted from the variant position. Thus, results from HTAS could be compared to results from Sanger sequencing, which refer to the coding sequence. The variant allele frequency (VAF) was computed by dividing the number of supporting reads with the coverage at the insertion site. Minimum cut-off for VAF was set to 0.5% (HTAS), based on empirical analysis of *FLT3*-ITD negative control samples, to exclude any sequencing background noise (non-specific variants). Off-target ITDs and ITDs which appeared in the *FLT3*-WT cell line HL60 were excluded from further analysis. Per sample the median coverage per amplicon was 157,100x (range: 63,890x – 488,300x).

**Statistical analysis.** SPSS (IBM, version 21.0) or R (GNU GPL, version 3.4.1) software was used for statistical analysis. Spearman rank correlation was used to examine correlations between continuous parameters. Two-sided log rank test was used for Kaplan-Meier diagrams to compute survival curves. Mann-Whitney-U test was performed to test for differences between groups. Results were considered as significant with a p-value less than 0.05. Univariate and multivariate Cox-Regression analysis was performed to evaluate prognostic variables for OS and RFS. RFS was calculated from the time span between diagnosis and relapse [9, 71], failure to achieve a complete remission (CR) [35], last follow-up or death. OS was evaluated from initial diagnosis to last follow up or death. The criteria of relapse, resistant disease and CR were assigned according to ELN [9]. Cox proportional hazard model was used to estimate hazard ratios for multivariate analysis.

## **ACKNOWLEDGEMENTS AND FUNDING**

We thank all patients and participating centers of the AMLCG trials. K.H.M., K.S., P.A.G. and W.H. acknowledge support by the German Research Foundation (DFG) within the Collaborative Research Centre (SFB) 1243 "Cancer Evolution" (Projects A06, A07 and A08). This work was supported by the Wilhelm-Sander-Stiftung (2013.086.2) to T.H. The statistical analysis was funded partly by the Jose Carreras Foundation (DJCLS H 09/01f, to DG). S.K.B. is supported by Leukaemia & Blood Cancer New Zealand and the family of Marijanna Kumerich. Finally, we thank Gudrun Mellert, Jutta Sturm, and Evelyn Zellmeier for technical assistance.

## **CONFLICTS OF INTERESTS**

The authors have no conflict of interest to declare.

- 496 1. Mrozek K, Marcucci G, Paschka P, Whitman SP, Bloomfield CD. Clinical relevance  
497 of mutations and gene-expression changes in adult acute myeloid leukemia with normal  
498 cytogenetics: are we ready for a prognostically prioritized molecular classification? *Blood*.  
499 2007; 109: 431-48. doi: 10.1182/blood-2006-06-001149.
- 500 2. Schnittger S, Schoch C, Dugas M, Kern W, Staib P, Wuchter C, Löffler H, Sauerland  
501 CM, Serve H, Buchner T, Haferlach T, Hiddemann W. Analysis of FLT3 length mutations in  
502 1003 patients with acute myeloid leukemia: correlation to cytogenetics, FAB subtype, and  
503 prognosis in the AMLCG study and usefulness as a marker for the detection of minimal  
504 residual disease. *Blood*. 2002; 100: 59-66. doi:
- 505 3. Metzeler KH, Herold T, Rothenberg-Thurley M, Amler S, Sauerland MC, Gorlich D,  
506 Schneider S, Konstandin NP, Dufour A, Braundl K, Ksienzyk B, Zellmeier E, Hartmann L, et  
507 al. Spectrum and prognostic relevance of driver gene mutations in acute myeloid leukemia.  
508 *Blood*. 2016; 128: 686-98. doi: 10.1182/blood-2016-01-693879.
- 509 4. Thiede C, Steudel C, Mohr B, Schaich M, Schakel U, Platzbecker U, Wermke M,  
510 Bornhauser M, Ritter M, Neubauer A, Ehninger G, Illmer T. Analysis of FLT3-activating  
511 mutations in 979 patients with acute myelogenous leukemia: association with FAB subtypes  
512 and identification of subgroups with poor prognosis. *Blood*. 2002; 99: 4326-35. doi:
- 513 5. Frohling S, Schlenk RF, Breitnick J, Benner A, Kreitmeier S, Tobis K, Dohner H,  
514 Dohner K, leukemia AMLSGUAm. Prognostic significance of activating FLT3 mutations in  
515 younger adults (16 to 60 years) with acute myeloid leukemia and normal cytogenetics: a study  
516 of the AML Study Group Ulm. *Blood*. 2002; 100: 4372-80. doi: 10.1182/blood-2002-05-  
517 1440.
- 518 6. Levis M, Small D. FLT3: ITDoes matter in leukemia. *Leukemia*. 2003; 17: 1738-52.  
519 doi: 10.1038/sj.leu.2403099.
- 520 7. Levis M. FLT3 mutations in acute myeloid leukemia: what is the best approach in  
521 2013? *Hematology Am Soc Hematol Educ Program*. 2013; 2013: 220-6. doi:  
522 10.1182/asheducation-2013.1.220.
- 523 8. Dohner H, Estey E, Grimwade D, Amadori S, Appelbaum FR, Buchner T, Dombret H,  
524 Ebert BL, Fenaux P, Larson RA, Levine RL, Lo-Coco F, Naoe T, et al. Diagnosis and  
525 management of AML in adults: 2017 ELN recommendations from an international expert  
526 panel. *Blood*. 2017; 129: 424-47. doi: 10.1182/blood-2016-08-733196.
- 527 9. Dohner H, Estey EH, Amadori S, Appelbaum FR, Buchner T, Burnett AK, Dombret  
528 H, Fenaux P, Grimwade D, Larson RA, Lo-Coco F, Naoe T, Niederwieser D, et al. Diagnosis  
529 and management of acute myeloid leukemia in adults: recommendations from an international  
530 expert panel, on behalf of the European LeukemiaNet. *Blood*. 2010; 115: 453-74. doi:  
531 10.1182/blood-2009-07-235358.
- 532 10. Schlenk RF, Kayser S, Bullinger L, Kobbe G, Casper J, Ringhoffer M, Held G,  
533 Brossart P, Lubbert M, Salih HR, Kindler T, Horst HA, Wulf G, et al. Differential impact of  
534 allelic ratio and insertion site in FLT3-ITD-positive AML with respect to allogeneic  
535 transplantation. *Blood*. 2014; 124: 3441-9. doi: 10.1182/blood-2014-05-578070.
- 536 11. Bornhauser M, Illmer T, Schaich M, Soucek S, Ehninger G, Thiede C, group ASs.  
537 Improved outcome after stem-cell transplantation in FLT3/ITD-positive AML. *Blood*. 2007;  
538 109: 2264-5; author reply 5. doi: 10.1182/blood-2006-09-047225.
- 539 12. Ho AD, Schetelig J, Bochtler T, Schaich M, Schafer-Eckart K, Hanel M, Rosler W,  
540 Einsele H, Kaufmann M, Serve H, Berdel WE, Stelljes M, Mayer J, et al. Allogeneic Stem  
541 Cell Transplantation Improves Survival in Patients with Acute Myeloid Leukemia  
542 Characterized by a High Allelic Ratio of Mutant FLT3-ITD. *Biol Blood Marrow Transplant*.  
543 2016; 22: 462-9. doi: 10.1016/j.bbmt.2015.10.023.

13. Rasko JEJ, Hughes TP. First Approved Kinase Inhibitor for AML. *Cell*. 2017; 171: 981. doi: 10.1016/j.cell.2017.11.007.
14. Levis M. Midostaurin approved for FLT3-mutated AML. *Blood*. 2017; 129: 3403-6. doi: 10.1182/blood-2017-05-782292.
15. Stone RM, Mandrekar SJ, Sanford BL, Laumann K, Geyer S, Bloomfield CD, Thiede C, Prior TW, Dohner K, Marcucci G, Lo-Coco F, Klisovic RB, Wei A, et al. Midostaurin plus Chemotherapy for Acute Myeloid Leukemia with a FLT3 Mutation. *N Engl J Med*. 2017; 377: 454-64. doi: 10.1056/NEJMoa1614359.
16. Kayser S, Schlenk RF, Londono MC, Breitenbuecher F, Wittke K, Du J, Groner S, Spath D, Krauter J, Ganser A, Dohner H, Fischer T, Dohner K, et al. Insertion of FLT3 internal tandem duplication in the tyrosine kinase domain-1 is associated with resistance to chemotherapy and inferior outcome. *Blood*. 2009; 114: 2386-92. doi: 10.1182/blood-2009-03-209999.
17. Schnittger S, Bacher U, Haferlach C, Alpermann T, Kern W, Haferlach T. Diversity of the juxtamembrane and TKD1 mutations (exons 13-15) in the FLT3 gene with regards to mutant load, sequence, length, localization, and correlation with biological data. *Genes Chromosomes Cancer*. 2012; 51: 910-24. doi: 10.1002/gcc.21975.
18. Breitenbuecher F, Markova B, Kasper S, Carius B, Stauder T, Bohmer FD, Masson K, Ronnstrand L, Huber C, Kindler T, Fischer T. A novel molecular mechanism of primary resistance to FLT3-kinase inhibitors in AML. *Blood*. 2009; 113: 4063-73. doi: 10.1182/blood-2007-11-126664.
19. Breitenbuecher F, Schnittger S, Grundler R, Markova B, Carius B, Brecht A, Duyster J, Haferlach T, Huber C, Fischer T. Identification of a novel type of ITD mutations located in nonjuxtamembrane domains of the FLT3 tyrosine kinase receptor. *Blood*. 2009; 113: 4074-7. doi: 10.1182/blood-2007-11-125476.
20. Heidel F, Solem FK, Breitenbuecher F, Lipka DB, Kasper S, Thiede MH, Brandts C, Serve H, Roesel J, Giles F, Feldman E, Ehninger G, Schiller GJ, et al. Clinical resistance to the kinase inhibitor PKC412 in acute myeloid leukemia by mutation of Asn-676 in the FLT3 tyrosine kinase domain. *Blood*. 2006; 107: 293-300. doi: 10.1182/blood-2005-06-2469.
21. Fischer M, Schnetzke U, Spies-Weissart B, Walther M, Fleischmann M, Hilgendorf I, Hochhaus A, Scholl S. Impact of FLT3-ITD diversity on response to induction chemotherapy in patients with acute myeloid leukemia. *Haematologica*. 2017; 102: e129-e31. doi: 10.3324/haematol.2016.157180.
22. Stirewalt DL, Kopecky KJ, Meshinchi S, Engel JH, Pogosova-Agadjanyan EL, Linsley J, Slovak ML, Willman CL, Radich JP. Size of FLT3 internal tandem duplication has prognostic significance in patients with acute myeloid leukemia. *Blood*. 2006; 107: 3724-6. doi: 10.1182/blood-2005-08-3453.
23. Schnittger S, Schoch C, Kern W, Hiddemann W, Haferlach T. FLT3 length mutations as marker for follow-up studies in acute myeloid leukaemia. *Acta Haematol*. 2004; 112: 68-78. doi: 10.1159/000077561.
24. Kusec R, Jaksic O, Ostojic S, Kardum-Skelin I, Vrhovac R, Jaksic B. More on prognostic significance of FLT3/ITD size in acute myeloid leukemia (AML). *Blood*. 2006; 108: 405-6; author reply 6. doi: 10.1182/blood-2005-12-5128.
25. Ponziani V, Gianfaldoni G, Mannelli F, Leoni F, Ciolli S, Guglielmelli P, Antonioli E, Longo G, Bosi A, Vannucchi AM. The size of duplication does not add to the prognostic significance of FLT3 internal tandem duplication in acute myeloid leukemia patients. *Leukemia*. 2006; 20: 2074-6. doi: 10.1038/sj.leu.2404368.
26. Schneider F, Hoster E, Unterhalt M, Schneider S, Dufour A, Benthaus T, Mellert G, Zellmeier E, Kakadia PM, Bohlander SK, Feuring-Buske M, Buske C, Braess J, et al. The FLT3ITD mRNA level has a high prognostic impact in NPM1 mutated, but not in NPM1

unmutated, AML with a normal karyotype. *Blood*. 2012; 119: 4383-6. doi: 10.1182/blood-2010-12-327072.

27. Thol F, Kolking B, Damm F, Reinhardt K, Klusmann JH, Reinhardt D, von Neuhoff N, Brugman MH, Schlegelberger B, Suerbaum S, Krauter J, Ganser A, Heuser M. Next-generation sequencing for minimal residual disease monitoring in acute myeloid leukemia patients with FLT3-ITD or NPM1 mutations. *Genes Chromosomes Cancer*. 2012; 51: 689-95. doi: 10.1002/gcc.21955.

28. Whitman SP, Archer KJ, Feng L, Baldus C, Becknell B, Carlson BD, Carroll AJ, Mrozek K, Vardiman JW, George SL, Kolitz JE, Larson RA, Bloomfield CD, et al. Absence of the wild-type allele predicts poor prognosis in adult de novo acute myeloid leukemia with normal cytogenetics and the internal tandem duplication of FLT3: a cancer and leukemia group B study. *Cancer Res*. 2001; 61: 7233-9. doi:

29. Kim Y, Lee GD, Park J, Yoon JH, Kim HJ, Min WS, Kim M. Quantitative fragment analysis of FLT3-ITD efficiently identifying poor prognostic group with high mutant allele burden or long ITD length. *Blood Cancer J*. 2015; 5: e336. doi: 10.1038/bcj.2015.61.

30. Bibault JE, Figeac M, Helevaut N, Rodriguez C, Quief S, Sebda S, Renneville A, Nibourel O, Rousselot P, Gruson B, Dombret H, Castaigne S, Preudhomme C. Next-generation sequencing of FLT3 internal tandem duplications for minimal residual disease monitoring in acute myeloid leukemia. *Oncotarget*. 2015; 6: 22812-21. doi: 10.18632/oncotarget.4333.

31. Luthra R, Patel KP, Reddy NG, Haghshenas V, Routbort MJ, Harmon MA, Barkoh BA, Kanagal-Shamanna R, Ravandi F, Cortes JE, Kantarjian HM, Medeiros LJ, Singh RR. Next-generation sequencing-based multigene mutational screening for acute myeloid leukemia using MiSeq: applicability for diagnostics and disease monitoring. *Haematologica*. 2014; 99: 465-73. doi: 10.3324/haematol.2013.093765.

32. Ilyas AM, Ahmad S, Faheem M, Naseer MI, Kumosani TA, Al-Qahtani MH, Gari M, Ahmed F. Next generation sequencing of acute myeloid leukemia: influencing prognosis. *BMC Genomics*. 2015; 16 Suppl 1: S5. doi: 10.1186/1471-2164-16-S1-S5.

33. Zuffa E, Franchini E, Papayannidis C, Baldazzi C, Simonetti G, Testoni N, Abbenante MC, Paolini S, Sartor C, Parisi S, Marconi G, Cattina F, Bochicchio MT, et al. Revealing very small FLT3 ITD mutated clones by ultra-deep sequencing analysis has important clinical implications in AML patients. *Oncotarget*. 2015; 6: 31284-94. doi: 10.18632/oncotarget.5161.

34. Frohling S, Scholl C, Levine RL, Loriaux M, Boggon TJ, Bernard OA, Berger R, Dohner H, Dohner K, Ebert BL, Teckie S, Golub TR, Jiang J, et al. Identification of driver and passenger mutations of FLT3 by high-throughput DNA sequence analysis and functional assessment of candidate alleles. *Cancer Cell*. 2007; 12: 501-13. doi: 10.1016/j.ccr.2007.11.005.

35. Schnittger S, Schoch C, Kern W, Mecucci C, Tschulik C, Martelli MF, Haferlach T, Hiddemann W, Falini B. Nucleophosmin gene mutations are predictors of favorable prognosis in acute myelogenous leukemia with a normal karyotype. *Blood*. 2005; 106: 3733-9. doi: 10.1182/blood-2005-06-2248.

36. Braess J, Spiekermann K, Staib P, Gruneisen A, Wormann B, Ludwig WD, Serve H, Reichle A, Peceny R, Oruzio D, Schmid C, Schiel X, Hentrich M, et al. Dose-dense induction with sequential high-dose cytarabine and mitoxantone (S-HAM) and pegfilgrastim results in a high efficacy and a short duration of critical neutropenia in de novo acute myeloid leukemia: a pilot study of the AMLCG. *Blood*. 2009; 113: 3903-10. doi: 10.1182/blood-2008-07-162842.

37. Schlenk RF, Dohner K, Krauter J, Frohling S, Corbacioglu A, Bullinger L, Habdank M, Spath D, Morgan M, Benner A, Schlegelberger B, Heil G, Ganser A, et al. Mutations and treatment outcome in cytogenetically normal acute myeloid leukemia. *N Engl J Med*. 2008; 358: 1909-18. doi: 10.1056/NEJMoa074306.



38. Gale RE, Green C, Allen C, Mead AJ, Burnett AK, Hills RK, Linch DC, Medical Research Council Adult Leukaemia Working P. The impact of FLT3 internal tandem duplication mutant level, number, size, and interaction with NPM1 mutations in a large cohort of young adult patients with acute myeloid leukemia. *Blood*. 2008; 111: 2776-84. doi: 10.1182/blood-2007-08-109090.
39. Schnittger S, Bacher U, Kern W, Alpermann T, Haferlach C, Haferlach T. Prognostic impact of FLT3-ITD load in NPM1 mutated acute myeloid leukemia. *Leukemia*. 2011; 25: 1297-304. doi: 10.1038/leu.2011.97.
40. Quentmeier H, Reinhardt J, Zaborski M, Drexler HG. FLT3 mutations in acute myeloid leukemia cell lines. *Leukemia*. 2003; 17: 120-4. doi: 10.1038/sj.leu.2402740.
41. McCall CM, Mosier S, Thiess M, Debeljak M, Pallavajjala A, Beierl K, Deak KL, Datto MB, Gocke CD, Lin MT, Eshleman JR. False positives in multiplex PCR-based next-generation sequencing have unique signatures. *J Mol Diagn*. 2014; 16: 541-9. doi: 10.1016/j.jmoldx.2014.06.001.
42. Hubmann M, Kohnke T, Hoster E, Schneider S, Dufour A, Zellmeier E, Fiegl M, Braess J, Bohlander SK, Subklewe M, Sauerland MC, Berdel WE, Buchner T, et al. Molecular response assessment by quantitative real-time polymerase chain reaction after induction therapy in NPM1-mutated patients identifies those at high risk of relapse. *Haematologica*. 2014; 99: 1317-25. doi: 10.3324/haematol.2014.104133.
43. Thiede C, Koch S, Creutzig E, Steudel C, Illmer T, Schaich M, Ehninger G. Prevalence and prognostic impact of NPM1 mutations in 1485 adult patients with acute myeloid leukemia (AML). *Blood*. 2006; 107: 4011-20. doi: 10.1182/blood-2005-08-3167.
44. Dohner K, Schlenk RF, Habdank M, Scholl C, Rucker FG, Corbacioglu A, Bullinger L, Frohling S, Dohner H. Mutant nucleophosmin (NPM1) predicts favorable prognosis in younger adults with acute myeloid leukemia and normal cytogenetics: interaction with other gene mutations. *Blood*. 2005; 106: 3740-6. doi: 10.1182/blood-2005-05-2164.
45. Verhaak RG, Goudswaard CS, van Putten W, Bijl MA, Sanders MA, Hugens W, Uitterlinden AG, Erpelinck CA, Delwel R, Lowenberg B, Valk PJ. Mutations in nucleophosmin (NPM1) in acute myeloid leukemia (AML): association with other gene abnormalities and previously established gene expression signatures and their favorable prognostic significance. *Blood*. 2005; 106: 3747-54. doi: 10.1182/blood-2005-05-2168.
46. Leung AY, Man CH, Kwong YL. FLT3 inhibition: a moving and evolving target in acute myeloid leukaemia. *Leukemia*. 2013; 27: 260-8. doi: 10.1038/leu.2012.195.
47. Au CH, Wa A, Ho DN, Chan TL, Ma ES. Clinical evaluation of panel testing by next-generation sequencing (NGS) for gene mutations in myeloid neoplasms. *Diagn Pathol*. 2016; 11: 11. doi: 10.1186/s13000-016-0456-8.
48. Bolli N, Manes N, McKerrell T, Chi J, Park N, Gundem G, Quail MA, Sathiaselan V, Herman B, Crawley C, Craig JI, Conte N, Grove C, et al. Characterization of gene mutations and copy number changes in acute myeloid leukemia using a rapid target enrichment protocol. *Haematologica*. 2015; 100: 214-22. doi: 10.3324/haematol.2014.113381.
49. Kottaridis PD, Gale RE, Frew ME, Harrison G, Langabeer SE, Belton AA, Walker H, Wheatley K, Bowen DT, Burnett AK, Goldstone AH, Linch DC. The presence of a FLT3 internal tandem duplication in patients with acute myeloid leukemia (AML) adds important prognostic information to cytogenetic risk group and response to the first cycle of chemotherapy: analysis of 854 patients from the United Kingdom Medical Research Council AML 10 and 12 trials. *Blood*. 2001; 98: 1752-9. doi: 10.1182/blood-2001-05-1752.
50. Abu-Duhier FM, Goodeve AC, Wilson GA, Gari MA, Peake IR, Rees DC, Vandenberghe EA, Winship PR, Reilly JT. FLT3 internal tandem duplication mutations in adult acute myeloid leukaemia define a high-risk group. *Br J Haematol*. 2000; 111: 190-5. doi: 10.1046/j.1365-2141.2000.01111.x.

51. Papaemmanuil E, Gerstung M, Malcovati L, Tauro S, Gundem G, Van Loo P, Yoon CJ, Ellis P, Wedge DC, Pellagatti A, Shlien A, Groves MJ, Forbes SA, et al. Clinical and biological implications of driver mutations in myelodysplastic syndromes. *Blood*. 2013; 122: 3616-27; quiz 99. doi: 10.1182/blood-2013-08-518886.
52. Schulz WLD, T.J.S.; Rinder, J.; Tormey, C.A.; Torres, R.; Smith, B.R.; Hager, K.M.; Howe, J.G.; Siddon, A.J. Impact of Molecular Clonality on Survival in Acute Myeloid Leukemia. *Blood*. 2015; 126: 3385. doi:
53. Borthakur G, Kantarjian H, Patel KP, Ravandi F, Qiao W, Faderl S, Kadia T, Luthra R, Pierce S, Cortes JE. Impact of numerical variation in FMS-like tyrosine kinase receptor 3 internal tandem duplications on clinical outcome in normal karyotype acute myelogenous leukemia. *Cancer*. 2012; 118: 5819-22. doi: 10.1002/cncr.27571.
54. Spencer DH, Abel HJ, Lockwood CM, Payton JE, Szankasi P, Kelley TW, Kulkarni S, Pfeifer JD, Duncavage EJ. Detection of FLT3 internal tandem duplication in targeted, short-read-length, next-generation sequencing data. *J Mol Diagn*. 2013; 15: 81-93. doi: 10.1016/j.jmoldx.2012.08.001.
55. Meshinchi S, Alonzo TA, Stirewalt DL, Zwaan M, Zimmerman M, Reinhardt D, Kaspers GJ, Heerema NA, Gerbing R, Lange BJ, Radich JP. Clinical implications of FLT3 mutations in pediatric AML. *Blood*. 2006; 108: 3654-61. doi: 10.1182/blood-2006-03-009233.
56. Ommen HB. Monitoring minimal residual disease in acute myeloid leukaemia: a review of the current evolving strategies. *Ther Adv Hematol*. 2016; 7: 3-16. doi: 10.1177/2040620715614529.
57. Cloos J, Goemans BF, Hess CJ, van Oostveen JW, Waisfisz Q, Corthals S, de Lange D, Boeckx N, Hahlen K, Reinhardt D, Creutzig U, Schuurhuis GJ, Zwaan Ch M, et al. Stability and prognostic influence of FLT3 mutations in paired initial and relapsed AML samples. *Leukemia*. 2006; 20: 1217-20. doi: 10.1038/sj.leu.2404246.
58. Kronke J, Bullinger L, Teleanu V, Tschurtz F, Gaidzik VI, Kuhn MW, Rucker FG, Holzmann K, Paschka P, Kapp-Schworer S, Spath D, Kindler T, Schittenhelm M, et al. Clonal evolution in relapsed NPM1-mutated acute myeloid leukemia. *Blood*. 2013; 122: 100-8. doi: 10.1182/blood-2013-01-479188.
59. Del Principe MI, Buccisano F, Maurillo L, Sconocchia G, Cefalo M, Consalvo MI, Sarlo C, Conti C, De Santis G, De Bellis E, Di Veroli A, Palomba P, Attrotto C, et al. Minimal Residual Disease in Acute Myeloid Leukemia of Adults: Determination, Prognostic Impact and Clinical Applications. *Mediterr J Hematol Infect Dis*. 2016; 8: e2016052. doi: 10.4084/MJHID.2016.052.
60. Perl AE, Altman JK, Cortes J, Smith C, Litzow M, Baer MR, Claxton D, Erba HP, Gill S, Goldberg S, Jurcic JG, Larson RA, Liu C, et al. Selective inhibition of FLT3 by gilteritinib in relapsed or refractory acute myeloid leukaemia: a multicentre, first-in-human, open-label, phase 1-2 study. *Lancet Oncol*. 2017; 18: 1061-75. doi: 10.1016/S1470-2045(17)30416-3.
61. Altman JKP, A.E.; Cortes, J.E.; Smith, C.C.; Litzow, M.R.; Hill, J.E.; Larson, R.A.; Liu, C.; Ritchie, E.K.; Strickland, S.A.; Wang, E.S.; Neubauer, A.; Martinelli, G.; Bahceci, E.; Levis, M.J. Deep molecular response to gilteritinib to improve survival in FLT3 mutation-positive relapsed/refractory acute myeloid leukemia. . *Journal of Clinical Oncology* 2017; 35: 7003. doi: 10.1200/JCO.2017.35.15\_suppl.7003
62. Bacher U, Haferlach C, Kern W, Haferlach T, Schnittger S. Prognostic relevance of FLT3-TKD mutations in AML: the combination matters--an analysis of 3082 patients. *Blood*. 2008; 111: 2527-37. doi: 10.1182/blood-2007-05-091215.
63. MacLeod RA, Kaufmann M, Drexler HG. Cytogenetic harvesting of commonly used tumor cell lines. *Nat Protoc*. 2007; 2: 372-82. doi: 10.1038/nprot.2007.29.

64. van Dongen JJ, Macintyre EA, Gabert JA, Delabesse E, Rossi V, Saglio G, Gottardi E, Rambaldi A, Dotti G, Griesinger F, Parreira A, Gameiro P, Diaz MG, et al. Standardized RT-PCR analysis of fusion gene transcripts from chromosome aberrations in acute leukemia for detection of minimal residual disease. Report of the BIOMED-1 Concerted Action: investigation of minimal residual disease in acute leukemia. *Leukemia*. 1999; 13: 1901-28. doi:
65. Kiyoi H, Naoe T, Yokota S, Nakao M, Minami S, Kuriyama K, Takeshita A, Saito K, Hasegawa S, Shimodaira S, Tamura J, Shimazaki C, Matsue K, et al. Internal tandem duplication of FLT3 associated with leukocytosis in acute promyelocytic leukemia. *Leukemia Study Group of the Ministry of Health and Welfare (Kohseisho)*. *Leukemia*. 1997; 11: 1447-52. doi:
66. Shih LY, Huang CF, Wu JH, Lin TL, Dunn P, Wang PN, Kuo MC, Lai CL, Hsu HC. Internal tandem duplication of FLT3 in relapsed acute myeloid leukemia: a comparative analysis of bone marrow samples from 108 adult patients at diagnosis and relapse. *Blood*. 2002; 100: 2387-92. doi: 10.1182/blood-2002-01-0195.
67. Li H, Handsaker B, Wysoker A, Fennell T, Ruan J, Homer N, Marth G, Abecasis G, Durbin R, Genome Project Data Processing S. The Sequence Alignment/Map format and SAMtools. *Bioinformatics*. 2009; 25: 2078-9. doi: 10.1093/bioinformatics/btp352.
68. Giardine B, Riemer C, Hardison RC, Burhans R, Elnitski L, Shah P, Zhang Y, Blankenberg D, Albert I, Taylor J, Miller W, Kent WJ, Nekrutenko A. Galaxy: a platform for interactive large-scale genome analysis. *Genome Res*. 2005; 15: 1451-5. doi: 10.1101/gr.4086505.
69. Blankenberg D, Hillman-Jackson J. Analysis of next-generation sequencing data using Galaxy. *Methods Mol Biol*. 2014; 1150: 21-43. doi: 10.1007/978-1-4939-0512-6\_2.
70. Ye K, Schulz MH, Long Q, Apweiler R, Ning Z. Pindel: a pattern growth approach to detect break points of large deletions and medium sized insertions from paired-end short reads. *Bioinformatics*. 2009; 25: 2865-71. doi: 10.1093/bioinformatics/btp394.
71. Cheson BD, Bennett JM, Kopecky KJ, Buchner T, Willman CL, Estey EH, Schiffer CA, Doehner H, Tallman MS, Lister TA, Lo-Coco F, Willemze R, Biondi A, et al. Revised recommendations of the International Working Group for Diagnosis, Standardization of Response Criteria, Treatment Outcomes, and Reporting Standards for Therapeutic Trials in Acute Myeloid Leukemia. *J Clin Oncol*. 2003; 21: 4642-9. doi: 10.1200/JCO.2003.04.036.
72. Opatz S, Polzer H, Herold T, Konstandin NP, Ksienzyk B, Zellmeier E, Vosberg S, Graf A, Krebs S, Blum H, Hopfner KP, Kakadia PM, Schneider S, et al. Exome sequencing identifies recurring FLT3 N676K mutations in core-binding factor leukemia. *Blood*. 2013; 122: 1761-9. doi: 10.1182/blood-2013-01-476473.

## TABLES

**Table 1. Patient characteristics.**

<b>Characteristics</b>	
<b>cohort size</b> (patients no.)	250
<b>median age</b> (years; range)	59; 18-80
<b>sex (m/f)</b> (patients no.; [%])	121/129; 48/52
<b>median follow-up</b> (months; range)	50; 0-136
<b>median overall survival</b> (months; range)	9; 0-136
<b>Morphologic parameters</b>	
<b>median WBC count</b> (n=243), (leucocytes/mL; range)	48,350; 100 – 391,200
<b>median BM-blasts</b> (n=229), ([%]; range)	83; 10-100
<b>median PLT</b> (n=243), (PLT/mL; range)	55,000; 1,220 – 592,000
<b>median LDH</b> (n=239), (LDH/mL; range)	691; 87-6,251
<b>AML type</b> (n=245)	<b>patients</b> (no.)
<b>de novo</b>	205
<b>s-AML</b>	27
<b>t-AML</b>	13
<b>FAB-type</b> (n=236)	<b>patients</b> (no.)
<b>M0</b>	9
<b>M1</b>	71
<b>M2</b>	60
<b>M3</b>	0
<b>M4</b>	67
<b>M5</b>	24
<b>M6</b>	4
<b>M7</b>	1
<b>Categories according to ELN (n=246)</b>	
<b>favourable</b>	0; 0
<b>intermediate-I</b>	172; 70
<b>intermediate-II</b>	52; 21
<b>adverse</b>	22; 9
<b>Karyotype</b> (n=250)	<b>patients</b> (no.; [%])
<b>Normal</b>	176; 70
<b>Complex</b>	74; 30
<b>Molecular genetics</b>	
<b><i>FLT3</i>-ITD+ (n=250)</b>	250; 100
<b><i>NPM1</i>+ (n=189)</b>	118; 47
<b><i>CEBPA</i>+ (n=116)</b>	9; 4
<b><i>KMT2A</i>-PTD+ (n=241)</b>	20; 8

WBC (white blood cell), PLT (platelet counts), BM (bone marrow), LDH (lactate dehydrogenase), AML (acute myeloid leukemia), MDS (myelodysplastic syndrome), ELN (European Leukemia Net), FAB (French American British Classification), ITD (internal tandem duplication), PTD (partial tandem duplication), no. (number).

**Table 2. *FLT3* primers.**

Primer for fragment analysis of <i>FLT3</i>		
	forward	reverse
<b>cDNA</b>	5'-FAM-tgt cga gca gta ctc taa aca tg-3' (R5)	5'-atc cta gta cct tcc caa act c-3' (R6)
<b>gDNA</b>	5'-FAM-gca aat tag gta tga aag cca gc-3' (11F)	5'-cct tca gca ttt tga cgg caa cc-3' (12R)
Primer for high-throughput amplicon sequencing of <i>FLT3</i>		
	forward	reverse
	5'-aat gat acg gcg aac aac gag atc tac act ctt tcc cta cac gac gct ctt ccg atc t – BARCODE– tgt cga gca gta ctc taa aca tg -3'	5' - caa gca gaa gac ggc ata cga gat cgg tct cgg cat tcc tgc tga acc gct ctt ccg atc t – BARCODE – atc cta gta cct tcc caa act c – 3'

FAM (fluorescein amidite).

**Table 3. *FLT3*-ITD localization and co-occurrence of mutations in other cancer related genes.**

mutation	juxtamembrane domain			tyrosine kinase domain		total
	switch motif	zipper motif	hinge region	beta1-sheet	NBL	
<b><i>FLT3</i>-PM (TKD)</b>	0	0(2)	3	2	1(1)	6(3)
<b><i>NPM1</i></b>	3	58	18	29	7	115
<b><i>CEBPA</i></b>	0	4	1	3	1	9
<b><i>KIT</i></b>	0	1	1	0	0	2
<b><i>IDH1/2</i></b>	0	7	2	5	0	14
<b><i>KMT2A</i>-PTD</b>	0	10	2	6	1	19
<b><i>FLT3</i>-ITDs</b>	4	128	35	62	13	242

Distribution of concurrent mutations among the patients, clustered according to ITD location in functional *FLT3* domain (n=242, according to *FLT3*-ITD position of the dominant clone by high-throughput amplicon sequencing (HTAS)). PM (point mutations; including D835N and V592L), ITD (internal tandem duplication), TKD (tyrosine kinase domain), NBL (nuclear binding loop), PTD (partial tandem duplication), no. (number).

## FIGURE LEGENDS

**Figure 1. Study design.** Flow chart illustrating the selection of patient samples. \*Residual patients were lost during follow-up. HTAS (high-throughput amplicon sequencing), ITD (internal tandem duplication).

**Figure 2. FLT3 mutations.** Schematic illustration displaying AML-specific FLT3 mutations according to their receptor domain localization (modified from Opatz et al. [72]). FLT3-ITDs are located within the juxtamembrane (JM) and tyrosine kinase domain (TKD) 1, whereas point mutations are frequently found in TKD1 and TKD2. *FLT3* cDNA region covered by HTAS and fragment analysis is indicated by the primer binding marks (R5 and R6). ITD (internal tandem duplication), JM-B (JM binding motif), JM-S (JM switch motif), JM-Z (JM zipper motif), HR (hinge region),  $\beta$ 1 ( $\beta$ 1-sheet), NBL (nucleotide binding loop),  $\beta$ 2 ( $\beta$ 2-sheet).

**Figure 3. FLT3-ITD detection output by fragment analysis and by HTAS.** Exemplary results are shown for UPN 42 **a)** Electropherogram displays *FLT3* amplicon signals as fragment peaks, with the distance of the peak positions corresponding to the size of the ITD and the area under the peak curves used for calculation of the mutational burden. **b)** Tabular representation of variant detection results from HTAS in VCF format (Pindel output). WT (wild type), ITD (internal tandem duplication), Chrom (Chromosome), Pos (cDNA position), Ref (reference sequence), Alt (alternative sequence), VAF (variant allele frequency), \*computed separately and added manually.

**Figure 4. FLT3-ITDs assigned to functional domains.** Distribution of detected *FLT3*-ITDs by HTAS across functional domains according to insertion site and clone size. ITD (internal tandem duplication), JM (juxtamembrane), TKD (tyrosine kinase domain), NBL (nuclear binding loop).

**Figure 5. FLT3-ITD subclone detection.** **a)** Number of detected *FLT3*-ITDs per patient (n=250), comparing HTAS to fragment analysis. **b)** Number of detected *FLT3*-ITDs per

method, comparing HTAS to fragment analysis according to clonal size. HTAS (high-throughput amplicon sequencing), ITD (internal tandem duplication), sub (subclone).

**Figure 6. Impact of the number of *FLT3*-ITD clones on relapse-free and overall survival.**

**a)** Relapse-free and **b)** overall survival of patients according to number of *FLT3*-ITD clones detected by HTAS with cDNA template (n=242; one *FLT3*-ITD per patient (n=191), more than one *FLT3*-ITD per patient (n=51)). **c)** Relapse-free and **d)** overall survival of patients according to number of *FLT3*-ITD clones detected by fragment analysis with cDNA template (n=242; one *FLT3*-ITD per patient (n=212), more than one *FLT3*-ITD per patient (n=30). HTAS (high-throughput amplicon sequencing), ITD (internal tandem duplication).

**Figure 7. Sensitivity of *FLT3*-ITD detection by HTAS compared to fragment analysis.**

*FLT3*-ITD from the heterozygous *FLT3*-ITD positive cell line MOLM-13 detected after serial dilution in the *FLT3*-WT cell line HL60 by HTAS or fragment analysis using cDNA (n=3; log(10); 95% confidence interval). Cell line cDNA was derived from five million cells each. For amplification 1µL cDNA template of each serial dilution was used. The dashed line represents the cut-off defined for ITD-analysis in patient samples. HTAS (high-throughput amplicon sequencing), ITD (internal tandem duplication).

**Figure 8. *FLT3*-ITD mutational burden measured by fragment analysis and HTAS.**

Correlation of the *FLT3*-ITD mRNA level according to fragment analysis or according to the variant allele frequency in HTAS with cDNA template (n=220). HTAS (high-throughput amplicon sequencing), ITD (internal tandem duplication).

**Figure 9. Mappability of *FLT3*-ITD sequence reads.**

Mappability of sequence reads from HTAS according to length of ITD. P-value was computed using Mann-Whitney-U test. nt (nucleotide), HTAS (high-throughput amplicon sequencing), ITD (internal tandem duplication).

Figure 1.

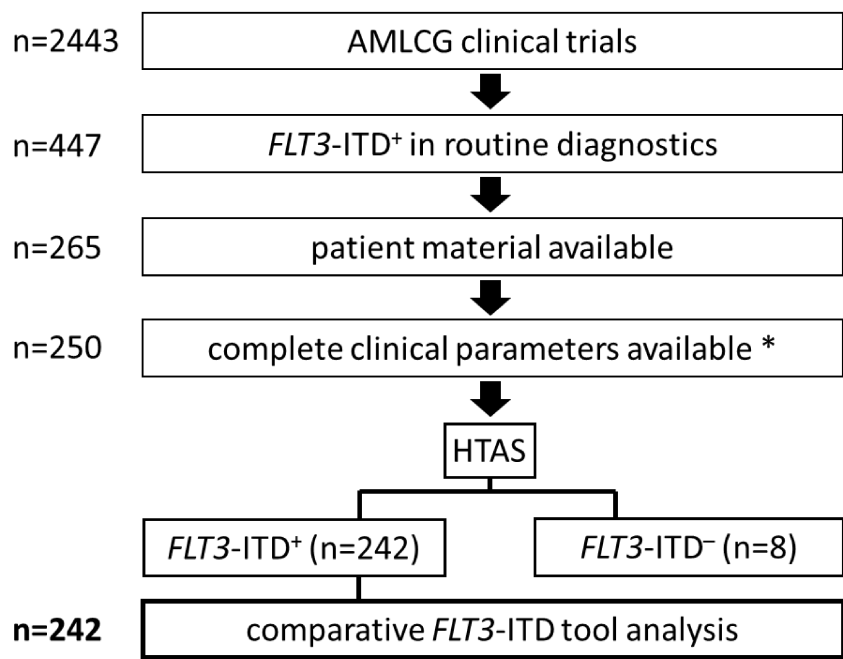


Figure 2.

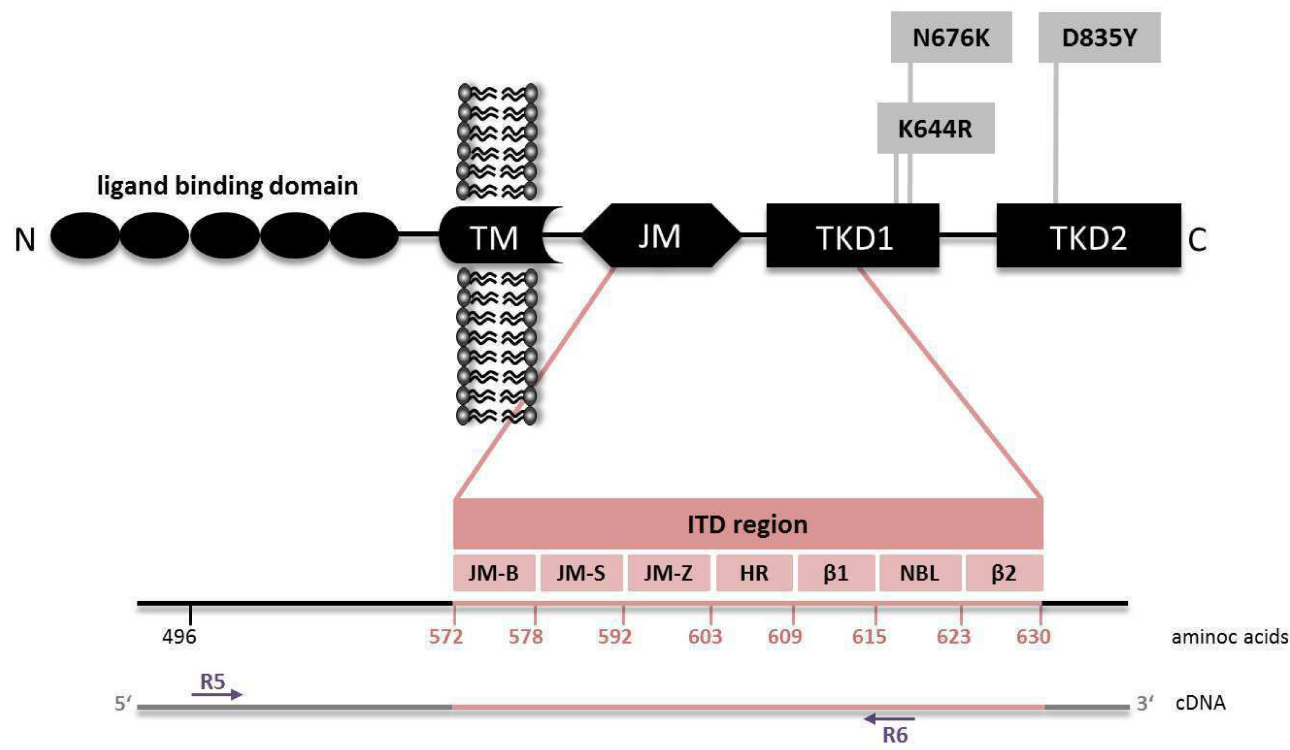




Figure 3.

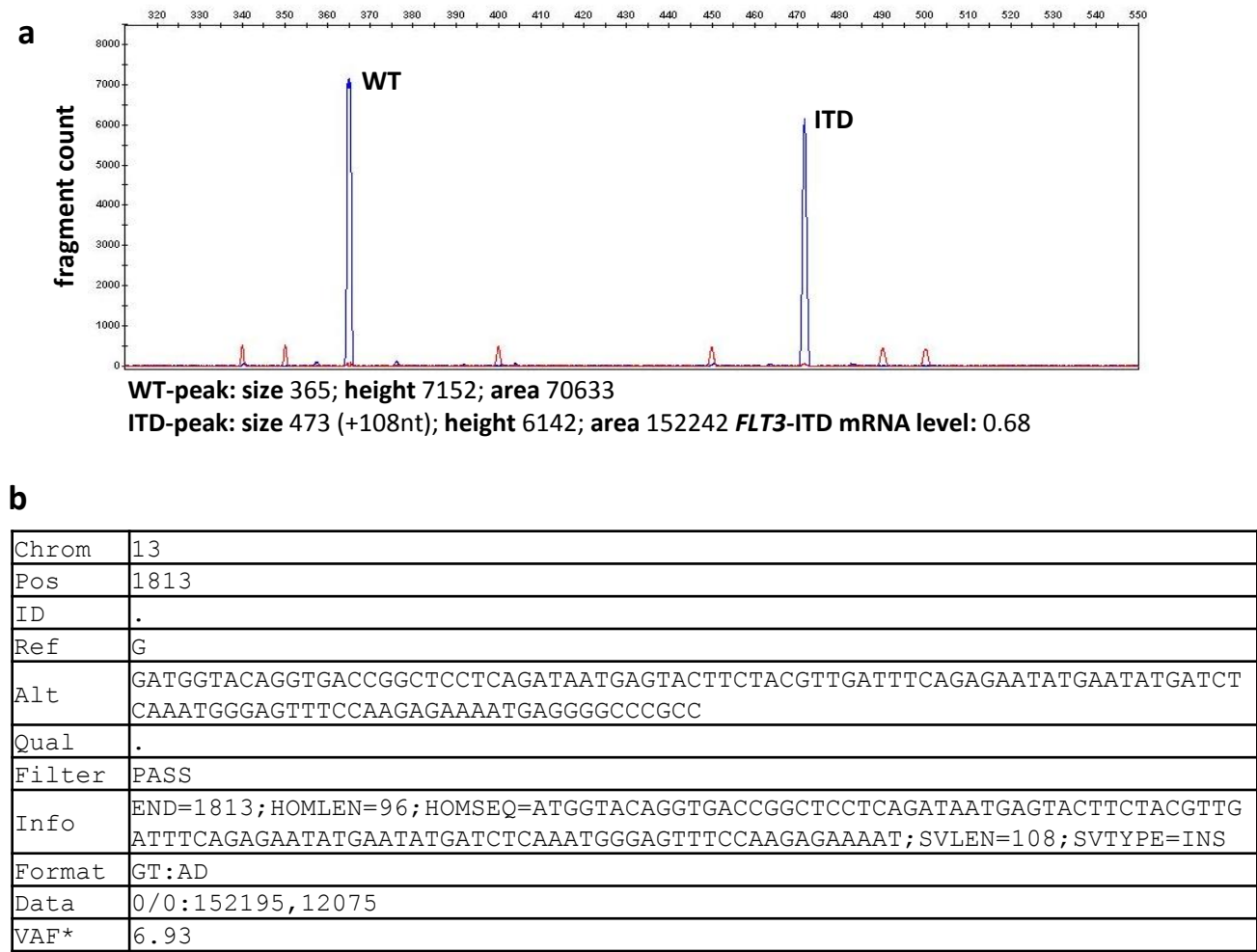


Figure 4.

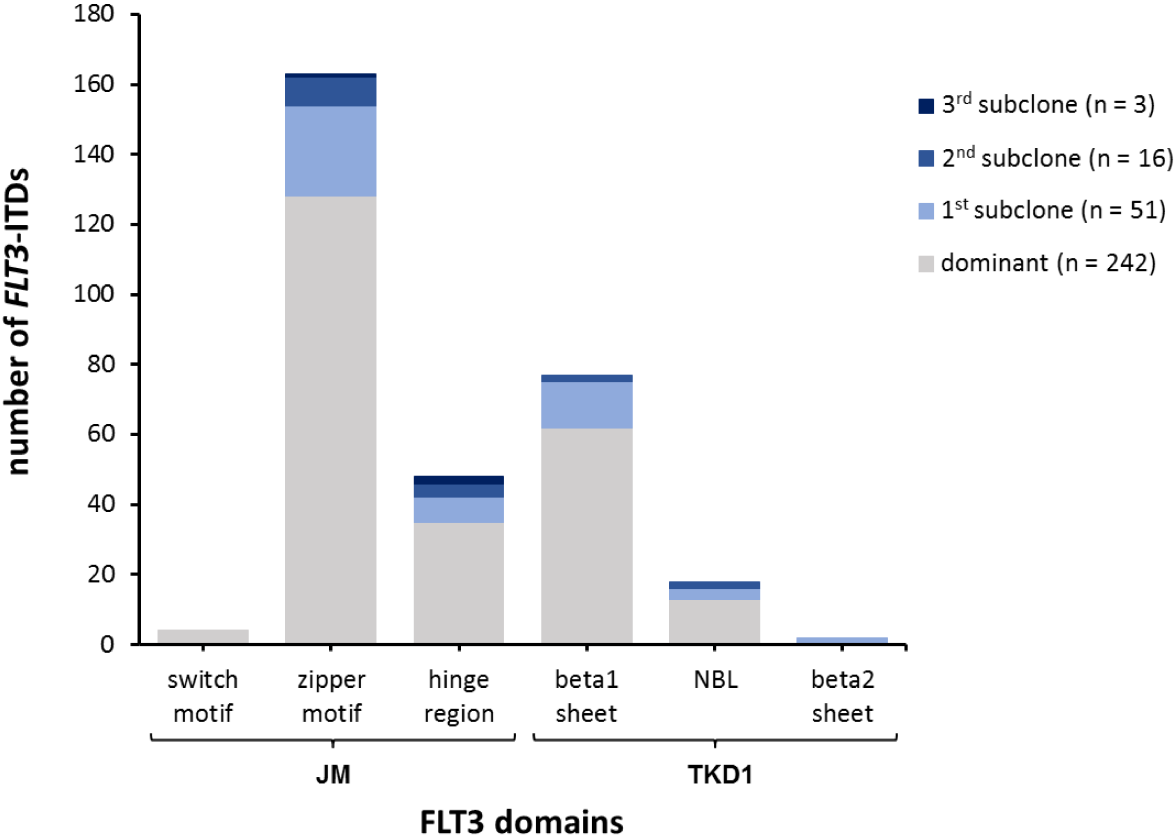
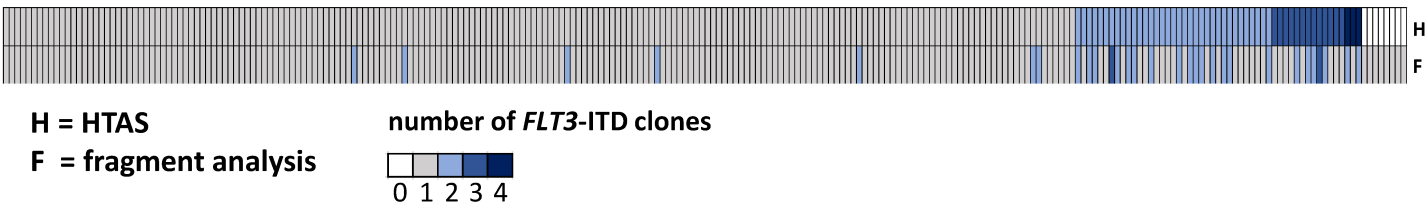


Figure 5.

a



b

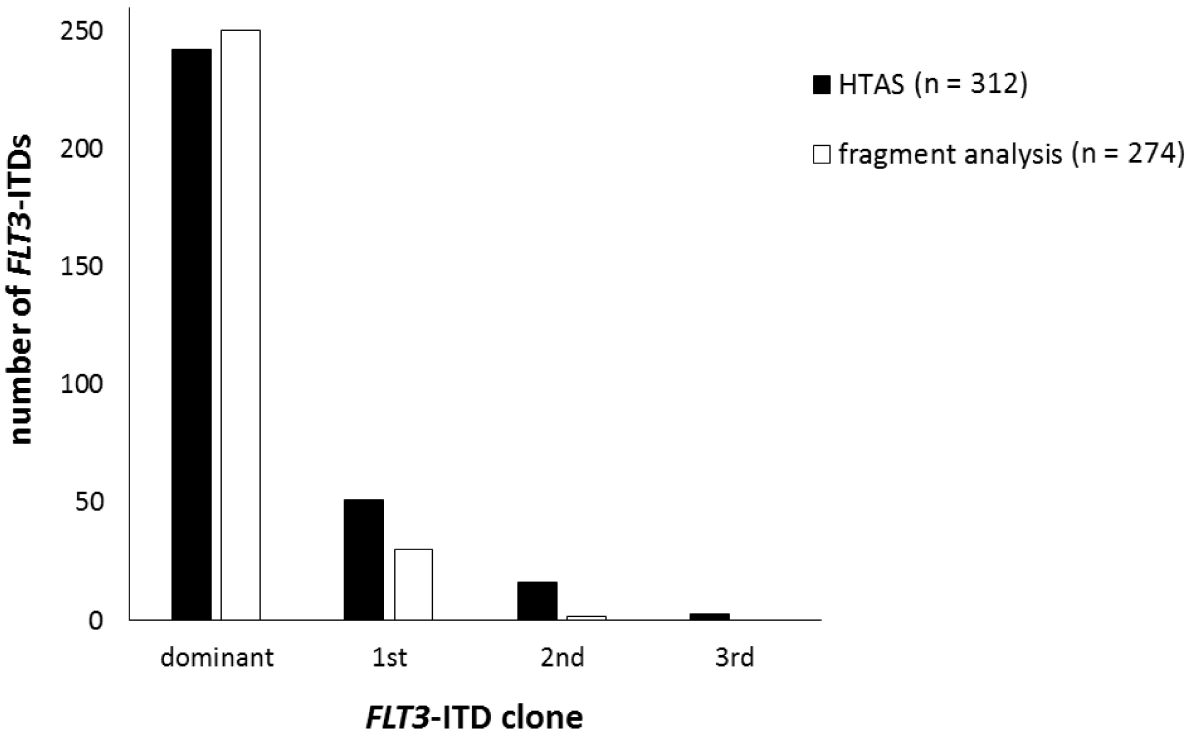


Figure 6.

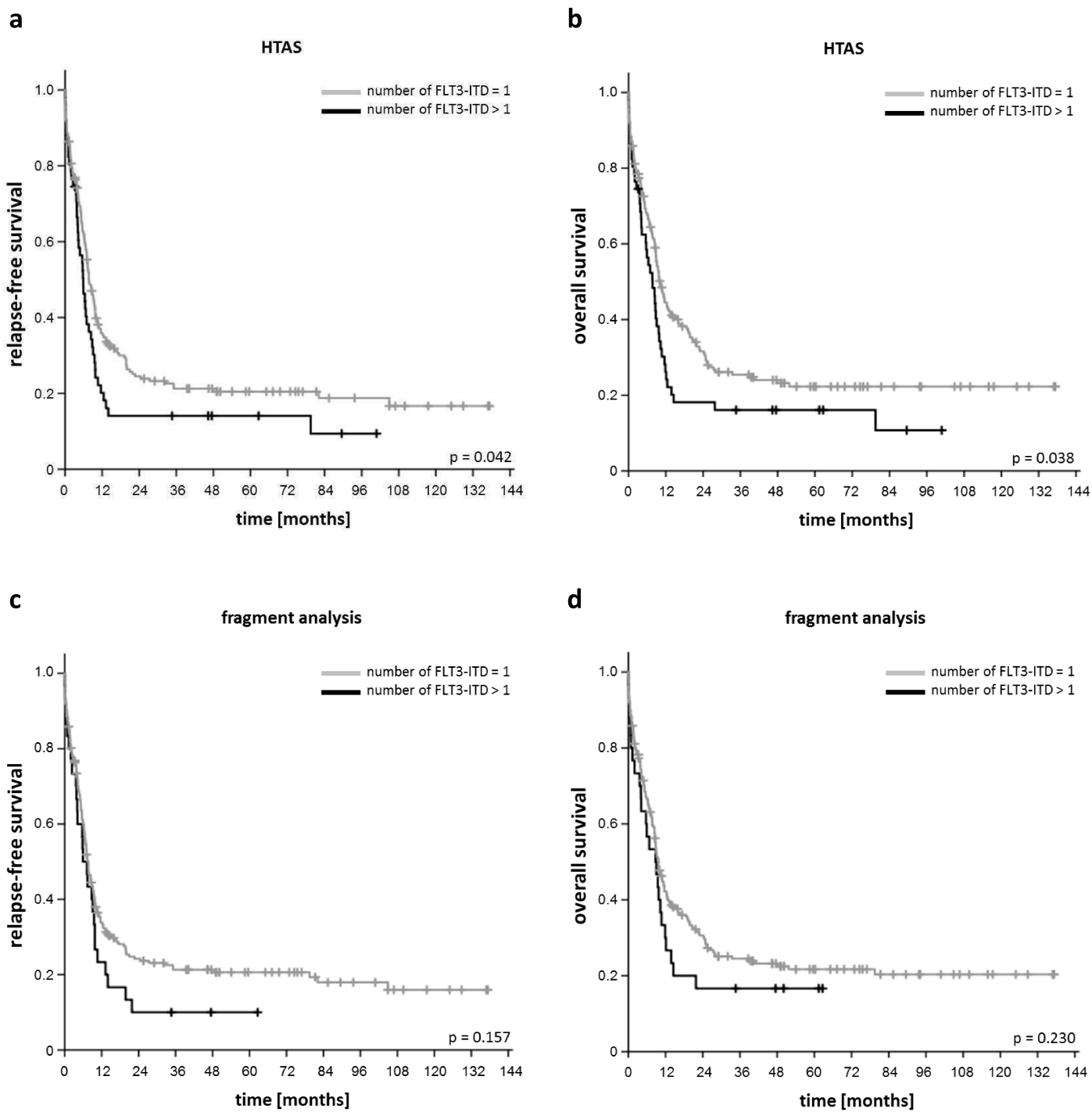


Figure 7.

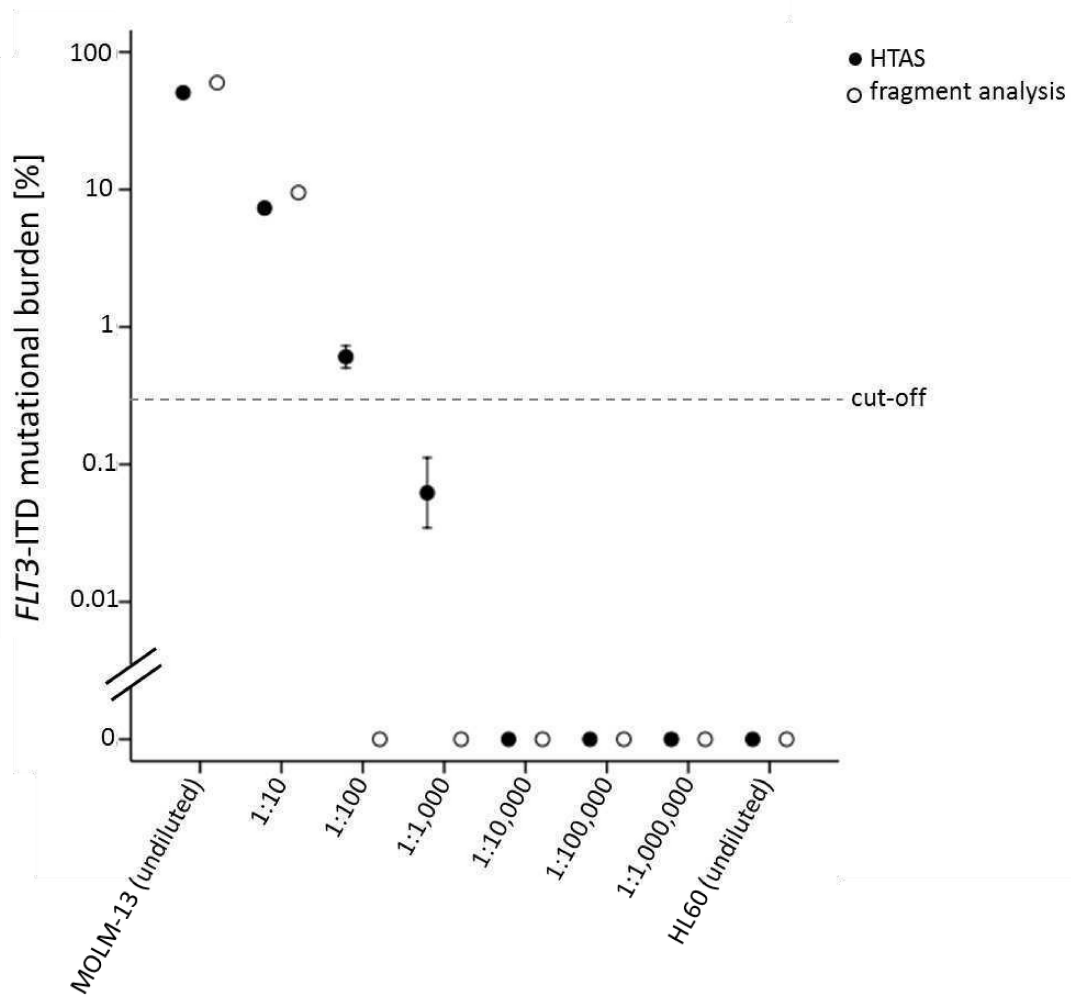


Figure 8.

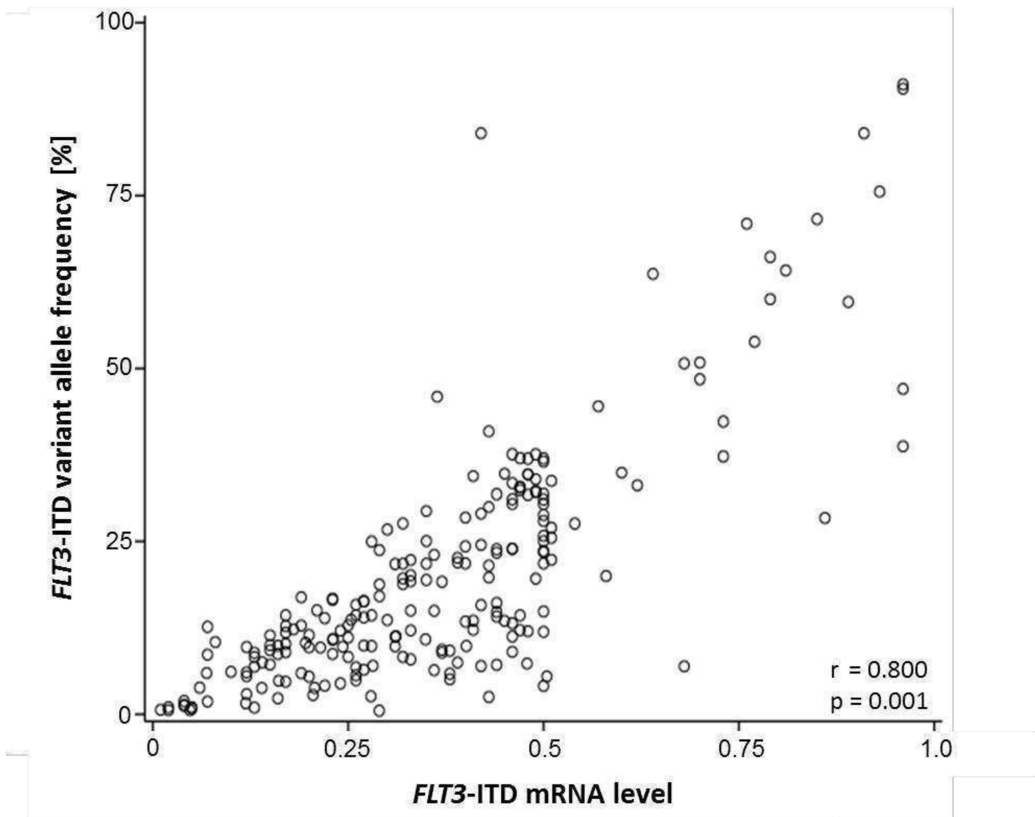
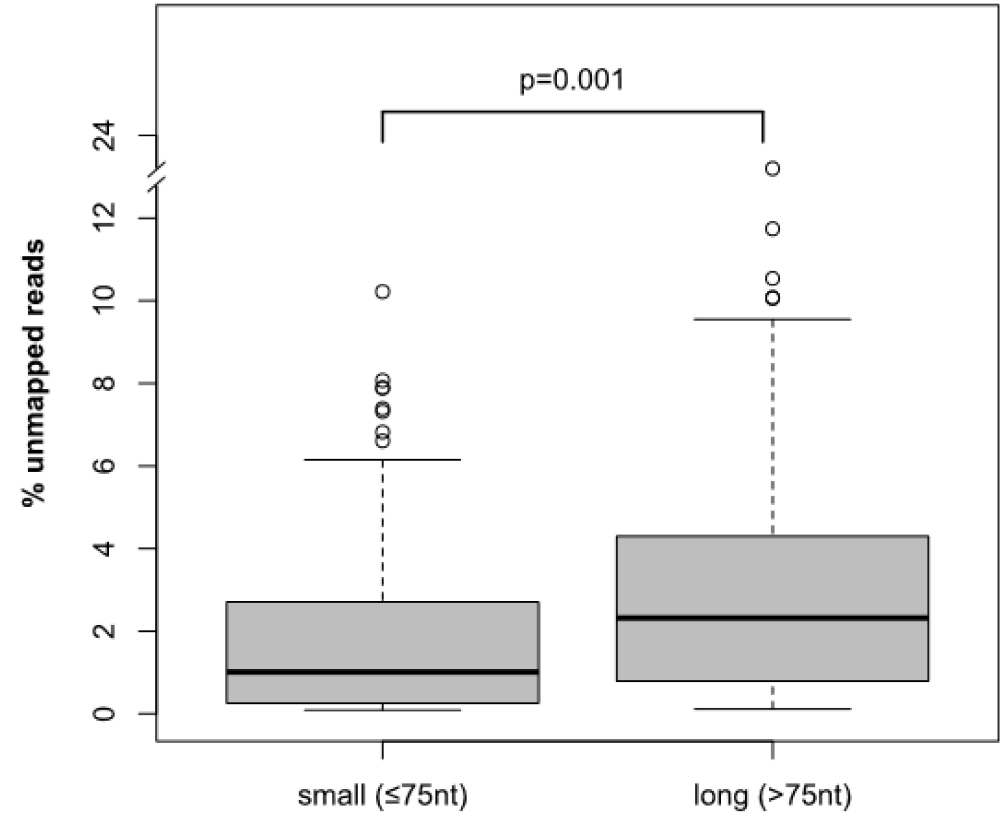


Figure 9.



## **SUPPLEMENTARY INFORMATION**

**Clonal heterogeneity of *FLT3*-ITD detected by high-throughput amplicon sequencing correlates with adverse prognosis in acute myeloid leukemia**

Schranz K. et al.

### **Content**

Supplementary Tables S1-S8

Supplementary Figures S1-S11

## Supplementary Tables

**Supplementary Table S1: *FLT3*-ITDs per patient detected by HTAS and fragment analysis, displaying ITD position, size, length and mutational burden.**

patient (UPN)	FLT3-ITD							exclusively
	cDNA position		length [nt]			mutational burden [%]		
	HTAS	S	HTAS	F	S	HTAS	F	
1	1804	NA	69	69	NA	0.59	1.57	no
2	1781	NA	66	65	NA	0.82	5.30	no
	neg	NA	neg	112	NA	neg	6.37	yes (F)
3	1840	1843	111	111	111	0.96	13.34	no
4	1793	NA	66	66	NA	1.01	1.96	no
	1800	NA	57	57	NA	0.64	0.99	no
5	1829	1831	75	75	75	1.02	4.94	no
6	1805	1804	87	NA	87	1.12	NA	no
7	1806	NA	63	63	NA	1.23	3.75	no
8	1839	NA	66	63	NA	1.38	3.66	no
9	1844	1882	153	NA	153	1.62	NA	no
10	1810	1813	39	39	39	1.85	6.54	no
11	1793	NA	24	24	NA	1.92	4.47	no
	1795	NA	21	neg	NA	0.50	neg	yes (H)
12	1811	1813	69	NA	69	2.01	NA	no
13	1842	1843	54	NA	54	2.29	NA	no
	1861	1867	78	NA	90	0.92	NA	no
	1804	neg	27	NA	neg	0.81	NA	yes (H)
	1802	neg	54	NA	neg	0.68	NA	yes (H)
14	1828	1831	93	93	93	2.32	15.54	no
15	1794	1813	24	24	24	21.77	35.36	no
	1831	neg	102	102	neg	2.77	20.51	no
16	1782	1783	63	63	63	2.92	11.50	no
17	1860	1867	81	NA	81	3.35	NA	no
18	1797	NA	18	18	NA	3.85	5.75	no
19	1825	1828	99	99	99	4.10	50.00	no
	1839	neg	57	neg	neg	2.50	neg	yes (H)
	1820	neg	33	neg	neg	4.52	neg	yes (H)
20	1803	1810	72	72	72	4.14	22.12	no
21	1836	NA	51	51	NA	4.46	23.55	no
22	1799	1810	24	24	24	4.71	17.01	no
	1876	neg	93	93	neg	5.96	6.89	no
23	1832	1834	63	63	63	4.93	25.93	no
24	1789	NA	63	63	NA	5.05	37.66	no
	1787	NA	33	neg	NA	0.94	neg	yes (H)
25	1862	1864	78	NA	78	5.20	NA	no
26	1794	1801	78	NA	78	5.21	NA	no
27	1830	NA	51	51	NA	5.44	19.87	no
28	1802	1804	54	54	54	5.49	11.66	no
29	1797	NA	78	78	NA	5.64	25.93	no
30	1783	1786	33	NA	33	5.80	NA	no
31	1869	1870	87	87	87	5.86	37.97	no

continued on next page



Supplementary Table S1 continued.

patient (UPN)	FLT3-ITD							exclusively
	cDNA position		length [nt]			mutational burden [%]		
	HTAS	S	HTAS	F	S	HTAS	F	
32	1836	1837	96	NA	96	5.91	NA	no
	1796	neg	27	NA	neg	4.70	NA	yes (H)
33	1797	1798	51	NA	51	5.94	NA	no
34	1852	1855	63	63	63	5.95	18.57	no
35	1807	1810	60	60	60	6.06	12.20	no
36	1794	1795	24	24	24	6.14	10.31	no
37	1841	NA	99	99	NA	6.38	36.39	no
	1794	NA	48	48	NA	45.95	36.39	no
	neg	NA	neg	30	NA	neg	22.12	yes (F)
38	1838	1840	60	60	60	6.43	27.33	no
39	1794	1795	78	NA	78	6.77	NA	no
40	1777	NA	63	63	NA	6.79	26.09	no
41	1818	NA	36	36	NA	6.89	13.12	no
42	1839	NA	108	108	NA	6.93	68.35	no
43	1838	1840	105	105	105	6.97	41.59	no
44	1788	1789	57	57	57	7.15	43.98	no
45	1825	NA	60	60	NA	7.20	15.47	no
46	1823	1825	96	NA	96	7.29	NA	no
47	1790	1792	72	72	72	7.48	39.02	no
	1824	neg	63	63	neg	7.33	47.89	no
48	1793	1795	57	57	57	7.50	13.79	no
49	1801	1804	69	NA	69	7.79	NA	no
	1799	neg	30	NA	neg	5.19	NA	yes (H)
50	1830	1831	90	90	90	7.94	33.20	no
	1838	neg	60	neg	neg	5.26	neg	yes (H)
	1793	neg	24	neg	neg	0.79	neg	yes (H)
	1814	neg	69	neg	neg	0.69	neg	yes (H)
51	1796	NA	27	27	NA	8.27	13.42	no
	1805	NA	96	96	NA	0.58	4.76	no
52	1829	1831	84	84	84	8.29	24.87	no
53	1792	1795	63	63	63	8.29	31.93	no
54	1838	1840	102	102	102	8.63	7.32	no
55	1831	1834	60	60	60	8.72	22.84	no
	1838	1840	63	63	63	4.85	16.11	no
56	1823	1825	39	39	39	8.73	15.97	no
57	1793	1795	24	24	24	8.89	13.04	no
58	1786	1789	57	57	57	8.91	36.51	no
	1786	neg	21	neg	neg	6.93	neg	yes (H)
	1809	neg	27	neg	neg	5.09	neg	yes (H)
59	1836	1837	66	66	66	8.99	17.08	no
60	1843	1834	117	117	117	9.03	45.95	no
61	1817	NA	102	102	NA	9.19	37.89	no
62	1794	NA	21	21	NA	9.26	14.68	no
63	1804	1807	48	48	48	9.33	37.38	no
64	1817	1819	99	NA	99	9.40	NA	no

continued on next page

Supplementary Table S1 continued.

patient (UPN)	FLT3-ITD							exclusively
	cDNA position		length [nt]			mutational burden [%]		
	HTAS	S	HTAS	F	S	HTAS	F	
65	1796	1798	24	NA	24	9.60	NA	no
66	1793	NA	51	51	NA	9.67	20.06	no
67	1790	1792	15	15	15	9.72	12.28	no
68	1856	1858	66	66	66	9.83	30.75	no
69	1802	1804	87	87	87	9.87	28.21	no
70	1789	1792	30	30	30	9.91	15.54	no
71	1839	NA	102	102	NA	9.93	27.27	no
	1805	NA	60	60	NA	10.83	34.90	no
	1827	NA	72	neg	NA	0.52	neg	yes (H)
72	1810	NA	21	21	NA	9.99	14.89	no
73	1803	NA	24	24	NA	10.17	16.53	no
74	1841	1843	72	72	72	10.44	8.26	no
	1819	neg	33	neg	neg	2.75	neg	yes (H)
	1805	neg	30	neg	neg	2.31	neg	yes (H)
75	1788	1789	75	75	75	10.77	23.49	no
76	1804	NA	72	72	NA	11.09	25.30	no
77	1861	1855	126	126	126	11.23	31.27	no
	1792	neg	78	neg	neg	0.64	neg	yes (H)
78	1834	1837	102	102	102	11.24	45.56	no
79	1829	1831	51	51	51	11.41	15.18	no
	1795	1798	36	36	36	7.02	28.16	no
	1819	neg	30	neg	neg	0.78	neg	yes (H)
80	1838	1840	30	30	30	11.44	20.32	no
	1796	1798	21	21	21	9.65	21.45	no
	1804	neg	60	neg	neg	0.93	neg	yes (H)
	1823	neg	51	neg	neg	0.52	neg	yes (H)
81	1825	1828	51	NA	51	11.66	NA	no
82	1834	1837	93	93	93	11.81	16.60	no
83	1802	1804	75	75	75	11.93	49.52	no
	1834	neg	60	neg	neg	0.54	neg	yes (H)
84	1781	NA	30	30	NA	12.01	47.62	no
	neg	NA	neg	15	NA	neg	7.75	yes (F)
85	1797	1798	63	NA	63	12.03	NA	no
86	1806	NA	60	60	NA	12.10	24.24	no
87	1844	1846	102	102	102	12.13	32.80	no
88	1791	1804	21	21	21	12.16	46.67	no
	1838	neg	36	36	neg	11.27	31.13	no
	1801	neg	21	neg	neg	8.54	neg	yes (H)
89	1818	NA	60	66	NA	12.21	40.83	no
90	1809	1810	27	27	27	12.27	18.17	no
91	1799	1801	63	NA	63	12.38	NA	no
92	1815	1816	30	30	30	12.64	7.49	no
	1793	neg	24	24	neg	3.82	20.70	no
93	1787	1789	18	18	18	12.76	17.15	no
94	1784	1786	69	NA	69	12.82	NA	no

continued on next page

Supplementary Table S1 continued.

patient (UPN)	FLT3-ITD							exclusively
	cDNA position		length [nt]			mutational burden [%]		
	HTAS	S	HTAS	F	S	HTAS	F	
95	1788	1789	39	39	39	12.84	18.50	no
	1825	neg	18	neg	neg	0.81	neg	yes (H)
96	1797	NA	42	42	NA	12.87	25.21	no
	neg	NA	neg	66	NA	neg	9.17	yes (F)
97	1817	1819	36	NA	36	12.93	NA	no
98	1784	1786	69	69	69	13.15	45.83	no
99	1838	1837	45	NA	45	13.24	NA	no
	1803	neg	15	NA	neg	3.82	NA	yes (H)
100	1867	1864	129	129	129	13.40	39.76	no
101	1848	NA	90	90	NA	13.50	44.90	no
102	1836	1837	90	90	90	13.54	40.93	no
103	1843	1846	63	63	63	13.63	29.63	no
	1784	neg	39	neg	neg	0.89	neg	yes (H)
104	1809	neg	30	30	neg	13.90	22.12	no
	1824	1828	93	93	93	10.33	19.55	no
	1833	neg	45	45	neg	3.81	13.94	no
105	1818	1819	36	36	36	14.01	26.79	no
	1808	neg	51	neg	neg	2.26	neg	yes (H)
	1819	neg	72	neg	neg	1.85	neg	yes (H)
106	1826	1828	51	51	51	14.13	43.57	no
	1840	1843	42	42	42	9.87	40.12	no
	1829	neg	78	neg	neg	0.64	neg	yes (H)
107	1798	NA	21	21	NA	14.31	27.59	no
108	1797	1798	81	81	81	14.31	47.09	no
109	1814	1814	21	21	21	14.31	16.94	no
	1835	neg	57	57	neg	10.89	23.08	no
110	1830	1831	54	54	54	14.32	26.25	no
111	1825	1828	87	87	87	14.82	44.44	no
112	1864	NA	75	75	NA	14.86	50.00	no
113	1839	NA	84	84	NA	14.96	35.98	no
114	1840	1843	60	60	60	14.99	33.16	no
115	1796	1798	21	21	21	15.04	21.26	no
116	1804	1807	18	18	18	15.80	42.20	no
	1778	neg	42	neg	neg	0.62	neg	yes (H)
117	1834	1837	60	60	60	15.84	25.54	no
118	1841	1843	66	NA	66	15.92	NA	no
119	1840	1843	90	90	90	16.09	43.91	no
120	1803	1804	30	30	30	16.34	27.01	no
	1793	1795	24	24	24	13.67	25.37	no
121	1799	1801	30	30	30	16.35	26.56	no
122	1841	NA	72	72	NA	16.56	22.53	no
123	1793	NA	24	24	NA	16.71	23.02	no
124	1793	1795	24	24	24	16.92	19.35	no
	1886	1888	114	114	114	2.60	27.90	no
125	1787	1789	45	45	45	17.07	29.43	no

continued on next page

Supplementary Table S1 continued.

patient (UPN)	FLT3-ITD							exclusively
	cDNA position		length [nt]			mutational burden [%]		
	HTAS	S	HTAS	F	S	HTAS	F	
126	1770	1771	48	NA	48	17.09	NA	no
127	1814	1816	18	18	18	18.77	29.18	no
128	1805	1807	21	21	21	18.83	31.97	no
	1856	1858	75	75	75	0.51	28.98	no
129	1847	NA	75	75	NA	19.16	36.67	no
130	1849	1819	45	45	45	19.23	32.89	no
	1817	neg	45	neg	neg	2.00	neg	yes (H)
	1809	neg	75	neg	neg	1.53	neg	yes (H)
131	1793	1795	57	NA	57	19.38	NA	no
	1794	neg	24	NA	neg	3.11	NA	yes (H)
132	1830	1831	54	54	54	19.42	35.40	no
133	1839	1840	96	96	96	19.62	49.11	no
134	1808	1810	45	45	45	19.65	32.25	no
135	1833	1834	51	51	51	19.78	43.28	no
	1832	1825	87	78	78	9.77	24.30	no
136	1793	1795	24	24	24	19.99	57.63	no
137	1799	1801	30	30	30	20.11	32.75	no
	1795	neg	36	neg	neg	9.91	neg	yes (H)
138	1838	1840	69	69	69	21.52	42.73	no
139	1792	1795	27	27	27	21.73	30.65	no
	neg	neg	neg	96	neg	neg	24.59	yes (F)
140	1868	NA	114	114	NA	2.50	42.63	no
141	1787	1789	18	18	18	21.78	32.20	no
142	1800	NA	24	24	NA	21.82	50.15	no
143	1823	1819	78	78	78	21.82	39.94	no
144	1807	1810	63	63	63	21.95	39.06	no
145	1842	1843	108	NA	108	22.05	NA	no
146	1782	1783	27	27	27	22.31	32.61	no
147	1840	1843	69	69	69	22.34	50.93	no
148	1826	1828	57	57	57	22.62	39.10	no
149	1795	1798	36	NA	36	23.07	NA	no
	1792	neg	21	NA	neg	4.22	NA	yes (H)
	1853	neg	72	NA	neg	0.50	NA	yes (H)
150	1804	1807	30	30	30	23.07	35.94	no
151	1843	1846	60	60	60	23.36	43.63	no
152	1847	1849	66	66	66	23.44	50.25	no
153	1839	NA	60	60	NA	23.62	50.00	no
154	1794	1795	60	NA	60	23.64	NA	no
155	1786	1789	27	27	27	23.74	28.88	no
156	1827	NA	33	33	NA	23.87	44.48	no
	neg	NA	neg	110	NA	neg	6.54	yes (F)
157	1800	1802	54	54	54	23.92	45.50	no
158	1839	NA	51	45	NA	23.93	45.86	no
159	1838	NA	36	36	NA	24.27	40.26	no
160	1830	1831	57	57	57	24.50	42.43	no

continued on next page

Supplementary Table S1 continued.

patient (UPN)	FLT3-ITD							exclusively
	cDNA position		length [nt]			mutational burden [%]		
	HTAS	S	HTAS	F	S	HTAS	F	
161	1826	NA	51	51	NA	24.98	27.54	no
	1817	NA	78	78	NA	1.60	11.89	no
162	1837	1840	66	66	66	25.01	49.55	no
	1834	neg	93	neg	neg	2.74	neg	yes (H)
	1792	neg	45	neg	neg	0.58	neg	yes (H)
163	1792	1795	21	21	21	25.05	34.77	no
164	1821	1822	42	42	42	25.53	50.52	no
165	1793	1795	48	NA	48	25.71	NA	no
166	1836	NA	48	48	NA	25.80	50.47	no
167	1785	NA	24	24	NA	26.71	29.78	no
	1804	NA	18	18	NA	5.47	50.42	no
168	1841	1843	57	NA	57	26.93	NA	no
169	1822	1825	39	NA	39	26.95	NA	no
170	1839	1840	63	63	63	26.97	50.74	no
171	1792	1795	54	NA	54	27.30	NA	no
172	1818	NA	72	72	NA	27.58	53.92	no
173	1802	1804	57	57	57	27.59	32.43	no
	1848	neg	108	neg	neg	0.60	neg	yes (H)
174	1795	1798	60	60	60	27.96	49.70	no
175	1797	1798	27	NA	27	28.11	NA	no
176	1811	1812	21	NA	21	28.26	NA	no
177	1793	1795	72	72	72	28.39	86.48	no
178	1795	NA	51	51	NA	28.44	40.41	no
179	1802	1804	63	63	63	28.83	50.27	no
180	1783	1786	42	42	42	29.03	41.55	no
181	1809	1810	30	NA	30	29.27	NA	no
182	1823	1825	75	75	75	29.40	35.32	no
	1787	neg	18	neg	neg	0.96	neg	yes (H)
183	1805	1807	36	36	36	29.98	43.15	no
	1797	neg	24	neg	neg	3.23	neg	yes (H)
184	1793	1795	24	24	24	30.42	45.95	no
185	1791	1792	51	51	51	30.42	49.75	no
186	1797	1798	51	NA	51	31.03	NA	no
187	1825	NA	54	54	NA	31.08	50.00	no
188	1792	1795	33	33	33	31.11	46.06	no
189	1778	1780	33	33	33	31.76	47.64	no
190	1793	NA	24	24	NA	31.84	44.17	no
191	1812	NA	33	33	NA	31.91	49.57	no
192	1819	NA	36	36	NA	32.15	48.85	no
193	1792	NA	39	39	NA	32.28	48.72	no
194	1837	1840	108	NA	108	32.42	NA	no
195	1810	1813	39	39	39	32.43	46.61	no
196	1839	1840	36	36	36	32.85	47.31	no
197	1805	1807	36	36	36	32.88	46.64	no

continued on next page

Supplementary Table S1 continued.

patient (UPN)	FLT3-ITD							exclusively
	cDNA position		length [nt]			mutational burden [%]		
	HTAS	S	HTAS	F	S	HTAS	F	
198	1793	NA	18	15	NA	33.12	61.98	no
	neg	NA	neg	48	NA	neg	5.66	yes (F)
199	1821	1822	27	27	27	33.43	45.74	no
200	1781	1795	12	24	24	33.75	50.98	no
201	1808	1810	33	33	33	34.00	49.49	no
202	1787	1789	18	18	18	34.46	41.18	no
203	1805	1807	21	21	21	34.68	48.32	no
204	1787	NA	18	18	NA	34.72	48.37	no
205	1808	1810	27	27	27	34.82	45.05	no
206	1819	1822	45	45	45	34.96	60.06	no
	1843	neg	54	neg	neg	3.89	neg	yes (H)
207	1801	1804	21	21	21	36.58	49.55	no
208	1788	1789	36	36	36	36.99	48.45	no
209	1771	NA	33	33	NA	37.02	50.00	no
210	1783	NA	33	33	NA	37.06	47.45	no
211	1836	1837	81	81	81	37.31	72.77	no
	1836	neg	53	neg	neg	11.06	neg	yes (H)
	1866	neg	175	neg	neg	1.72	neg	yes (H)
212	1800	1801	21	21	21	37.60	48.72	no
213	1809	NA	15	15	NA	37.63	46.47	no
214	1792	1795	42	NA	42	38.60	NA	no
215	1787	1789	60	60	60	38.76	96.15	no
216	1773	1774	27	NA	27	39.75	NA	no
217	1830	1831	27	27	27	40.94	43.28	no
218	1841	1843	60	60	60	42.35	72.50	no
	1793	neg	24	neg	neg	5.43	neg	yes (H)
219	1794	1795	51	51	51	44.55	56.52	no
220	1798	1801	48	48	48	47.08	96.15	no
	1826	neg	90	neg	neg	19.21	neg	yes (H)
221	1838	1840	81	NA	81	48.06	NA	no
222	1794	1795	54	NA	54	48.17	NA	no
223	1826	1828	57	57	57	48.46	69.83	no
224	1809	NA	33	33	NA	50.73	68.35	no
225	1838	1840	36	36	36	50.85	69.81	no
226	1795	1795	21	NA	66	52.06	NA	no
227	1827	1828	33	33	33	53.86	76.61	no
228	1784	1786	30	NA	30	58.71	NA	no
	1843	1846	72	NA	72	7.70	NA	no
229	1826	1828	90	90	90	59.62	88.95	no
230	1808	1810	51	51	51	60.04	79.38	no
231	1830	1831	27	27	27	63.68	64.41	no
232	1779	1780	36	36	36	64.18	81.35	no
233	1801	1804	21	21	21	66.13	79.46	no
	1796	neg	21	neg	neg	0.58	neg	yes (H)
234	1792	NA	54	54	NA	70.94	75.83	no

continued on next page

Supplementary Table S1 continued.

patient (UPN)	FLT3-ITD							exclusively
	cDNA position		length [nt]			mutational burden [%]		
	HTAS	S	HTAS	F	S	HTAS	F	
235	1839	1840	57	57	57	71.60	84.62	no
236	1837	NA	57	57	NA	75.57	92.88	no
	neg	NA	neg	24	NA	neg	17.50	yes (F)
237	1841	1843	60	NA	60	79.49	NA	no
238	1801	1804	60	NA	60	80.19	NA	no
239	1798	NA	33	33	NA	84.02	90.79	no
240	1798	1843	33	66	66	84.02	42.26	no
241	1797	1798	42	42	42	90.46	95.79	no
242	1793	1795	24	24	24	91.08	96.15	no
243	(1840)	NA	(102)	102	NA	(0.46)	1.96	yes (F)
244	neg	1784	neg	3	3	neg	41.42	yes (F)
245	neg	NA	neg	10	NA	neg	48.90	yes (F)
246	neg	NA	neg	84	NA	neg	6.54	yes (F)
247	neg	1813	neg	NA	57	neg	NA	yes (F)
248	(1794)	NA	(78)	78	NA	(0.22)	2.25	yes (F)
249	(1788)	1783	(87)	NA	81	(0.34)	NA	yes (F)
250	(1833)	1834	(78)	NA	78	(0.35)	NA	yes (F)
C-1	1804	neg	30	neg	neg	0.58	neg	yes (H)

Underlined ITD lengths highlight those which were not in-frame. Bold and italic ITD lengths highlight those which were different by HTAS and fragment analysis / Sanger sequencing. Values in light grey and brackets were detected by HTAS below the VAF cut-off level (< 0.5%). UPN (unique patient number), C- (control, assessed *FLT3*-ITD negative according to routine diagnostics), HTAS (high-throughput amplicon sequencing), F (fragment analysis using cDNA), S (Sanger sequencing), nt (nucleotide), NA (not available), neg (negative, not detected).

**Supplementary Table S2. Validation of *FLT3*-ITD length for cases displaying length differences between HTAS and fragment analysis.**

patient (UPN)	<i>FLT3</i> -ITD												
	cDNA position			length [nt]					mutational burden [%]				validated length
	HTAS	S	T(g)	HTAS	F	S	T(g)	F(g)	HTAS	F	T(g)	F(g)	
<b>2</b>	1781	NA	NA	<b>66</b>	<u>65</u>	NA	NA	66	0.82	5.30	NA	2.53	HTAS
<b>8</b>	1839	NA	NA	<b>66</b>	<b>63</b>	NA	NA	66	1.38	3.66	NA	1.67	HTAS
<b>13</b>	1861	1867	NA	<b>78</b>	NA	<b>90</b>	NA	78	0.92	NA	NA	2.82	HTAS
<b>89</b>	1818	NA	NA	<b>60</b>	<b>66</b>	NA	NA	NA	12.21	40.83	NA	NA	NA
<b>135</b>	1832	1825	1824	<b>87</b>	<b>78</b>	<b>78</b>	78	78	9.77	24.30	9.30	21.88	F
<b>158</b>	1839	NA	NA	<b>51</b>	<b>45</b>	NA	NA	45	23.93	45.86	NA	1.09	F
<b>198</b>	1793	NA	NA	<b>18</b>	<b>15</b>	NA	NA	18	33.12	61.98	NA	26.63	HTAS
<b>200</b>	1781	1795	1794	<b>12</b>	<b>24</b>	<b>24</b>	24	24	33.75	50.98	40.33	44.13	F
<b>226</b>	1795	1795	NA	<b>21</b>	NA	<b>66</b>	NA	66	52.06	NA	NA	57.90	F
<b>240</b>	1798	1843	NA	<b>33</b>	<b>66</b>	<b>66</b>	NA	66	84.02	42.26	NA	39.80	F
<b>249</b>	(1788)	1783	NA	(87)	NA	<b>81</b>	NA	neg	(0.34)	NA	NA	neg	NA

Underlined ITD lengths highlight those which were not in-frame. Bold and italic ITD lengths highlight those which were different by HTAS and gDNA fragment analysis / targeted genome sequencing. UPN (unique patient number), HTAS (high-throughput amplicon sequencing), F (fragment analysis using cDNA), S (Sanger sequencing), T(g) (targeted haloplex sequencing using gDNA), F(g) (fragment analysis using gDNA), nt (nucleotide), NA (not available), neg (negative, not detected).



**Supplementary Table S3: Impact of *FLT3*-ITD length on OS, RFS and occurrence with *NPM1*, *KMT2A*-PTD and *CEBPA* mutations.**

<i>FLT3</i> -ITDs	<i>FLT3</i> -ITD length [nt]	no. of patients	median OS [days]	hazard ratio	p-value	median RFS [days]	hazard ratio	p-value	no. of <i>NPM1</i> <sup>+</sup> (n=115)	no. of <i>KMT2A</i> -PTDs <sup>+</sup> (n=19)	no. of <i>CEBPA</i> <sup>+</sup> (n=9)
dominant clone by H (n=242)	<50	107	288 vs. 264	1.021	0.891	209 vs. 210	1.137	0.378	47	3	5
	51-100	120	258 vs. 289	1.062	0.685	209 vs. 214	0.981	0.893	58	16	3
	>100	15	327 vs. 262	0.716	0.305	291 vs. 209	0.643	0.175	10	0	1
dominant clone by F (n=242)	<50	106	292 vs. 261	0.957	0.771	217 vs. 207	1.015	0.919	48	3	5
	51-100	121	255 vs. 294	1.132	0.405	199 vs. 228	1.097	0.525	57	15	3
	>100	15	327 vs. 262	0.716	0.305	291 vs. 209	0.643	0.175	10	0	1

Length of *FLT3*-ITD was assigned according to the dominant clone (n=242) by both methods. OS (overall survival), RFS (relapse free survival), ITD (internal tandem duplication), PTD (partial tandem duplication), nt (nucleotides), no. (number), H (HTAS, high-throughput amplicon sequencing), F (fragment analysis using cDNA).

**Supplementary Table S4: Impact of *FLT3*-ITD localization of the dominant clone (n=242) detected by HTAS according to functional domain on CR after induction therapy, RFS and OS.**

survival parameter	FLT3 domain				
	JM switch motif (n=4)	JM zipper motif (n=128)	JM hinge region (n=35)	TKD1 beta1-sheet (n=62)	NBL (n=13)
CR after induction therapy	2 (50%)	70 (61%)	20 (67%)	38 (63%)	6 (55%)
(no. (%), X <sup>2</sup> , p-value)	0.253	0.049	0.308	0.053	0.281
	0.615*	0.825*	0.579*	0.817*	0.596*
RFS (HR, p-value)	1.261	0.943	1.200	1.070	0.592
	0.691**	0.743**	0.361**	0.683**	0.148**
OS (HR, p-value)	1.330	0.900	1.171	1.152	0.626
	0.625**	0.478**	0.436**	0.401**	0.196**

ITD (internal tandem duplication), TKD1 (tyrosine kinase domain 1), JM (juxtamembrane), NBL (nucleotide binding loop), RFS (relapse free survival), CR (clinical remission), OS (overall survival), HR (hazard ratio), no. (number). \*Chi-Square test \*\*Cox-regression model.

**Supplementary Table S5: Validation of subclonal *FLT3*-ITDs detected by HTAS exclusively.**

patient (UPN)	FLT3-ITD								validated
	cDNA position		length [nt]			mutational burden [%]			
	HTAS	T(g)	HTAS	T(g)	F(g)	HTAS	T(g)	F(g)	
11	1795	neg	21	neg	15	0.50	neg	0.99	(yes)
13	1804	neg	27	neg	27	0.81	neg	1.09	yes
	1802	neg	54	neg	24	0.68	neg	0.60	(yes)
19	1839	NA	57	NA	57	2.50	NA	3.66	yes
	1820	NA	33	NA	33	4.52	NA	20.57	yes
24	1787	NA	33	NA	neg	0.94	NA	neg	no
32	1796	NA	27	NA	27	4.70	NA	6.37	yes
49	1799	1800	30	30	30	5.19	10.83	10.31	yes
50	1838	1837	60	60	60	5.26	13.53	17.15	yes
	1793	1794	24	24	24	0.79	1.56	2.15	yes
	1814	1815	69	69	69	0.69	1.25	1.77	yes
58	1786	1788	21	21	21	6.93	14.40	11.82	yes
	1809	1810	27	27	27	5.09	8.90	11.03	yes
71	1827	NA	72	NA	72	0.52	NA	2.44	yes
74	1819	1820	33	33	33	2.75	2.02	3.48	yes
	1805	1806	30	30	30	2.31	1.52	5.12	yes
77	1792	1794	78	78	78	0.64	0.87	1.96	yes
79	1819	NA	30	NA	30	0.78	NA	1.67	yes
80	1804	NA	60	NA	neg	0.93	NA	neg	no
	1823	NA	51	NA	neg	0.52	NA	neg	no
83	1834	neg	60	neg	neg	0.54	neg	neg	no
88	1801	NA	21	NA	12	8.54	NA	1.38	(yes)
95	1825	NA	18	NA	51	0.81	NA	0.99	(yes)
99	1803	NA	15	NA	15	3.82	NA	7.41	yes
103	1784	neg	39	neg	39	0.89	neg	1.09	yes
105	1808	1809	51	51	51	2.26	2.03	4.67	yes
	1819	1821	72	72	72	1.85	1.58	5.66	yes
106	1829	NA	78	NA	78	0.64	NA	1.38	yes
116	1778	1779	42	42	42	0.62	3.20	6.80	yes

continued on next page

Supplementary Table S5 continued.

patient (UPN)	FLT3-ITD								validated
	cDNA position		length [nt]			mutational burden [%]			
	HTAS	T(g)	HTAS	T(g)	F(g)	HTAS	T(g)	F(g)	
130	1817	neg	45	neg	neg	2.00	neg	neg	no
	1809	neg	75	neg	neg	1.53	neg	neg	no
131	1794	1797	24	24	24	3.11	1.40	3.29	yes
137	1795	1800	36	36	36	9.91	13.87	19.49	yes
149	1792	NA	21	NA	21	4.22	NA	1.28	yes
	1853	NA	72	NA	neg	0.50	NA	neg	no
162	1771	1800	93	30	57	2.74	1.37	1.28	(yes)
	1792	1789	45	45	45	0.58	2.86	3.20	yes
173	1848	neg	108	neg	105	0.60	neg	5.66	(yes)
182	1787	neg	18	neg	NA	0.96	neg	NA	no
183	1797	NA	24	NA	24	3.23	NA	9.75	yes
206	1843	1837	54	54	54	3.89	4.90	9.50	yes
211	1836	neg	53	neg	165	11.06	neg	18.70	(yes)
	1866	1838	175	175	174	1.72	2.60	90.01	(yes)
218	1793	1794	24	24	24	5.43	10.29	11.74	yes
220	1826	NA	90	NA	39	19.21	NA	8.00	(yes)
233	1796	neg	21	neg	12	0.58	neg	3.10	(yes)
C-1	1804	NA	30	NA	neg	0.58	NA	neg	no

Underlined ITD lengths highlight those which were not in-frame. Bold and italic ITD lengths highlight those which were different by HTAS and gDNA fragment analysis / targeted genome sequencing. UPN (unique patient number), C- (control), HTAS (high-throughput amplicon sequencing), T(g) (targeted haloplex sequencing using gDNA), F(g) (fragment analysis using gDNA), nt (nucleotide), NA (not available), neg (negative, not detected).

**Supplementary Table S6: Multivariate analysis of *FLT3*-ITD number and *FLT3*-ITD mutational burden as independent prognostic factor for RFS and OS.**

variable	RFS		OS	
	HR (95% CI)	p-value	HR (95% CI)	p-value
<b><i>FLT3</i>-ITD number – single clone (H)</b>	0.675 (0.450 – 1.014)	0.058	0.753 (0.500 – 1.134)	0.175
<b><i>NPM1</i> mutation status positive</b>	0.626 (0.438 – 0.896)	0.010*	0.666 (0.465 – 0.954)	0.027*
<b>normal karyotype</b>	0.611 (0.350 – 1.065)	0.082	0.653 (0.368 – 1.157)	0.144

variable	RFS		OS	
	HR (95% CI)	p-value	HR (95% CI)	p-value
<b><i>FLT3</i>-ITD number – single clone (F)</b>	0.740 (0.455 – 1.205)	0.227	0.849 (0.509 – 1.416)	0.531
<b><i>NPM1</i> mutation status positive</b>	0.649 (0.455 – 0.926)	0.017*	0.674 (0.470 – 0.964)	0.031*
<b>normal karyotype</b>	0.593 (0.341 – 1.031)	0.064	0.634 (0.358 – 1.120)	0.117

variable	RFS		OS	
	HR (95% CI)	p-value	HR (95% CI)	p-value
<b>total VAF &lt;50% (H)</b>	0.511 (0.284 – 0.919)	0.025*	0.647 (0.361 – 1.157)	0.142
<b><i>NPM1</i> mutation status positive</b>	0.609 (0.424 – 0.872)	0.007*	0.648 (0.451 – 0.931)	0.019*
<b>normal karyotype</b>	0.585 (0.337 – 1.016)	0.057	0.636 (0.360 – 1.123)	0.119

variable	RFS		OS	
	HR (95% CI)	p-value	HR (95% CI)	p-value
<b>total <i>FLT3</i>-ITD mRNA level &lt;50% (F)</b>	0.565 (0.377 – 0.845)	0.005*	0.615 (0.408 – 0.928)	0.020*
<b><i>NPM1</i> mutation status positive</b>	0.714 (0.489 – 1.042)	0.080	0.714 (0.487 – 1.047)	0.085
<b>normal karyotype</b>	0.726 (0.403 – 1.309)	0.288	0.735 (0.400 – 1.351)	0.322

n = 182; \*p-values <0.05; H (high-throughput amplicon sequencing), F (fragment analysis using cDNA); RFS (relapse-free survival); OS (overall survival).

**Supplementary Table S7: Exclusion of sequencing non-specific variants detected in the *FLT3* wild-type cell line HL60 and a type of artificial ITD detected in patient samples.**

variant type	cDNA position	sequence	<i>FLT3</i> -ITD length [nt]
non-specific variant	1712	<u>A</u> AAAGGTAAAAGC	12
non-specific variant	1787	<u>A</u> AAGGTAAAAGCAAAGGTAAAAATTCATTATTCTTTCCTCTATCT GCAGAACTGCCTATTCTCTAACTGACTCATCATTTTCATCTCTG	86
artificial ITD (exemplary)	1896	<u>G</u> GTAATCGAGAATATGAATATGATCTCAAATGGGAGTTTCCAA <b>GAGAAAATTTAGAGTTT*</b>	59
corresponding dominant clone	1843	<u>A</u> GAGAATATGAATATGATCTCAAATGGGAGTTTCCAAGAGAA <b>AATTTAGAGTTTGGTAATC*</b>	60

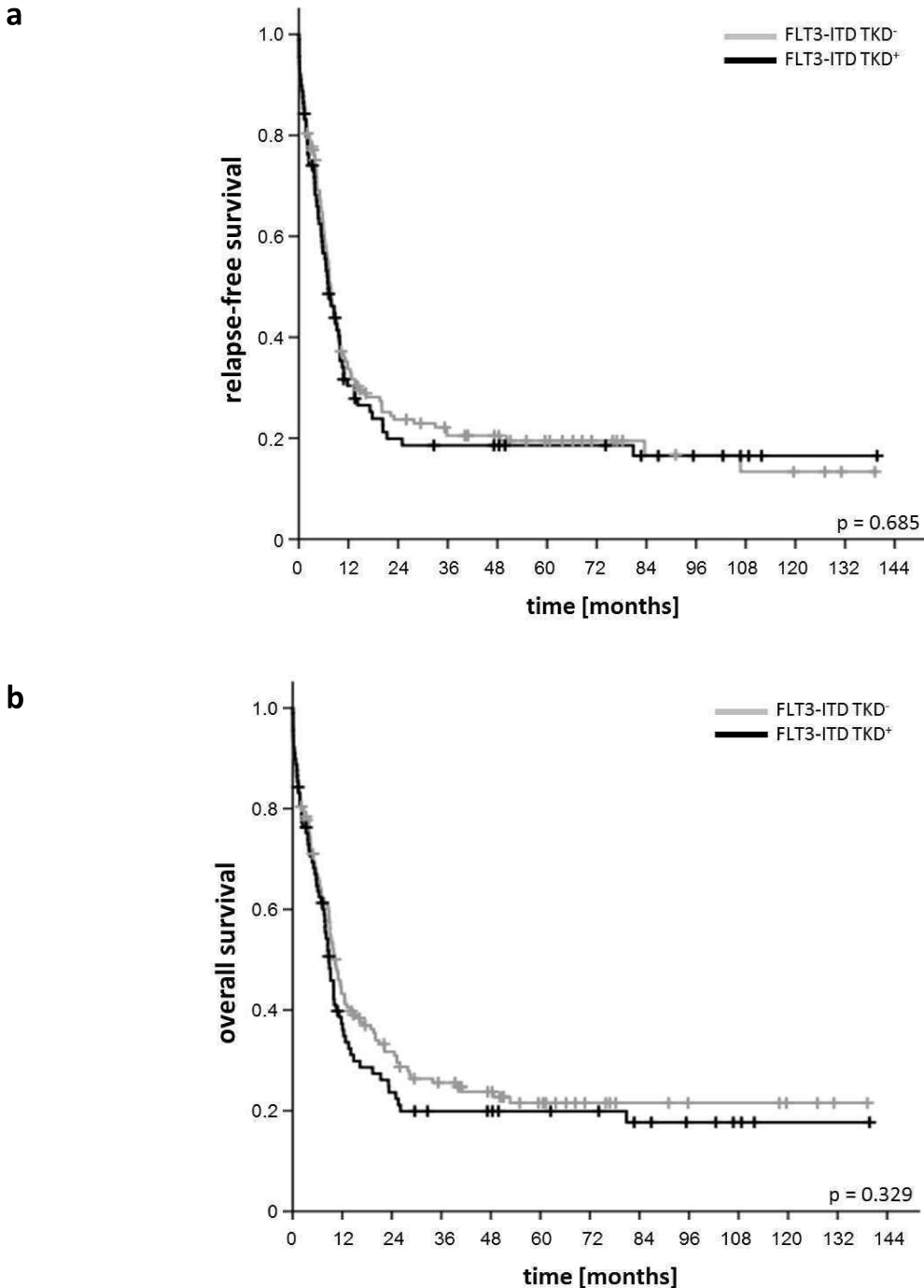
The underlined nucleotide represents the reference base at the given position. \*Overlapping sequence between artificial ITD and corresponding dominant clone is displayed in bold.

**Supplementary Table S8: Custom-designed barcode-sequences for next generation *FLT3* amplicon sequencing, enabling a multiplex run of up to 96 samples by primer-combinations.**

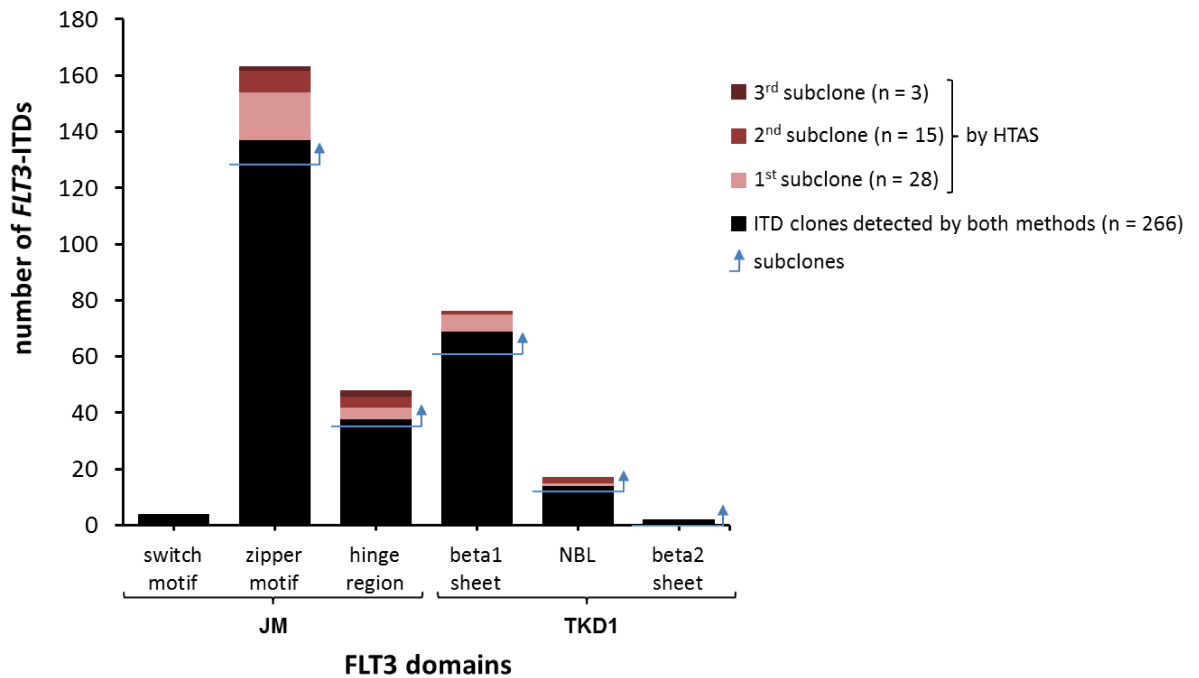
BARCODE		
primer no.	forward	reverse
1	ACCA	ACGCCC
2	AGAT	ATCTGT
3	CTTC	CGACCT
4	GGTT	CGGAGC
5	TATC	CGTTGT
6	TGCT	CTGTTA
7	ATAA	GAAAGT
8	GACC	GCTAAT
9	NA	GCTGCA
10	NA	GTCACC
11	NA	TGACAA
12	NA	TCGTCA

NA (not available), no. (number).

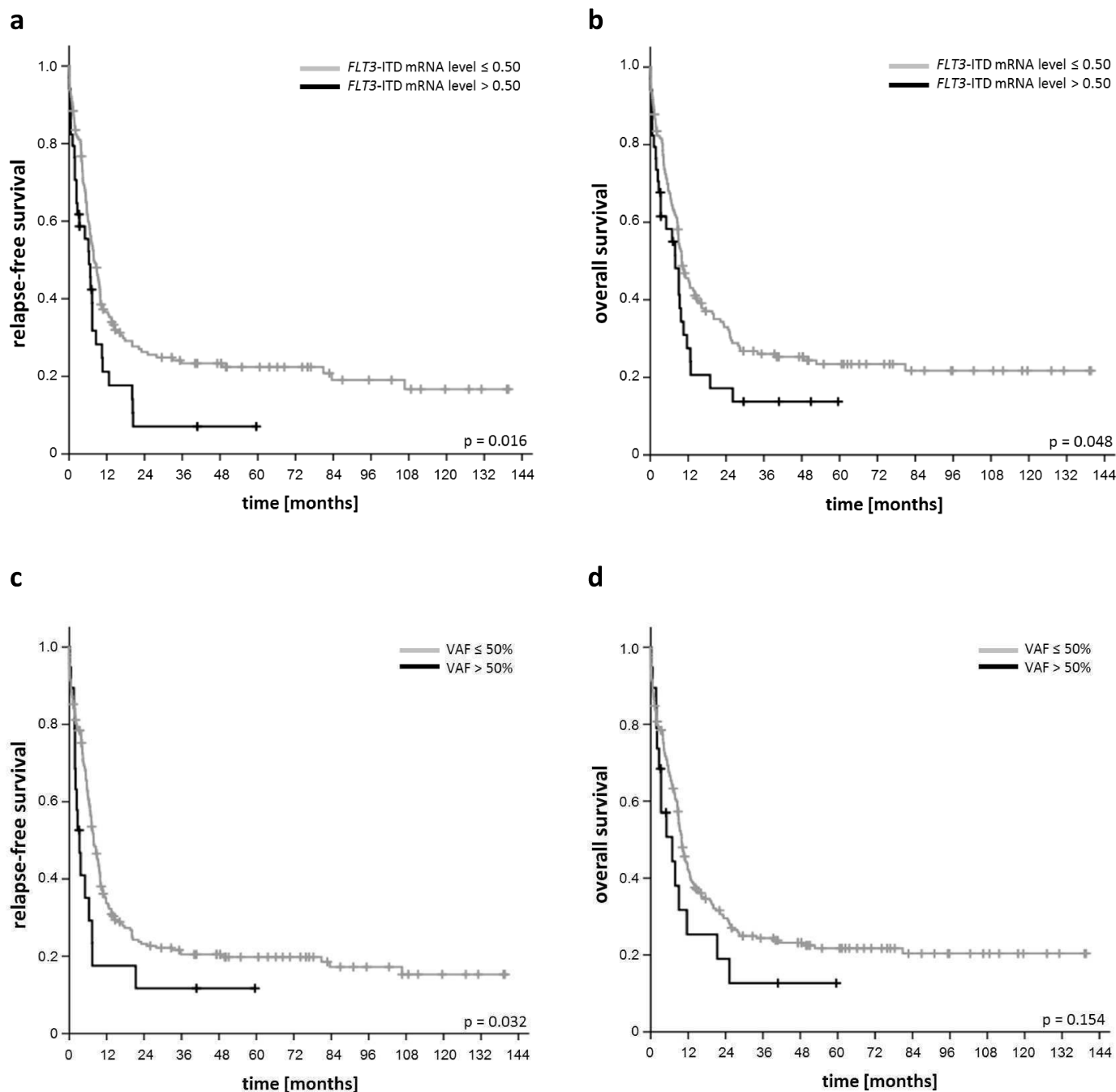
## Supplementary Figures



**Supplementary Figure S1: Impact of the occurrence of *FLT3*-ITD in the TKD on RFS and OS.** **a)** Relapse-free survival (RFS) and **b)** overall survival (OS) of patients according to harbouring a *FLT3*-ITD inside the TKD (*FLT3*-ITD TKD<sup>+</sup>) compared to those located in the JM (*FLT3*-ITD TKD<sup>-</sup>; considering all *FLT3*-ITD clones per patient; n=242; *FLT3*-ITD TKD<sup>+</sup> (n=89), *FLT3*-ITD TKD<sup>-</sup> (n=153)). ITD (internal tandem duplication), TKD (tyrosine kinase domain).

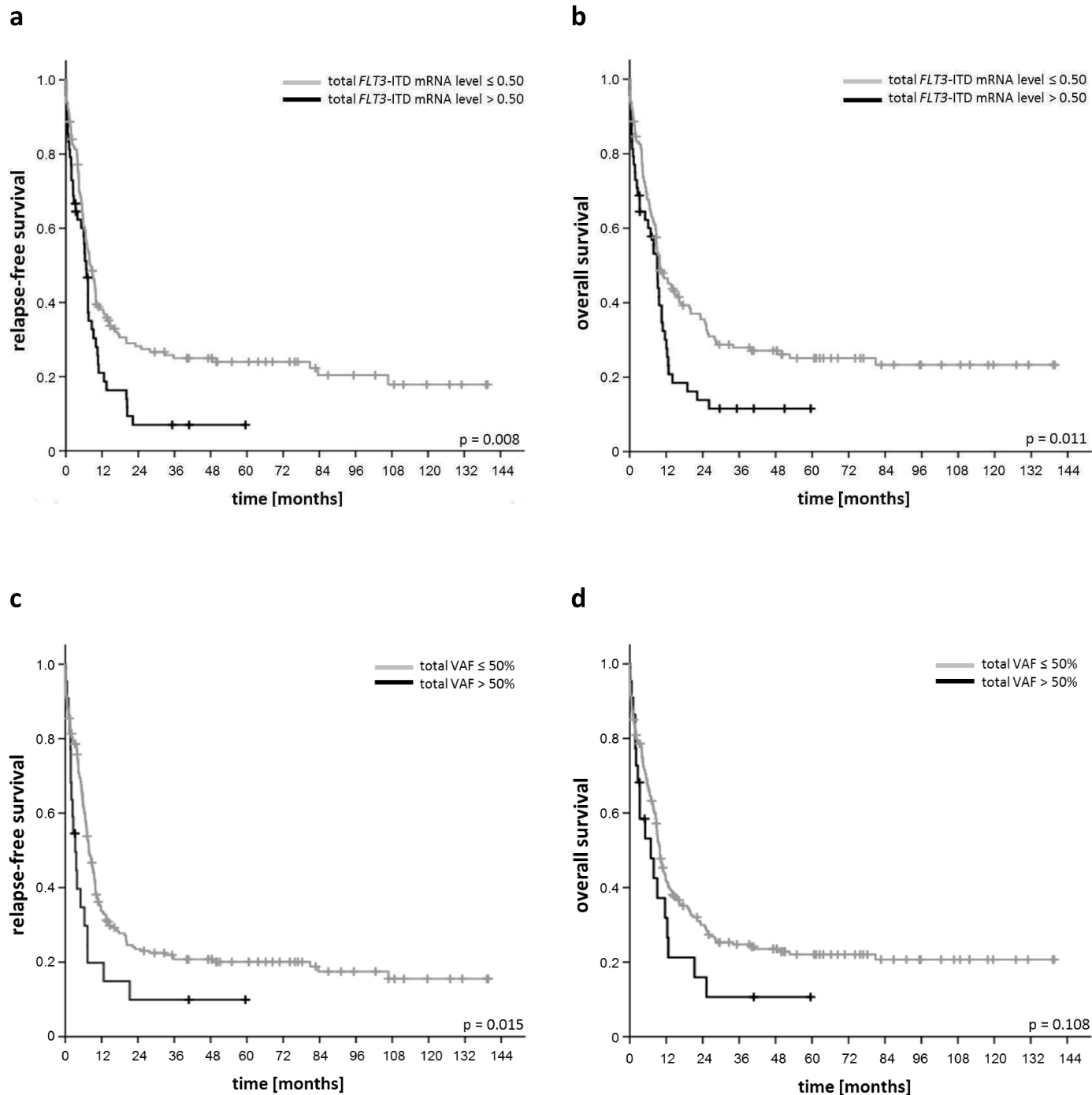


**Supplementary Figure S2: Subclonal ITDs exclusively detected by HTAS according to FLT3 domain.** Of 320 detected ITDs in total (detected by HTAS and/or fragment analysis with cDNA template), 312 ITDs are shown (for the 8 sub-clonal ITDs detected by fragment analysis exclusively no information about ITD position was available). HTAS (high-throughput amplicon sequencing), ITD (internal tandem duplication).

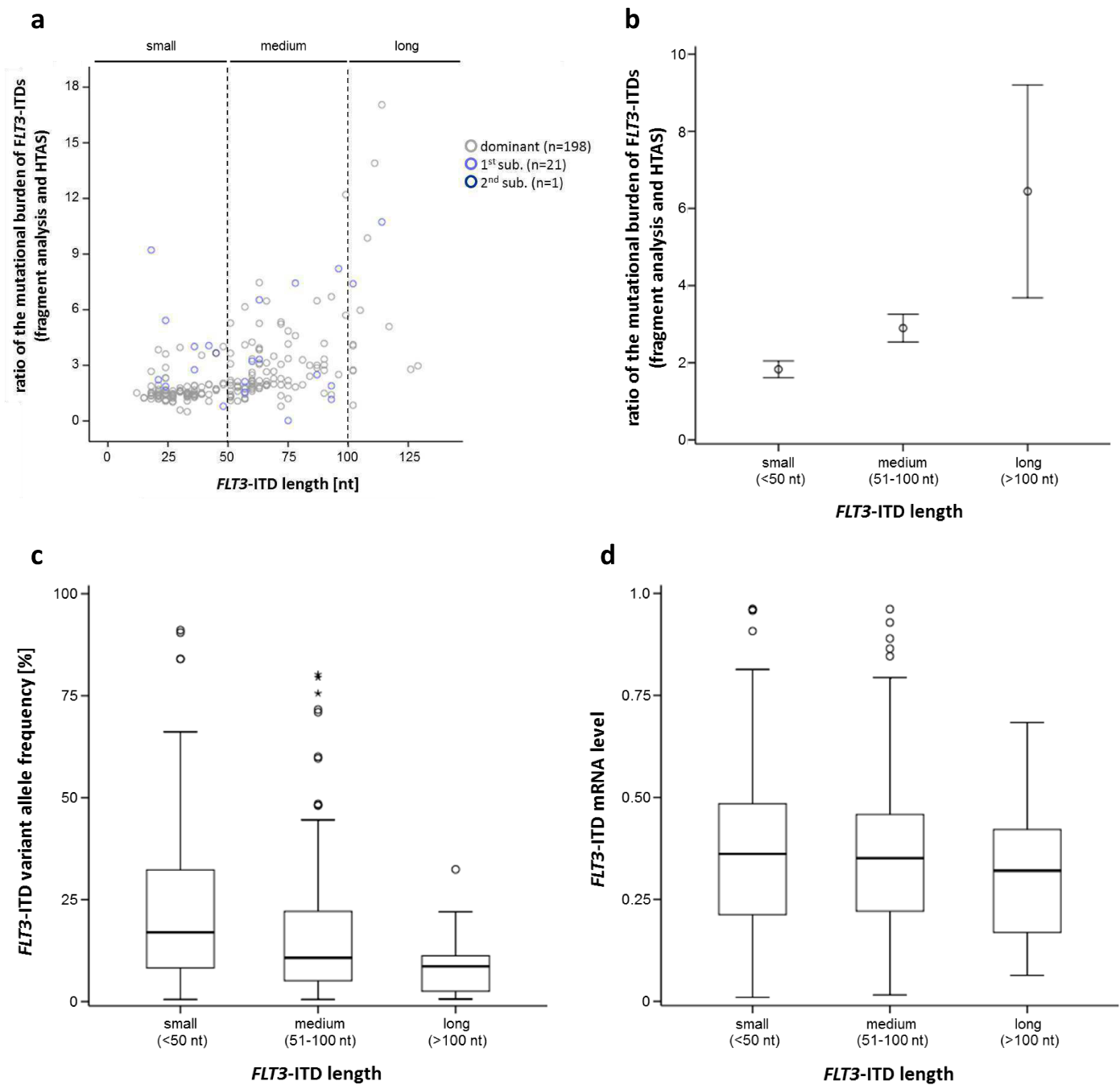


**Supplementary Figure S3: Impact of the *FLT3*-ITD mutational burden of the dominant clone on relapse-free and overall survival.** **a)** Relapse-free and **b)** overall survival according to the *FLT3*-ITD mRNA level measured by fragment analysis with cDNA template (n=198; *FLT3*-ITD mRNA level  $\leq 0.50$  (n=164), *FLT3*-ITD mRNA level  $> 0.50$  (n=34)). **c)** Relapse-free and **d)** overall survival according to the *FLT3*-ITD variant allele frequency (VAF) measured by HTAS with cDNA template (n=242; VAF  $\leq 50\%$  (n=223), VAF  $> 50\%$  (n=19)). HTAS (high-throughput amplicon sequencing), ITD (internal tandem duplication).

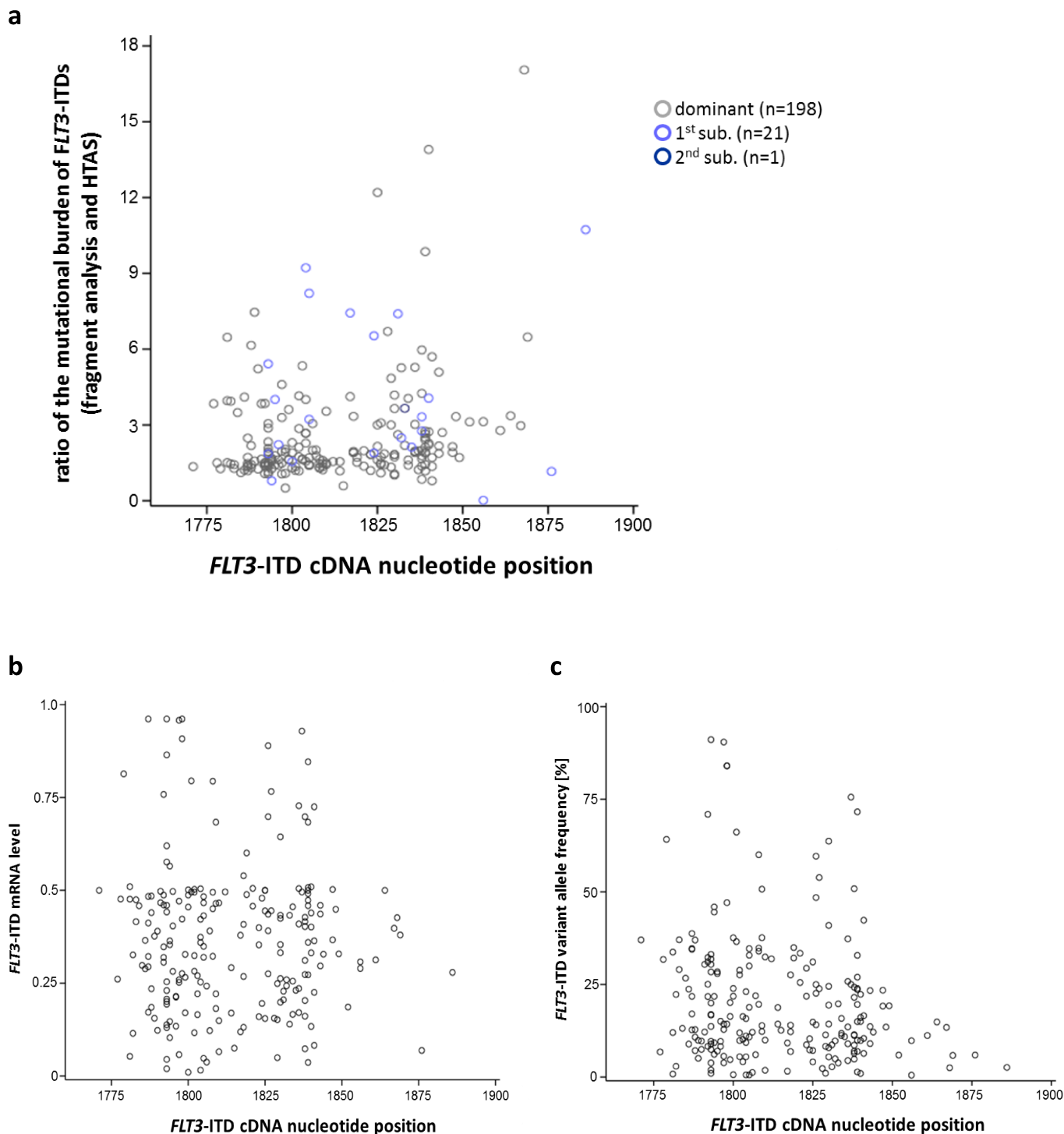




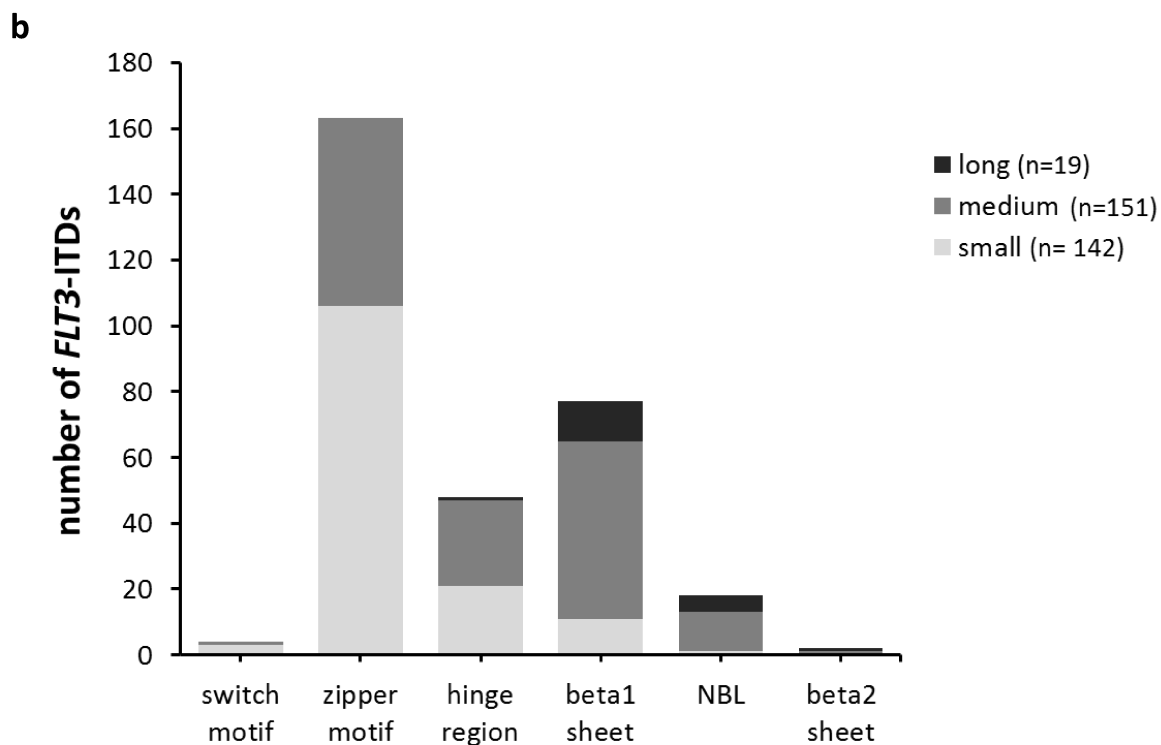
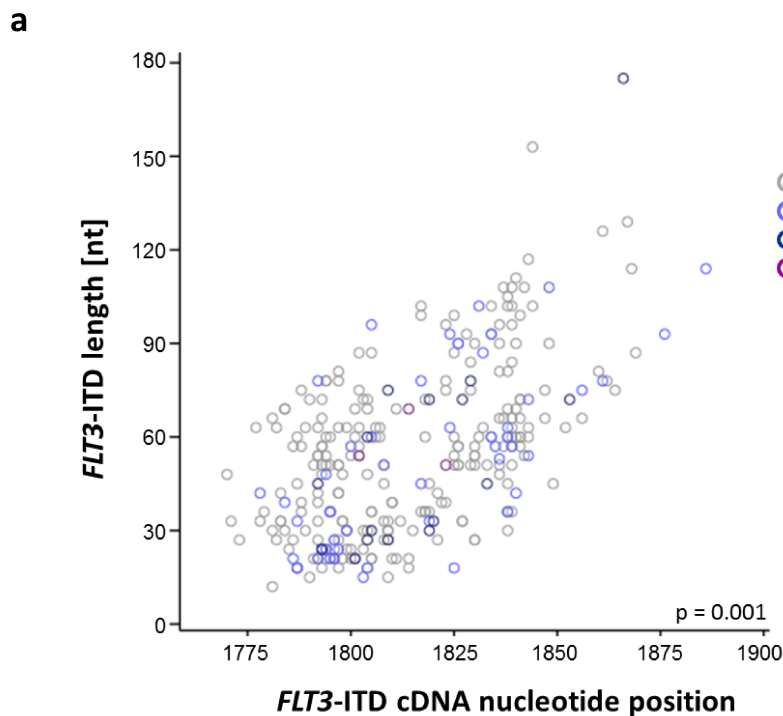
**Supplementary Figure S4: Impact of the *FLT3*-ITD mutational burden of all detected *FLT3*-ITD clones on relapse-free and overall survival.** **a)** Relapse-free and **b)** overall survival according to the total *FLT3*-ITD mRNA level of all *FLT3*-ITD clones measured by fragment analysis with cDNA template ( $n=198$ ; *FLT3*-ITD mRNA level  $\leq 0.50$  ( $n=150$ ), *FLT3*-ITD mRNA level  $> 0.50$  ( $n=48$ )). **c)** Relapse-free and **d)** overall survival according to the total *FLT3*-ITD variant allele frequency (VAF) of all *FLT3*-ITD clones measured by HTAS with cDNA template ( $n=242$ ; VAF  $\leq 50\%$  ( $n=220$ ), VAF  $> 50\%$  ( $n=22$ )). HTAS (high-throughput amplicon sequencing), ITD (internal tandem duplication).



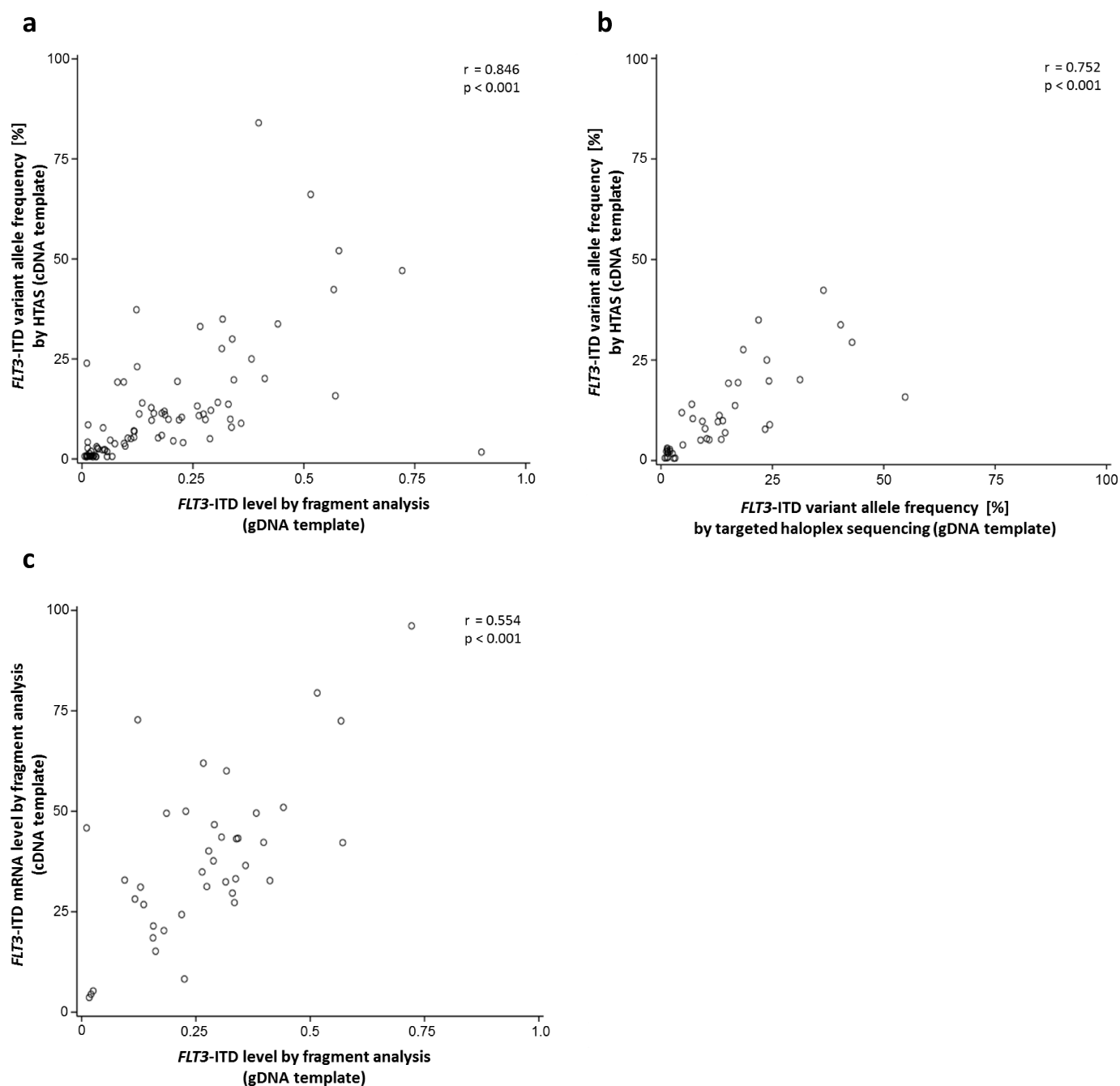
**Supplementary Figure S5: Variance of the mutational burden of *FLT3*-ITD clones according to *FLT3*-ITD size.** Divergence of the mutational burden of *FLT3*-ITDs generated by high-throughput amplicon sequencing (HTAS) and fragment analysis using cDNA template compared to *FLT3*-ITD length (n=220; min.=12 nt, max.=129 nt), classified into three groups: small (<50 nt; n=101), median (51–100 nt; n=105) and long (>100 nt; n=14) of **a**) all data points and **b**) mean values with the corresponding confidence interval CI(95%). **c**) Distribution of the mutational burden of *FLT3*-ITDs generated by HTAS clustered according to *FLT3*-ITD size (n=312; small n=141, medium n=151, long n=19). **d**) Distribution of the mutational burden of *FLT3*-ITDs generated by fragment analysis clustered according to *FLT3*-ITD size (n=228; small n=106, medium n=107, long n=15). nt (nucleotide), ITD (internal tandem duplication), sub (subclone).



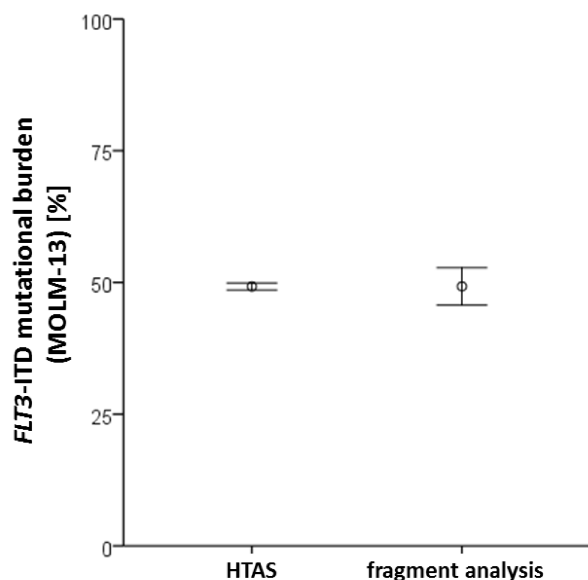
**Supplementary Figure S6: *FLT3*-ITD clone size in relation to *FLT3*-ITD cDNA nucleotide position.** **a)** Divergence of VAF generated by cDNA-based high-throughput amplicon sequencing (HTAS) and fragment analysis compared to *FLT3*-ITD position (determined by HTAS, n=220). Correlation of the *FLT3*-ITD cDNA nucleotide position (determined by HTAS) with **b)** the *FLT3*-ITD mRNA level by fragment analysis and **c)** the variant allele frequency by high-throughput amplicon sequencing (HTAS, n=220). VAF (variant allele frequency), ITD (internal tandem duplication), sub (subclone).



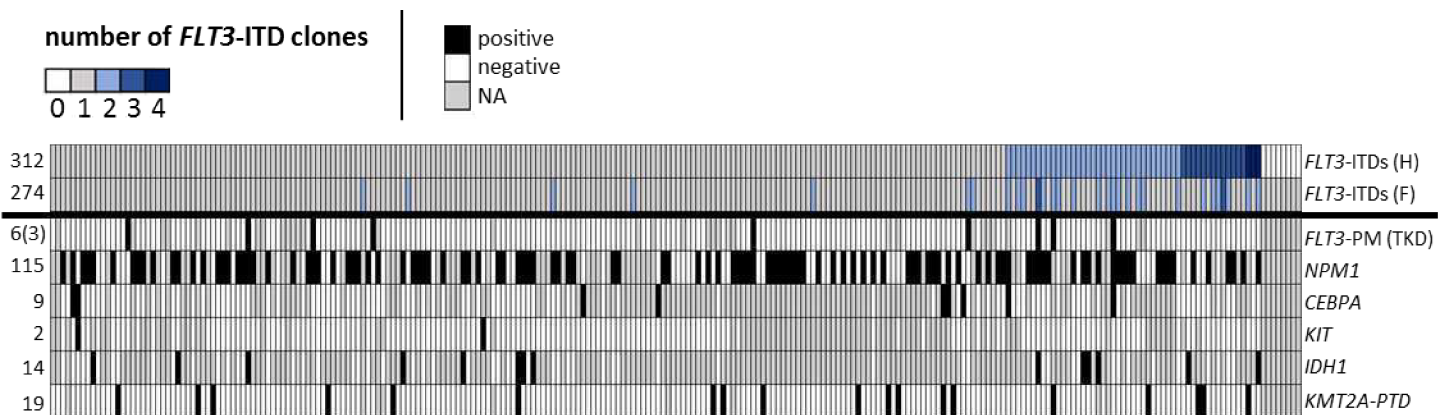
**Supplementary Figure S7: FLT3-ITD length in relation to FLT3-ITD cDNA nucleotide position determined by HTAS. a)** Localization of ITDs according to cDNA nucleotide position in relation to ITD size, displaying a clustering of ITDs according to clonal size. **b)** Localization of ITDs according to functional FLT3 domain, grouping ITDs into three groups depending on insertion size (small (<50nt), medium (51-100nt), large (>100nt)). HTAS (high-throughput amplicon sequencing), ITD (internal tandem duplication), sub (subclone).



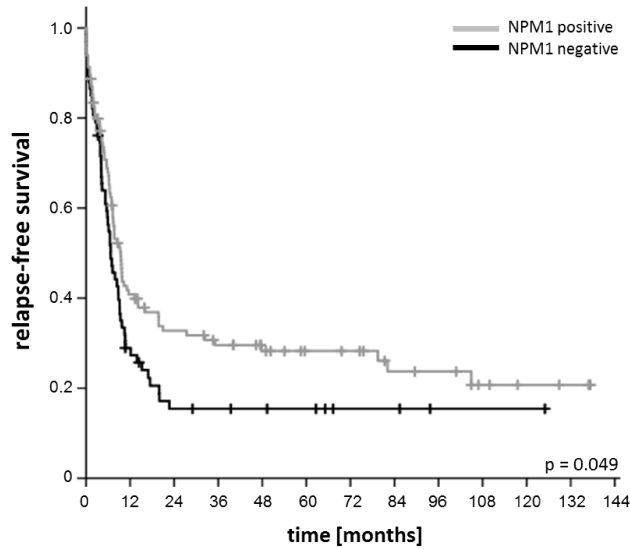
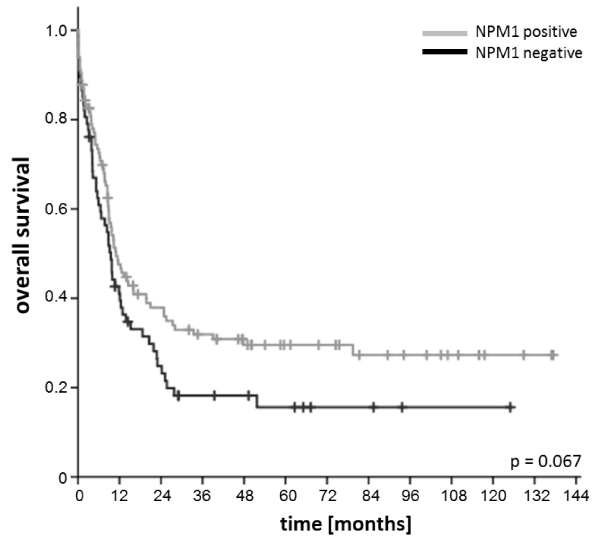
**Supplementary Figure S8: *FLT3*-ITD mutational burden of validated subclones using cDNA versus gDNA template.** Correlation of the variant allele frequency determined by HTAS using cDNA template compared **a)** to the *FLT3*-ITD level determined by fragment analysis using gDNA template (n=86 ITDs, in 42 patient samples) and **b)** to the variant allele frequency determined by targeted haloplex sequencing using gDNA template (n=41 ITDs, in 22 patient samples). **c)** Correlation of the *FLT3*-ITD mRNA level by fragment analysis using cDNA template compared to the *FLT3*-ITD level determined by fragment analysis using gDNA template (n=40 ITDs, in 34 patient samples). HTAS (high-throughput amplicon sequencing), ITD (internal tandem duplication).



**Supplementary Figure S9: Experimental variance of the *FLT3*-ITD mutational burden of MOLM-13.** Experimental variance of the mutational burden for the 21 nt *FLT3*-ITD detected in MOLM-13 cDNA for both *FLT3*-ITD detection methods high-throughput amplicon sequencing (HTAS) and fragment analysis respectively (n=4; mean values with confidence interval CI(95%)). ITD (internal tandem duplication), nt (nucleotide).



**Supplementary Figure S10: Number of *FLT3*-ITDs and co-occurrence of mutations in other cancer related genes.** PM (point mutations; including D835N and V592L), TKD (tyrosine kinase domain), ITD (internal tandem duplication), H (high-throughput amplicon sequencing; HTAS), F (fragment analysis using cDNA), PTD (partial tandem duplication), NA (not available).

**a****b**

**Supplementary Figure S11: Impact of *NPM1* mutation status on RFS and OS.** **a)** Relapse-free survival (RFS) and **b)** overall survival (OS) of *FLT3*-ITD positive patients according to *NPM1* mutation (n=182; *NPM1*<sup>+</sup> (n=115), *NPM1*<sup>-</sup> (n=67)). ITD (internal tandem duplication).





---

## **4.2 The new and recurrent FLT3 juxtamembrane deletion mutation shows a dominant negative effect on the wild-type FLT3 receptor**

---

# SCIENTIFIC REPORTS

OPEN

## The new and recurrent FLT3 juxtamembrane deletion mutation shows a dominant negative effect on the wild-type FLT3 receptor

Received: 12 January 2016

Accepted: 23 May 2016

Published: 27 June 2016

Nadine Sandhöfer<sup>1,2,3,\*</sup>, Julia Bauer<sup>1,\*</sup>, Katrin Reiter<sup>1,2,3</sup>, Annika Dufour<sup>1</sup>, Maja Rothenberg<sup>1</sup>, Nikola P. Konstandin<sup>1</sup>, Evelyn Zellmeier<sup>1</sup>, Belay Tizazu<sup>1</sup>, Philipp A. Greif<sup>1,2,3</sup>, Klaus H. Metzeler<sup>1</sup>, Wolfgang Hiddemann<sup>1,2,3</sup>, Harald Polzer<sup>1,2,3</sup> & Karsten Spiekermann<sup>1,2,3</sup>

In acute myeloid leukemia (AML), the Fms-like tyrosine kinase 3 (*FLT3*) is one of the most frequently mutated genes. Recently, a new and recurrent juxtamembrane deletion mutation (p.Q569Vfs\*2) resulting in a truncated receptor was identified. The mutated receptor is expressed on the cell surface and still binds its ligand but loses the ability to activate ERK signaling. FLT3 p.Q569fs-expressing Ba/F3 cells show no proliferation after ligand stimulation. Furthermore, coexpressed with the FLT3 wild-type (WT) receptor, the truncated receptor suppresses stimulation and activation of the WT receptor. Thus, FLT3 p.Q569Vfs\*2, to our knowledge, is the first *FLT3* mutation with a dominant negative effect on the WT receptor.

The Fms-like tyrosine kinase 3 (*FLT3*) gene encodes a receptor tyrosine kinase (RTK), which is mostly expressed on hematopoietic progenitor cells and enables these cells to proliferate and differentiate. The high prevalence of activating mutations of the *FLT3* gene in acute myeloid leukemia (AML) indicates the importance of *FLT3* for physiological hematopoiesis<sup>1,2</sup>. The most common alterations occur in two functional domains of the receptor. Internal tandem duplications (ITD) disrupt the autoinhibitory function of the juxtamembrane domain and convey ligand-independent phosphorylation and activation of *FLT3*<sup>3</sup>. Point mutations within the activation loop of the tyrosine kinase domain (TKD) mark another class of gain-of-function *FLT3* mutations<sup>4</sup>. Both, ITD and TKD mutations, lead to a constitutive activation of downstream signaling pathways such as the ERK and STAT5 pathway<sup>3,4</sup>. With the technical improvement of sequencing methods over recent years the number of novel identified *FLT3* mutations is increasing. However, the evaluation of functional relevance remains difficult, since the mutation's position in a mutational hotspot or in an important functional receptor domain alone cannot predict its oncogenic potential<sup>5</sup>. In this study we functionally characterized a novel frameshift deletion mutation in the juxtamembrane region (JM) of *FLT3* found in a relapsed patient with AML. We investigated the functional properties of the truncated FLT3 receptor since truncated variants of other receptors have been shown to promote hematopoietic malignancies<sup>6–9</sup>.

### Materials and Methods

**FLT3 mutation analysis.** A patient was referred to our hospital for treatment of AML relapse. Mononuclear cells were isolated from bone marrow aspirates and conventional cytogenetic and mutational analyses were performed in accordance with described protocols<sup>10</sup>. Sequencing of the *FLT3* gene was performed using Sanger sequencing. The FLT3 variant was described according to the guidelines of the Human Genome Variation Society (HGVS) (<http://varnomen.hgvs.org>). Mutations in further AML-related genes were analyzed using a targeted, multiplexed amplicon resequencing approach as previously described<sup>10</sup>. The experimental protocols were approved by the Institutional Review Board of the Department of Internal Medicine III, University Hospital Grosshadern, Ludwig-Maximilians-University (LMU), Munich, Germany and written informed consent was obtained in accordance with the Declaration of Helsinki. The methods were performed in accordance with the approved guidelines.

<sup>1</sup>Department of Internal Medicine III, University Hospital Grosshadern, Ludwig-Maximilians-University (LMU), Munich, Germany. <sup>2</sup>German Cancer Consortium (DKTK), Heidelberg, Germany. <sup>3</sup>German Cancer Research Center (DKFZ), Heidelberg, Germany. \*These authors contributed equally to this work. Correspondence and requests for materials should be addressed to K.S. (email: Karsten.spiekermann@med.uni-muenchen.de)

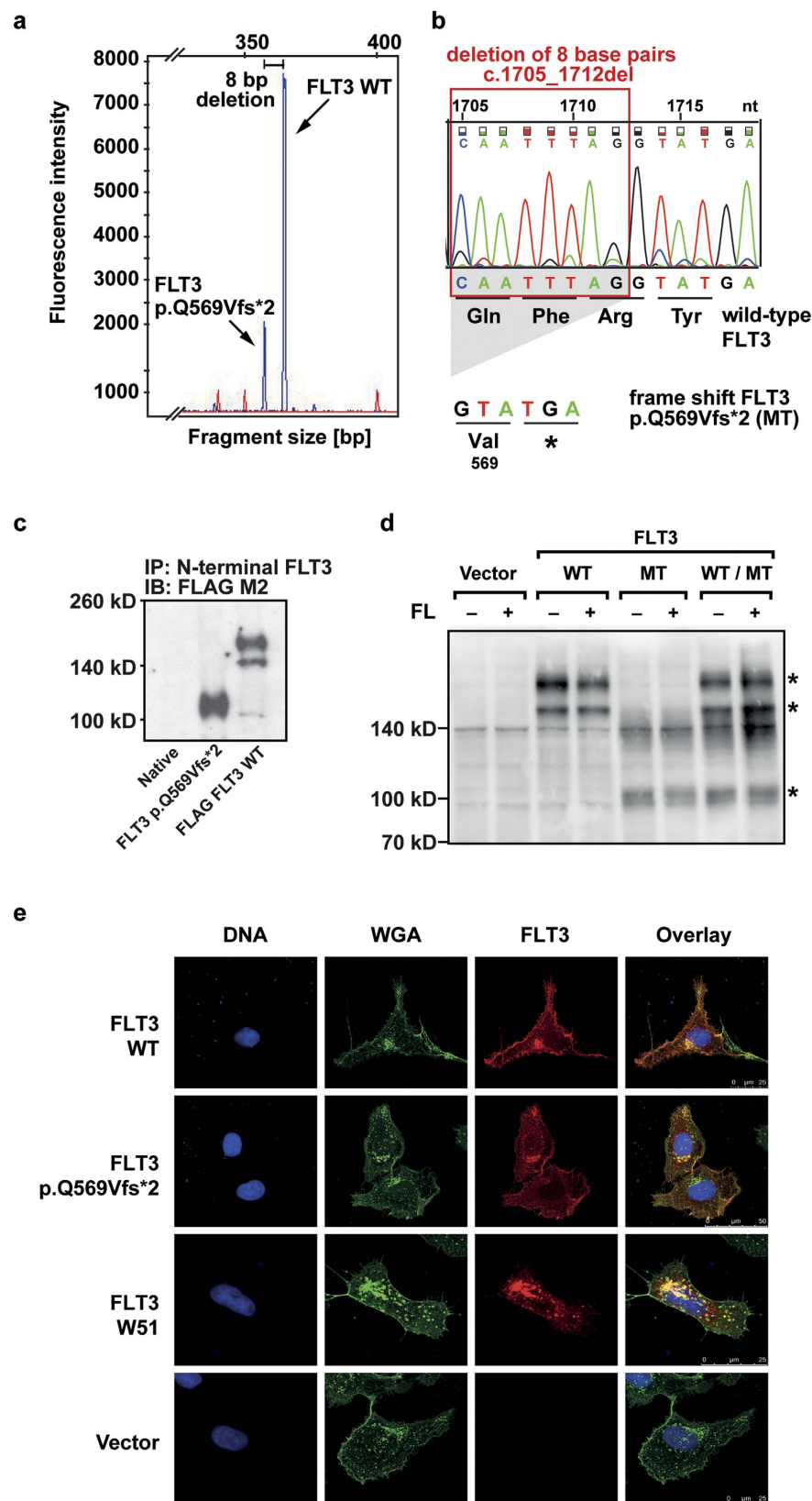


**Figure 1. Identification of the mutation in the patient sample and expression of the truncated FLT3 p.Q569Vfs\*2 receptor.** (a) Blast cells were isolated from the bone marrow of a relapsed AML patient. mRNA was isolated and reverse transcribed. The *FLT3* cDNA was amplified and fragment analysis was performed. Arrows indicate fragments for *FLT3* WT and *FLT3* p.Q569Vfs\*2. The peaks differ by eight base pairs in their fragment size. (b) Sanger sequencing revealed a deletion of eight nucleotides, leading to a frameshift and a premature stop codon within the *FLT3* gene. The chromatogram is shown for the wild-type *FLT3*, nucleotide triplets and the corresponding amino acids are shown for the *FLT3* WT and the frameshift mutation *FLT3*

p.Q569Vfs\*2 sequence. (c) Phoenix eco cells were transfected with FLAG-tagged *FLT3* WT and FLAG-tagged *FLT3* p.Q569Vfs\*2. After cell lysis the FLT3 protein was immunoprecipitated from whole cell lysates with an N-terminal FLT3 antibody (SF1.340). After blotting the FLAG-tagged FLT3 was detected with an FLAG M2 antibody. One representative experiment is shown. The blot was cropped to improve the clarity of the image. (d) Ba/F3 cells stably expressing the indicated constructs. After cell lysis the FLT3 protein was detected with an N-terminal FLT3 antibody (4B12). One representative experiment is shown. FLT3 bands are indicated by asterisks. The blot was cropped to improve the clarity of the image (MT = FLT3 p.Q569Vfs\*2). (e) Immunofluorescence of FLT3 (red), glycoconjugates (green) and counterstaining of DNA (blue) in transiently transfected U2OS cells. One representative image of each construct is shown.

**Cell culture and reagents.** The Ba/F3, Hek-293T, and WEHI-3B cell lines were obtained from DSMZ (Braunschweig, Germany), the U2OS cell line from ATCC (Wesel, Germany) and cultured according to the supplier's recommendation. The retroviral packaging cell line Phoenix eco was purchased from Orbigen (San Diego, CA, USA). Recombinant human FLT3 ligand (FL) was obtained from PromoKine (Heidelberg, Germany), recombinant murine IL-3 from ImmunoTools (Friesoythe, Germany) and AC220 was obtained from Selleck Chemicals (Houston, TX, USA).

**Generation of cell lines.** The *FLT3* p.Q569Vfs\*2 and the FLAG *FLT3* p.Q569Vfs\*2 cDNA were synthesized by GENEART (Life Technologies, Regensburg, Germany) and subcloned into the MSCV-IRES-eYFP retroviral expression vector. The empty vector, MSCV-IRES-eGFP-*FLT3*-WT, and MSCV-IRES-eGFP-*FLT3*-W51 have been described previously<sup>11</sup>. For the stable transduction of Ba/F3 cells the retroviral supernatant of Phoenix eco cells was used<sup>11</sup>. Stable expression of the receptor was confirmed by real time-PCR, Western blot, immunoprecipitation and flow cytometry as described elsewhere<sup>11,12</sup>. The following antibodies were used as recommended by the manufacturer: anti FLAG (M2), alpha-Tubulin (T6199), goat anti rabbit secondary antibody from Sigma-Aldrich (St. Louis, MO, USA), FLT3 (SF1.340, S-18), phospho-tyrosine (PY99), goat anti mouse and goat anti rat secondary antibodies from Santa Cruz Biotechnology (CA, USA), ERK and phospho-ERK (Thr202/Tyr204) from Cell Signaling Technology (Danvers, MA, USA). The FLT3-antibody (4B12) was provided by Dr. Elisabeth Kremmer (Helmholtz Center Munich).

**Cell proliferation assay.**  $4 \times 10^4$ /mL Ba/F3 cells were cultured in the presence or absence of 10 ng IL-3 and 50 ng FL for 72 hours. Viable cells were counted by trypan blue exclusion using the cell viability analyzer Vi-CELL AS (Beckman Coulter, Krefeld, Germany)<sup>11</sup>.

**FL binding assay.** Binding of the FL was analyzed using the Fluorokine biotinylated human FL kit (NFFK0) and streptavidin-allophycocyanin (APC) (F0050) (R&D Systems, Minneapolis, MN, USA) according to the supplier's recommendations. As a negative staining control cells were stained with biotinylated soybean trypsin inhibitor. To confirm staining specificity cells were incubated with unbiotinylated FL in parallel.

**Immunofluorescent staining.** U2OS cells were transiently transfected using the PolyFect transfection reagent (QIAGEN, Hilden, Germany). 50,000 cells were seeded on coverslips one day prior transfection. For transfection 1.5 µg plasmid DNA, 5 µL of transfection reagent and Opti-MEM Reduced Serum Medium (Thermo Fisher Scientific, Braunschweig, Germany) were used. The medium was changed six hours later. Glycoconjugates were stained 48 hours post-transfection using anti-wheat germ agglutinin (WGA)-488 fluorescein conjugate (1:1000; Life Technologies, Carlsbad, CA, USA) for 10 minutes. Thereafter cells were fixed on ice for 10 minutes using pre-cooled methanol and blocked for 1 hour with 2% BSA in DPBS. Cells were then incubated with monoclonal mouse or polyclonal rabbit FLT3 (SF1.340, S-18) antibody (1:200; Santa Cruz Biotechnology) for 1 hour, followed by washing with DPBS-T (0.1% Tween 20; Carl Roth, Karlsruhe, Germany). Secondary antibody incubation was performed for 1 hour with anti-mouse IgG (H + L), F (ab')<sub>2</sub> fragment Alexa Fluor 594 Conjugate (1:500; Cell Signaling Technology). For counterstaining 1 µg/mL 4',6-diamidino-2-phenylindole (DAPI) was used (Sigma-Aldrich), followed by mounting. Specimens were finally analyzed utilizing a confocal fluorescence laser scanning system (TCS SP5 II; Leica, Wetzlar, Germany). For image acquisition and processing we used the LAS AF Lite Software (Leica).

## Results

**The FLT3 mutation (p.Q569Vfs\*2), present only at relapse, results in a truncated FLT3 receptor lacking essential parts for autophosphorylation.** The *FLT3* mutation (FLT3 p.Q569Vfs\*2) was found during routine diagnostics in a patient with relapsed AML and 15% blasts in the bone marrow (Supplemental Table S1). Fragment size analysis from cDNA showed the *FLT3* wild-type (WT) peak and an additional smaller and shorter fragment (Fig. 1a), indicating a smaller proportion of cells with an alternative *FLT3* transcript. The allele frequency of the detected mutation could not be determined as there was no patient gDNA material available. At the time point of first diagnosis, this fragment was not present (Supplemental Table S1). At the time point of initial diagnosis, the major leukemic clone carried an *IDH2* mutation with an allele frequency of 20.4%. *NPM1c* was present only in a subfraction (7.2% allele frequency) and *FLT3*-ITD/TKD mutations were undetectable (Supplemental Table S1). By Sanger sequencing a deletion in the *FLT3* gene of eight base pairs leading to a frameshift followed by a premature stop codon was identified (Fig. 1b). The mutant is predicted to result in a truncated FLT3 protein, consisting of 570 amino acids and lacking the intracellular parts essential for autophosphorylation of the receptor and downstream signal transduction (Fig. S1). Due to lack of adequate patient material, it was not possible to finally prove the expression of the truncated protein in the patient's bone marrow. To characterize

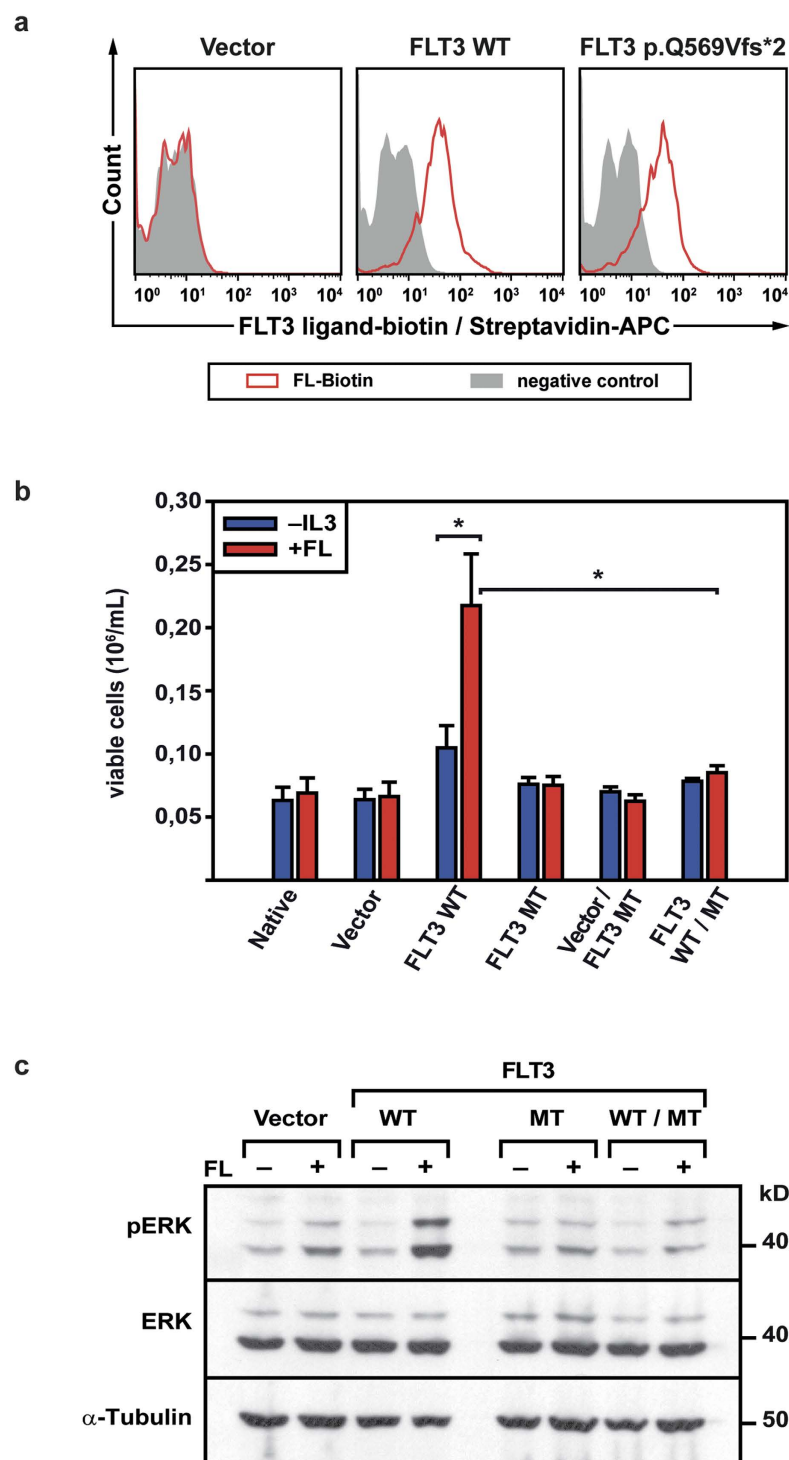


**Figure 2.** FL binding by the truncated FLT3 p.Q569Vfs\*2 receptor, downstream signaling pathways, and proliferation of Ba/F3 cells. **(a)** Ba/F3 cells stably expressing the indicated constructs were incubated with biotinylated human FL. Receptor bound biotinylated FL was detected with streptavidin-APC using flow cytometry. As a negative control biotinylated soybean trypsin inhibitor was used. One out of at least three independent experiments is shown. **(b)** Ba/F3 cells stably expressing the indicated constructs were seeded at a density of  $4 \times 10^4$ /mL in the presence or absence of 50 ng FL. Viable cells were counted by trypan blue exclusion after 72 hours. Shown are mean values  $\pm$  SEM of at least three independent experiments;  $*p < 0.05$  (MT = FLT3 p.Q569Vfs\*2). **(c)** Ba/F3 cells stably expressing the empty vector, FLT3 WT, FLT3 p.Q569Vfs\*2 alone or both FLT3 WT and FLT3 p.Q569Vfs\*2 were starved for 24 hours in cell culture media containing 0.3% fetal calf serum. Cells were left untreated (–) or stimulated (+) with 100 ng/mL FL for 60 minutes prior to cell lysis. Phosphorylation of ERK was analyzed by western blot. One representative experiment is shown. The blot was first incubated with phospho ERK antibody, stripped and reblotted with ERK and  $\alpha$ -Tubulin antibody. The blot was cropped to improve the clarity of the image (MT = FLT3 p.Q569Vfs\*2).

the functional consequences of the deletion mutation we thus generated Ba/F3 cells stably expressing *FLT3* WT and *FLT3* p.Q569Vfs\*2. In Western Blot analysis we observed a band of lower molecular weight (110 kD) in *FLT3* p.Q569Vfs\*2-expressing cells in comparison to the WT receptor (140/160 kDa), confirming the expression of a truncated protein (Fig. 1c,d, the full-length blots are shown in supplemental Fig. S4a–c).

### The loss of function *FLT3* p.Q569Vfs\*2 mutant suppresses *FLT3* WT in a dominant negative manner by forming heterodimers with the WT *FLT3* receptor.

*FLT3* p.Q569Vfs\*2 receptor expression on the cell surface was confirmed by flow cytometry and immunofluorescent staining (Fig. 1e, Supplemental Fig. S2) and binding of FL by FL binding assays with biotinylated FL (Fig. 2a). After adding of unbiotinylated FL to the sample, the binding capacity for biotinylated FL decreased in a dose dependent manner indicating the specificity of the FL binding assay (Supplemental Fig. S3). By immunoprecipitation the truncated *FLT3* protein in double-transfected Hek-293T cells, and immunoblot against a C-terminal *FLT3* epitope, heterodimerisation of the truncated and the wildtype *FLT3* receptor became detectable (Fig. S5b). In contrast to *FLT3* WT, *FLT3* p.Q569Vfs\*2-expressing Ba/F3 cells did not proliferate after FL stimulation (Fig. 2b). Furthermore, coexpression of WT and mutant *FLT3* receptor also abolished the WT receptor's proliferative effect on Ba/F3 cells when stimulated with FL (Fig. 2b). This observation was confirmed by analyzing the downstream signaling pathway. Stimulation of *FLT3* WT-expressing cells with FL led to strong *FLT3* and subsequent ERK phosphorylation which were absent in *FLT3* p.Q569Vfs\*2-expressing and *FLT3* p.Q569Vfs\*2/*FLT3* WT-coexpressing cells, respectively (Fig. 2c, the full-length blots are shown in supplemental Fig. S4d,e and Fig. S5c,d).

In order to address a possible growth advantage of the *FLT3* p.Q569Vfs\*2-expressing cells, we performed proliferation assays in Ba/F3 cells treated with the highly potent *FLT3* inhibitor AC220 in two different concentrations. Neither the *FLT3* p.Q569Vfs\*2 cells nor the double-transduced cells had a growth advantage under the chosen conditions (see supplemental Fig. S5a).

## Discussion

AML-specific mutations within the *FLT3* gene have been of high interest and were studied in detail over the past decades. In contrast to the highly prevalent activating mutations the impact of receptor truncating mutations in *FLT3* remains largely unknown, especially regarding their proliferative activity. To our knowledge, this is the first study to functionally characterize a patient derived loss-of-function *FLT3* mutation resulting in a dominant negative effect on the WT receptor. Our analysis demonstrated that the truncated *FLT3* receptor lack both TKDs that are crucial for signal transduction, thus being unable to activate ERK phosphorylation and proliferation upon ligand binding. These effects were dominant negative on *FLT3* WT in cells coexpressing both *FLT3* WT and p.Q569Vfs\*2.

In analogy, kinase-negative or truncated EGF receptors can exert a dominant negative effect on WT receptors by inhibiting the tyrosine kinase activity and suppressing the mitogenic response of WT receptors through heterodimerisation<sup>13,14</sup>. However, the receptor truncation does not always imply a loss of function. Alterations of the *CSF3R* gene, which lead to a truncated cytoplasmic tail, showed an activating and hyperresponsive phenotype and have been linked to the development of AML, chronic myeloid and neutrophilic leukemia<sup>6,7</sup>. Similarly, truncations in the extracellular domain of the TrkA receptor ("Delta TrkA") constitutively activate the receptor in fibroblast and epithelial cell lines<sup>8,9</sup>.

The loss-of-function phenotype of *FLT3* p.Q569Vfs\*2 suggests that the patient's AML blasts proliferate independently of *FLT3* kinase activity. We cannot exclude that *FLT3* p.Q569Vfs\*2 is a passenger mutation in a mutational hotspot region of the *FLT3* gene and does not influence leukemogenesis. However, the same somatic deletion mutation has been reported recently as a somatic and recurrent mutation, detected in two out of 6843 unselected AML patients resulting in a frequency of 0.03%<sup>15</sup>. It is tempting to speculate that a leukemic cell may benefit from truncating *FLT3* mutations through escape from the *FLT3* receptor mediated growth regulation. Functional characterization of *FLT3* mutations nevertheless is of major importance to identify driver mutations, validate therapeutic targets and analyze the mechanisms of receptor interaction and activation. Our study shows that mutations of *FLT3* do not always accompany a gain of function and functional relevance has to be investigated on an individual basis.

## References

1. Schnittger, S. *et al.* Analysis of *FLT3* length mutations in 1003 patients with acute myeloid leukemia: correlation to cytogenetics, FAB subtype, and prognosis in the AMLCG study and usefulness as a marker for the detection of minimal residual disease. *Blood*. **100**(1), 59–66 (2002).
2. Thiede, C. *et al.* Analysis of *FLT3*-activating mutations in 979 patients with acute myelogenous leukemia: association with FAB subtypes and identification of subgroups with poor prognosis. *Blood*. **99**(12), 4326–35 (2002).
3. Kiyoi, H. *et al.* Internal tandem duplication of the *FLT3* gene is a novel modality of elongation mutation which causes constitutive activation of the product. *Leukemia*. **12**(9), 1333–7 (1998).
4. Yamamoto, Y. *et al.* Activating mutation of D835 within the activation loop of *FLT3* in human hematologic malignancies. *Blood*. **97**(8), 2434–9 (2001).
5. Frohling, S. *et al.* Identification of driver and passenger mutations of *FLT3* by high-throughput DNA sequence analysis and functional assessment of candidate alleles. *Cancer Cell*. **12**(6), 501–13 (2007).
6. Liongue, C. & Ward, A. C. Granulocyte colony-stimulating factor receptor mutations in myeloid malignancy. *Front Oncol*. **4**, 93 (2014).
7. Maxson, J. E. *et al.* Oncogenic *CSF3R* mutations in chronic neutrophilic leukemia and atypical CML. *N Engl J Med*. **368**(19), 1781–90 (2013).
8. Meyer, J. *et al.* Remarkable leukemogenic potency and quality of a constitutively active neurotrophin receptor, deltaTrkA. *Leukemia*. **21**(10), 2171–80 (2007).
9. Reuther, G. W. *et al.* Identification and characterization of an activating TrkA deletion mutation in acute myeloid leukemia. *Mol Cell Biol*. **20**(23), 8655–66 (2000).



10. Sandhofer, N. *et al.* Dual PI3K/mTOR inhibition shows antileukemic activity in MLL-rearranged acute myeloid leukemia. *Leukemia*. **29**(4), 828–38 (2015).
11. Polzer, H. *et al.* Casitas B-lineage lymphoma mutants activate AKT to induce transformation in cooperation with class III receptor tyrosine kinases. *Exp Hematol*. **41**(3), 271–80 e4 (2013).
12. Janke, H. *et al.* Activating FLT3 mutants show distinct gain-of-function phenotypes *in vitro* and a characteristic signaling pathway profile associated with prognosis in acute myeloid leukemia. *PLoS One*. **9**(3), e89560 (2014).
13. Basu, A. *et al.* Inhibition of tyrosine kinase activity of the epidermal growth factor (EGF) receptor by a truncated receptor form that binds to EGF: role for interreceptor interaction in kinase regulation. *Mol Cell Biol*. **9**(2), 671–7 (1989).
14. Kashles, O. *et al.* A dominant negative mutation suppresses the function of normal epidermal growth factor receptors by heterodimerization. *Mol Cell Biol*. **11**(3), 1454–63 (1991).
15. Chatain, N. *et al.* Rare FLT3 deletion mutants may provide additional treatment options to patients with AML: an approach to individualized medicine. *Leukemia*. **29**(12), 2434–8 (2015).

## Acknowledgements

We thank Prof. Dr. Thorsten Haferlach for providing first diagnosis material and Elisabeth Kremmer for generating the N-terminal FLT3 antibody.

## Author Contributions

N.S., J.B., H.P., N.P.K., W.H., K.H.M. and K.S. designed the experiments; J.B., N.S., H.P., K.R., E.Z. and B.T. performed the experiments; J.B., N.S., H.P., M.R., A.D., P.A.G. and K.H.M. analyzed and interpreted the data; N.S., J.B., K.R., H.P. and K.S. wrote the manuscript.

## Additional Information

**Supplementary information** accompanies this paper at <http://www.nature.com/srep>

**Competing financial interests:** The authors declare no competing financial interests.

**How to cite this article:** Sandhöfer, N. *et al.* The new and recurrent FLT3 juxtamembrane deletion mutation shows a dominant negative effect on the wild-type FLT3 receptor. *Sci. Rep.* **6**, 28032; doi: 10.1038/srep28032 (2016).



This work is licensed under a Creative Commons Attribution 4.0 International License. The images or other third party material in this article are included in the article's Creative Commons license, unless indicated otherwise in the credit line; if the material is not included under the Creative Commons license, users will need to obtain permission from the license holder to reproduce the material. To view a copy of this license, visit <http://creativecommons.org/licenses/by/4.0/>

## **Supplementary information**

### **The new and recurrent FLT3 deletion mutation (p.Glu569fs) shows a dominant negative effect on the wild type FLT3 receptor**

*Nadine Sandhöfer, Julia Bauer, Katrin Reiter, Annika Dufour, Maja Rothenberg, Nikola Konstandin, Evelyn Zellmeier, Philipp A. Greif, Klaus H. Metzeler, Wolfgang Hiddemann, Harald Polzer, and Karsten Spiekermann*

### **Supplemental Tables:**

- Supplemental Table S1: Overview about available material and performed analyses.

### **Supplemental Figures:**

- Supplemental Figure S1: Schematic representation of the truncated FLT3 receptor in comparison to the WT receptor.
- Supplemental Figure S2: Cell surface expression of FLT3 constructs.
- Supplemental Figure S3: Binding capacity for biotinylated FLT3 ligand.
- Supplemental Figure S4: Full-length immuno blots of figure 1 and 2.
- Supplemental Figure S5: Dominant negative effect of FLT3 p.Q569fs and heterodimerisation



**Supplemental Table S1: Overview about available material and performed analyses.**

	<b>Initial diagnosis</b>	<b>Relapse</b>
<b>Blast cells</b>	39% (pB)	15% (BM)
<b>Available patient material</b>		
<b>gDNA</b>	x	NA
<b>cDNA</b>	x	x
<b>Mutational analyses on cDNA</b>	NPM1 c.860_863dup	NPM1 c.860_863dup
	/	FLT3 c.1705_1712del
<b>Mutational analyses on gDNA (Allele frequency)</b>	IDH2 (20.39%)	NA
	NPM1c (7.17%)	NA
<b>Karyotype</b>	no dividing cells	ND

x: available, BM: bone marrow, pB: peripheral blood, NA: not available, ND: not determined

**Figure S1**

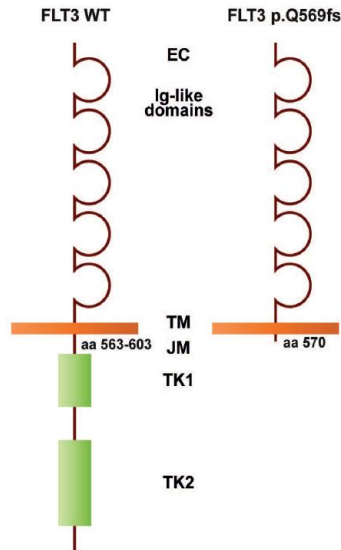


**Figure S1: Schematic representation of the truncated FLT3 receptor in comparison to the FLT3 WT receptor.** The truncated receptor lacks a large proportion of the juxtamembrane domain as well as other intracellular domains, especially the tyrosine kinase domains 1/2.  
aa: amino acid, EC: extracellular domain, Ig-like domain: Immunglobuline-like domain, TM: transmembrane domain, JM: juxtamembrane domain, TK1/2: tyrosine kinase domain 1/2.

**Figure S2**

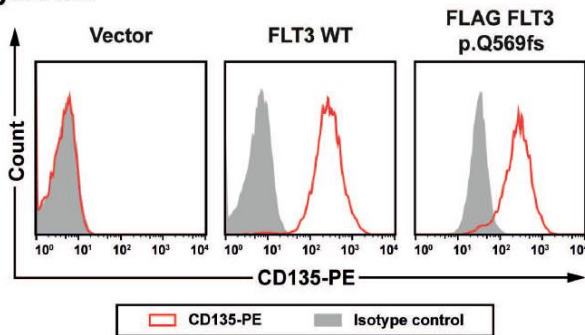


**Figure S2: Cell surface expression of the FLT3 constructs.** Ba/F3 cells stably expressing the indicated constructs were stained with CD135 antibody (red) or isotype control (grey) and analyzed by flow cytometry. One representative example is shown.

**Figure S3**

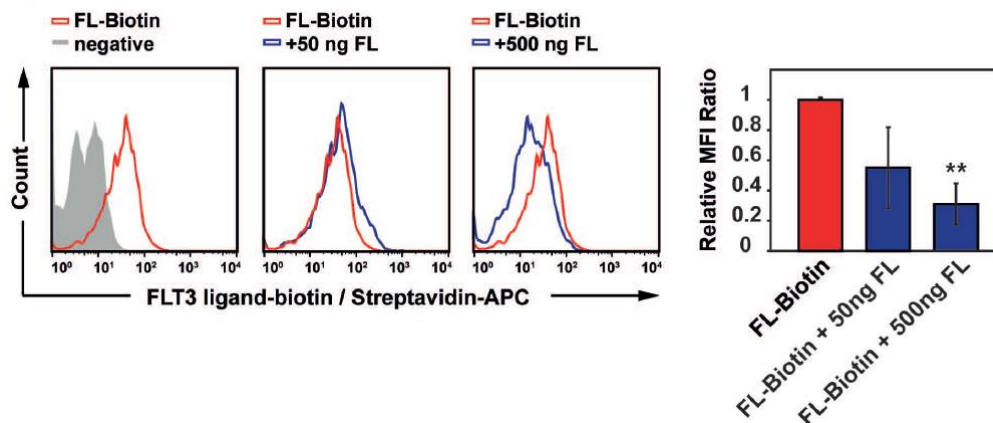


**Figure S3: Binding capacity for biotinylated FLT3 ligand.** Ba/F3 cells stably expressing FLT3 p.Q569fs were incubated with biotinylated human FLT3 ligand (FL). Receptor bound biotinylated FL was detected with streptavidin-APC using flow cytometry. As a negative control biotinylated soybean trypsin inhibitor was used. Different amounts of unbiotinylated FL (50 ng; 500 ng) were added to determine the staining specificity. One representative example is shown (left). Binding of biotinylated FL to FLT3 p.Q569fs without addition of unbiotinylated FL is set as 1. Shown are mean values of the relative mean fluorescence intensity ratios (MFI)  $\pm$  SEM of at least three independent experiments (right); \*\* p<0.01.

**Figure S4**

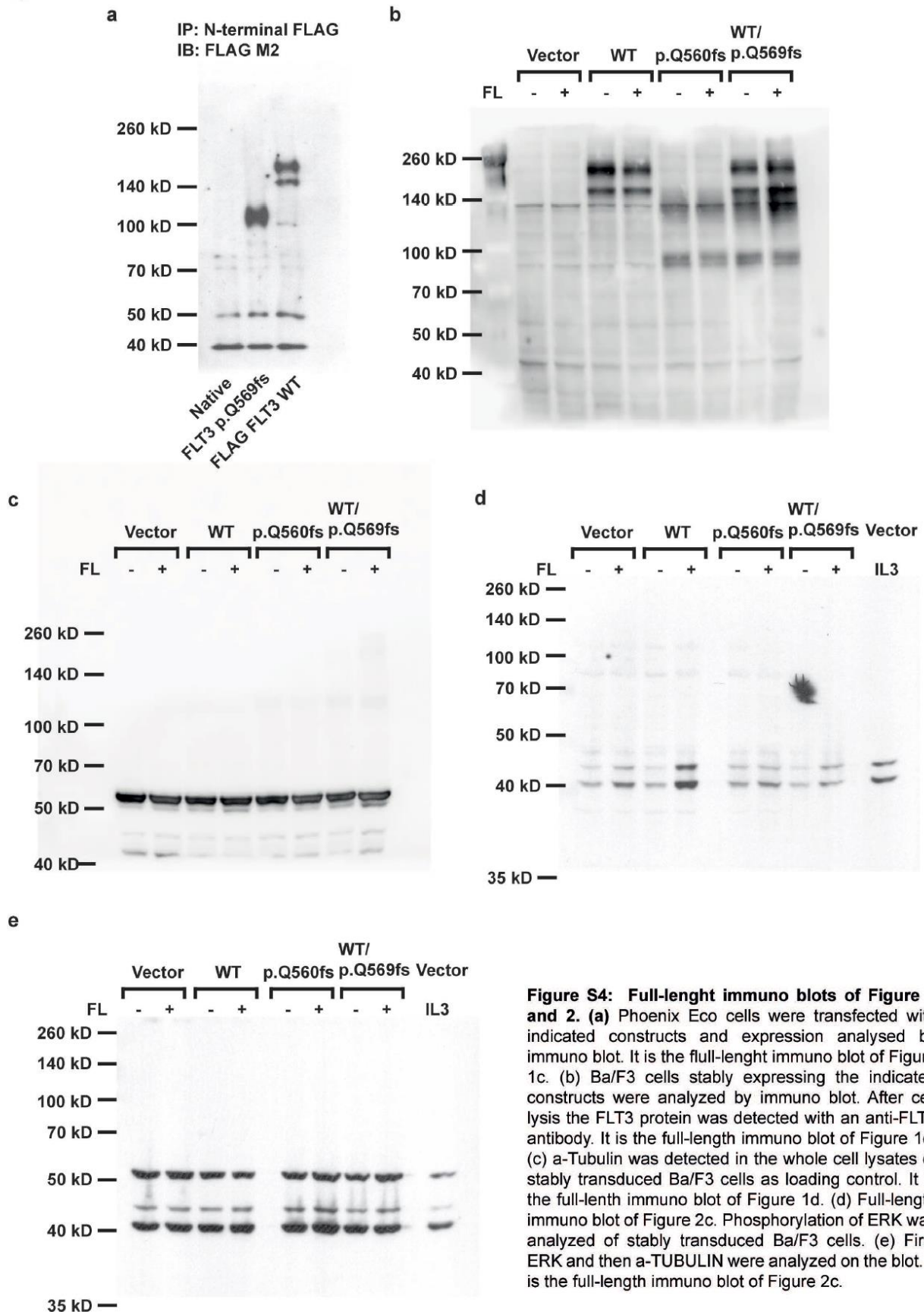


**Figure S4: Full-length immuno blots of Figure 1 and 2.** (a) Phoenix Eco cells were transfected with indicated constructs and expression analysed by immuno blot. It is the full-length immuno blot of Figure 1c. (b) Ba/F3 cells stably expressing the indicated constructs were analyzed by immuno blot. After cell lysis the FLT3 protein was detected with an anti-FLT3 antibody. It is the full-length immuno blot of Figure 1d. (c) a-Tubulin was detected in the whole cell lysates of stably transduced Ba/F3 cells as loading control. It is the full-length immuno blot of Figure 1d. (d) Full-length immuno blot of Figure 2c. Phosphorylation of ERK was analyzed of stably transduced Ba/F3 cells. (e) First ERK and then a-TUBULIN were analyzed on the blot. It is the full-length immuno blot of Figure 2c.

**Figure S5**

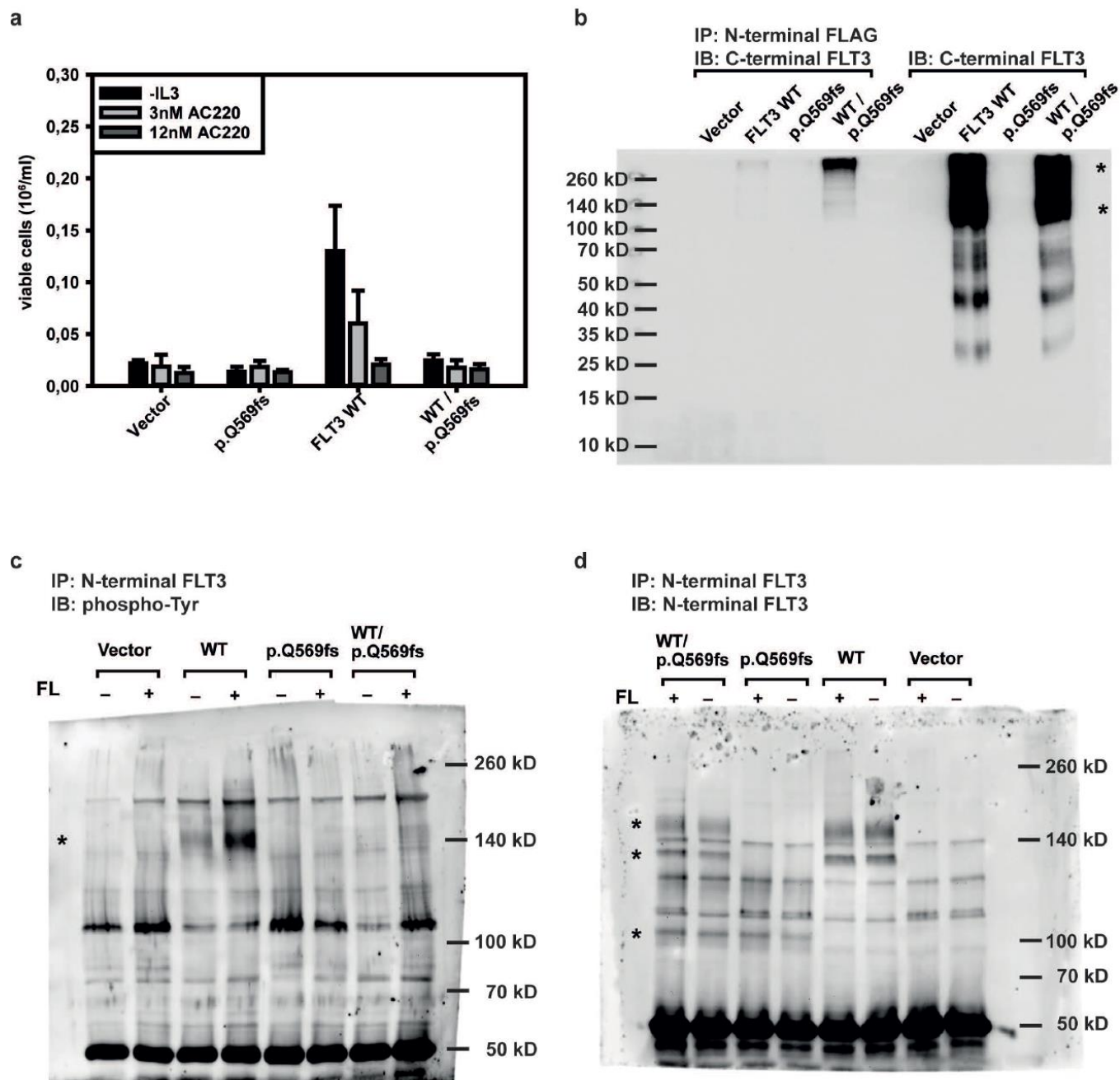


**Figure S5: Dominant negative effect of FLT3 p.Q569fs and heterodimerisation.** (a) Ba/F3 cells stably expressing the indicated constructs were seeded at a density of  $4 \times 10^4$ /mL in the absence of cytokines and indicated concentrations of AC220. Viable cells were counted by trypan blue exclusion after 72 hours. Shown are mean values  $\pm$  SEM of three independent experiments. (b) HEK 293T were transfected with indicated constructs. After lysis FLT3 p.Q569fs was immunoprecipitated via its FLAG-tag from whole cell lysates. SDS-gel was run without reducing agents and in MOPS buffer. After blotting the FLT3 WT was detected with a C-terminal FLT3 antibody (\* indicating FLT3 dimer and monomer). (c,d) From whole cell lysates of stable Ba/F3 cells the FLT3 protein was immunoprecipitated with an N-terminal FLT3 antibody (\* indicating FLT3 specific bands). After blotting the phosphorylation status of FLT3 was detected by a pTyr antibody (c) and total FLT3 protein with a different N-terminal FLT3 antibody (d).

---

### **4.3 Tyrosine kinase inhibition increases the cell surface localization of FLT3-ITD and enhances FLT3-directed immunotherapy of acute myeloid leukemia**

---



## ORIGINAL ARTICLE

# Tyrosine kinase inhibition increases the cell surface localization of FLT3-ITD and enhances FLT3-directed immunotherapy of acute myeloid leukemia

K Reiter<sup>1,2,3,12</sup>, H Polzer<sup>1,2,3,12</sup>, C Krupka<sup>1,4</sup>, A Maiser<sup>5</sup>, B Vick<sup>2,6</sup>, M Rothenberg-Thurley<sup>1,2,3</sup>, KH Metzeler<sup>1,2,3</sup>, D Dörfel<sup>7,8</sup>, HR Salih<sup>3,7,8</sup>, G Jung<sup>9</sup>, E Nößner<sup>10</sup>, I Jeremias<sup>2,6,11</sup>, W Hiddemann<sup>1,2,3</sup>, H Leonhardt<sup>5</sup>, K Spiekermann<sup>1,2,3</sup>, M Subklewe<sup>1,2,3,4,12</sup> and PA Greif<sup>1,2,3,12</sup>

The *fms*-related tyrosine kinase 3 (FLT3) receptor has been extensively studied over the past two decades with regard to oncogenic alterations that do not only serve as prognostic markers but also as therapeutic targets in acute myeloid leukemia (AML). Internal tandem duplications (ITDs) became of special interest in this setting as they are associated with unfavorable prognosis. Because of sequence-dependent protein conformational changes FLT3-ITD tends to autophosphorylate and displays a constitutive intracellular localization. Here, we analyzed the effect of tyrosine kinase inhibitors (TKIs) on the localization of the FLT3 receptor and its mutants. TKI treatment increased the surface expression through upregulation of FLT3 and glycosylation of FLT3-ITD and FLT3-D835Y mutants. In T cell-mediated cytotoxicity (TCMC) assays, using a bispecific FLT3 × CD3 antibody construct, the combination with TKI treatment increased TCMC in the FLT3-ITD-positive AML cell lines MOLM-13 and MV4-11, patient-derived xenograft cells and primary patient samples. Our findings provide the basis for rational combination of TKI and FLT3-directed immunotherapy with potential benefit for FLT3-ITD-positive AML patients.

*Leukemia* advance online publication, 12 September 2017; doi:10.1038/leu.2017.257

## INTRODUCTION

In acute myeloid leukemia (AML), approximately one-third of patients carry an activating mutation in the *fms*-related tyrosine kinase 3 (FLT3) gene, prevalently an internal tandem duplication (ITD) of varying length (affecting 20–30% of adult AML).<sup>1,2</sup> FLT3-ITD is associated with an unfavorable prognosis, characterized by shorter event-free survival (EFS) and overall survival (OS) as well as a high relapse rate.<sup>2–6</sup> On a cellular level, the mutant FLT3 receptor promotes cell proliferation of hematopoietic stem and myeloid progenitor cells.<sup>2,3,6</sup> FLT3-ITD mutations lead to sequence-dependent protein conformational changes in the receptor and, thus, to an endoplasmatic reticulum-retained intracellular localization, constitutive autophosphorylation and induction of growth factor signaling pathways.<sup>7–11</sup> Therefore, FLT3-targeting therapies are highly warranted to impede disease progression, alternatively or in addition to conventional chemotherapy. Promising agents are second-generation tyrosine kinase inhibitors (TKIs), including AC220 (quizartinib), PKC412 (midostaurin) and BAY43-9006 (sorafenib, nexavar), that block FLT3 phosphorylation.<sup>12–17</sup> Although complete remission rates reach a moderate level, clinical response to TKI monotherapy remains limited by the high risk of relapse that often occurs within months.<sup>18–21</sup> However, the SORAML trial (NCT00893373) demonstrated sorafenib to be a

beneficial antileukemic additive to conventional chemotherapy with regard to increased EFS and relapse-free survival for patients aged ≤60 years, regardless of FLT3 status.<sup>22</sup> Furthermore, the CALGB 10603/RATIFY trial (NCT00651261) demonstrated significantly improved EFS and OS for patients, harboring a FLT3 mutation, when treated with PKC412 in addition to induction chemotherapy and 1 year of maintenance therapy.<sup>23</sup> Nevertheless, TKIs still lack the efficiency to eradicate all FLT3-mutated AML cells because of resistance mechanisms. In FLT3-ITD-positive AML, resistance is frequently mediated by specific insertion sites of ITDs (including β1- or β2-sheet), emerging secondary FLT3 point mutations (PMs; such as D835Y, N676K), protection by the stromal microenvironment and/or altered pathway signaling.<sup>24–31</sup> The subcellular localization of FLT3 matters for activation of signaling cascades. For example, FLT3-N676K displays a mere wild-type (WT)-like membrane localization and activates mitogen-activated protein kinase signaling, whereas FLT3-D835Y localizes to the ER and activates the signal transducer and activator of transcription 5 pathway.<sup>10,32</sup> However, the effect of TKIs on the subcellular localization of FLT3 and its mutants has not yet been examined systematically. Therefore, we investigated the localization of FLT3 mutants under TKI treatment and observed an increase of FLT3 on the cell surface that facilitated the application of FLT3-directed immunotherapy.

<sup>1</sup>Department of Medicine III, University Hospital, LMU Munich, Munich, Germany; <sup>2</sup>German Cancer Consortium (DKTK), partner site Munich, Munich, Germany; <sup>3</sup>German Cancer Research Center (DKFZ), Heidelberg, Germany; <sup>4</sup>Department of Translational Cancer Immunology, Gene Center Munich, LMU Munich, Munich, Germany; <sup>5</sup>Department of Biology II, LMU Munich, Munich, Germany; <sup>6</sup>Department of Gene Vectors, Helmholtz Zentrum München, German Research center for Environmental Health, Munich, Germany; <sup>7</sup>Department of Medical Oncology, Hematology, Immunology, Rheumatology and Pulmology, Eberhard Karls Universität Tübingen, University Hospital Tübingen, Tübingen, Germany; <sup>8</sup>Clinical Collaboration Unit Translational Immunology, German Cancer Consortium (DKTK) and German Cancer Research Center (DKFZ), partner site Tübingen, Tübingen, Germany; <sup>9</sup>Department of Immunology, Eberhard Karls Universität Tübingen, Tübingen, Germany; <sup>10</sup>Immunoanalytics-Tissue control of Immuncytes, Helmholtz Zentrum München, German Research Center for Environmental Health, Munich, Germany and <sup>11</sup>Department of Pediatrics, Dr von Hauner Children's Hospital, LMU Munich, Munich, Germany. Correspondence: Dr PA Greif, Department of Medicine III, University Hospital, Max-Lebsche-Platz. 30, LMU Munich, München 81337, Germany. E-mail: p.greif@dkfz-heidelberg.de or pgreif@med.uni-muenchen.de

<sup>12</sup>These authors contributed equally to this work.

Received 7 April 2017; revised 14 July 2017; accepted 1 August 2017; accepted article preview online 14 August 2017

## MATERIALS AND METHODS

### Cell lines and reagents

All cell lines were purchased from the German Collection of Microorganisms and Cell Culture (DSMZ, Braunschweig, Germany), except for U2OS cells that were obtained from ATCC (American Type Culture Collection, Wesel, Germany) and Phoenix eco, which were purchased from Orbigen (San Diego, CA, USA). The B-cell lymphoma cell line OCI-Ly8 was a kind gift from O Weigert (Department of Internal Medicine III, University Hospital of the LMU Munich, Munich, Germany).<sup>33,34</sup> All cell lines were cultivated according to supplier's instructions or as described elsewhere.<sup>35</sup> Stably transduced Ba/F3 cell lines were generated as described previously.<sup>36,37</sup> Recombinant human FLT3 ligand (FL) was obtained from Promokine (Heidelberg, Germany), recombinant murine interleukin-3 from Immunotools (Friesoythe, Germany), cycloheximide and 2-deoxy-D-glucose from Sigma-Aldrich (Taufkirchen, Germany). TKIs sorafenib (BAY43-9006, nexavar), midostaurin (PKC412) and quizartinib (AC220) were purchased from Selleck Chemicals (Houston TX, USA). Cell lines were tested for a mycoplasma contamination on a regular basis (MycopAlert Mycoplasma Detection Kit, Lonza Rockland Inc., Rockland, ME, USA).

### Plasmid constructs and mutagenesis

The following DNA constructs and vectors have been described before:<sup>32,37,38</sup> the expression vectors pcDNA6.2-V5-HisA, pcDNA6.2-V5-HisA-FLT3-WT, pcDNA6.2-V5-HisA-FLT3-K602R(7) (described as W51) and pcDNA6.2-V5-HisA-FLT3-E611C(28) (described as NPOS); the retroviral expression vectors pMSCV-IRES-EYFP, pMSCV-IRES-EYFP-FLT3-WT, pMSCV-IRES-EYFP-FLT3-N676K, pMSCV-IRES-EYFP-FLT3-D835Y and pMSCV-IRES-EYFP-FLT3-E611C(28) (described as NPOS). The constructs pMSCV-IRES-puro-EYFP-FLT3-WT, pMSCV-IRES-puro-EYFP-FLT3-E611V(32), pMSCV-IRES-puro-EYFP-FLT3-G613E(33), pMSCV-IRES-puro-EGFP-FLT3-598/599(12), pMSCV-IRES-puro-EGFP-FLT3-598/599(22), pMSCV-IRES-puro-EGFP-FLT3-L601H(10) and pMSCV-IRES-puro-EGFP-FLT3-K602R(7) have been previously described<sup>39</sup> and kindly provided by FH Heide (Center of Internal Medicine, Otto-von-Guericke University Magdeburg, Magdeburg, Germany). Denotation of all FLT3-ITDs was adapted from a recent publication.<sup>39</sup> The mutations N676K and D835Y were introduced into pcDNA6.2-V5-HisA-FLT3-WT and pMSCV-IRES-EYFP-FLT3-E611C(28), using the QuikChange II XL Site-Directed Mutagenesis Kit (Agilent, Santa Clara, CA, USA) according to the supplier's instructions as previously described.<sup>32</sup> Mutations were confirmed by Sanger sequencing.

### Proliferation assay

Proliferation assays were performed as described before, utilizing the Vi-Cell XR (Beckman Coulter, Munich, Germany).<sup>36</sup> AML cell lines were seeded at a density of  $3 \times 10^5$ /ml. Experiments were performed in biological triplicates.

### Immunofluorescence staining

Transient transfection of U2OS cells and subsequent immunofluorescence staining was performed as previously described<sup>40</sup> using the following antibodies: anti-wheat germ agglutinin-488 fluorescein conjugate (catalog number: W11261; Invitrogen–ThermoFisher Scientific, Munich, Germany), rabbit anti-FLT3 (catalog number: sc-480, clone: S-18; Santa Cruz Biotechnology, Heidelberg, Germany) and anti-rabbit IgG (H+L) F(ab')<sub>2</sub> fragment Alexa Fluor 594 Conjugate (catalog number: 88895; Cell Signaling Technology, Leiden, The Netherlands). Fixation was performed for 10 min at room temperature with Dulbecco's phosphate-buffered saline (DPBS) 2% formaldehyde (37% stock solution; Merck Schuchardt, Hohenbrunn, Germany), followed by permeabilization for 10 min with DPBS 0.5% Triton X-100 (Carl Roth, Karlsruhe, Germany). Before staining, cells were treated with 50 nM AC220 for 6 h, whereas controls were left untreated. For suspension cells, 8-well chamber slides (ibidi, Munich, Germany) were precoated with poly-L-lysine hydrobromide (Sigma-Aldrich) according to the supplier's recommendations. Before seeding, cells were treated with 50 nM AC220, whereas controls were left untreated, washed twice with DPBS and dissolved in H2F buffer (1× Hanks' balanced salt solution (w/o calcium, magnesium and phenol red, ThermoFisher Scientific), 2% fetal bovine serum (Biochrom, Berlin, Germany), 1% 1 M Hepes (Sigma-Aldrich) and 1% penicillin/streptomycin (PAN Biotech, Aidenbach, Germany). After

30 min of detachment at 4 °C, glycoconjugates were stained as described previously,<sup>40</sup> followed by cell fixation using DPBS 4% formaldehyde for 5 min. For blocking, DPBS with 0.1% Tween 20 (Carl Roth) and 10% fetal bovine serum (Biochrom) was used. Subsequent steps of the staining procedure were performed as for U2OS cells.

### T cell-mediated cytotoxicity (TCMC) assay

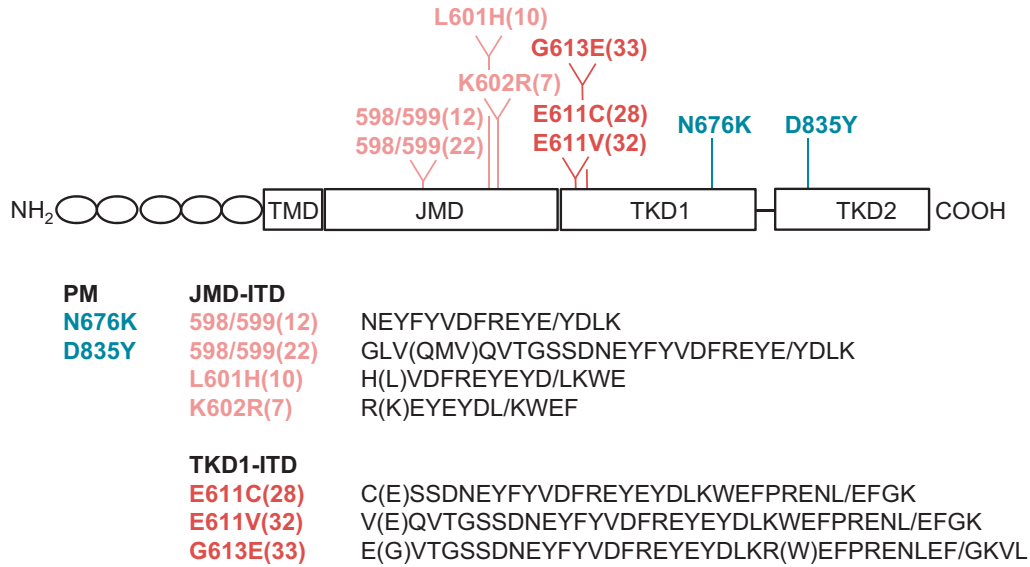
The *in vitro* cytotoxicity assays against AML cells were performed as described previously.<sup>35,41</sup> The bispecific FLT3×CD3 antibody construct (4G8×UCHT1, Fabsco-format) was utilized as reported elsewhere.<sup>42</sup> Confirmatory antibody serial dilution experiments with an effector-to-target ratio of 1:2.5 were performed using CD3-positive isolated T cells from healthy donors. For TCMC assays, AML cells and T cells were co-cultured with an effector-to-target ratio between 1:2.5 and 1:4. Then 50 nM AC220 and 1–10 µg/ml FLT3×CD3 antibody were added at the beginning of each experiment, whereas controls were left untreated. After 72 h, cell counting and flow cytometry analysis was performed, determining the percentage of cytotoxicity as described previously.<sup>35,41</sup> FLT3 (CD135) surface expression was assessed simultaneously. Estimation of a potential additive effect of combined treatment was computed based on the fractional product method.<sup>43</sup> Competitive lysis experiments were performed as described previously,<sup>35</sup> using 1–5 µg/ml FLT3×CD3 antibody. Untreated AML cells (HL60 or MV4-11) were mixed 1:1 with corresponding 6 h AC220-pre-treated AML cells (HL60 or MV4-11) and cultured with healthy donor T cells at an effector-to-target ratio of 1:1 for 20–24 h. Cell membrane staining of untreated AML cells (HL60 and MV4-11) was performed using the PKH26 red fluorescent cell linker kit (Sigma-Aldrich) according to the manufacturer's protocol. Experiments were performed once, if not stated otherwise. Additional materials and methods are provided in the Supplementary Information.

## RESULTS

TKIs increase the membrane localization of FLT3-V592A, FLT3-D835Y and FLT3-ITD mutants

Cellular localization studies of seven ITD constructs with varying length and position, as well as two activating PMs of FLT3 (Figure 1a), revealed an altered localization of FLT3 mutants D835Y and ITDs upon TKI treatment. FLT3-ITD or FLT3-D835Y protein was retained in the perinuclear ER and after addition of AC220 a cell membrane localization similar to FLT3-WT or FLT3-N676K was observed (Figures 1b and 2a). Flow cytometry confirmed that FLT3 (CD135) surface expression differed significantly between treated and untreated FLT3-expressing Ba/F3 cells (Figure 2b and Supplementary Figure S1a) not only for ITD and D835Y but also for WT and N676K. However, the increase in surface FLT3 was significantly higher in FLT3-D835Y or FLT3-ITD compared with FLT3-WT-expressing cells (Student's *t*-test:  $P = 0.003$  and  $P < 0.001$ , respectively). In light of the recently reported *in vitro* and *in vivo* experiments, displaying juxtamembrane domain (JMD)-ITD to be more sensitive towards TKI-therapy than tyrosine kinase domain 1 (TKD1)-ITD,<sup>39</sup> we evaluated four JMD-ITD and three TKD1-ITD constructs with regard to TKI-induced FLT3 surface expression and did not observe any significant differences (Figure 2b). In AML cell lines, FLT3 surface expression levels were hardly altered in cells with FLT3-WT status (THP-1, OCI-AML3) or a heterozygous FLT3-ITD (MOLM-13, PL-21), whereas the cell lines MV4-11 with FLT3-loss of heterozygosity (LOH) and MONO-MAC-6 (MM6) with an activating PM FLT3-V592A<sup>44</sup> responded with a significant increase in FLT3 surface expression upon AC220 treatment (Table 1 and Figures 3a and b). The TKI response of MV4-11 was also obvious in immunofluorescence staining (Supplementary Figure S1b). Additional FLT3-WT AML cell lines (HL60, Kasumi-1, EOL-1, NOMO-1, MUTZ-2) confirmed this observation, except for MUTZ-2 (Student's *t*-test:  $P < 0.001$ ; Supplementary Figures S1c and d). In the AML cell line KG-1a, the CML cell line K-562 and the B-cell lymphoma cell line OCI-Ly8, we did not detect any FLT3 surface expression, regardless of TKI treatment. In a time-course experiment over 24 h with TKI-treatment, MV4-11 cells showed a steady increase in FLT3 surface expression, whereas untreated cells remained stable in

a



b

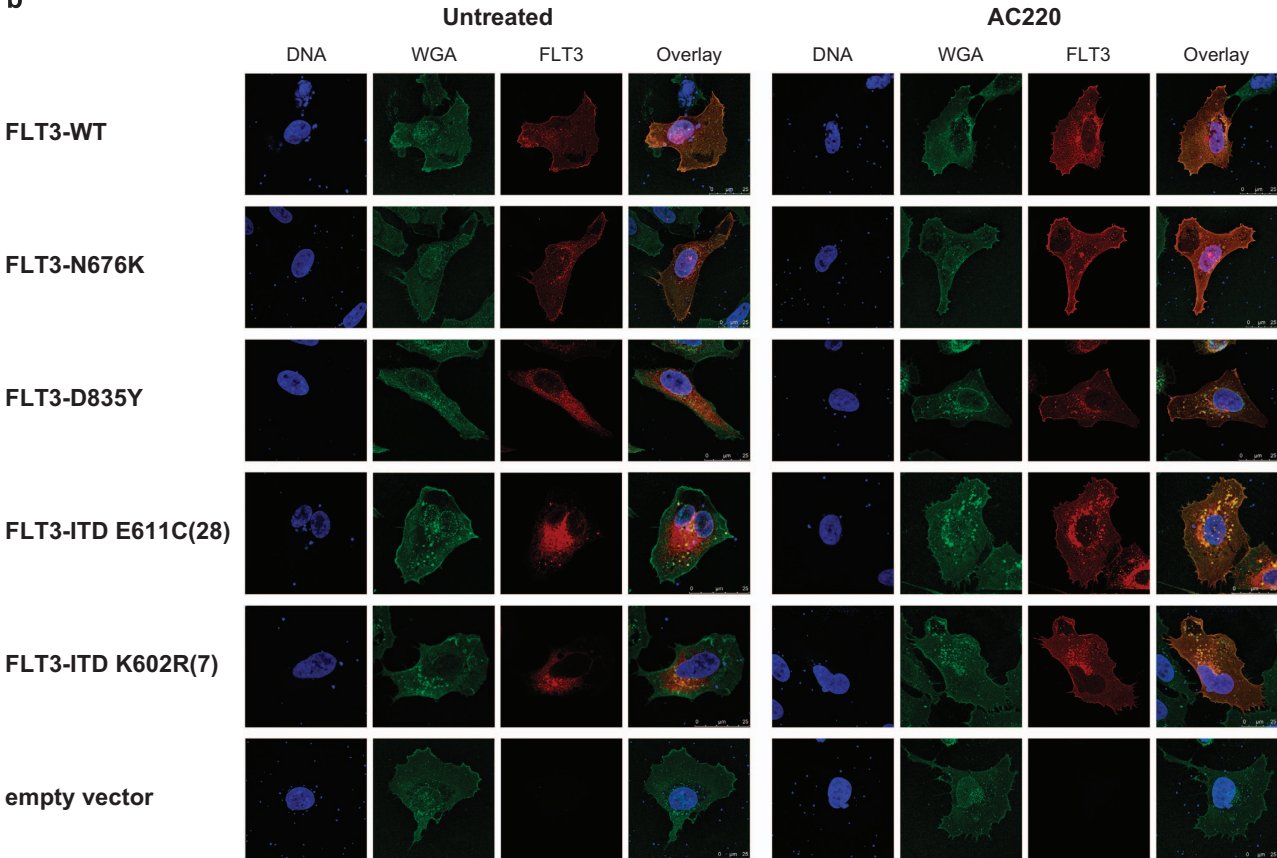


**Figure 1.** FLT3 mutants and their subcellular localization with and without TKI treatment. (a) Schematic illustration of the FLT3 protein (NP\_004110.2) and mutant constructs with indication of amino acid substitutions and insertion sequences (modified from Arreba-Tutusaus et al.<sup>39</sup>). (b) Immunofluorescence staining of FLT3-WT, FLT3 mutants or empty vector with or without AC220 treatment in transiently transfected U2OS cells. WGA (wheat germ agglutinin). Scale bar: 25 µm.

FLT3 surface expression (Supplementary Figure S2a). MOLM-13 cells started to diverge from untreated cells after 12 h of TKI treatment. Other TKIs (PKC412 and sorafenib) induced a similar response in MV4-11 cells, however, with AC220 the effect was strongest, when applying equal concentrations (Supplementary

Figures S2b and c). A dose escalation experiment, applying concentrations up to 100 nM of AC220, sorafenib or PKC412, revealed that AC220 was most efficient in inducing FLT3 surface expression at concentrations from 5 to 25 nM (Supplementary Figure S2d).



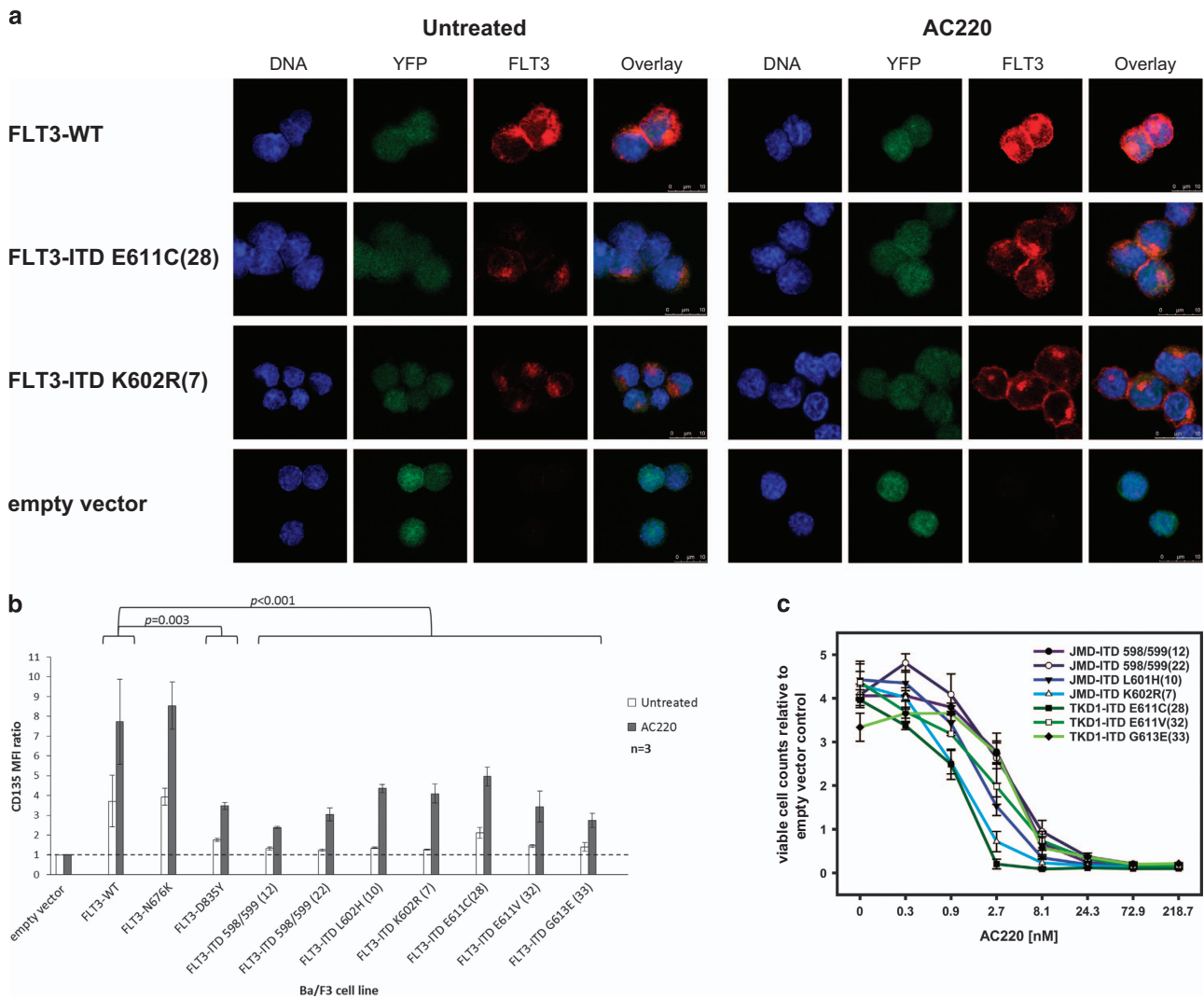


**Figure 2.** TKI treatment response of FLT3-expressing Ba/F3 cells. **(a)** Immunofluorescence staining of stably transduced Ba/F3 cells expressing FLT3-WT, FLT3-ITD or empty vector with or without AC220 treatment. WGA (wheat germ agglutinin). Scale bar: 10  $\mu$ m. **(b)** FLT3 surface expression levels with or without AC220 treatment (mean  $\pm$  s.d.). **(c)** Viable cell counts of Ba/F3 cells expressing the indicated FLT3 mutants, normalized to the empty vector transduced control cells, after 72 h of treatment with increasing concentrations of AC220 ( $n = 3$ , mean  $\pm$  s.d.).

**Table 1.** Classification of FLT3-mutated AML cell lines and PDX cells into FLT3 genotype categories: heterozygous FLT3-ITD and FLT3-LOH

AML cell lines/PDX cells	FLT3 genotype	ITD type	ITD insertion sequence
MOLM-13	Heterozygous	Y631F(7)	F(Y)DFREYE/YDLK
PL-21	Heterozygous	569/570(42)	F <u>K</u> S <u>V</u> QVTGSSDNEYFYVDFREYEDLKWEFPRENLEFGKNGM
AML-573	Heterozygous	E604D(21)	D(E)PSDNEYFYVDFREYEDLKW/EFPR
AML-640	Heterozygous	L610F(28)	F(L)GSSDNEYFYVDFREYEDLKWEFPREN/LEFG
		F612V(20)	V(F)DFREYEDLKWEFPRENLE/FGKV
MV4-11	LOH	H633L(10)	H(L)VDFREYED/LKWE
AML-415	LOH	E598D(6)	D(E)FREYE/EYDL
AML-579	LOH	E598Y(8)	Y(E)VDFREYE/EYDL

Abbreviations: FLT3, fms-related tyrosine kinase 3; ITD, internal tandem duplication; LOH, loss of heterozygosity; PDX, patient-derived xenograft. Underlined amino acids are inserted before the ITD.

TKI-induced increase in FLT3 surface expression in FLT3-mutated cells correlates inversely with proliferation

Treatment of Ba/F3 cells, expressing various FLT3-ITD constructs, with AC220 at nontoxic concentrations ( $\leq 500$  nM) revealed a variable inhibition of proliferation without any obvious correlation to ITD length or position (Figure 2c and Supplementary Table S1).

However, the AC220-mediated reduction in proliferation of FLT3-ITD-positive cells correlated with the increase in surface FLT3 (Pearson:  $-0.931$ ,  $P = 0.002$ ,  $n = 7$ ). Moreover, we confirmed that the TKI resistance-mediating PMs<sup>32,45</sup> reduced the TKI response with regard to FLT3 surface expression when combined with ITD (Supplementary Figures S3a–c and Supplementary Table S1).

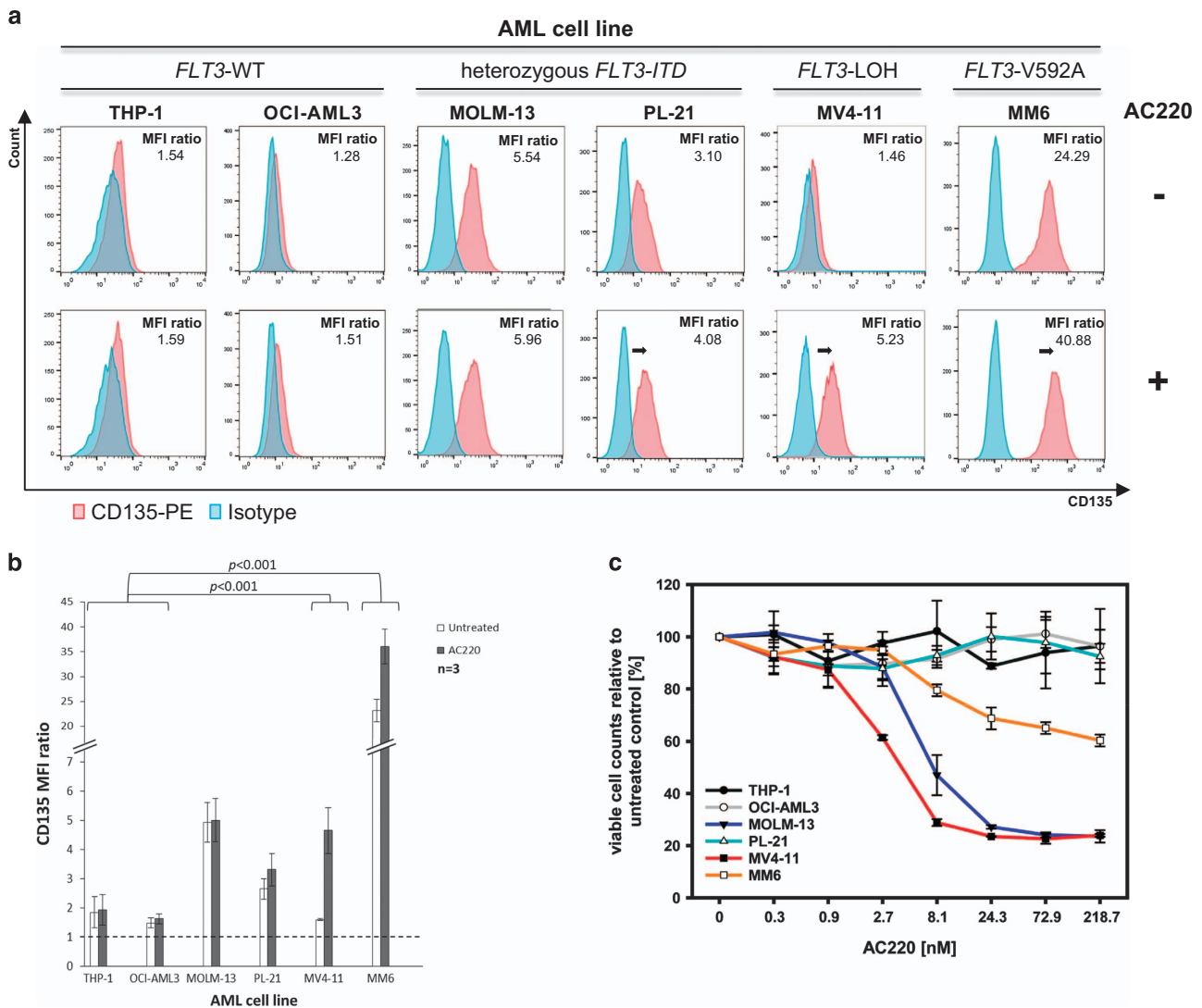


**Figure 3.** TKI treatment response of AML cells. **(a)** Representative flow cytometry plots and **(b)** bar graph showing the FLT3 surface expression in AML cells, harboring different *FLT3* genotypes, with or without AC220 treatment (mean  $\pm$  s.d.). A mean fluorescence intensity (MFI) ratio increase of  $\geq 0.50$  is highlighted by an arrow. **(c)** Viable cell counts of selected AML cells, normalized to untreated control, after 72 h of treatment with increasing concentrations of AC220 ( $n = 3$ , mean  $\pm$  s.d.).

The *FLT3*-LOH cell line MV4-11, which showed the highest increase in FLT3 surface location upon TKI treatment, was more sensitive to AC220, compared with the heterozygous *FLT3*-ITD cell lines MOLM-13 and PL-21 (Figure 3c). Of note, PL-21 cells did not respond to AC220 treatment during the proliferation assay, although carrying a heterozygous *FLT3*-ITD and showing a slight increase in FLT3 surface expression. Targeted multiplexed amplicon sequencing revealed that the cell line PL-21 harbored a KRAS mutation (c.437C > T:p.A146V, NM\_033360), constituting a potential mechanism of TKI resistance. The AML cell line MM6 with a *FLT3*-V592A PM displayed a prominent increase in FLT3 surface expression after AC220 treatment and responded with a moderate decrease in proliferation (Figure 3c and Supplementary Table S2). The *FLT3*-WT cell lines THP-1 and OCI-AML3 were resistant to AC220 treatment. When comparing the antiproliferative potential of various TKIs (PKC412, sorafenib, AC220) in the *FLT3*-LOH cell line MV4-11, AC220 was the most potent agent at low nanomolar levels (Supplementary Figure S2e and Supplementary Table S2). Of note, several other *FLT3*-WT cell lines (HL60, MUTZ-2, NOMO-1) and *FLT3*-expression-negative cell lines (KG-1a, K-562) also showed TKI resistance. In contrast, the *FLT3*-WT cell lines Kasumi-1 and

EOL-1, which carry alterations of other receptor tyrosine genes (*KIT* c.2466T > A:p.N822K, NM\_000222 in Kasumi-1 and FIP1L1-PDGFR $\alpha$  rearrangement; del(4)(q12q12) in EOL-1), both responded, consistent with the known target profile of the tested TKIs<sup>12,30</sup> (Supplementary Table S2).

#### Induction of FLT3 surface expression depends on the pretreatment *FLT3*-ITD mRNA levels

The AC220-induced FLT3 increase on the cell surface (CD135 mean fluorescence intensity ratio change, Supplementary Table S2) tended to correlate with the pretreatment *FLT3*-ITD mRNA levels (Supplementary Figure S4a) in tested AML cell lines (Pearson: 0.864,  $P = 0.059$ ,  $n = 5$ ). Patient-derived xenograft (PDX) cells with either *FLT3*-WT, heterozygous *FLT3*-ITD mutation or *FLT3*-LOH status (Table 1) revealed a stable FLT3 surface expression in *FLT3*-WT PDX cells (AML-372, AML-491), whereas the heterozygous *FLT3*-ITD PDX cells (AML-573, AML-640) showed a minimal response to AC220 treatment (Figures 4a and b). However, both PDX cells with *FLT3*-LOH (AML-415, AML-579) showed a significant FLT3 surface expression increase upon AC220 treatment (Student's  $t$ -test: both  $P < 0.001$ ). Thus, a difference between *FLT3*-WT

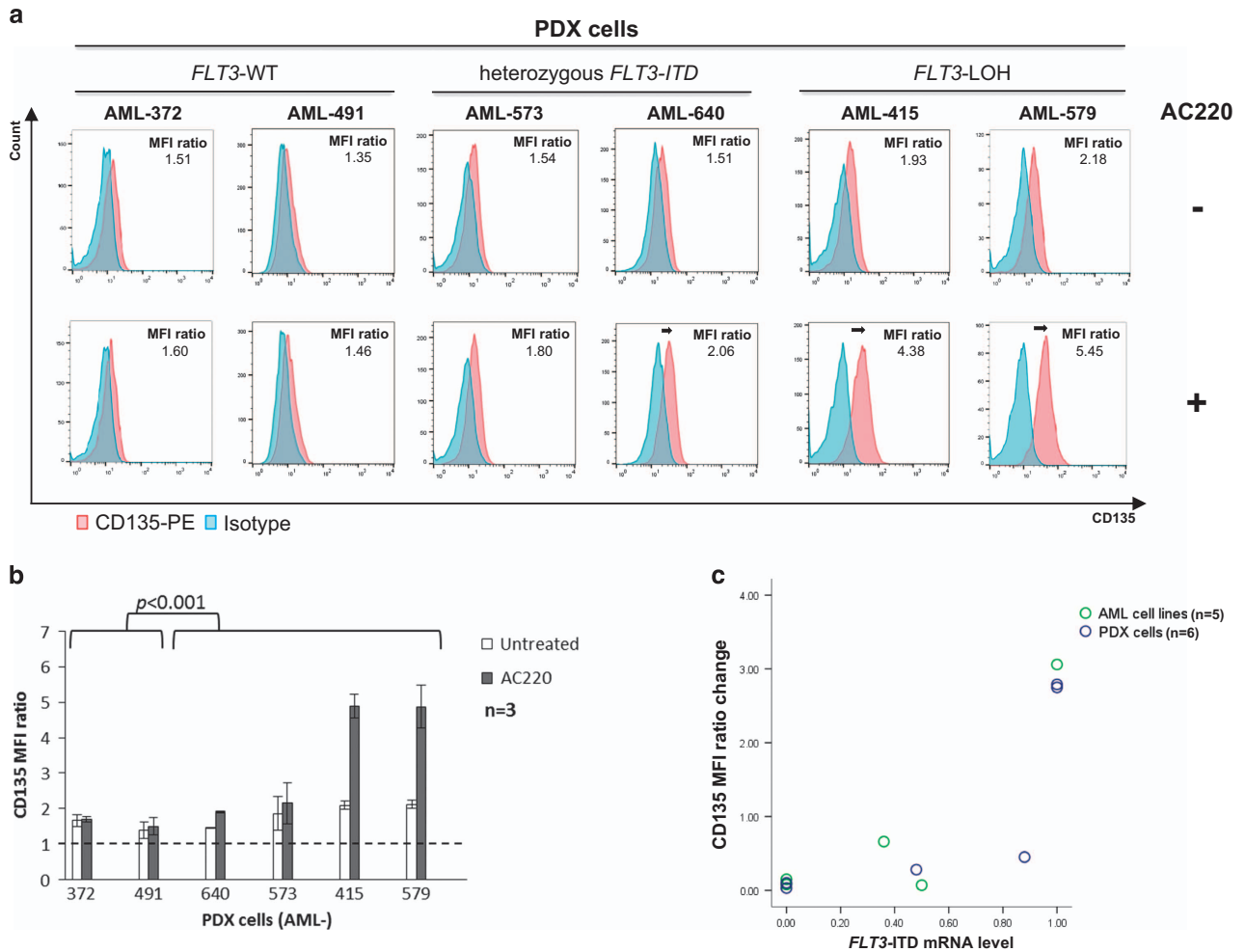


**Figure 4.** TKI treatment response of PDX cells and correlation with *FLT3*-ITD mRNA level. **(a)** Representative flow cytometry plots and **(b)** bar graph showing the *FLT3* surface expression in PDX cells, with and without AC220 treatment (mean  $\pm$  s.d.). A mean fluorescence intensity (MFI) ratio increase of  $\geq 0.50$  is highlighted by an arrow. **(c)** Scatter plot showing the correlation of the pretreatment *FLT3*-ITD mRNA level and the AC220 treatment-induced MFI ratio change representing the increase in *FLT3* surface expression.

and *FLT3*-ITD samples was observed (Student's *t*-test:  $P < 0.001$ ). In addition, there was a positive correlation of the *FLT3* expression increase at the cell surface upon AC220 treatment with the pretreatment *FLT3*-ITD mRNA level (Spearman: 0.971,  $P = 0.001$ ,  $n = 6$ ; in case of AML-640, the pretreatment *FLT3*-ITD mRNA level of the dominant clone was used for statistics). The correlation remained significant when combining the data generated from AML cell lines and PDX cells (Figure 4c; Spearman: 0.840,  $P = 0.001$ ,  $n = 11$ ). Characteristics of PDX cells have been recently published<sup>46</sup> and are summarized in Supplementary Table S3. The pretreatment *FLT3*-ITD mRNA levels of the PDX cells are shown in Supplementary Figure S4b.

#### FLT3 surface expression is glycosylation dependent

Western blot analysis showed an increase of the fully glycosylated mature (160 kDa) form of all *FLT3* constructs expressed in Ba/F3 cells after 6 h of TKI treatment (Figure 5a). This effect was also obvious in the *FLT3*-LOH AML cell line MV4-11 and apparent in the AML cell line MM6 that carries a *FLT3*-V592A PM. In contrast, *FLT3*-WT and *FLT3*-expression-negative cell lines (KG-1a, K-562, OCI-Ly8) remained mostly unaffected (Figure 5b and Supplementary Figures S5a and b). The increase of mature *FLT3* after TKI treatment was smaller or absent, when combining ITD with a resistance-mediating PM (Supplementary Figure S5c). Thus, the

altered glycosylation pattern of *FLT3*, represented by relative changes of the two differentially glycosylated forms, was consistent with the increase in surface *FLT3* upon TKI treatment. Consistently, the *FLT3*-WT PDX cells did not show any obvious difference in glycosylation pattern after AC220 treatment, in contrast to PDX cells harboring a *FLT3*-ITD, especially those with *FLT3*-LOH (Figure 5c). Treatment of MV4-11 cells with 2-deoxy-D-glucose, a compound inhibiting *N*-linked glycosylation,<sup>47</sup> alone or in combination with AC220, demonstrated that TKI not only affects phosphorylation but also *N*-linked glycosylation (Figure 5d). After a 24 h TKI treatment period, the glycosylated form of *FLT3* was increased 1.5- and four-fold for the *FLT3*-ITD-positive cell lines MOLM-13 and MV4-11, whereas the immature form decreased to 0.8-fold (Supplementary Figures S5d and e). Moreover, the TKI-treated MV4-11 cells showed an increase in total amount of *FLT3* protein levels likely because of upregulation of *FLT3* mRNA expression (Supplementary Figure S5f). Whereas in MOLM-13 cells the overall *FLT3* mRNA level was not altered by AC220 treatment, the ratio of *FLT3*-WT to *FLT3*-ITD changed significantly (Student's *t*-test:  $P < 0.001$ ) pointing toward allelic expression in favour of the WT allele (Supplementary Figures S5g and h). In addition, cycloheximide treatment indicated that TKI-mediated differential expression of mature and immature *FLT3* depends on biosynthesis. Furthermore, we confirmed that PKC412

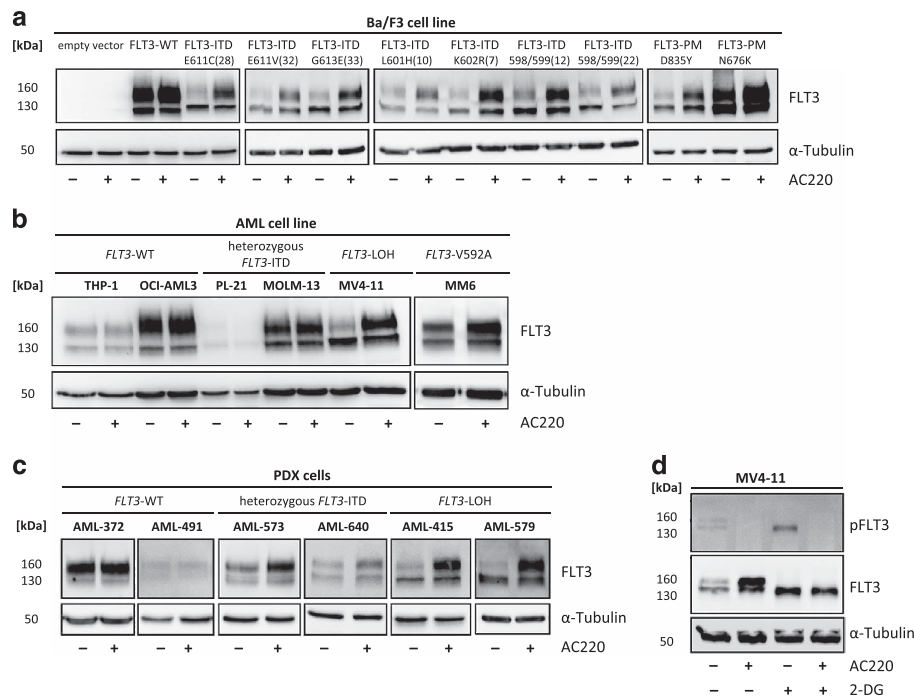


**Figure 5.** TKI increases the glycosylation of FLT3-ITD. Western blot analysis of FLT3 or phospho-FLT3 (130 and 160 kDa) and  $\alpha$ -tubulin (50 kDa) in whole-cell lysates with or without AC220 and/or 2-DG (2-deoxy-D-glucose) of (a) Ba/F3 cells transduced with empty vector, FLT3-WT or indicated FLT3 mutant construct, (b) AML cell lines, (c) PDX cells and (d) MV4-11 cells.

and sorafenib also have the potential to increase the glycosylation of FLT3 in MV4-11 cells (Supplementary Figure S5i).

#### FLT3 upregulation by TKI *in vivo*

*In vivo*, cells of two AML patients with mutated FLT3 who received sorafenib treatment (TKI-PT#1 and TKI-PT#2), after conventional therapy had failed, showed a prominent increase in FLT3 surface expression when comparing FLT3 expression at diagnosis of relapse and after sorafenib treatment (Figure 6a). Sorafenib treatment schemes are shown in Figure 6b and corresponding patient characteristics are detailed in Supplementary Table S5 and Supplementary Figure S6. For TKI-PT#1, sorafenib maintenance monotherapy resulted in a reduction of leukemia burden (blast count: 40% at diagnosis of relapse and 15% after 21 days of treatment), whereas in TKI-PT#2, leukemic burden showed a persistent increase over time (blast count: 48% at diagnosis of relapse and 90% after 53 days of treatment).

#### AC220 treatment boosts FLT3 $\times$ CD3 antibody-mediated cytotoxicity against FLT3-ITD-positive AML cells

Besides TKIs, an alternative strategy to target FLT3 is immunotherapy using a FLT3-directed antibody construct.<sup>42,48</sup> However, FLT3-directed immunotherapy might be limited by insufficient antigen expression levels. In light of our findings, we hypothesized that TKIs will increase anti-FLT3-directed antibody-mediated cytotoxicity through upregulation of the FLT3 target antigen (Figure 7a). Therefore, we performed T-cell-mediated cytotoxicity (TCMC) assays using a bispecific FLT3  $\times$  CD3 antibody construct<sup>42</sup> in combination with AC220. FLT3-expression-specific cell lysis by the FLT3  $\times$  CD3 antibody was demonstrated by an antibody serial dilution (Supplementary Figure S7a). Assessment of expression kinetics of FLT3-ITD-positive AML cells over 72 h showed a steady increase of FLT3 surface expression in MV4-11 cells upon addition of AC220, whereas MOLM-13 cells showed a maximum at 24 h (Supplementary Figure S7b). The FLT3 surface expression level in

the FLT3-WT AML HL60 cells was not significantly changed by addition of AC220. In TCMC experiments, the combination of TKI and FLT3  $\times$  CD3 in HL60 cells showed no significant change in cytotoxicity (Figure 7b and Supplementary Table S4). In contrast, FLT3-ITD-positive MV4-11 cells were almost completely eradicated by combined treatment with a mean CD33+ cell count lower than the computed additive effect (Figure 7b and Supplementary Table S4), pointing toward a synergism of TKI and FLT3-directed immunotherapy. The difference between single-agent and combined treatment was significant (Student's *t*-test:  $P < 0.001$  AC220 only and  $P = 0.028$  FLT3  $\times$  CD3 only). For the heterozygous FLT3-ITD cell line MOLM-13, the FLT3  $\times$  CD3 antibody treatment alone was very efficient in eradicating nearly all CD33+ cells (Figure 7b and Supplementary Table S4), and therefore no conclusion about synergistic or additive effects could be drawn regarding the increased lysis by combined treatment. Representative flow cytometry plots of the TCMC assays are shown in Supplementary Figure S7c. Competitive lysis experiments of untreated and AC220-pretreated AML cells confirmed a preferential killing of AC220-pretreated MV4-11 cells with higher FLT3 surface expression levels (Supplementary Figure S7d). For PDX cells a considerable increase in cytotoxicity was observed when applying the combined treatment, especially in PDX cells with FLT3-LOH (AML-415, AML-579; Figure 7c). For the heterozygous FLT3-ITD PDX cells AML-573 the single FLT3  $\times$  CD3 antibody treatment already resulted in almost complete eradication of CD33+ cells, similar to the heterozygous FLT3-ITD cell line MOLM-13 (Figures 7b and c). Moreover, two primary AML samples (PT#1, PT#2) showed a decrease in CD33+ cells by combined treatment below the computed additive effect (Figure 7c and Supplementary Table S4). Patient characteristics are shown in Supplementary Table S5; corresponding fragment analyses representing the pretreatment FLT3-ITD mRNA level of the primary samples are depicted in Supplementary Figure S6. Representative flow cytometry plots of the TCMC assays are shown in Supplementary Figure S7e.



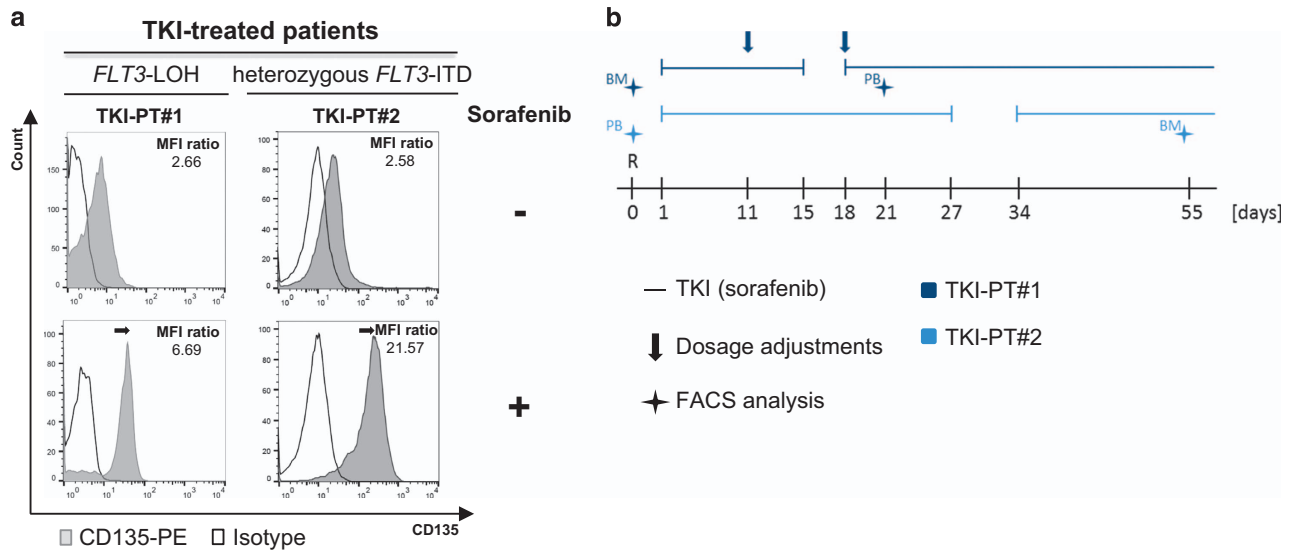


**Figure 6.** TKI effect on FLT3 surface expression in patients. **(a)** Flow cytometry plots showing the FLT3 surface expression before (day 0) and after (indicated day) TKI treatment. A mean fluorescence intensity (MFI) ratio increase of  $\geq 0.50$  is highlighted by an arrow. **(b)** Sorafenib treatment scheme with indication of the time point of relapse (R), sampling of bone marrow (BM) and peripheral blood (PB) for the assessment of treatment response. Arrows indicate dosage adjustments.

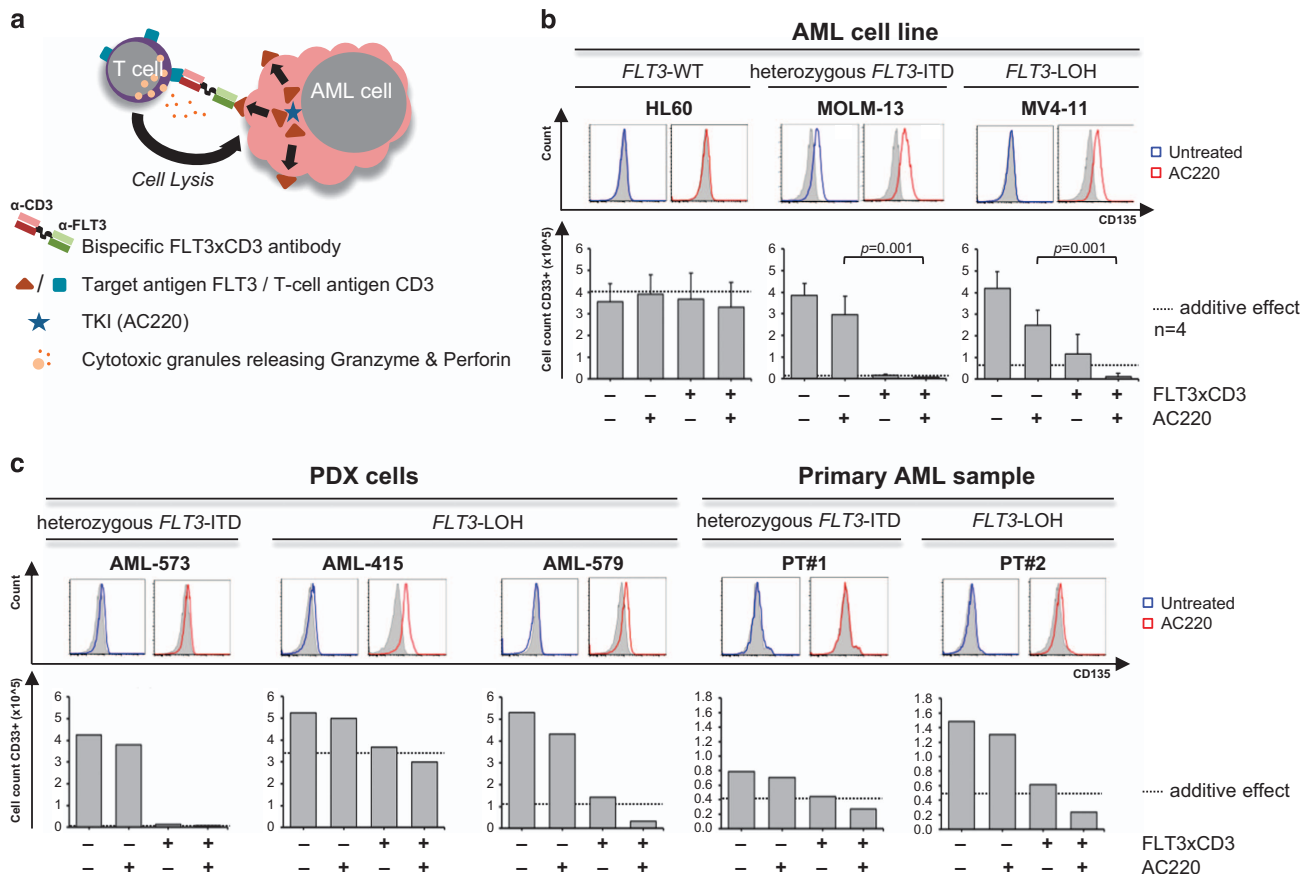


**Figure 7.** TKI- and FLT3-directed antibody combination mediates cytotoxicity against AML cells. **(a)** Mechanistic mode of action when combining TKI treatment with FLT3-directed immunotherapy. Response to FLT3 $\times$ CD3 or AC220 alone or in combination with regard to FLT3 surface expression (representative flow cytometry plots) and specific T cell-mediated lysis of **(b)** AML cell lines (effector-to-target (E/T) 1:2.5–4, FLT3 $\times$ CD3 10  $\mu$ g/ml) (mean  $\pm$  s.d.), **(c)** PDX cells and primary AML cells (E/T 1:3, FLT3 $\times$ CD3 1  $\mu$ g/ml). The computed additive effect is shown as dotted line.

## DISCUSSION

FLT3-ITD is a common mutation in AML, associated with increased relapse rates and poor prognosis.<sup>4,16</sup> Novel treatment approaches are therefore highly warranted for patients who are not eligible for intensive treatment as well as for patients with failure of conventional therapy or allogeneic stem cell transplantation. Moreover, targeting FLT3 seems to be attractive for minimal residual disease eradication during consolidation or maintenance therapy to minimize relapse rates and to prolong EFS and OS. So far, TKI is a promising approach to target FLT3, for instance as a bridging therapy before stem cell transplantation and as treatment of medically unfit patients. However, clinical trials using TKI as a single agent indicate the need for combinatorial therapies in order to prevent resistance toward TKI and to achieve prolonged remission.<sup>18,20,21,49,50</sup> The application of PKC412 in combination with induction chemotherapy in the CALGB 10603/RATIFY trial (NCT00651261) prolonged EFS and OS in FLT3-ITD- or FLT3-TKD-positive patients.<sup>23</sup> In our study, we demonstrated that FLT3 surface expression could be significantly increased by TKI treatment, particularly in FLT3-ITD- and FLT3-D835Y-mutant cells. Of note, cells harboring FLT3-ITD in combination with a resistance mediating point mutation showed a reduced FLT3 surface increase upon TKI treatment consistent with TKI resistance.<sup>27,29</sup> In contrast to CEP701 (Lestaurtinib), which was reported to increase FLT3 surface expression in certain AML patients upon treatment<sup>51</sup> irrespective of FLT3 genotype, we showed that AML cell lines and PDX cells responded to AC220 depending on the FLT3 genotype and pretreatment FLT3-ITD mRNA level. An exception was the AML cell line PL-21—although carrying a heterozygous ITD, the TKI was not effective in reducing proliferation, likely because of the presence of a KRAS mutation that is known to be associated with TKI resistance.<sup>52,53</sup> In line with previous reports,<sup>12</sup> comparison of several TKIs confirmed that the second-generation TKI AC220 was more potent than multikinase inhibitors, such as PKC412 and sorafenib. In this context, FLT3-ITD-positive patients may benefit from the combination of TKI and therapeutic FLT3-directed antibodies. This strategy may not only overcome the limitation of FLT3 antigen availability in FLT3-ITD-positive AML cells but could also prevent adaptive TKI-resistance—a frequent problem in single-agent TKI-treatment. Although the overall impact of TKI on immune response remains controversial,<sup>54–57</sup> we provide evidence that the combination of TKI and FLT3 × CD3 antibodies enhance the T cell-mediated lysis of FLT3-ITD-positive AML cell lines, PDX cells and primary AML patient samples. Beyond increased FLT3 surface expression in FLT3-mutated cells as potential mechanism, TKI treatment may also modulate immune response through post-translational modifications as glycosylation matters in major histocompatibility complex peptide presentation and antigen recognition of T cells.<sup>58</sup> This may be linked to the demonstrated increase in the mature, fully glycosylated form of FLT3 in FLT3-ITD-positive cells after TKI treatment, in accordance with other publications.<sup>47,59,60</sup> This result suggests that autophosphorylation of the FLT3-ITD receptor may prevent physiological processing that is required for maturation and surface expression and possibly also for antigen processing and recognition. Of note, altered FLT3 mRNA expression also seems to contribute to the TKI-mediated increase in surface FLT3 that has been demonstrated in FLT3-TKI-resistant cells,<sup>21,61</sup> pointing toward a feedback response mechanism to compensate the lack of mature FLT3 receptor in the FLT3-mutated cellular setting.

Taken together, we do not only provide insights into the cellular effects of TKIs but also open up avenues to eradicate FLT3-mutated AML by combination of FLT3-targeting strategies. Further preclinical models and ultimately clinical trials are needed to translate our findings into novel therapeutic approaches.

## CONFLICT OF INTEREST

The authors declare no conflict of interest.

## ACKNOWLEDGEMENTS

This study was supported by the German Research Council (DFG) within the Collaborative Research Centre (SFB) 1243 'Cancer Evolution' (projects A01, A05, A06, A07, A08 and A10). We thank Bianka Ksienzyk, Gudrun Mellert, Jutta Sturm, Belay Tizazu, Maike Fritschle and Miriam Krekel for technical support.

## REFERENCES

- Schnittger S, Schoch C, Dugas M, Kern W, Staib P, Wuchter C et al. Analysis of FLT3 length mutations in 1003 patients with acute myeloid leukemia: correlation to cytogenetics, FAB subtype, and prognosis in the AMLCG study and usefulness as a marker for the detection of minimal residual disease. *Blood* 2002; **100**: 59–66.
- Levis M, Small D. FLT3: ITD does matter in leukemia. *Leukemia* 2003; **17**: 1738–1752.
- Mrozek K, Marcucci G, Paschka P, Whitman SP, Bloomfield CD. Clinical relevance of mutations and gene-expression changes in adult acute myeloid leukemia with normal cytogenetics: are we ready for a prognostically prioritized molecular classification? *Blood* 2007; **109**: 431–448.
- Santos FP, Jones D, Qiao W, Cortes JE, Ravandi F, Estey EE et al. Prognostic value of FLT3 mutations among different cytogenetic subgroups in acute myeloid leukemia. *Cancer* 2011; **117**: 2145–2155.
- Frohling S, Schlenk RF, Breitnick J, Benner A, Kreitmeier S, Tobis K et al. Prognostic significance of activating FLT3 mutations in younger adults (16 to 60 years) with acute myeloid leukemia and normal cytogenetics: a study of the AML Study Group Ulm. *Blood* 2002; **100**: 4372–4380.
- Steffen B, Muller-Tidow C, Schwable J, Berdel WE, Serve H. The molecular pathogenesis of acute myeloid leukemia. *Crit Rev Oncol Hematol* 2005; **56**: 195–221.
- Koch S, Jacobi A, Ryser M, Ehninger G, Thiede C. Abnormal localization and accumulation of FLT3-ITD, a mutant receptor tyrosine kinase involved in leukemogenesis. *Cells Tissues Organs* 2008; **188**: 225–235.
- Chan PM. Differential signaling of FLT3 activating mutations in acute myeloid leukemia: a working model. *Protein Cell* 2011; **2**: 108–115.
- Choudhary C, Olsen JV, Brandts C, Cox J, Reddy PN, Bohmer FD et al. Mislocalized activation of oncogenic RTKs switches downstream signaling outcomes. *Mol Cell* 2009; **36**: 326–339.
- Choudhary C, Schwable J, Brandts C, Tickenbrock L, Sargin B, Kindler T et al. AML-associated FLT3 kinase domain mutations show signal transduction differences compared with FLT3 ITD mutations. *Blood* 2005; **106**: 265–273.
- Schmidt-Arras D, Bohmer SA, Koch S, Muller JP, Blei L, Cornils H et al. Anchoring of FLT3 in the endoplasmic reticulum alters signaling quality. *Blood* 2009; **113**: 3568–3576.
- Zarrinkar PP, Gunawardane RN, Cramer MD, Gardner MF, Brigham D, Belli B et al. AC220 is a uniquely potent and selective inhibitor of FLT3 for the treatment of acute myeloid leukemia (AML). *Blood* 2009; **114**: 2984–2992.
- Levis M. Quizartinib in acute myeloid leukemia. *Clin Adv Hematol Oncol* 2013; **11**: 586–588.
- Knapper S. FLT3 inhibition in acute myeloid leukaemia. *Br J Haematol* 2007; **138**: 687–699.
- Grunwald MR, Levis MJ. FLT3 inhibitors for acute myeloid leukemia: a review of their efficacy and mechanisms of resistance. *Int J Hematol* 2013; **97**: 683–694.
- Levis M. FLT3 mutations in acute myeloid leukemia: what is the best approach in 2013? *Hematology Am Soc Hematol Educ Program* 2013; **2013**: 220–226.
- Cortes JE, Kantarjian H, Foran JM, Ghirdaladze D, Zodelava M, Borthakur G et al. Phase I study of quizartinib administered daily to patients with relapsed or refractory acute myeloid leukemia irrespective of FMS-like tyrosine kinase 3-internal tandem duplication status. *J Clin Oncol* 2013; **31**: 3681–3687.
- Wiernik PH. FLT3 inhibitors for the treatment of acute myeloid leukemia. *Clin Adv Hematol Oncol* 2010; **8**: 429–436, 444.
- Fischer T, Stone RM, Deangelo DJ, Galinsky I, Estey E, Lanza C et al. Phase IIB trial of oral Midostaurin (PKC412), the FMS-like tyrosine kinase 3 receptor (FLT3) and multi-targeted kinase inhibitor, in patients with acute myeloid leukemia and high-risk myelodysplastic syndrome with either wild-type or mutated FLT3. *J Clin Oncol* 2010; **28**: 4339–4345.
- Pawar R, Bali OP, Malhotra BK, Lamba G. Recent advances and novel agents for FLT3 mutated acute myeloid leukemia. *Stem Cell Investig* 2014; **1**: 7.
- Kindler T, Lipka DB, Fischer T. FLT3 as a therapeutic target in AML: still challenging after all these years. *Blood* 2010; **116**: 5089–5102.
- Rollig C, Serve H, Huttman A, Noppeney R, Muller-Tidow C, Krug U et al. Addition of sorafenib versus placebo to standard therapy in patients aged 60 years or

- younger with newly diagnosed acute myeloid leukaemia (SORAML): a multi-centre, phase 2, randomised controlled trial. *Lancet Oncol* 2015; **16**: 1691–1699.
- 23 Stone RM, Mandrekas S, Sanford BL, Geyer S, Bloomfield CD, Dohner K *et al*. The Multi-Kinase Inhibitor Midostaurin (M) Prolongs Survival Compared with Placebo(P) in Combination with Daunorubicin(D)/Cytarabine(C) Induction (ind), High-Dose C Consolidation (consol), and As Maintenance (maint) Therapy in Newly Diagnosed Acute Myeloid Leukemia (AML) Patients (pts) Age 18-60 with FLT3 Mutations (muts): An International Prospective Randomized (rand) P-Controlled Double-Blind Trial (CALGB 10603/RATIFY [Alliance]). 57th ASH Annual Meeting. Orlando, FL, Blood, 2015, p 6.
  - 24 Breitenbuecher F, Markova B, Kasper S, Carius B, Stauder T, Bohmer FD *et al*. A novel molecular mechanism of primary resistance to FLT3-kinase inhibitors in AML. *Blood* 2009; **113**: 4063–4073.
  - 25 Smith CC, Lin K, Stecula A, Sali A, Shah NP. FLT3 D835 mutations confer differential resistance to type II FLT3 inhibitors. *Leukemia* 2015; **29**: 2390–2392.
  - 26 Weisberg E, Sattler M, Ray A, Griffin JD. Drug resistance in mutant FLT3-positive AML. *Oncogene* 2010; **29**: 5120–5134.
  - 27 von Bubnoff N, Engh RA, Aberg E, Sanger J, Peschel C, Duyster J. FMS-like tyrosine kinase 3-internal tandem duplication tyrosine kinase inhibitors display a non-overlapping profile of resistance mutations in vitro. *Cancer Res* 2009; **69**: 3032–3041.
  - 28 Man CH, Fung TK, Ho C, Han HH, Chow HC, Ma AC *et al*. Sorafenib treatment of FLT3-ITD(+) acute myeloid leukemia: favorable initial outcome and mechanisms of subsequent nonresponsiveness associated with the emergence of a D835 mutation. *Blood* 2012; **119**: 5133–5143.
  - 29 Heidele F, Solem FK, Breitenbuecher F, Lipka DB, Kasper S, Thiede MH *et al*. Clinical resistance to the kinase inhibitor PKC412 in acute myeloid leukemia by mutation of Asn-676 in the FLT3 tyrosine kinase domain. *Blood* 2006; **107**: 293–300.
  - 30 Kampa-Schittenhelm KM, Heinrich MC, Akmut F, Dohner H, Dohner K, Schittenhelm MM. Quizartinib (AC220) is a potent second generation class III tyrosine kinase inhibitor that displays a distinct inhibition profile against mutant-FLT3, -PDGFRα and -KIT isoforms. *Mol Cancer* 2013; **12**: 19.
  - 31 Cools J, Mentens N, Furet P, Fabbro D, Clark JJ, Griffin JD *et al*. Prediction of resistance to small molecule FLT3 inhibitors: implications for molecularly targeted therapy of acute leukemia. *Cancer Res* 2004; **64**: 6385–6389.
  - 32 Opatz S, Polzer H, Herold T, Konstandin NP, Ksienzyk B, Zellmeier E *et al*. Exome sequencing identifies recurring FLT3 N676K mutations in core-binding factor leukemia. *Blood* 2013; **122**: 1761–1769.
  - 33 Tweeddale ME, Lim B, Jamal N, Robinson J, Zalberg J, Lockwood G *et al*. The presence of clonogenic cells in high-grade malignant lymphoma: a prognostic factor. *Blood* 1987; **69**: 1307–1314.
  - 34 Mehra S, Messner H, Minden M, Chaganti RS. Molecular cytogenetic characterization of non-Hodgkin lymphoma cell lines. *Genes Chromosomes Cancer* 2002; **33**: 225–234.
  - 35 Krupka C, Kufer P, Kischel R, Zugmaier G, Bogeholz J, Kohnke T *et al*. CD33 target validation and sustained depletion of AML blasts in long-term cultures by the bispecific T-cell-engaging antibody AMG 330. *Blood* 2014; **123**: 356–365.
  - 36 Polzer H, Janke H, Schmid D, Hiddemann W, Spiekermann K. Casitas B-lineage lymphoma mutants activate AKT to induce transformation in cooperation with class III receptor tyrosine kinases. *Exp Hematol* 2013; **41**: 271–280 e274.
  - 37 Reindl C, Bagrintseva K, Vempati S, Ellwart JW, Wenig K *et al*. Point mutations in the juxtamembrane domain of FLT3 define a new class of activating mutations in AML. *Blood* 2006; **107**: 3700–3707.
  - 38 Kelly LM, Liu Q, Kutok JL, Williams IR, Boulton CL, Gilliland DG. FLT3 internal tandem duplication mutations associated with human acute myeloid leukemias induce myeloproliferative disease in a murine bone marrow transplant model. *Blood* 2002; **99**: 310–318.
  - 39 Arriba-Tutusaus P, Mack TS, Bullinger L, Schnoder TM, Polanetzki A, Weinert S *et al*. Impact of FLT3-ITD location on sensitivity to TKI-therapy in vitro and in vivo. *Leukemia* 2016; **30**: 1220–1225.
  - 40 Sandhofer N, Bauer J, Reiter K, Dufour A, Rothenberg M, Konstandin NP *et al*. The new and recurrent FLT3 juxtamembrane deletion mutation shows a dominant negative effect on the wild-type FLT3 receptor. *Sci Rep* 2016; **6**: 28032.
  - 41 Krupka C, Kufer P, Kischel R, Zugmaier G, Lichtenegger FS, Kohnke T *et al*. Blockade of the PD-1/PD-L1 axis augments lysis of AML cells by the CD33/CD3 BiTE antibody construct AMG 330: reversing a T-cell-induced immune escape mechanism. *Leukemia* 2016; **30**: 484–491.
  - 42 Durben M, Schmiedel D, Hofmann M, Vogt F, Nubling T, Pyz E *et al*. Characterization of a bispecific FLT3 X CD3 antibody in an improved, recombinant format for the treatment of leukemia. *Mol Ther* 2015; **23**: 648–655.
  - 43 Chou TC. Theoretical basis, experimental design, and computerized simulation of synergism and antagonism in drug combination studies. *Pharmacol Rev* 2006; **58**: 621–681.
  - 44 Spiekermann K, Dirschinger RJ, Schwab R, Bagrintseva K, Faber F, Buske C *et al*. The protein tyrosine kinase inhibitor SU5614 inhibits FLT3 and induces growth arrest and apoptosis in AML-derived cell lines expressing a constitutively activated FLT3. *Blood* 2003; **101**: 1494–1504.
  - 45 Polzer H, Janke H, Schneider S, Hiddemann W, Subklewe M, Spiekermann K. Individualized treatment strategy with small-molecular inhibitors in acute myeloid leukemia with concurrent FLT3-ITD and FLT3-TKD mutation. *J Clin Case Rep* 2015; **5**: 622.
  - 46 Vick B, Rothenberg M, Sandhofer N, Carlet M, Finkenzeller C, Krupka C *et al*. An advanced preclinical mouse model for acute myeloid leukemia using patients' cells of various genetic subgroups and in vivo bioluminescence imaging. *PLoS ONE* 2015; **10**: e0120925.
  - 47 Larrue C, Saland E, Vergez F, Serhan N, Delabesse E, Mansat-De Mas V *et al*. Antileukemic activity of 2-deoxy-D-glucose through inhibition of N-linked glycosylation in acute myeloid leukemia with FLT3-ITD or c-KIT mutations. *Mol Cancer Ther* 2015; **14**: 2364–2373.
  - 48 Hofmann M, Grosse-Hovest L, Nubling T, Pyz E, Bamberg ML, Aulwurm S *et al*. Generation, selection and preclinical characterization of an Fc-optimized FLT3 antibody for the treatment of myeloid leukemia. *Leukemia* 2012; **26**: 1228–1237.
  - 49 Metzelder S, Wang Y, Wollmer E, Wanzel M, Teichler S, Chaturvedi A *et al*. Compassionate use of sorafenib in FLT3-ITD-positive acute myeloid leukemia: sustained regression before and after allogeneic stem cell transplantation. *Blood* 2009; **113**: 6567–6571.
  - 50 Small D. Targeting FLT3 for the treatment of leukemia. *Semin Hematol* 2008; **45** (3 Suppl 2): S17–S21.
  - 51 Knapper S, Burnett AK, Littlewood T, Kell WJ, Agrawal S, Chopra R *et al*. A phase 2 trial of the FLT3 inhibitor lestaurtinib (CEP701) as first-line treatment for older patients with acute myeloid leukemia not considered fit for intensive chemotherapy. *Blood* 2006; **108**: 3262–3270.
  - 52 Smith CC, Viny AD, Massi ES, Kandath C, Socci ND, Hsu H *et al*. Recurrent mutations in CCND3 confer clinical resistance to FLT3 inhibitors. *Blood* 2015; **126**: 677.
  - 53 Zhang H, Watanabe-Smith KM, Bottomly D, Wilmot B, McWeeney SK, Kantarjian HM *et al*. Exome sequencing informs mechanisms of clinical resistance to the FLT3-D835 inhibitor crenolanib. *Blood* 2015; **126**: 2468.
  - 54 Wolleschak D, Mack TS, Perner F, Frey S, Schnoder TM, Wagner MC *et al*. Clinically relevant doses of FLT3-kinase inhibitors quizartinib and midostaurin do not impair T-cell reactivity and function. *Haematologica* 2014; **99**: e90–e93.
  - 55 Zhao W, Gu YH, Song R, Qu BQ, Xu Q. Sorafenib inhibits activation of human peripheral blood T cells by targeting LCK phosphorylation. *Leukemia* 2008; **22**: 1226–1233.
  - 56 Whartenby KA, Small D, Calabresi PA. FLT3 inhibitors for the treatment of autoimmune disease. *Expert Opin Investig Drugs* 2008; **17**: 1685–1692.
  - 57 Kreutzman A, Porkka K, Mustjoki S. Immunomodulatory effects of tyrosine kinase inhibitors. *Int Trends Immun* 2013; **1**: 17–28.
  - 58 Wolfert MA, Boons GJ. Adaptive immune activation: glycosylation does matter. *Nat Chem Biol* 2013; **9**: 776–784.
  - 59 Natarajan K, Xie Y, Burcu M, Linn DE, Qiu Y, Baer MR. Pim-1 kinase phosphorylates and stabilizes 130 kDa FLT3 and promotes aberrant STAT5 signaling in acute myeloid leukemia with FLT3 internal tandem duplication. *PLoS One* 2013; **8**: e74653.
  - 60 Weisberg E, Boulton C, Kelly LM, Manley P, Fabbro D, Meyer T *et al*. Inhibition of mutant FLT3 receptors in leukemia cells by the small molecule tyrosine kinase inhibitor PKC412. *Cancer Cell* 2002; **1**: 433–443.
  - 61 Chu SH, Small D. Mechanisms of resistance to FLT3 inhibitors. *Drug Resist Updat* 2009; **12**: 8–16.



This work is licensed under a Creative Commons Attribution-NonCommercial-NoDerivs 4.0 International License. The images or other third party material in this article are included in the article's Creative Commons license, unless indicated otherwise in the credit line; if the material is not included under the Creative Commons license, users will need to obtain permission from the license holder to reproduce the material. To view a copy of this license, visit <http://creativecommons.org/licenses/by-nc-nd/4.0/>

© The Author(s) 2017

Supplementary Information accompanies this paper on the Leukemia website (<http://www.nature.com/leu>)

# SUPPLEMENTARY INFORMATION

**Tyrosine kinase inhibition increases the cell surface localization of FLT3-ITD and enhances FLT3-directed immunotherapy of acute myeloid leukemia**

***Running title:*** *Targeting FLT3-ITD AML with TKI and immunotherapy*

*Reiter K. et al.*

## **Content**

Supplementary Material and Methods

Supplementary References

Supplementary Tables S1-S5

Supplementary Figures S1-S7



## Supplementary Material and Methods

**Primary patient samples.** Informed written consent was obtained from all patients in accordance with the Declaration of Helsinki. Institutional review board approval was obtained by the Ethics Committee of the participating centers. Patient samples were collected at the University Hospital of the LMU Munich, Medical Hospital for Haematology and Oncology, at the Charité Berlin, and at the University Hospital Tübingen at the time point of first diagnosis or follow up. Mononuclear cells were isolated from bone marrow (BM) aspirates or peripheral blood (PB) and subjected to routine diagnostics for conventional cytogenetic and routine mutational analysis of molecular markers, including *FLT3*-ITD, according to standard protocols.<sup>1,3,4</sup> From the residual patient material and from PB of healthy donors, mononuclear cells were isolated by standard density gradient centrifugation procedure utilizing Biocoll Separating Solution (density 1.077 g/ml; Biochrom, Berlin, Germany) and DPBS 0.2% BSA (DPBS from Biochrom; Specific Albumin from Medion Diagnostics, Berlin, Germany), followed by cryoconservation at  $\leq -80^{\circ}\text{C}$  in 80% FBS (Biochrom) and 20% dimethyl sulfoxide (AppliChem, Darmstadt, Germany).

**Patient derived xenograft (PDX) cells.** Primary patient cells were engrafted and serially passaged in NOD.Cg-*Prkdc<sup>scid</sup> Il2rg<sup>tm1Wjl</sup>/SzJ* (NSG) mice as reported recently.<sup>5</sup> PDX cells were reisolated from mouse BM or spleen and cultured in StemPro-34 SFM Medium (StemCell Technologies, Vancouver, Canada) containing 2% FCS, 1% Pen/Strep, 1% L-Glutamine, 10 ng/ml SCF, TPO and IL-3 (all R&D, Abingdon, UK) according to standard protocols.<sup>6</sup>

**Patient treatment with sorafenib.** Upon diagnosis of AML relapse after conventional therapy, patients received palliative treatment with 200 mg sorafenib, at the University Hospital Tübingen. Sorafenib was taken orally under clinical surveillance. Disease progression and tolerability of the drug were assessed in regular intervals. Patient 1 (TKI-PT#1) received 400 mg twice daily. On day 11 sorafenib dosage was reduced to 400 mg in the morning and 200 mg in the evening, due to thrombocytopenia ( $<100$  G/L). Treatment was paused for four days from day 15, due to thrombocytopenia ( $<20$  G/L) and neutropenia ( $\leq 500/\mu\text{l}$ ), continuing the treatment on day 18 with 200 mg twice daily. Patient 2 (TKI-PT#2) received 400 mg daily. Treatment was paused for seven days from day 27, due to a bacterial infection (C-reactive protein (CRP): 21 mg/dl), continuing the treatment on day 34. *FLT3*-expression was monitored *ex-vivo* by flow cytometry of the patient's BM or PB at relapse (day 0) and during TKI-treatment (indicated day) as described in the Materials & Methods section.

**Mutation profiling.** Mutational analysis of *FLT3* and further AML-related genes was performed for PDX cells and *FLT3*-ITD-positive cell lines, using a targeted, multiplexed amplicon sequencing approach as previously described.<sup>5</sup> *FLT3*-ITD mutational status and *FLT3*-ITD mRNA level respectively, was assessed by qPCR for *FLT3* amplification followed by fragment length analysis as described elsewhere.<sup>1,4</sup>

**Immunoblotting.** AML cell lines, stably transduced Ba/F3 and freshly isolated PDX cells ( $5 \times 10^6$  cells each) were treated for 6 h in the presence or absence of TKI (50 nM) and / or 2-DG (10 mM). Selected AML cell lines were treated for 24 h in the presence or absence of AC220 (50 nM) and / or cycloheximide (10  $\mu$ M). Western blotting of whole-cell lysates was performed according to standard procedures as described previously,<sup>2</sup> utilizing an 8% SDS-PAGE and the following antibodies as recommended by the supplier: rabbit anti-FLT3 (catalog number: sc-480, clone: S-18; Santa Cruz Biotechnology), rabbit anti-pFLT3 (Tyr969, catalog number: 3463S, clone: C24D9; Cell Signaling Technology), mouse anti-GAPDH (catalog number: 32233, clone: 6C5; Santa Cruz Biotechnology), mouse anti-alpha-Tubulin (catalog number: T6199; Sigma-Aldrich), goat anti-rabbit IgG-HRP, goat anti-mouse IgG-HRP, goat anti-rat IgG-HRP (catalog numbers: sc-2004, sc-2005, sc-2006 respectively, Santa Cruz Biotechnology). Proteins were visualized by enhanced chemiluminescence using ECL Plus Western Blot Detection Kit (GE Health Care, Munich, Germany) utilizing the FusionSL detection system (PeqLab, Erlangen, Germany). Quantification of protein levels was performed by densitometry using Fusion software (PeqLab) according to the user manual. Experiments were performed once, if not stated otherwise.

**Flow cytometry.** AML cell lines, stable transduced Ba/F3 and freshly isolated PDX cells ( $1 \times 10^6$  cells each) were treated for 6 h with TKI (50 nM, unless otherwise specified) or left untreated. Cells were incubated with the following antibodies in the dark for 10 min at RT: mouse anti-CD135-PE (catalog number: IM-2234U, clone: SF1.340; Beckman Coulter, Munich, Germany) or isotype control IgG1-FITC/IgG1-PE (catalog number: A07794, clone: 679.1Mc7; Beckman Coulter). For analysis of the TKI-treated patient, whole blood or bone marrow (BM) was incubated with mouse anti-CD135-PE (catalog number: 558996, clone: 4G8 (RUO); BD Biosciences), mouse anti-CD45-FITC (catalog number: 347463, clone: 2D1 (RUO); BD Biosciences) or respective isotype control IgG1-FITC / IgG1-PE-CF594 (catalog number: 562292, clone: X40 (RUO); BD Biosciences) for 15 min in the dark at RT. Furthermore, the sample was incubated with OptiLyse B (Beckman Coulter) for 15 min, followed by distilled water for the same time. For analysis of cells harvested from *in-vitro* cytotoxicity and AC220 inhibition assays on MS-5 feeder cells the following antibodies were used: mouse anti-CD135-PE (catalog number: 558996, clone: 4G8 (RUO); BD Biosciences), mouse anti-CD2-FITC (catalog number: 309218, clone: TS1/8; BioLegend, Hamburg, Germany), mouse CD33-PE-Cy7 (catalog number: 25-0338-42, clone: WM53; e-bioscience, ThermoFisher Scientific, Munich, Germany), each in combination with the respective isotype control IgG1-FITC/IgG1-PE (catalog number: A07794, clone: 679.1Mc7; Beckman Coulter). In addition, these cells were fixed with 2% paraformaldehyde upon dissolving in FACS buffer (DPBS, 2% FBS (Biochrom) and 5  $\mu$ g/ml Propidiumiodide (Carl Roth). All samples were analyzed in FACS buffer using a FACS Calibur or LS II instrument and Cell Quest Software (BD Biosciences, Heidelberg, Germany). Data were analyzed using FlowJo software (Tree Star, FlowJo LCC, Ashland, OR, USA). Surface expression intensity, defined as mean fluorescence intensity (MFI) ratios, was calculated using the geometric mean values of each antibody sample and corresponding isotype control. Experiments were performed once, if not stated otherwise.

**Quantitative real-time RT-PCR.** Selected AML cell lines were treated for 24 h in the presence or absence of AC220 (50 nM). RNA was isolated using the RNeasy Mini Kit (Qiagen, Hilden, Germany) according to the manufacturer's instructions, followed by reverse transcription of 2 µg RNA using the cDNA Synthesis Kit (ThermoFisher Scientific). Quantitative polymerase chain reaction was performed utilizing a LightCycler 480 (Roche, Basel, Switzerland), 500 ng cDNA, the QuantiTect SYBR Green PCR Kit (Qiagen) and the following primers: CTGAATTGCCAGCCACATTTTG (*FLT3*, forward primer), GGAACGCTCTCAGATATGCAG (*FLT3*, reverse primer; melting temperature for both: 78°C), AATGAAGGGGTCATTGATGG (*GAPDH*, forward primer) and AAGGTGAAGGTCGGAGTCAA (*GAPDH*, reverse primer; melting temperature for both: 81.5°C).<sup>7,8</sup> PCR steps included amplification (45 cycles at 58°C annealing temperature) and melting curve analysis (65°C - 95°C; using a temperature gradient of 0.11°C/sec). The quality of amplified PCR products was confirmed by agarose-gel-electrophoresis. Relative quantification of *FLT3* in comparison to *GAPDH* was performed using a mathematical model as described previously.<sup>9</sup> Experiments were performed in biological triplicates.

**Statistics.** Statistical significance was assessed for *in-vitro* results using Student's t-test, Mann-Whitney-U-test, Pearson and Spearman Rho correlation (all two-tailed and unpaired) utilizing the SPSS (IBM, version 23.0) software. Variance and normality of data was evaluated using the Levene-test and Kolmogoroff-Smirnov-test, respectively. Results were considered significant at a *P*-value <0.05.

## Supplementary References

1. Schnittger S, Schoch C, Dugas M, Kern W, Staib P, Wuchter C, et al. Analysis of FLT3 length mutations in 1003 patients with acute myeloid leukemia: correlation to cytogenetics, FAB subtype, and prognosis in the AMLCG study and usefulness as a marker for the detection of minimal residual disease. *Blood* 2002 Jul 1; 100(1): 59-66.
2. Polzer H, Janke H, Schmid D, Hiddemann W, Spiekermann K. Casitas B-lineage lymphoma mutants activate AKT to induce transformation in cooperation with class III receptor tyrosine kinases. *Exp Hematol* 2013 Mar; 41(3): 271-280 e274.
3. Bacher U, Haferlach C, Kern W, Haferlach T, Schnittger S. Prognostic relevance of FLT3-TKD mutations in AML: the combination matters--an analysis of 3082 patients. *Blood* 2008 Mar 1; 111(5): 2527-2537.
4. Schneider F, Hoster E, Unterhalt M, Schneider S, Dufour A, Benthaus T, et al. The FLT3ITD mRNA level has a high prognostic impact in NPM1 mutated, but not in NPM1 unmutated, AML with a normal karyotype. *Blood* 2012 May 10; 119(19): 4383-4386.
5. Vick B, Rothenberg M, Sandhofer N, Carlet M, Finkenzeller C, Krupka C, et al. An advanced preclinical mouse model for acute myeloid leukemia using patients' cells of various genetic subgroups and in vivo bioluminescence imaging. *PLoS One* 2015 Mar 20; 10(3): e0120925.
6. Wermke M, Camgoz A, Paszkowski-Rogacz M, Thieme S, von Bonin M, Dahl A, et al. RNAi profiling of primary human AML cells identifies ROCK1 as a therapeutic target and nominates fasudil as an antileukemic drug. *Blood* 2015 Jun 11; 125(24): 3760-3768.
7. Wang X, Spandidos A, Wang H, Seed B. PrimerBank: a PCR primer database for quantitative gene expression analysis, 2012 update. *Nucleic Acids Res.* 2012 Nov 15; 40(D1): D1144–D1149.
8. Jiang W, Zhang D, Bursac N, Zhang Y. WNT3 is a biomarker capable of predicting the definitive endoderm differentiation potential of hESCs. *Stem Cell Reports* 2013 Jun 4; 1: 46-52.
9. Pfaffl MW. A new mathematical model for relative quantification in real-time RT-PCR. *Nucleic Acids Res.* 2001 May 1; 29(9): e45.

## Supplementary Tables

**Supplementary Table S1: TKI-sensitivity of FLT3 expressing Ba/F3 cell lines.**

FLT3 expression	IC(50)	TKI-sensitivity	CD135 MFI ratio change		
	AC220 [nM]		(mean)	(s.d.)	(range)
FLT3-WT	60.80	(yes)	4.02	0.91	2.98 - 5.20
FLT3-N676K	3.00	yes	4.61	0.87	3.80 - 5.82
FLT3-D835Y	8.30	yes	1.71	0.23	1.39 - 1.88
FLT3-ITD 598/599(12)	3.80	yes	1.07	0.12	0.91 - 1.21
FLT3-ITD 598/599(22)	3.50	yes	1.80	0.37	1.50 - 2.32
FLT3-ITD L601H(10)	1.80	yes	2.99	0.23	2.81 - 3.31
FLT3-ITD K602R(7)	1.20	yes	2.84	0.49	2.19 - 3.39
FLT3-ITD E611C(28)	1.20	yes	2.85	0.47	2.19 - 3.22
FLT3-ITD E611V(32)	2.30	yes	1.99	0.74	1.40 - 3.03
FLT3-ITD G613E(33)	4.30	yes	1.34	0.23	1.04 - 1.59
FLT3-ITD-PM E611C(28)-N676K	43.70	yes	1.20	0.37	0.83 - 1.71
FLT3-ITD-PM E611C(28)-D835Y	>220	no	0.65	0.36	0.31 - 1.41

FLT3 (Fms-related tyrosine kinase 3); WT (wild-type); ITD (internal tandem duplication); TKI (tyrosine kinase inhibitor); MFI (mean fluorescence intensity); CD135 (cluster of differentiation antigen 135) s.d. (standard deviation).

**Supplementary Table S2: TKI-sensitivity of AML cell lines.**

AML cell line	FLT3 expression	IC(50)	IC(50)	IC(50)	TKI-sensitivity	CD135 MFI ratio change		
		AC220 [nM]	PKC412 [nM]	Sorafenib [nM]		(mean)	(s.d.)	(range)
THP-1	yes	>220	>220	>220	no	0.08	0.06	0.02 - 0.17
OCI-AML3	yes	>220	>220	>220	no	0.15	0.01	0.14 - 0.16
MOLM-13	yes	5.10	53.70	44.10	yes	0.07	0.09	-0.02 - 0.20
PL-21	yes	>220	>220	>220	no	0.66	0.21	0.50 - 0.95
MV4-11	yes	1.80	45.70	10.90	yes	3.06	0.79	2.07 - 4.00
MM6	yes	>220*	>220*	>220*	yes*	12.94	3.37	6.18 - 16.60
HL60	no	>220	>220	>220	no	0.01	0.02	-0.02 - 0.05
Kasumi-1	no	197.5	>220*	185.7	yes	-0.04	0.02	-0.06 - -0.01
EOL-1	yes	1.1	73	0.9	yes	-0.26	0.31	-0.44 - 0.03
MUTZ-2	yes	>220	>220	>220	no	1.13	0.19	0.92 - 1.40
NOMO-1	yes	>220	>220	>220	no	0.12	0.12	-0.01 - 0.33
KG-1a	no	>220	>220	>220	no	0.01	0.02	-0.02 - 0.04
K-562	no	>220	>220	>220	no	-0.01	0.05	-0.07 - 0.07

FLT3 (Fms-related tyrosine kinase 3); ITD (internal tandem duplication); TKI (tyrosine kinase inhibitor); MFI (mean fluorescence intensity); CD135 (cluster of differentiation antigen 135); s.d. (standard deviation); \*IC(70) [nM] for MM6: 21 (AC220), 160 (PKC412), 155 (Sorafenib); IC(70) [nM] for Kasumi-1: 135 (PKC412).

**Supplementary Table S3: Characteristics of PDX cells.**

PDX cell	Diagnosis	FAB	Disease Stage	SCT	Cytogenetics	NPM1	FLT3	Further mutated genes	Sex	Age [y]	PB/BM	Blasts [%]
<b>AML-372</b>	AML	M0	relapse	yes	adverse	WT	WT	KRAS, NRAS, TP53	M	42	PB	67
<b>AML-491</b>	AML	NA	relapse	yes	aberrant	WT	WT	DNMT3A, RUNX1, ETV6, PTPN11, BCOR, KRAS, NRAS	F	53	PB	44
<b>AML-573</b>	AML	M1	relapse	no	aberrant	WT	ITD (63nt)	WT1, DNMT3A, IDH2	F	64	BM	90
<b>AML-640</b>	AML	ND	relapse	no	adverse	Mut	ITD (60nt)	IDH1	M	79	PB	90
							ITD (84nt)					
<b>AML-415</b>	AML	NA	relapse	no	normal	Mut	ITD (18nt); LOH	DNMT3A, IDH1	F	68	BM	NA
<b>AML-579</b>	AML	ND	relapse	no	normal	Mut	ITD (24nt); LOH	DNMT3A, IDH1	M	51	PB	77

PDX (patient derived xenograft); FAB (French-American-British classification system); SCT (stem cell transplantation); NPM1 (nucleophosmin-1); FLT3 (Fms-related tyrosine kinase 3); WT (wild-type); Mut (mutated); ITD (internal tandem duplication); LOH (loss of heterozygosity); F (female); M (male); PB (peripheral blood); BM (bone marrow); NA (not available); ND (not determined); KRAS (Kirsten rat sarcoma proto-oncogene); NRAS (neuroblastoma ras proto-oncogene); TP53 (tumor protein p53); DNMT3A (DNA methyltransferase 3 alpha); RUNX1 (runt related transcription factor 1); ETV6 (ETS variant 6); PTPN11 (protein tyrosine phosphatase, non-receptor type 11); BCOR (BCL6 corepressor); WT1 (Wilms tumor 1); IDH (isocitrate dehydrogenase (NADP(+))).

**Supplementary Table S4: Lysis of AML cells by combination or single-agent treatment (FLT3xCD3 or AC220).**

AML cell	CD33+ cells relative to control [%] (s.d.; range)				experimental replicate (no.)
	AC220	FLT3xCD3	combination	computed additive effect	
<b>HL60</b>	112 (22; 97 - 150)	102 (15; 82 - 119)	92 (16; 76 - 110)	114	4
<b>MOLM-13</b>	76 (12; 61 - 93)	4 (2; 1 - 6)	2 (2; 0 - 5)	3	4
<b>MV4-11</b>	59 (12; 43 - 78)	25 (17; 3 - 43)	2 (3; 0 - 7)	15	4
<b>AML-573</b>	89	3	2	3	1
<b>AML-415</b>	95	70	57	67	1
<b>AML-579</b>	82	27	6	22	1
<b>PT#1</b>	90	57	34	51	1
<b>PT#2</b>	88	41	16	36	1

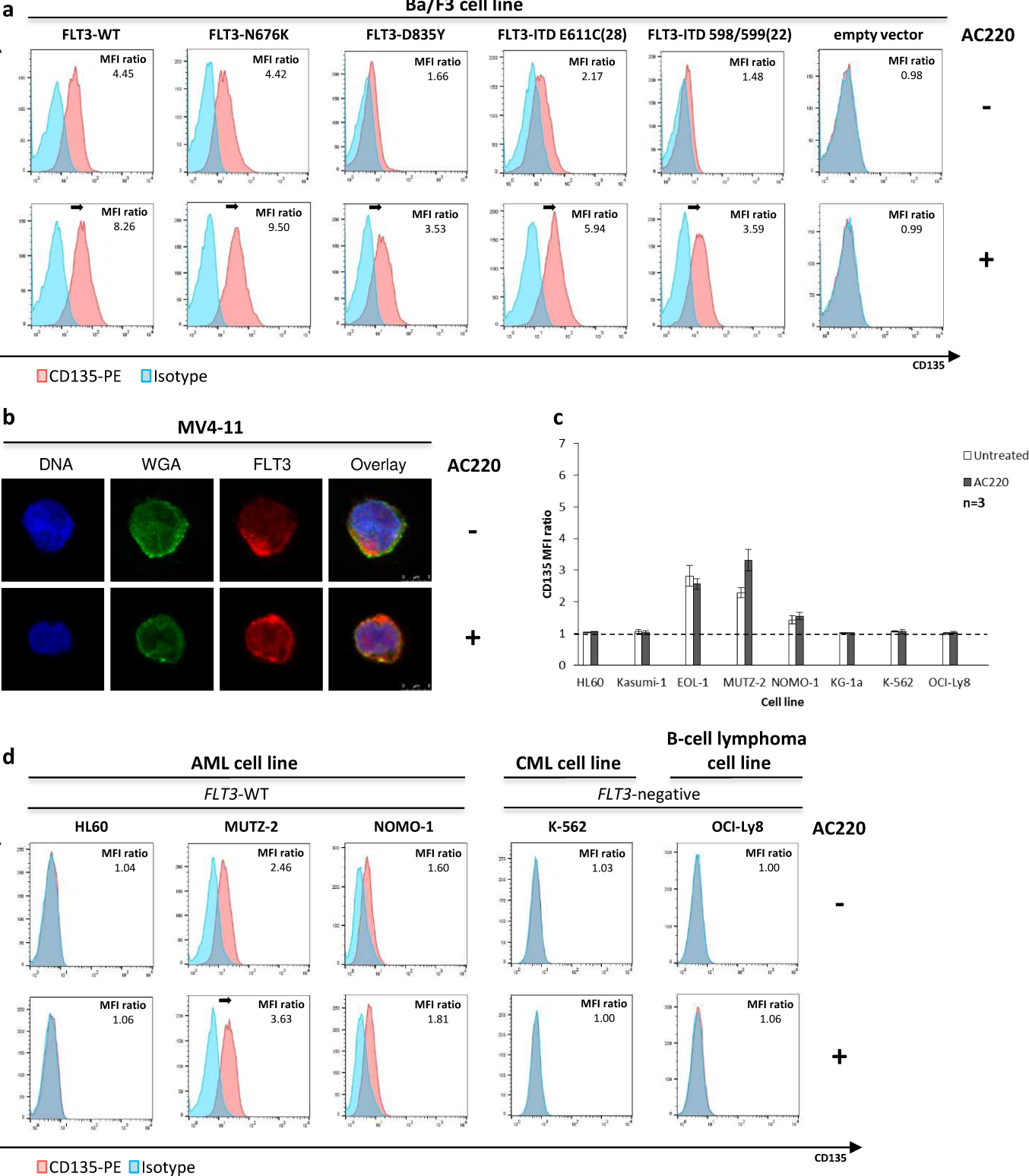
PDX (patient derived xenograft); no. (number); FLT3 (Fms-related tyrosine kinase 3); CD3 (cluster of differentiation antigen 3); s.d. (standard deviation).

**Supplementary Table S5: Characteristics of primary patient samples.**

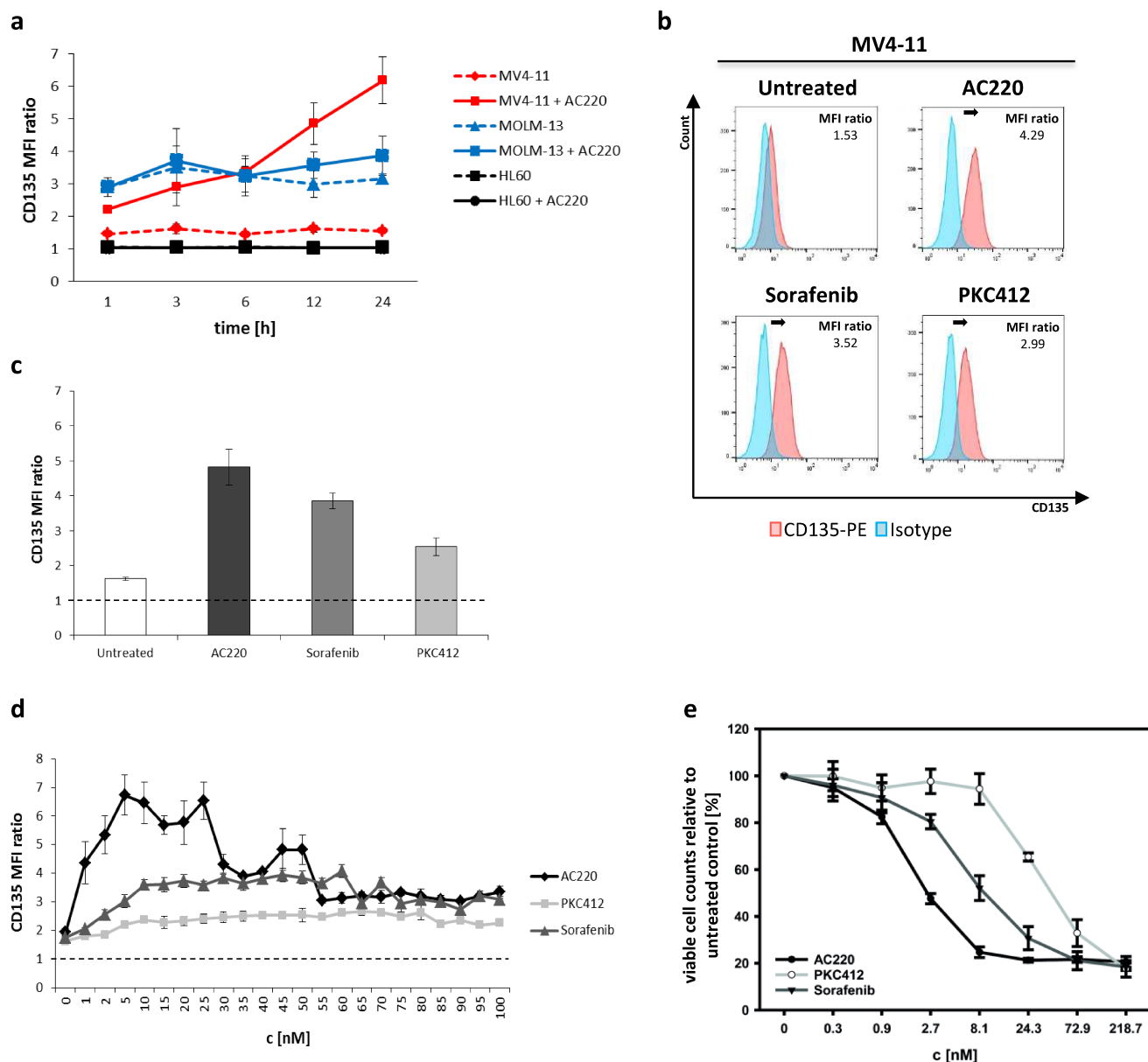
Sample	Diagnosis	FAB	Disease Stage	SCT	Cytogenetics	NPM1	FLT3	Sex	Age [y]	PB/BM	Blasts [%]
<b>TKI-PT#1</b>	AML	M2	relapse	yes	complex	WT	ITD (84nt); level: 0.96	M	29	BM	40
<b>TKI-PT#2</b>	AML	M5	relapse	yes	normal	ND	ITD (216nt); level: 0.84	M	24	PB	48
<b>PT#1</b>	AML	M4	first diagnosis	no	normal	Mut	ITD (60nt); level: 0.50	M	71	PB	78
<b>PT#2</b>	AML	NA	first diagnosis	no	aberrant	ND	ITD (24nt); level: 1	M	74	BM	NA

FAB (French-American-British classification system); SCT (stem cell transplantation); NPM1 (nucleophosmin-1); WT (wild-type); Mut (mutated); FLT3 (Fms-related tyrosine kinase 3); ITD (internal tandem duplication); TKD (tyrosine kinase domain); F (female); M (male); PB (peripheral blood); BM (bone marrow); NA (not available); ND (not determined). The FLT3-ITD mRNA level was calculated according to Schneider et al.<sup>4</sup>.

Supplementary Figures

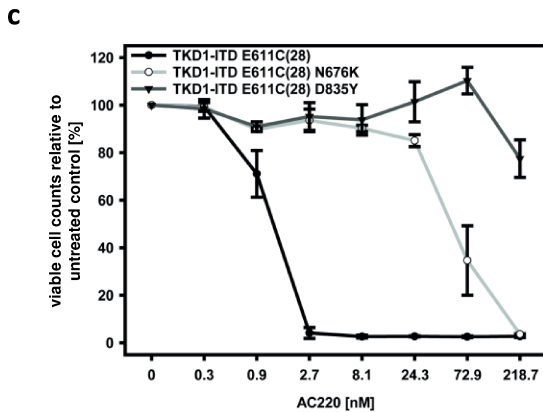
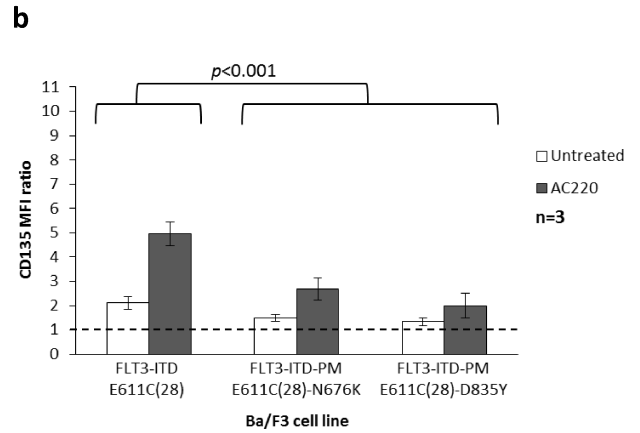
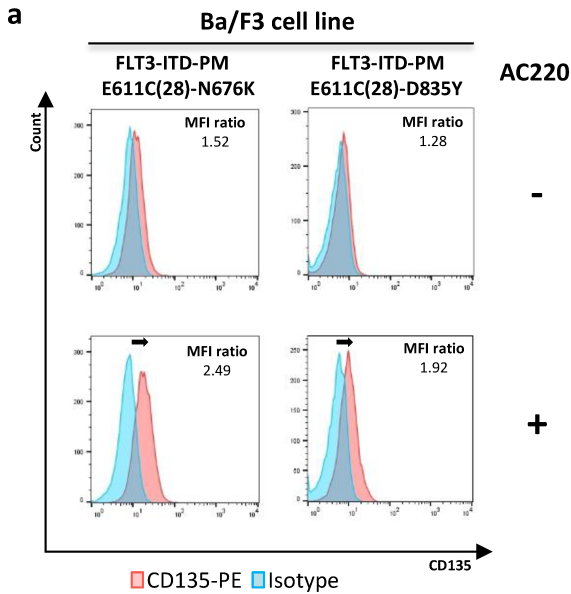


**Supplementary Figure S1: TKI effect on FLT3 surface expression in AML cells. (a)** Representative flow cytometry plots showing the FLT3 surface expression of Ba/F3 cells stably transduced with *FLT3*-WT, *FLT3*-ITD or empty vector with or without AC220-treatment. **(b)** Immunofluorescence staining of *FLT3*-ITD-positive MV4-11 cells with and without AC220-treatment. Scale bar: 5  $\mu$ m. **(c)** FLT3 surface expression levels with or without AC220-treatment (mean  $\pm$  s.d.). **(d)** Representative flow cytometry plots showing the FLT3 surface expression of *FLT3*-WT AML cell lines or *FLT3* negative hematopoietic cell lines (K-562, OCI-Ly8), with or without AC220-treatment. A MFI ratio increase  $\geq 0.5$  is highlighted by an arrow. WGA (wheat germ agglutinin), s.d. (standard deviation).



**Supplementary Figure S2: TKI-treatment response of AML cell lines with regards to dynamics and efficiency. (a)** FLT3 surface expression with or without AC220-treatment over time (mean  $\pm$  s.d.,  $n=3$ ). **(b)** Representative flow cytometry plots showing the FLT3 (CD135) surface expression of MV4-11 cells with or without TKI-treatment. A MFI ratio increase  $\geq 0.50$  is highlighted by an arrow. **(c)** FLT3 surface expression levels with or without TKI-treatment (mean  $\pm$  s.d.,  $n=3$ ). **(d)** FLT3 surface expression levels without or with increasing concentrations of TKI (mean  $\pm$  s.d.,  $n=3$ ). **(e)** Viable cell counts of MV4-11 cells after 72 h treatment with increasing concentrations of TKI (mean  $\pm$  s.d.,  $n=3$ ). s.d. (standard deviation).

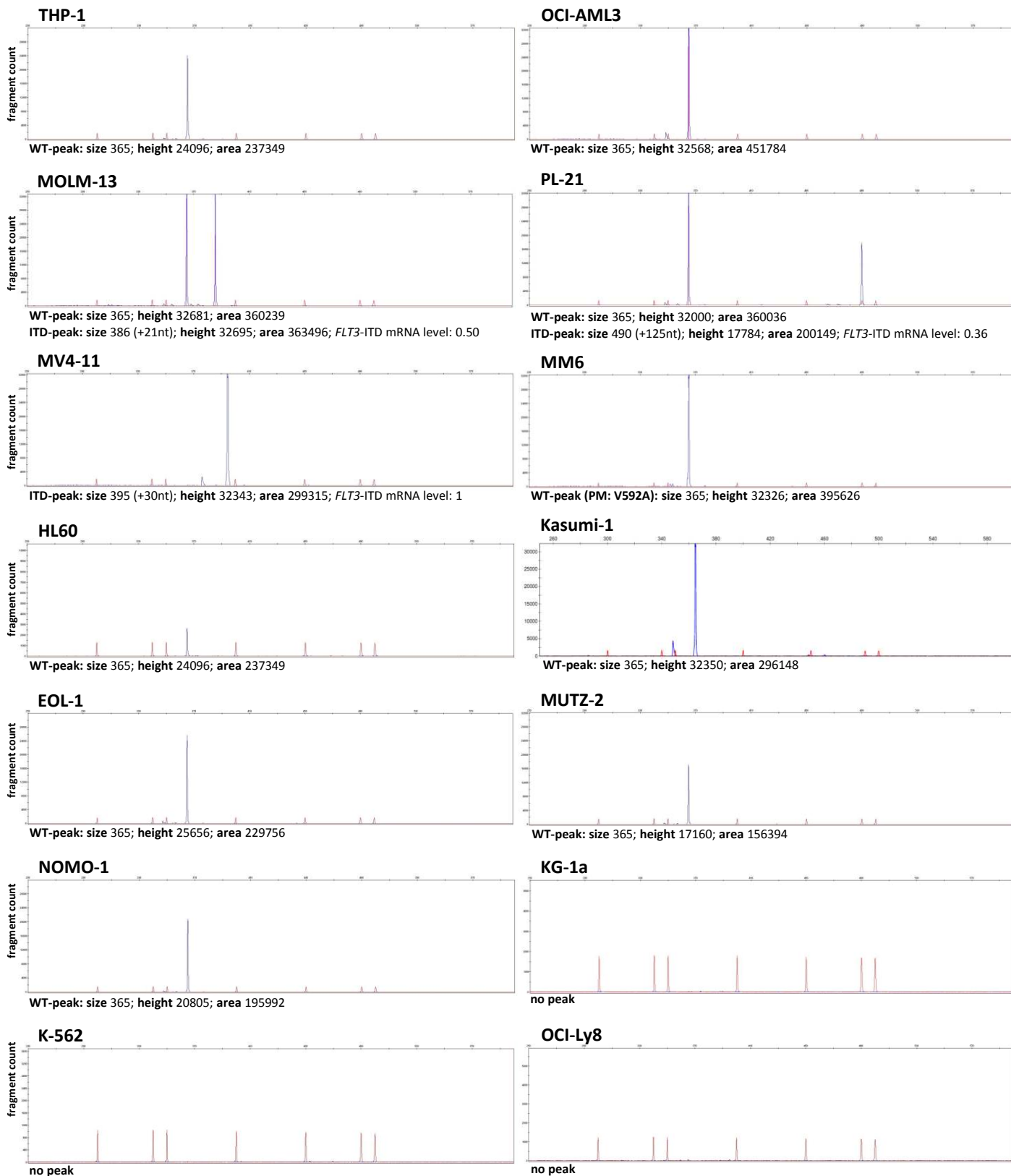




**Supplementary Figure S3: TKI-treatment response of Ba/F3 cells stably transduced with *FLT3*-ITD-PM.**

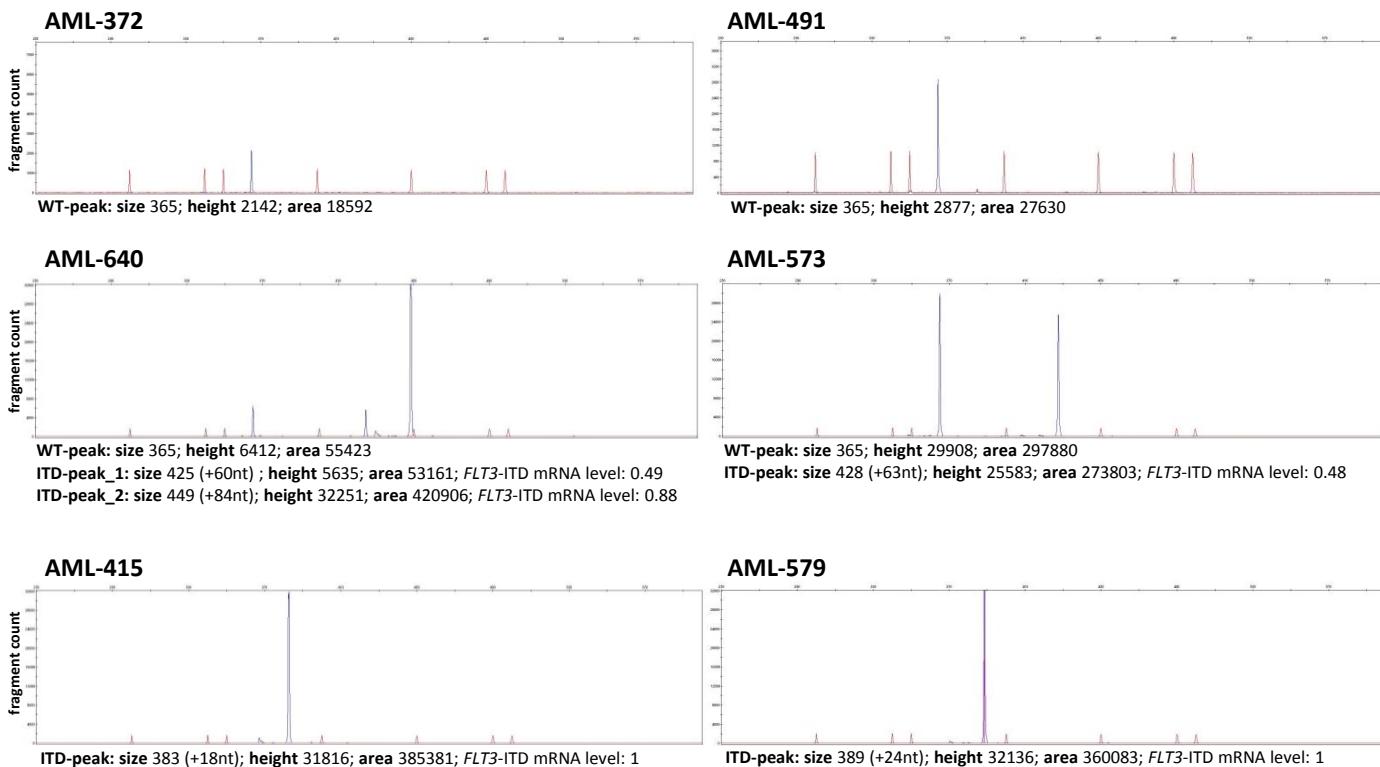
**(a)** Representative flow cytometry plots showing the FLT3 surface expression of Ba/F3 cells stably transduced with *FLT3*-ITD-PM with or without AC220-treatment. A MFI ratio increase  $\geq 0.50$  is highlighted by an arrow. **(b)** FLT3 surface expression levels with or without AC220-treatment (mean  $\pm$  s.d.). **(c)** Viable cell counts of Ba/F3 cells expressing the indicated FLT3 mutants after 72 h treatment with increasing concentrations of AC220 (mean  $\pm$  s.d., n=3). s.d. (standard deviation)

**a**

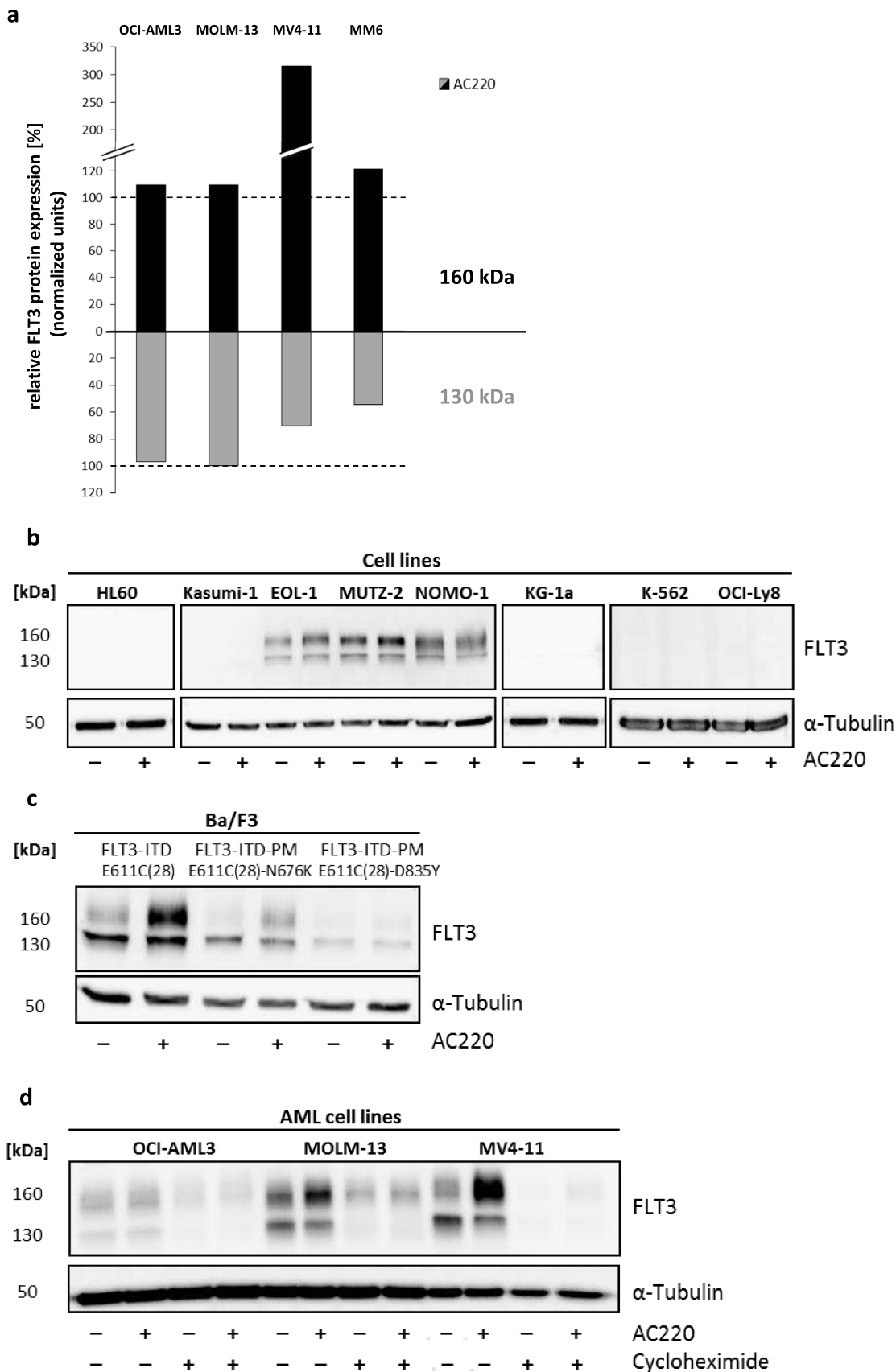


**Supplementary Figure S4: *FLT3*-ITD mRNA levels based on fragment analysis by capillary electrophoresis.**

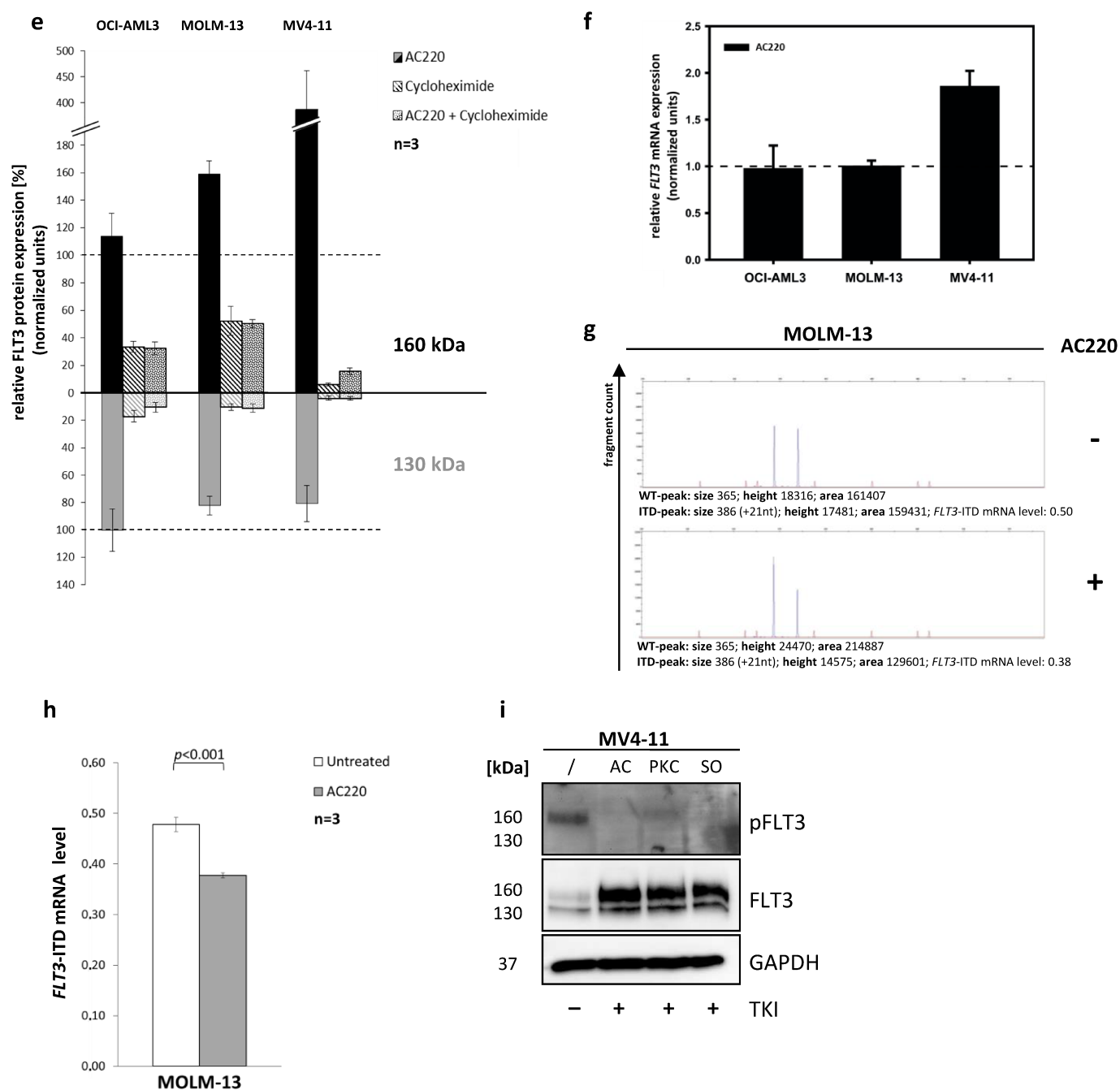
b



**Supplementary Figure S4 continued: *FLT3*-ITD mRNA levels based on fragment analysis by capillary electrophoresis.**  
(a) AML, CML and B-cell lymphoma cell lines and (b) PDX cells.

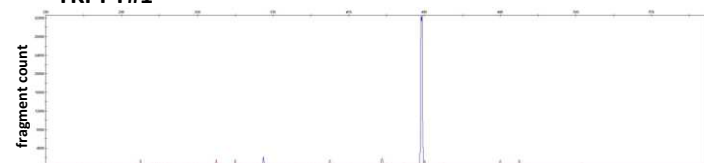


Supplementary Figure S5: TKI-efficiency to increase the amount and glycosylation of FLT3.



**Supplementary Figure S5 continued: TKI-efficiency to increase the amount and glycosylation of FLT3.** (a) Relative FLT3 protein expression of AML cell lines after treatment with AC220 for 6 h (relative values normalized to the FLT3 protein expression of untreated control (dotted line) and alpha-Tubulin). Western blot analysis of FLT3 (130 and 160 kDa) and alpha-Tubulin (50 kDa) in whole cell lysates with or without AC220-treatment and / or cycloheximide of (b) *FLT3*-WT or *FLT3* negative hematopoietic cell lines, (c) Ba/F3 cells transduced with *FLT3*-ITD or *FLT3*-ITD-PM and (d) *FLT3*-WT or *FLT3*-ITD AML cell lines. Relative (e) FLT3 protein and (f) *FLT3* mRNA expression of AML cell lines after treatment with AC220 for 24 h (relative values normalized to the untreated control (dotted line) as well as alpha-Tubulin and *GAPDH* respectively; mean  $\pm$  s.d.). (g) Representative fragment analysis of MOLM-13 cells before and after treatment with AC220 for 24 h. (h) *FLT3*-ITD mRNA levels of MOLM-13 cells with or without AC220-treatment for 24 h measured by fragment analysis (mean  $\pm$  s.d.). The *FLT3*-ITD mRNA level was calculated according to Schneider et al.<sup>4</sup> (i) Western blot analysis of FLT3 or phospho-FLT3 (130 and 160 kDa) and GAPDH (37 kDa) in whole cell lysates with or without AC220-treatment of MV4-11 cells. / (untreated), AC (AC220), SO (sorafenib), PKC (PKC412), s.d. (standard deviation).

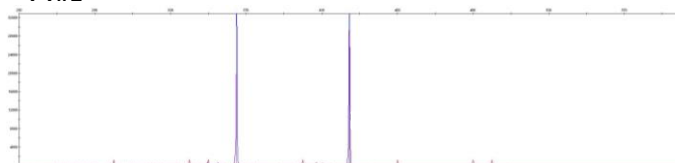
**TKI-PT#1**



**WT-peak:** size 365; height 2121; area 20005

**ITD-peak:** size 449 (+84nt); height 32592; area 459341; *FLT3*-ITD mRNA level: 0.96

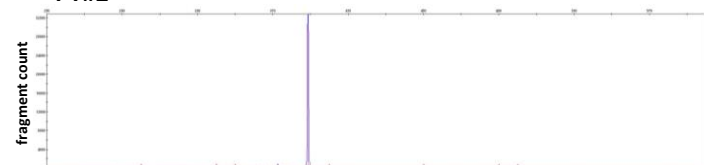
**PT#1**



**WT-peak:** size 365; height 32914; area 333733

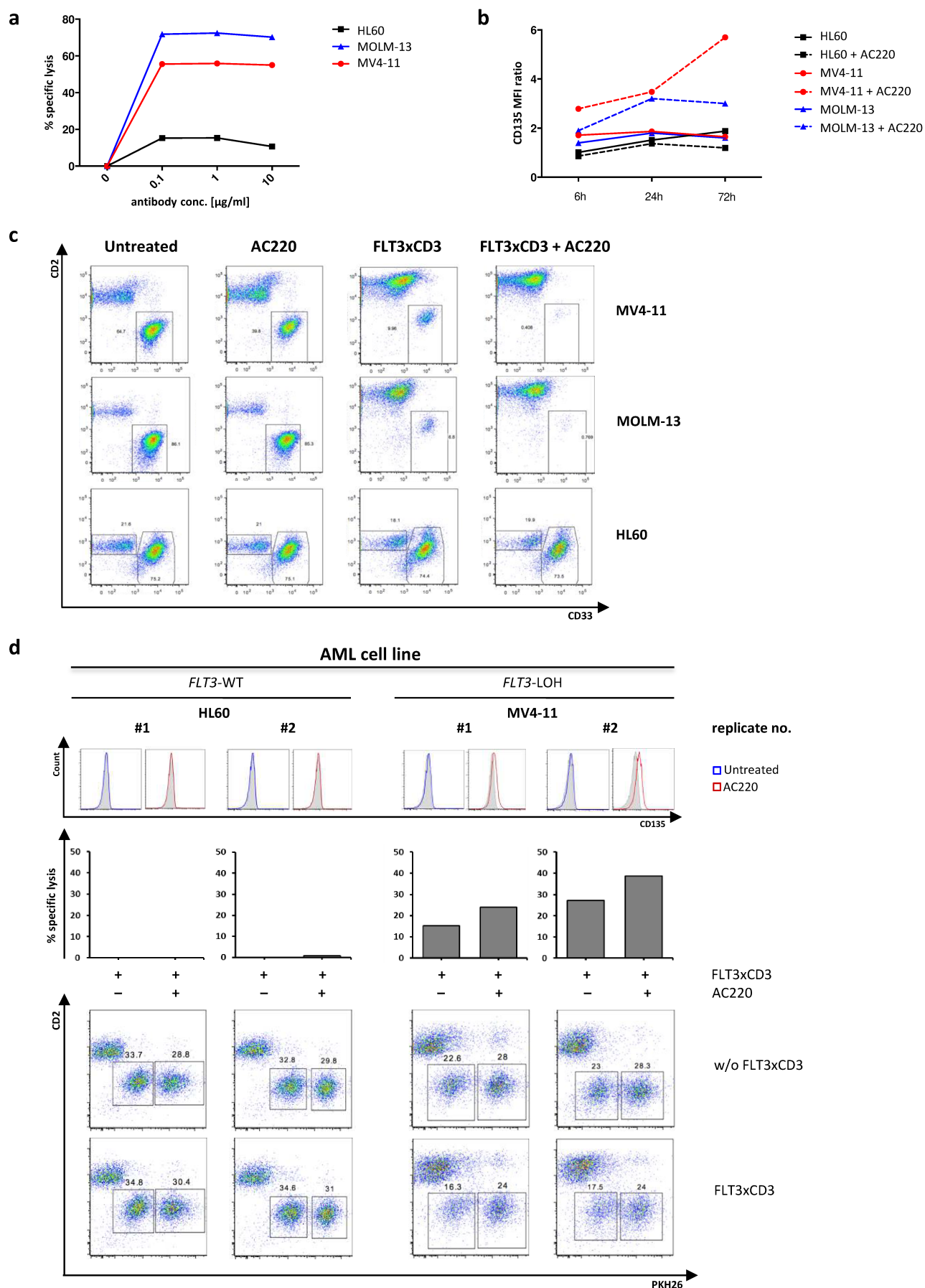
**ITD-peak:** size 425 (+60nt); height 32686; area 339409; *FLT3*-ITD mRNA level: 0.50

**PT#2**



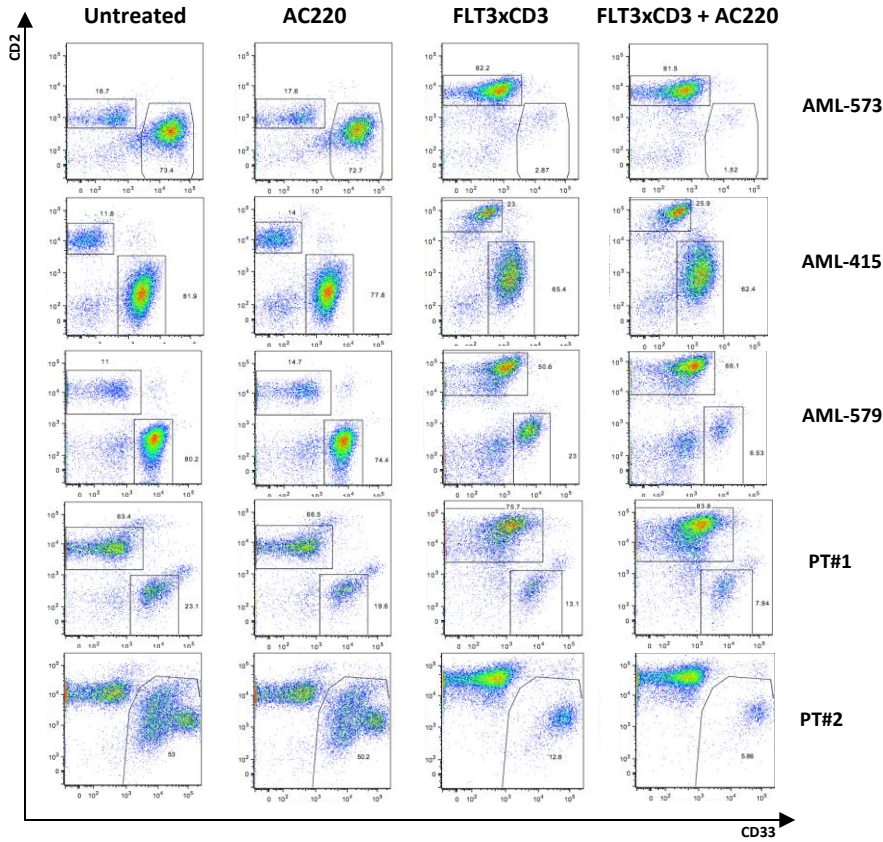
**ITD-peak:** size 389 (+24nt); height 32821; area 378274; *FLT3*-ITD mRNA level: 1

**Supplementary Figure S6: *FLT3*-ITD mRNA levels of primary AML samples.**



Supplementary Figure S7: Lysis of AML cells with regards to dynamics and antibody concentration.

e



**Supplementary Figure S7 continued: Lysis of AML cells with regards to dynamics and antibody concentration. (a)** Lysis of AML cell lines after 72 h treatment with increasing concentrations of FLT3xCD3. **(b)** FLT3 surface expression levels with or without AC220-treatment at time points while TCMC assay. Representative flow cytometry plots with or without FLT3xCD3, AC220 alone or in combination with regards to specific T-cell mediated lysis of **(c)** AML cell lines, **(e)** PDX and primary AML cells. **(d)** Impact of FLT3 surface expression on specific T-cell mediated lysis comparing untreated PKH26<sup>+</sup> to AC220-pre-treated PKH26<sup>-</sup> AML cells. no. (number), w/o (without)



## 5 Discussion

AML is an aggressive hematologic malignancy that, although being treated with well-defined chemotherapy regimens and HSCT, is ultimately fatal in half of all cases. [352, 368] Mutations in *FLT3* are frequently observed in AML patients. If implicated in oncogenic receptor activation, *FLT3* mutations impact negatively on therapy response and outcome. Especially *FLT3*-ITDs with a high mutational burden are associated with adverse prognosis, implicating high relapse rates and a poor OS. [12, 145, 187, 369] Over recent years, studies have highlighted the prognostic relevance of *FLT3*-ITDs, leading to their implementation in the ELN risk stratification. [9, 50, 189, 197, 202, 233, 244, 245, 262] Investigations on *FLT3*-targeted therapy have succeeded in the FDA-approval of Midostaurin in combination with chemotherapy as new treatment option for *FLT3*-mutated AML patients in 2017. Thus, screening of the *FLT3* mutational status at initial diagnosis is highly recommended for AML patients more than ever. [92, 93, 323, 343]

### 5.1 The applicability of NGS-based *FLT3*-ITD detection compared to standard routine assays

Recently, NGS-based approaches for the detection of known AML-driver genes have gained increasing importance. For *FLT3*-targeted NGS screening, benefits in the detection of *FLT3* mutations regarding sensitivity and MRD monitoring were highlighted. [259, 281, 286, 287, 370] Beyond sensitivity, equally important for diagnostic applications is the reliable detection of *FLT3* mutations. As comparison of *FLT3*-targeted NGS-approaches and standard methods has not been performed extensively, this was addressed within the first project of this doctoral work. This project provided insights into the methodological challenges and benefits of *FLT3*-ITD detection by high-throughput amplicon sequencing (HTAS).

#### 5.1.1 Challenges in *FLT3*-ITD detection based on NGS applications

While HTAS detected nearly all dominant ITD clones (97%) in line with routine diagnostics, technical limitations occurred when detecting ITDs combined with a deletion nearby or within the duplicated sequence. Secondly, false-positive calls, termed as non-specific and artificial ITDs, had to be excluded manually. Empirical evaluation of these ITD artifacts led to the definition of a cut-off value, eliminating the sequencing background noise. Furthermore, challenges in the quantification of the *FLT3*-ITD mutational burden of long ITDs were encountered, when compared to fragment analysis. Although *FLT3*-ITD mRNA levels correlated with the variant allele frequencies (VAFs), the estimation of the *FLT3*-ITD mutational load was up to five-fold lower compared to those measured by fragment analysis. This was reflected by a weaker correlation of allelic *FLT3*-ITD/*FLT3*-WT ratio and total *FLT3*-ITD mutational burden, respectively, with clinical outcome (RFS and OS). The cause was likely inappropriate mapping of long ITDs ( $\geq 75$  nt) to the

reference sequence. This phenomenon has been shown by recent studies in smaller cohorts too. They demonstrated that the ITD detection by Pindel is dependent on the length and on the relative position of the amplicon [282, 371, 372]. Therefore, algorithms for read mapping and variant detection are currently limiting the accurate calculation of the mutational load of long ITDs. To overcome this limitation, an increase in read length (more than 2x250 base pairs paired-end) and thus bi-directional coverage may be beneficial. Since the *FLT3*-ITD mutational burden is of prognostic relevance [11, 130, 189, 237, 257, 373], optimization of the VAF calculation by HTAS is indispensable. A recent study compared *FLT3*-ITD sequencing results generated by capillary electrophoresis and an NGS-based approach, analysing refractory or relapsed AML patients (n=241) that underwent TKI-treatment with Gilteritinib (CHRYSLIS Phase I/II study, clinical trial identifier: NCT02014558 [322]). In contrast to our approach, they used genomic DNA, while utilizing the same instrument (Illumina MiSeq). Their results were similar with regards to the *FLT3*-ITD mutational burden of the dominant ITD clone using both methods (concordance rate  $R^2$ : 0.987). [374]

In conjunction with improvements in bioinformatics algorithms for the detection of *FLT3*-ITDs, two novel tools have been presented in 2016. The first one, called ITDseek, shows improved detection of *FLT3*-ITD of varying length and position, being superior to Pindel with regards to the detection of long ITDs and those with a low mutational burden. [371] The other one, ITDetect, shows a profound ITD detection, revealing more ITDs than other reported ITD callers, including Pindel. Using this tool on whole-exome sequencing (WES) data, the authors stated to reveal additional clinically-relevant subclones. [375] ITD calling of Pindel versus ITDseek and ITDetect is shown in Figure 13a. These tools have only been tested in a small series of *FLT3*-ITD positive AML samples so far (n= 11 and 12, respectively), without providing evidence that the additional ITD subclones are valid. Re-evaluation of our cohort with these tools might be helpful to clarify whether the discrepancies of Pindel and fragment analysis could be diminished or if the same or even further valid ITD subclones would be detected. The other limitation in our study regarding the failure to call ITDs combined with deletion is unlikely to be overcome by these tools. Although NGS-approaches should be able to detect a deletion in combination with an ITD, current ITD detection tools fail to output the data correspondingly. Only by manual visualization of the raw sequencing reads of the BAM files in the IGV browser an ITD combined with a deletion can be assumed based on read drop outs (Figure 13b) [371].

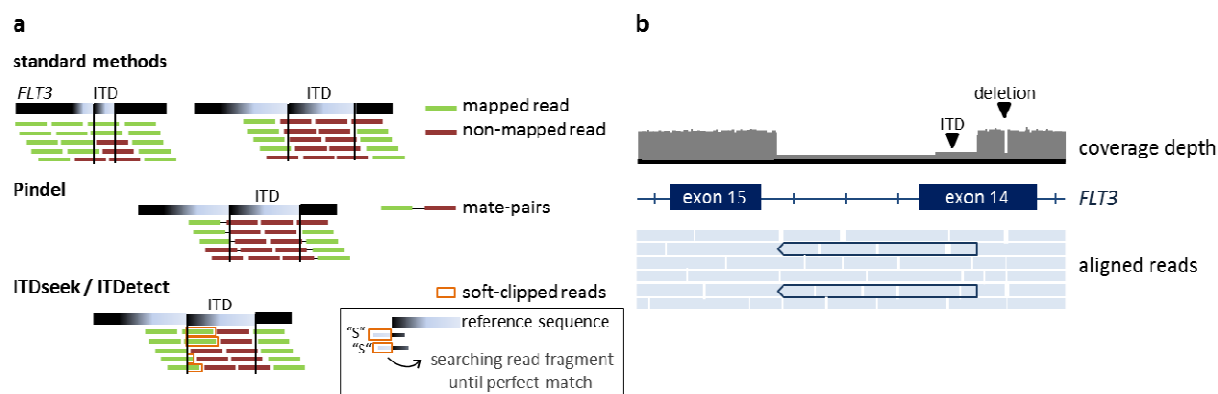


**Figure 13: Read-mapping of ITD detection tools and identification of ITDs combined with deletions.**

**a)** Detection of ITDs by Pindel versus standard NGS tools and novel ITDseek and ITDetect. Standard NGS callers, such as SamTools, are not capable of detecting long nucleotide insertions. This is due to insufficient sequence similarity to align reads. Small insertions are aligned if the inserted sequence is flanked by the homologous WT sequence. ITD callers, including Pindel use a pattern growth approach to identify breakpoints of variants from short paired-end reads for the detection of tandem duplications. They require long enough WT sequences upstream and downstream of the ITD for proper alignment to the FLT3 reference sequence. In contrast, ITDseek and ITDetect make use of any additional duplicated nucleotides that are marked as soft-clipped ("S"), in case the ITD is too long and/or too close to either end of amplicon. They correlate these soft-clipping points with any corresponding primary alignment plus compare points of soft-clipping in sequence read pairs for the detection of ITDs. **b)** Detection of ITDs combined with a deletion, represented by a schematic NGS sequencing histogram covering exon 14 and 15. Deletions are shown by read drop outs in raw reads of the BAM files, followed by the duplicated sequence corresponding to the ITD. The drop in sequencing depth at the region of the single-nucleotide deletion affects the coverage of the ITD *in trans* (modified from Spencer 2013, Shin 2016 and Au 2016). [282, 371, 375, 376]

False-positive ITD calls in turn would still require intra- and inter-run controls, when designating NGS-based assays for diagnostic routine. This was exemplified in our study by artificial ITDs detected within the background signal in FLT3-WT samples. They required the definition of a cut-off at 0.5% VAF for their exclusion. The same cut-off value was also used in another recent study [374]. Furthermore, FLT3-ITDs detected within or near the primer region have to be evaluated carefully to exclude artificial ITDs as seen in 15% of our investigated samples. An adaptive technique designed to aid in error-corrected sequencing and in normalization for any amplification bias in PCR-based methods for MRD detection is the implementation of unique molecular indexes (UMIs) for targeted sequencing. UMIs are barcoded sequences that enable an unbiased quantification of mutations. They can also be applied to exclude amplification errors, such as artificial variants, by setting a threshold of equal to or more than 90% for identical variant calls within read families in order to yield true mutations (Figure 14). [377] For our approach, implementing UMIs into the primer sequence might have helped to avoid false-positive calls, which were identified by manual exclusion of artificial variants above the 0.5% VAF cut-off level. In addition, compliance with quality assurance and management according to diagnostic standards is essential to use any NGS-application in a certified laboratory. To this end, laboratory accreditation checklists and guidelines assuring validation of NGS assays, assigned to the requirements for upstream analytical processes and downstream bioinformatic analysis for

NGS in clinical applications, were published. [378-380] Nonetheless, bioinformatics expertise is required in accurately assessing true mutations by a defined workflow so far [381].

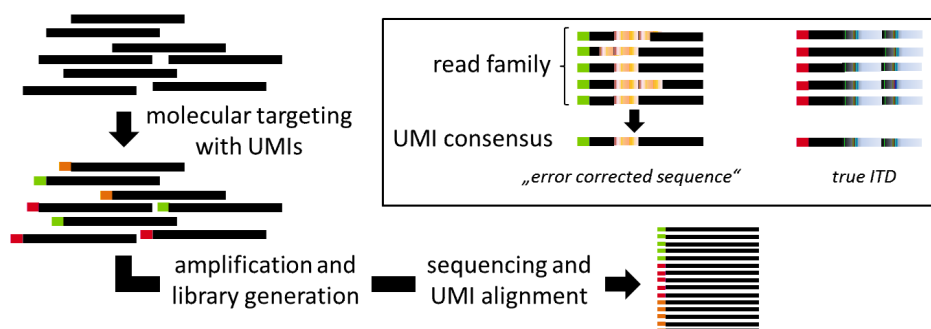


**Figure 14: The function of UMIs in amplification-based approaches.**

Identification of false-positive variants by implementing UMIs for targeted amplicon sequencing. Molecules are individually tagged with permanent UMI. The tag enables to count the number of original target molecules present in the sample despite PCR amplification bias. Sporadic errors introduced during PCR are excluded after discrimination of true variants within aligned read families sorted by UMIs (black rectangle). Double-UMIs, using the combined information of different UMI sequences for forward and reverse primer increase the error identification rate (adapted from Roloff 2017). [377]

In the future, data evaluation may be further supported by an artificial intelligence (AI). Algorithms are based on machine learning systems that can be applied for clinical predictions. Initial trials of such adaptive systems assisting in precision medicine diagnostics are already underway. Compared to human molecular tumour boards, cognitive computing identified additional genomic events in NGS of cancer patients. Many of those genetic events were considered clinically actionable based on recent publications and novel biomarker-selected clinical trials. [382, 383]

### 5.1.2 Clinical relevance of *FLT3*-ITD detection with high sensitivity

A feature HTAS was superior to conventional *FLT3*-ITD detection methods was its higher sensitivity in detecting *FLT3*-ITD subclones. A serial dilution demonstrated that the heterozygous ITD in MOLM-13 can be detected down to  $10^{-3}$  in our 96 sample multiplex setting. In contrast, fragment analysis detected levels down to  $10^{-1}$ . For fragment analysis, adaption of the annealing temperature and increased number of cycles as well as amount and concentration of PCR product has been shown to increase the maximum sensitivity down to  $10^{-2}$  [384]. In contrast, sensitivities down to  $10^{-5}$  can be achieved by NGS for homozygous ITDs, when adapting sample size per run to gain a higher coverage [281, 385]. A higher sensitivity results in identifying ITDs in samples that have been assessed *FLT3*-negative by standard diagnostics, due to ITD levels below the detection limit of routine methods [371]. This was also the case for one out of 17 tested samples in our study. Others have shown that techniques with a higher sensitivity thus can reveal ITDs in samples from initial diagnosis at very low levels that promoted relapse, detectable with conventional methods only at relapse [106, 259]. Regarding the *FLT3*-ITD positive patients, HTAS detected 46 additional subclones, not identified by fragment analysis or Sanger

sequencing. The majority of them could be validated on a genomic level. The number of ITDs by HTAS had a prognostic impact on RFS and OS, which was seen only as a trend in Kaplan-Meier survival curves by standard routine assays. In multivariate analysis, single *FLT3*-ITD mutations detected by HTAS were associated with a trend for longer RFS. In line with this, a low ITD mutation load correlated significantly with longer RFS in multivariate analysis. The correlation of additional clonal *FLT3*-ITD complexity by HTAS with adverse clinical outcome is in line with recent findings, demonstrating that the number of driver mutations per patient has prognostic relevance in MDS and AML [386-388]. Concordantly, similar results for the impact of *FLT3*-ITD subclones on therapy response and outcome have been obtained. This suggests the implementation of the number of *FLT3*-ITD clones into prognostic stratification [189, 257, 259, 389-391]. Contrarily, in a study of pediatric AML no effect of multiple ITD clones on outcome has been observed [392].

A higher sensitivity impacts on the therapy decision when considering the selection of patients for TKI treatment with Midostaurin in combination with induction chemotherapy or for TKI monotherapy bridging towards an HSCT. Therefore, a reliable and sensitive identification of *FLT3*-mutations in AML, including ITDs, is essential for initial risk assessment and therapeutic intervention. The additionally detected ITD subclones resulting from higher sensitivity would in turn contribute to the total *FLT3*-ITD mutational burden and *FLT3*-ITD/*FLT3*-WT ratio accordingly. In line with this, a higher clonal *FLT3*-ITD heterogeneity probably drives disease progression by variations of ITD clone sizes and of the *FLT3*-ITD/*FLT3*-WT ratio, respectively. Hence, a higher load of ITD mRNA level may result in more *FLT3*-mutated protein. Although *FLT3*-ITD is a rather variable marker during therapy and disease progression, with mutational plasticity between diagnosis and relapse [27, 106, 268, 269, 276], several studies have pointed out the potential of NGS approaches for *FLT3*-ITD MRD assessment in first CR over conventional diagnostic applications for the prediction of relapse [80, 189, 249, 259, 268, 270, 279, 281, 282, 286]. This also applies to the measurement of the anti-leukemic activity of TKI inhibitors in identifying patients who may require a more intensive treatment. In a recently published study, *FLT3*-ITD detection by NGS could distinguish patients with a good TKI-response, showing prolonged OS, from patients with a poor TKI-response based on their subclonal *FLT3*-ITD level ( $\leq 10^{-2}$ ; CHRYSALIS Phase I/II trial patients receiving Gilteritinib). They confirmed that the presence of an ITD at MRD level ( $>10^{-4}$ ) is predictive for OS in patients achieving clinical remission. By now, this *FLT3*-ITD MRD NGS test is commercially available. [287, 385] Consistently, other studies report that *FLT3* positivity in first remission impacts negatively on outcome in HSCT, even at MRD level [370, 393]. In contrast, this correlation was not observed in a cohort of *FLT3*-ITD positive patients who received T-cell repleted haploidentical stem cell transplantation. [394, 395] Overall, *FLT3*-ITD monitoring thus seems to be a powerful prognostic tool by assessment of the kinetics of early phase treatment response, apart from being used for initial risk stratification at diagnosis.

### 5.1.3 NGS compared to other sensitive *FLT3*-ITD detection strategies

Besides NGS, researchers also investigate the applicability of other strategies for a sensitive *FLT3*-ITD detection and monitoring, including PCR-based tools such as real-time quantitative RT-PCR (RQ-PCR) and digital droplet PCR (ddPCR).

Utilizing RQ-PCR for the detection of *FLT3*-ITD transcripts, a sensitivity of  $10^{-3}$  to  $10^{-4}$  can be achieved [80]. Similar to NGS studies [259, 281], the higher sensitivity enables the detection of small transcript levels in follow-up samples during CR. These are not measurable by conventional PCR [278]. A 3-log reduction in the *FLT3*-ITD level by RQ-PCR forecasts a better outcome of AML patients compared to those showing lower reductions and MRD levels above 0.1% [396, 397]. A benefit of RQ-PCR is the normalization of *FLT3*-ITD transcripts to the transcripts of a housekeeping gene, preferably Abelson murine leukemia viral oncogene homolog 1 (*ABL1*) [286]. The implementation of this control might also be useful for cDNA based NGS-approaches. Since being PCR-based also RQ-PCR requires a threshold which might be above low level transcripts in remission samples [283]. A method with strong potential to discriminate ITDs from the background signal is ddPCR (Figure 15a). ddPCR performs multiple PCRs of separated target DNA molecules in parallel, yielding ITD levels approximately 2-fold higher than VAFs measured by NGS variant calling of *FLT3*-ITD [377, 398]. To discriminate WT from ITD amplicons and to enable a precise quantification of ITD copies this technique, similar to RQ-PCR, requires ITD clone-specific primer-probes for each patient. Being resource-consuming, is a major drawback of both RQ-PCR and ddPCR. Regarding MRD monitoring, RQ-PCR and ddPCR both are unable to detect subclonal ITDs, undiscovered by conventional tools at initial diagnosis. Subsequently, they fail to detect clinically relevant low-level subclones outgrowing at relapse. [283, 286, 377, 398]

Other approaches try to improve the specificity and sensitivity of conventional PCR by using multiple standard set of primers. Examples are delta-PCR (using a triple-primer strategy) or nested-PCR (using two primer sets sequentially). Although revealing additional and clinically relevant *FLT3*-ITD subclones at initial diagnosis, that have not been detected with conventional methods but may grow out during disease progression, sensitivity appropriate for MRD cannot be reached. [280, 375] Another approach intends to solely detect duplication specific amplicons to reduce any WT allele competitive amplification bias that may limit ITD detection sensitivity of PCR-based assays. This inverse PCR method is named tandem duplication PCR (Figure 15b). Tandem duplication PCR has been shown to detect long ITDs with high sensitivity (up to  $10^{-4}$ ), but it fails to identify ITDs smaller than 40 nt, whereby up to 40% of ITDs may be missed. Additionally, in two out of 24 BM samples of healthy transplant donors an ITD was detected, each not-in frame indicating that this technique still requires further validation. [279, 399]

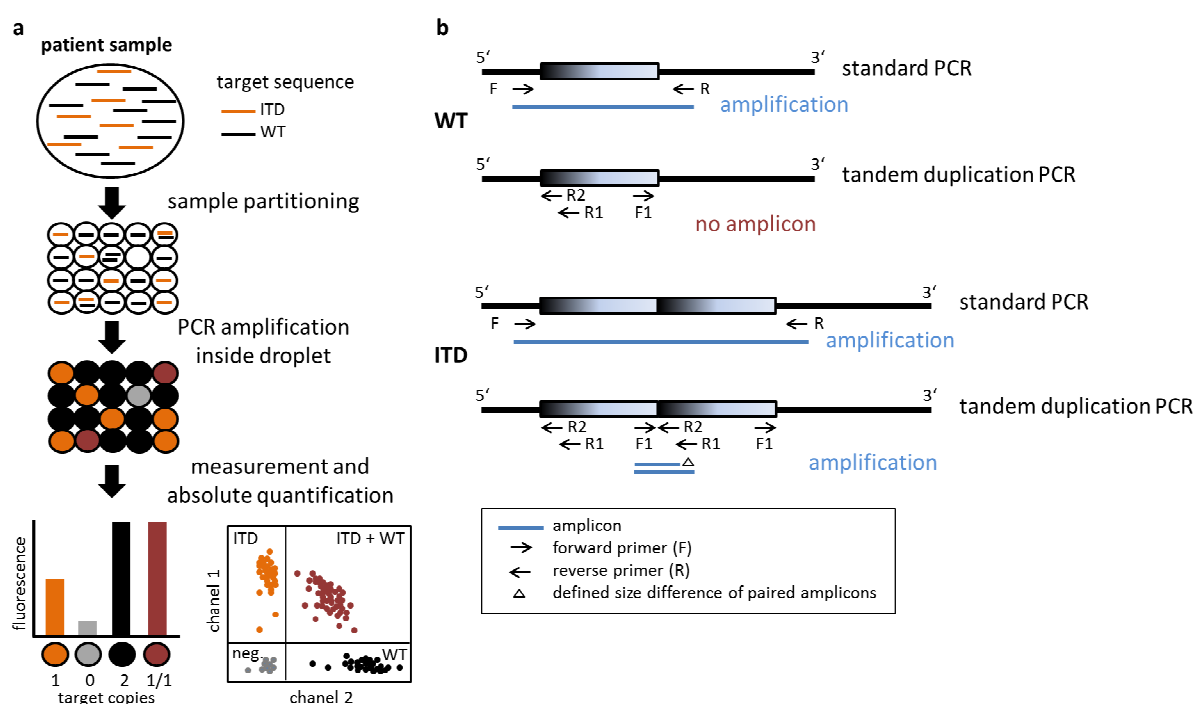


**Figure 15: Conventional PCR compared to inverse PCR and ddPCR.**

**a)** ddPCR is accomplished by nanofluidic chips which distribute the DNA-PCR mixture into single reaction water-oil droplets. Each droplet contains single or multiple copies of WT, mutant allele, WT plus mutant or no target DNA. The readout of each PCR is performed separately by fluorescence signal measurement, displayed in a graphical output as illustrated. Of note, only single-positive clusters can be used for quantification of the total number of mutant sequences (adapted from Roloff 2017 and Whale 2016). [377, 398, 400] **b)** Primers for specific tandem duplication amplification face away from each other, resulting in an amplicon only when the duplication junction is present. No template-specific amplification occurs from the WT allele or if one or both primers bind outside the duplicated sequence. A third primer ensures specificity of PCR amplification. By standard PCR template-specific amplicons are generated irrespective of WT or duplicated allele, competing for primer binding (adapted from Lin 2013). [279]

In total, the variety of techniques and variability of assay performance and cut-off levels for data evaluation hardly provide an exact guideline for consistent measurements underlying treatment decisions worldwide up to date. Standardization of *FLT3*-ITD detection and quantification for comparable results between routine laboratories is thus urgently required.

#### 5.1.4 The impact of the sample material on *FLT3*-ITD detection sensitivity

Irrespective of the used technique, the sample material impacts on sensitivity. Several discussions are ongoing about preferably screening BM aspirates instead of PB samples. Due to a usually higher tumor load and thus higher sensitivity BM is favored, especially for MRD assessment during therapy. [80, 283] The practicability of BM sampling with regards to sample collection is, however, questionable when considering short monitoring intervals. Another issue is about whether to use gDNA or reversely transcribed cDNA as input. Concordant with other reports [195], we demonstrated a good correlation of *FLT3*-ITD levels irrespective of input DNA - although differences in *FLT3*-ITD levels were obvious in some samples. This is probably attributed to transcriptional imbalance, favouring the expression of one allele. According to the

revised version of the ELN guideline 2017 [50], gDNA is recommended as input for *FLT3*-ITD fragment analysis, avoiding any transcription bias. However, the assessment of cDNA might still be worthwhile and recommendable, since the pretreatment *FLT3*-ITD ratio based on cDNA seems to correlate with TKI response (as demonstrated by the third project of this doctoral work and by a study investigating *ex vivo* pediatric AML samples treated with Gilteritinib [392]). On the cDNA level any influence of TKI treatment on the *FLT3*-ITD ratio might however complicate accurate treatment response measurements. Hence, changes in *FLT3*-ITD mRNA level in the AML cell line MOLM-13 upon TKI treatment were observed. Further evaluation of this phenomenon in the heterozygous setting is required. So far, several NGS-based *FLT3*-mutation detection tools have been designed to analyse gDNA input, including targeted haloplex sequencing. The recently commercialized *FLT3*-ITD MRD NGS assay also relies on gDNA input. In our study the use of gDNA from selected samples seemed to further ease the identification of ITDs - especially those being expressed at low levels as determined by fragment analysis. A higher number of ITDs was detected by gDNA compared to cDNA fragment analysis, affirming additional subclones detected by HTAS. Since *FLT3* is a rather variable marker during disease progression [106, 268, 269, 276, 283] with ITDs often being subclonal or expressed at low levels at initial diagnosis and then promoting relapse, a sensitive determination irrespective of transcriptional bias is relevant. Nonetheless, sensitivity might be still a matter of technique rather than input DNA.

### 5.1.5 Prospective NGS-application in future *FLT3*-ITD routine diagnostics

Our and other published results highlight the potential and reliability of NGS-based *FLT3*-ITD detection applications for diagnosis as well as therapy response monitoring [259, 281, 385]. Therefore, the use for routine diagnostics seems promising and reasonable. With increasing read length the covered sequence within *FLT3* may even be expanded to the TKD2 region. This would enable to simultaneously identify activating *FLT3*-PMs, such as D835Y, which mediate TKI resistance. Within our cohort a preliminary test with the six patient samples would be possible, which were routinely-assessed and harbour a TKD mutation. Including *FLT3*-PMs in the assay would follow the recent recommendation by the ELN to perform *FLT3* testing for both ITD and TKD for all patients diagnosed with AML. With regards to the therapeutic application of Midostaurin in combination with chemotherapy they suggest the assessment of *FLT3*-mutation status receiving results within 3 days. [50, 401] Regarding our 96-well setting this would require down-scaling according to the needs in routine diagnostics based on incoming samples and an established bioinformatic output system. With decreasing sample number the sensitivity as well as the costs per sample will rise. Therefore, it might be worth to expand our approach to assess several prognostic markers at once by multiplexing different target-amplicons from mutational hotspots in further genes, including *NPM1*, *CEBPA* and *WT1*. Sequencing multiple targets in parallel, performing a gene panel, in turn reduces sensitivity for either target. When maintaining sensitivity, higher costs per sample are implicated. However, this would save time compared to multiple Sanger sequencing runs [381]. An all-in-one genetic assay would enable classification of patients more accurately, considering that co-occurrence with an *NPM1* mutation partially improves response and survival outcomes of *FLT3*-ITD positive or *FLT3*-D835 mutated patients. [402-404]. Especially for diagnosis, the assessment of a gene panel is attractive to accurately



classify molecularly heterogeneous AML patients and to define their best personalized therapeutic option.

## 5.2 The relevance of new and recurrent *FLT3* deletion mutations in AML

Since not all mutations in the *FLT3* gene found in AML patients have biological consequences [229], deciphering passenger from driver mutations remains essential. The second project provided insights about the impact of a new and recurrent FLT3 mutant p.Q569Vfs\*2 on receptor function and downstream signalling.

### 5.2.1 Deciphering the biological consequences of *FLT3* p.Q569Vfs\*2

The *FLT3* mutation p.Q569Vfs\*2 was found in an AML patient at relapse. P.Q569Vfs\*2 in *FLT3* leads to a frameshift deletion generating a truncated FLT3 receptor in transduced Ba/F3 cells, which likely represented the processed protein in the patient sample. In a study of a large AML cohort this mutation was detected with a frequency of 0.03% (two out of 6843 unselected AML patients) [405]. Functional characterization of AML patient-derived *FLT3* mutations causing a truncated FLT3 receptor have not been performed yet. Only the combination of a JMD-ITD with an engineered truncation of the kinase domains has been investigated to demonstrate the JMD-mediated impact on receptor activation and proliferation [220]. In contrast, FLT3-p.Q569Vfs\*2 only comprised the first amino acids of the JMD, while lacking the residual internal receptor region responsible for signalling activation. The FLT3 tyrosine residues 589 and 591 in the JMD have been reported to be essential for ligand-dependent activation of FLT3-WT as well as for the transforming potential of oncogenic FLT3 mutants [406]. Hence, a FLT3-mediated proliferation advantage was questionable. As expected, Ba/F3 cells expressing the truncated FLT3 mutant showed no proliferation upon ligand stimulation. This effect also occurred in the heterozygous setting. FLT3-p.Q569Vfs\*2 influenced FLT3-WT receptor signalling in a dominant-negative way, due to the formation of receptor heterocomplexes. mRNA levels of FLT3-p.Q569Vfs\*2 were lower compared to FLT3-WT in the patient sample. Nonetheless, evidence in Ba/F3 cells is required to proof that FLT3 heterodimerization is favoured compared to homodimerization upon FL stimulation. Subsequently, the amount of serum FL level in the patient sample might be informative. Nonetheless, heterodimer formation and influence on FLT3-WT has been shown for the engineered truncated JMD-ITD mutant too [220]. Similarly, for the truncated EGFR CD-533 a dominant negative effect on WT receptors has been observed, proposing heterodimerization as responsible mechanism for abrogation of tyrosine kinase activity and suppression of mitogenic response of WT receptors. [407, 408] Similar to the investigated truncated FLT3 variant p.Q569Vfs\*2, EGFR CD-533 contains a premature stop following a few amino acids after the transmembrane domain, lacking all cytoplasmic phosphorylation residues. Therefore, autophosphorylation and subsequent receptor activation upon dimerization with the truncated form seems to be inhibited. Interestingly, the presence of EGFR CD-533 furthermore reduced the

amount of high-affinity ligand binding sites and subsequently the internalization of WT receptors in NIH 3T3 cells expressing both receptor types, slowing down receptor degradation. [408] This might also be the case for the heterozygous setting with FLT3 WT and FLT3 p.Q569Vfs\*2 in Ba/F3 cells which requires confirmation.

The dominant negative effect of FLT3 p.Q569Vfs\*2 on receptor signalling suggests that the patient's AML blasts proliferate independently of FLT3 kinase activity. This raises the question about the role of this mutant in cancer evolution, disease progression and other mechanisms involved in the evasion of anti-leukaemia treatment. A potential role in the pathogenesis of AML might be the escape of FLT3 dependent signalling modulated by FL. However, the proof of protein expression of FLT3-p.Q569Vfs\*2 in the patient sample was not possible due to lack of appropriate patient material. Following the evidence from expression in the Ba/F3 model system, FLT3-p.Q569Vfs\*2 expression should be investigated in AML cell lines. Using targeted genome editing, for example clustered regularly interspaced short palindromic repeats (CRISPR) and CRISPR-associated protein 9 nuclease (Cas9), may be used to genetically introduce the p.Q569Vfs\*2 mutation into *FLT3* in AML cells. This would provide insights whether nonsense-mediated mRNA decay (NMD) mechanisms affect this mutant in the setting of AML. In physiological conditions, NMD acts as surveillance mechanism balancing the abundance of cellular RNAs and as a translation-dependent quality control mechanism eliminating mRNA transcripts that contain premature stop codons. Thus, NMD prevents any dominant cellular toxicity of mutant proteins. [409, 410] However, the susceptibility to NMD seems to be different from case to case. For example, the truncated p53 protein encoded by the 770delT allele is as abundant as the WT protein due to increased protein stability governed by the removal of the C-terminal p53 domain. [411] In AML cells, NMD activity declines during chemotherapy and during treatment using the hypomethylating agent Azacitidine. This results in an inefficient destruction of mRNAs containing a premature stop codon. [409, 412] In theory, upon treatment pressure with hypomethylating or chemotherapeutic agents, AML cells with FLT3-p.Q569Vfs\*2 would have received a cell survival benefit, if FLT3-p.Q569Vfs\*2 mediated oncogenic transformation. Same accounts for any TKI response to AC220 treatment, since the type II TKI competes with ATP binding targeting intracellular receptor regions lacking in the truncated variant. As expected, a growth advantage of mutant without or in combination with FLT3-WT under TKI treatment using AC220 in the Ba/F3 model system was not observed. Nonetheless, competitive growth of CRISPR-Cas9-modified AML cells under treatment might be different - although reconstruction of the complete biological picture as present in the AML patient sample would require a complete mutational profile. Due to the lack of remaining gDNA patient material mutational analysis of known driver genes was not possible. Only RNA patient material was available. Examination of allelic expression of interesting candidates by RNA sequencing might be worth it, to assess molecular alterations potentially causing the relapse aside from the detected *FLT3* alteration.

Although investigation of the truncated variant FLT3-p.Q569Vfs\*2 conferred a loss-of-function phenotype with repression of FLT3-WT in an heterozygous cell culture setting, similar to the behaviour of EGFR CD-533, examples of truncated receptors fostering the onset of AML exist.

### 5.2.2 Consequences of truncations in other receptors associated with AML

Truncated receptors showing the potential to promote leukemogenesis are for instance truncated variants of the colony-stimulating factor 3 receptor (CSF3R). CSF3R is a key player in neutrophil production, belonging to the hematopoietin receptor superfamily. In about 20% of patients suffering from severe congenital neutropenia (SCN), C-terminal truncated variants of CSF3R are detectable. They confer an increased risk of developing AML. Unlike RTKs, hematopoietin receptors are not capable of autophosphorylation. They require the recruitment of cytoplasmic tyrosine kinases of the JAK or Src kinase families for downstream signalling. Receptor signalling is furthermore tightly regulated by members of the suppressors of cytokine signalling (SOCS) family and tyrosine phosphatases SHP-1 and SHP-2. [413-415] Somatic mutations in *CSF3R*, that generate C-terminally truncated proteins lacking 82 to 98 amino acids implying tyrosine residues required for downstream signalling, typically affect a single allele. Nonetheless, truncated CSF3R mediates increased growth and abrogated maturation in response to their ligand CSF3 based on increased STAT5/STAT3 activation ratio. Thereby, truncated CSF3R act dominantly over CSF3R-WT. Compared to CSF3R-WT, truncated receptors are featured with a hyper-responsiveness to CSF3 inducing a higher and more sustained receptor activation, while facing a substantially reduced “off-rate”. This is based on defective internalization of truncated receptors as well as on abrogated negative feedback mechanisms on STAT5 activation, implicating the loss of tyrosine residues recruiting SOCS3 and SHP-2 (Figure 16a). Compared to FLT3-p.Q569Vfs\*2, AML-associated truncated CSF3R still contains sites required for the recruitment of cytoplasmic tyrosine kinases as well as membrane-proximal region residing residues for STAT5 binding. In addition, truncated CSF3R frequently lacks both receptor inhibitory sites and sites required for mediators of cell differentiation. Although mediating a proliferative advantage, the mere expression of truncated CSF3R in mice is not leukemogenic. Only in cooperation with PML-RARA a CSF3-dependent decreased latency in AML induction is observable, accompanied by higher blast counts and increased myelosuppression. [413, 415] This demonstrates that the interplay of cooperating mechanisms such as other genetic alterations are essential to recapitulate and understand the complete mode of action truncated receptors can exert in forcing AML induction or progression.

Another example of a truncated receptor being associated with AML is delta-tropomyosin-related kinase A (TrkA). TrkA is involved in neuronal survival and maintenance. Beyond its function in neurons, TrkA is expressed at several stages of haematopoiesis and in primary leukemic cells from AML patients. [416] Delta-TrkA is an AML-patient derived truncated variant of the neutrophin receptor TrkA, lacking 75 amino acids of the extracellular domain. This includes the loss of the main part of the second Ig-like domain, responsible to inhibit spontaneous dimerization and subsequent autophosphorylation of the receptors, while intracellular receptor parts remain unaffected (Figure 16b). [417] Delta-TrkA thus leads to a constitutive activation of the receptor, mediating a leukemic transformation of primary murine HSCs via activation of PI3K and mammalian target of rapamycin (mTOR), but not STAT and MAPK pathway. Lin-negative BM cells transduced with delta-TrkA induced acute leukemia with signs of a maturation arrest of myeloid blasts when transplanted into mice. While half of the mice

developed AML with necrotic tumor emboli in the blood vessels of the lung, liver and kidney, the other half, surviving the early blast crisis, subsequently developed ALL or MPD-like myeloid leukemia with meningeal infiltration of leukemic cells. [416]

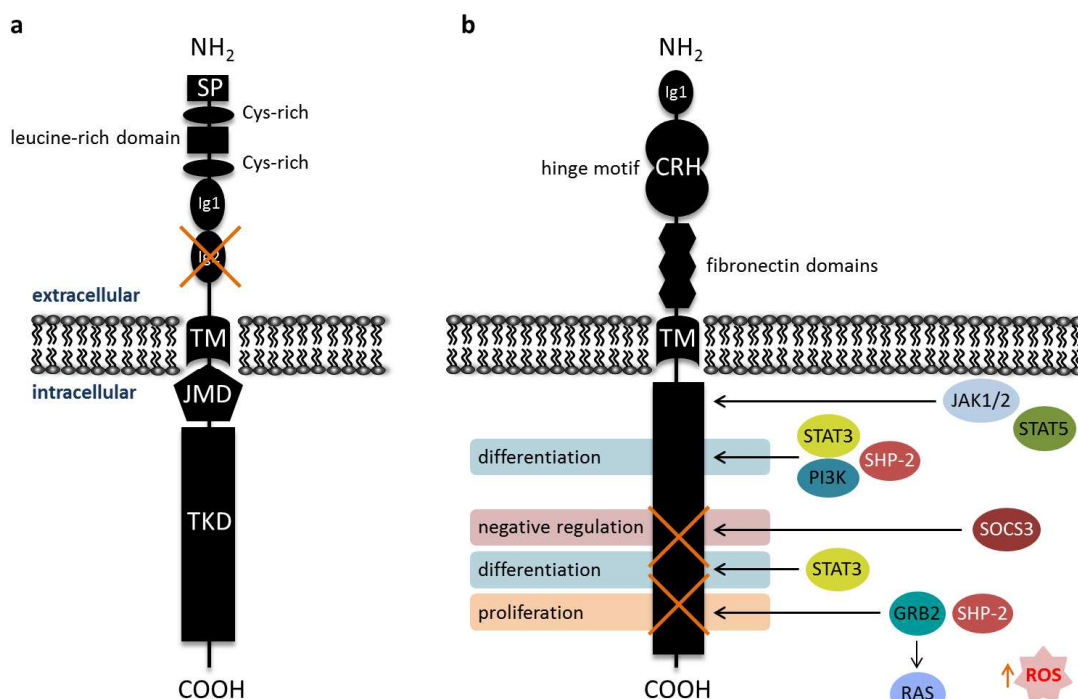


**Figure 16: Truncated CSF3R and TrkA.**

Illustration of the truncated receptors **a)** delta-TrkA, which contains a 75 amino acid deletion of the extracellular second immunoglobulin-like domain (modified from Reuther 2000 and Tacconelli 2005) and **b)** CSF3R lacking cytoplasmic regions, involved in mediating differentiation and proliferation signalling (orange crossed domains). The hinge motif separates the cytokine receptor homology (CRH) domain. Truncated CSF3R have also been shown to increase the production of reactive oxygen species (ROS), creating genotoxic stress (adapted from Liongue 2014). SP (signal peptide), Cys-rich (cysteine-rich cluster), TM (transmembrane domain), JMD (juxtamembrane domain), TKD (tyrosine kinase domain). [415, 417, 418]

These examples provide insights into the mechanisms involving truncating variants in leukemogenesis. They further indicate that at least parts of the domains responsible for receptor autophosphorylation and thus signalling are required for any oncogenic potential. Although there still might be a contributory role of dominant-negative mutants in oncogenesis, their leukemogenic potential tends to be marginal. Nonetheless, consequences of new and recurrent mutations on receptor signalling require elucidation, since alterations mediating a gain-of-function may be targetable.

### 5.3 TKI-mediated effects on FLT3 and the potential for a combination with FLT3-directed immunotherapy in AML

With regards to TKI single-agent treatment variable responses of AML patients have been observed, irrespective of *FLT3* state. [289] Therefore, systematic evaluation of the TKI response

on FLT3 localization and cell proliferation in differentially *FLT3* mutated settings was performed in the third project of this doctoral work. The project revealed a TKI-mediated increase in FLT3 surface expression based on the *FLT3* genotype. This FLT3 surface increase was *N*-linked glycosylation-dependent and correlated inversely with proliferation. Sufficient target presentation at the cell surface is required for profound immunotherapy responses. Hence, this mechanism provided the basis for a rational combination of TKIs with FLT3-directed immunotherapy for the treatment of *FLT3*-mutated AML. Proof-of-principle experiments affirmed a synergistic anti-leukemic effect of Quizartinib and a bispecific FLT3xCD3 antibody in *FLT3*-ITD positive AML cells. This therapeutic approach might be especially interesting for elderly patients, harboring a *FLT3*-ITD mutation, neither eligible for the combination of TKI with chemotherapy nor for HSCT.

### 5.3.1 The role of the *FLT3*-genotype on TKI response

In our study TKIs increased the membrane localization of the FLT3-PM V592A, D835Y as well as of FLT3-ITDs. The increase in surface FLT3 correlated positively with the pretreatment *FLT3*-ITD mRNA level (also referred to as ITD ratio), being most prominent in samples harboring a homozygous ITD. Heterozygous ITD positive samples responded with a lower FLT3 surface increase after 6 hours. This is reflected by outliers in the respective scatter plot displaying the correlation between the change in FLT3 expression and the *FLT3*-ITD mRNA level. However, as shown for the AML cell line MOLM-13 – where FLT3 surface levels increased at a later time point – this might be attributed to a delay in TKI response. In line with this, a high increase in surface FLT3 was observed for an *ex vivo* sample of a *FLT3*-ITD heterozygous patient after day 55 of TKI treatment. Concordantly, a phase II trial with Lestaurtinib shows an increase in FLT3 surface levels in *FLT3*-mutated (ITD and TKD) AML patients at day 14, 28 and 56 after treatment [289], but also for patients with a *FLT3*-WT genotype. Thus, TKI-mediated changes in FLT3 surface expression might also be a matter of time in FLT3-WT expressing AML patients. Of note, also WT-expressing cells demonstrate a reduction of BM blasts after Lestauritinib treatment, whilst one ITD-positive patient did not respond. Any late FLT3 expression increase during Lestauritinib treatment does not correlate with clinical outcome. [289] This was also the case for a Sorafenib-treated ITD patient in our study, who demonstrated no reduction in blast count, although showing higher levels of FLT3 compared to prior treatment. Any late TKI responses might therefore be irrespective of the *FLT3*-genotype - which should be examined further. Early responses after 6 hours of Quizartinib treatment seem to depend on the mutation level of *FLT3*. Neither *FLT3*-WT AML nor PDX cells showed a significant increase in surface FLT3 in our study, except for the *FLT3*-WT AML cell line MUTZ-2. The underlying mechanisms of the early increase of FLT3 surface expression in this cell line should be investigated more closely, since it may indicate intracellularly retained FLT3 before treatment. Alternatively, transcriptional upregulation may be the cause for increased FLT3 surface levels. Moreover, the correlation between the pretreatment *FLT3*-ITD mRNA level and the early TKI-mediated increase in FLT3 surface expression should be confirmed, since the sample number was relatively low in our study (n=11). Retrospective data analysis of TKI-treated patients regarding this correlation could be

done rather easily now, as Midostaurin has now been approved by the FDA for the treatment of *FLT3*-mutated AML patients in combination with chemotherapy [343, 419, 420].

Theoretically, a high ITD ratio implies a quantitatively greater expression of constitutively active *FLT3*, combined with a greater dependency on *FLT3* signalling for cell survival and thus better TKI response [115]. In accordance, the increase in surface *FLT3* correlated inversely with proliferation in our study. Nevertheless, also in this case, sample size should be increased to confirm the correlation of the early *FLT3* surface increase and cytotoxicity in primary AML blasts. Subsequent investigations should also include a larger set of TKIs. In line with our findings, a study of 348 *FLT3*-ITD positive and 135 *FLT3*-ITD negative *ex vivo* samples showed *FLT3*-ITD to be predictably the strongest association with Midostaurin-response *in vitro*. In analogy, the ITD mutant allele fraction correlated strongly with the extent of Midostaurin sensitivity. Interestingly, *FLT3*-TKD positive samples showed responses similar to *FLT3*-WT samples after Midostaurin treatment. [421] Investigations with Sorafenib and Quizartinib affirmed that samples with a mutant allelic burden above 50% are more sensitive to the TKIs *in vitro* compared to those with a low ITD ratio [369]. An ITD ratio dependent cytotoxic response for the TKIs Lestauritinib and Gilteritinib is confirmed by *ex vivo* treatment of pediatric AML samples [115, 392]. With regards to Lestauritinib, *FLT3*-WT and *FLT3*-TKD positive samples showed similar cytotoxicity, with responses in approximately 30% of cases in each group [115]. Biologically, the predictability of the ITD ratio for TKI response has been shown to be based on the amount of co-expressed *FLT3*-WT. Co-expression of *FLT3*-WT attenuates the inhibitory effect of TKIs in heterozygous *FLT3*-ITD AML cells in a FL-dependent manner *in vitro* and *in vivo* [422]. Thus, samples with a high mutant allelic burden are more likely to be responsive to *FLT3* inhibition, compared to samples with a low mutant allelic burden.

Dose responses for samples with a low ITD ratio are concordant with the selectivity scores for the different TKIs [369]. Thus cytotoxic efficacy relies on the target spectrum of the TKI, since target selectivity affects target affinity [291, 292, 369]. In line with previous reports [291, 369, 423], our study confirmed that the second-generation TKI Quizartinib was most potent against *FLT3*-ITD compared to multi-kinase inhibitors, such as Midostaurin and Sorafenib. Early increases in *FLT3* surface level were highest at concentrations of 5 to 25 nM for the *FLT3*-ITD positive cell line MV4-11. Of importance, Midostaurin and Lestauritinib target both, *FLT3*-WT and mutant *FLT3* (ITD and TKD), whilst Quizartinib and Sorafenib show higher potencies against *FLT3*-ITD than *FLT3*-TKD and *FLT3*-WT [301, 369, 422, 424]

Although there might be a significant difference *in vitro*, clinical trials suggest that the benefit of TKIs might be irrespective of the *FLT3*-mutation state (TKD or ITD) or the ITD ratio. Within the CALGB10603/RATIFY trial the benefit of Midostaurin on outcome after conventional therapy was consistent across all *FLT3*-mutant subtypes (TKD mutated, low/high ITD ratio) [93, 425]. Similarly, the SORAML trial administering Sorafenib demonstrated Sorafenib to be a beneficial additive to conventional therapy irrespective of the *FLT3* genotype [337]. Also *FLT3*-ITD positive patients treated with Gilteritinib within the CHRYSALIS trial benefited from TKI treatment irrespective of initial mutational ITD burden. *FLT3*-TKD positive patients with a mutational burden above 5% VAF in contrast tended to show a better OS response after 10 months of treatment. [287, 323,

374] This is probably attributed to the high efficacy of Gilteritinib in eradicating *FLT3*-TKD and *FLT3*-ITD-TKD mutant AML cells [426]. Furthermore, Gilteritinib has been shown to decrease the expression of anti-apoptotic proteins in MV4-11 cells, such as MCL-1 and survivin, which are reported to be essential in chemotherapy sensitivity [427]. No overall clinical benefit was observed when adding Lestauritinib to chemotherapy in *FLT3*-mutated AML (CALBG106603 trial). Lower rates of relapse and improved OS were only seen in patients who achieved sustained *FLT3* inhibition (more than 85%). [312] Insufficient *FLT3*-target inhibition might be due to resistance mechanisms, whereby broad-range TKIs might be of advantage – but also their efficacy has limits. Investigations on combining chemotherapy with the most potent *FLT3* inhibitor Quizartinib are still ongoing. An interim analysis revealed that Quizartinib combined with low-dose Cytarabine is highly active in AML patients with a *FLT3*-ITD mutation. [92, 428, 429]

With regards to resistance, in our study the heterozygous *FLT3*-ITD positive AML cell line PL-21 did neither respond with an increase in surface *FLT3* nor with a reduction in proliferation, as expected based on the ITD ratio. This was likely due to its *KRAS* mutation, which is known to be associated with TKI-resistance [430, 431]. This is in line with previous reports, demonstrating sustained proliferation of *FLT3*-ITD positive samples not entirely relying on *FLT3* signalling [369]. Mutations in *KRAS* and *TP53* amongst *FLT3*-ITD positive patients are predictive towards Midostaurin resistance, while t(15;17) in ITD-positive patients increases Midostaurin efficiency. In contrast, in *FLT3*-ITD negative samples inv(16) confers increased sensitivity to Midostaurin. [421] Moreover, acquisition of activating PM in *FLT3*-ITD positive patients mediates resistance to TKI treatment [252, 253, 263, 264]. Concordantly, in our study, resistance mediating PM combined with an ITD required higher dose of Quizartinib to induce a reduction in proliferation compared to cells with ITD only. The TKI-mediated cell proliferation inhibition as well as the increase in *FLT3* surface expression seemed not to be influenced by the ITD position. In contrast, a recent report demonstrated JMD-ITDs to be more sensitive towards TKI-therapy than TKD1-ITDs *in vitro* and *in vivo* [251].

An exception of the inverse correlation of *FLT3* surface increase and proliferation was the *FLT3*-WT AML cell line MUTZ-2. MUTZ-2 did not show any inhibition of proliferation, although showing a significant increase in surface *FLT3* levels upon TKI treatment. Phosphorylation levels of *FLT3* should thus be examined for any involvement of direct targeting by Quizartinib. Inhibition of *FLT3* phosphorylation in turn should result in a reduction in cell proliferation. According to the online available cytogenetic profile provided by the DSMZ, MUTZ-2 harbors additional chromosomes 8 and 10, including the oncogenes *MYC* and *RUNX1*. Deregulated *MYC* and *RUNX1* have been shown to confer resistance to *FLT3* inhibitors by mediating cell survival (Figure 17) – a mechanism frequently exploited by *FLT3*-ITD positive AML cells [215, 222, 223, 432].

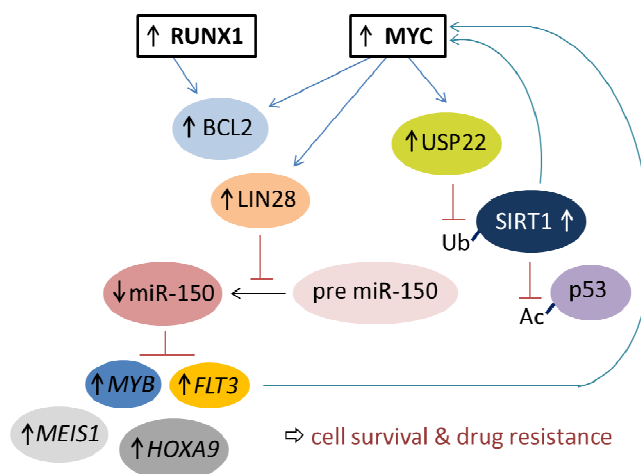


**Figure 17: Consequences of deregulated MYC and RUNX1 in FLT3-ITD positive AML cells.**

Upregulation of RUNX1 leads to chromatin remodeling and regulation of anti-apoptotic genes, including *BCL2* [215, 222-224]. Elevated MYC expression disrupts apoptosis through increased expression of *BCL2* or loss of either BIM or p53 function. Inhibition of p53 signalling, by enhanced p53 protein deacetylation, is mediated by stabilization of the NAD-dependent deacetylase sirtuin 1 (SIRT1) by a MYC-mediated increase in USP22 deubiquitinase expression. Stabilized SIRT1 in turn mediates a positive feedback-loop towards MYC deacetylation. [432, 433] Moreover, deregulated MYC results in a block of micro RNA 150 (miR-150) maturation, a negative regulator of *FLT3*, *HOXA9* and *MEIS1* [434, 435]. Notably, *HOXA9* and *MEIS1* have been shown to passively upregulate *FLT3* expression [436, 437] and to disrupt myeloid differentiation [438]; (modified from Kuo 2016 and Jiang 2012) [434, 439].

Other exceptions of the inverse correlation of FLT3 surface level increase with proliferation in our study were the *FLT3*-WT AML cell lines Kasumi-1 and EOL-1. Kasumi-1 and EOL-1 showed no increase in surface FLT3 expression, but they were sensitive to TKI treatment. Sensitivity to the tested TKIs could be assigned to their alterations in other tyrosine receptors namely KIT and PDGFRA – both are known targets of the tested TKIs [291, 303]. Concordant, the IC(50) was lower for the multi-kinase inhibitor Sorafenib. Hence, any influence of concomitant mutations on the TKI target profile or other alterations known to mediate TKI resistance should be assessed beforehand to more accurately predict responses. Of note, in EOL-1, FLT3 is further constitutively activated in an autocrine manner by the expression of FL [178, 440]. This indicates that the TKI probably also inhibits activated FLT3-WT in this cell line. Confirmation of the FLT3 phosphorylation level prior and after treatment as well as the intrinsically produced FL amount may therefore be informative about any FLT3-specific response. The *FLT3*-WT ALL cell line REH also expresses FL and would be another candidate to confirm this phenomenon [178]. Besides frequently expressed in an autocrine manner by leukemic blasts, FL is produced *in vivo* in the BM stromal microenvironment [178, 441]. Interestingly, FL was demonstrated to augment the cytotoxicity in *FLT3*-WT and *FLT3*-PM pediatric AML patients that were responsive to Lestauritinib treatment, suggesting that their AML cells rely on FLT3 signalling. [115] In certain AML *FLT3*-WT cases, a combination of a TKI with a FLT3-directed antibody therapy could thus be beneficial. Investigations about any late-term surface FLT3 increase in *FLT3*-WT patients as well as any anti-proliferative activity could be informative for the potential exploitability in targeted therapy. Since CN *FLT3*-WT patients have a predictably rather favorable outcome with



conventional treatment, TKI treatment in combination with chemotherapy might not be essential.

Although there is emerging evidence that the *FLT3*-genotype matters in TKI efficiency *in vitro* [115, 301, 369, 422], the biological picture might be more complex *in vivo*. Hence, clinical responses in *FLT3*-mutated as well as *FLT3*-WT cases might be influenced by intrinsic and extrinsic effects, involving alternative oncogenic pathways. Therefore, concomitant molecular alterations aiding in predicting TKI sensitivity or resistance should be routinely assessed when intending to apply TKIs. Moreover, biological mechanisms underlying TKI response or resistance have to be fully understood to apply TKIs as tailored as possible.

### 5.3.2 Biological mechanisms behind the increase in surface FLT3

Concordant with other reports [207, 442-447], our experiments revealed an increase of the fully glycosylated mature (160 kDa) form of FLT3 after TKI-treatment. The increase in the mature form was in compliance with the increase in surface FLT3. In the *FLT3*-ITD positive cell lines MOLM-13 and MV4-11 as well as in the *FLT3*-PM cell line MM6, a decrease in the immature form was observed. On a biological level the increase in surface FLT3 by TKIs was dependent on *N*-linked glycosylation, as demonstrated by inhibition with 2-deoxy-D-glucose (2-DG). In line with this observation, others report that complex glycosylation of FLT3 at the Golgi compartment is important for its protein stability and trafficking to the cell surface [207, 208, 444, 448]. Thereby, the extracellular domains of FLT3 are of importance, because they carry most potential glycosylation sites [207]. Kinase activity involving tyrosine residue 842 and serine residue 935 are decisive for appropriate receptor folding and maturation in a chaperone-dependent manner. Consequently, also kinase inactivation promotes FLT3 maturation mediating the shift from the immature towards the mature receptor form. Inhibition of STAT5 activation in *FLT3*-ITD positive AML cells abrogates the positive feedback mechanism governed by its downstream target PIM1. The serine/threonine kinase PIM1 is capable of phosphorylating and stabilizing immature FLT3 receptors in conjunction with the chaperones calnexin and heat shock protein 90 (HSP90). They assure glycoprotein maturation quality in the ER or cytosol, prior processing towards the Golgi complex. Immature but activated FLT3 is prevented from proteasomal degradation and enabled to further activate STAT5. [206-208, 217, 444, 449] Therefore, inhibition of STAT5 activation may release the cytosolic retained immature *FLT3*-ITD. Of note, MOLM-13 cells made resistant to Midostaurin (by sustained low-dose supplementation to the culture medium) showed higher levels and a reduced turnover of FLT3 with prolonged half-life [362, 442].

Besides phosphorylation and *N*-glycosylation, our experiments showed that the FLT3 surface expression was linked to transcriptional regulation of *FLT3*. Dependency on biosynthesis was indicated by experiments with cycloheximide. In the *FLT3*-ITD homozygous AML cell line MV4-11, a transcriptional upregulation of *FLT3* mRNA expression upon Quizartinib treatment was observed, elevating the total amount of FLT3 protein. In the heterozygous *FLT3*-ITD AML cell line MOLM-13, *FLT3* mRNA expression levels did not change significantly upon Quizartinib treatment. A transcriptional imbalance favoring the WT allele was observed. This might be attributed to the

delayed increase of surface FLT3 after TKI-treatment. The underlying cascade mediating these feedback responses should be investigated more closely to decipher which transcriptional activators are involved. Confirmation of this phenomenon in primary samples by other TKIs should be performed. Transcriptional upregulation of *FLT3* in MV4-11 might somehow be associated with CD99 (MIC2) expression. Inhibition of CD99 expression leads to elevated FLT3 levels in MV4-11 cells - a dual pattern also inducible upon Midostaurin treatment. [450] Anyhow, transcriptional upregulation of *FLT3* and increase in protein stability may be an adaptive cellular attempt to rescue FLT3-mediated signalling by the concept of “oncogene addiction” to tolerate target inhibition. Frequently, gain of secondary point mutations mediating TKI resistance in *FLT3*-ITD positive patients restores the activation of the FLT3 pathway [352, 451]. Compensatory upregulation of *FLT3*-WT might be an alternative way to increase the possibility for FL stimulation. In line with the transcriptional shift towards *FLT3*-WT seen in MOLM-13 in our study, co-expression of *FLT3*-WT has been shown to attenuate the inhibitory effect of TKIs when stimulated with FL via MAPK activation of fully glycosylated FLT3 [422]. Glycosylation is thereby the key to the FL-dependent resistance to TKIs [422].

The TKI-mediated increase in mature surface FLT3 may also provide enhanced access to FL activation. Intrinsic upregulation of FL expression has been observed in response to TKI-treatment in MV4-11 cells made resistant to FLT3 inhibitors [212]. After chemotherapy treatment, elevated serum FL levels are detectable in AML patients. [422, 452-454] Enhanced FL-induced FLT3 activation might thus impede the efficacy of TKIs up to several fold in *FLT3*-ITD positive patients, hence being identified as potential resistance mechanism [115, 352, 422, 451-453]. In adult *FLT3*-ITD positive AML patients, an increased level of FL was associated with decreased TKI sensitivity, requiring higher doses of Lestauritinib to overcome the lowered inhibitory efficacy [452]. Nevertheless, the combination of Midostaurin as well as Sorafenib with conventional chemotherapy improved patient outcomes in AML patients (CALGB 10603 / RATIFY and SORAML trial) [93, 337, 420]. Similarly, elevated FL levels might efficiently compete with FLT3-directed antibodies for target binding, lowering the pharmacodynamics and requiring higher antibody-doses. So far, initial experiments with anti-FLT3 antibodies indicate that they are still cytotoxic to FLT3 TKI-resistant clones and that they bind FLT3 regardless of the concentration of FL [354, 455].

Beyond these resistance mechanisms, the increase in surface FLT3 mediated by the TKI probably promoted NADPH oxidase (NOX)-generated ROS formation. Recently, researchers discovered that AKT signalling induced by FLT3 located at the plasma membrane is required for NOX-generated ROS induction. NOX-generated ROS act as a pro-survival signal. However, concentrations beyond the tolerable threshold can enforce apoptosis inducing selective cytotoxicity. [456, 457] In response to oxidative stress, cells can induce autophagy as a protective response mechanisms [458]. Whether the TKI-mediated increase in surface FLT3 induces cytotoxic ROS levels should be evaluated to assess any pro-survival feedback mechanism.

Nonetheless, with regards to target recognition in immunotherapy, increased FLT3 surface expression might overcome the limitation of FLT3-antigen availability in *FLT3*-ITD positive AML

cells. Full glycosylation mediated by the TKI might also modulate immune response through post-translational modifications as glycosylation matters in major histocompatibility complex (MHC) peptide presentation and antigen recognition of T-cells. [459]

Since TKI treatment seems to implicate a lot of biological responses based on individual molecular compositions, their therapeutic exploitability as well as the need for intervention has to be further investigated. Any of these response mechanisms should subsequently be carefully examined to determine the clinical applicability of the combination of TKIs with FLT3-directed immunotherapy.

### 5.3.3 Clinical applicability of combining TKIs with FLT3-directed immunotherapy

Relapse in *FLT3*-ITD positive AML patients remains common, due to resistance mechanisms towards standard treatment or novel single-agent targeted therapeutic approaches [212, 260, 263, 267, 377, 451, 460-462]. Therefore, combinatorial approaches are highly warranted. In our study, we investigated the combination of TKIs with FLT3-targeted immunotherapy in T-cell mediated cytotoxicity (TCMC) assays, based on the finding that TKIs induced an increase in surface FLT3 presentation. A synergistic effect of Quizartinib with a bispecific FLT3xCD3 antibody was observed against homozygous *FLT3*-ITD positive MV4-11 cells, PDX samples and a primary AML patient sample. In the heterozygous *FLT3*-ITD AML cell line MOLM-13 as well as in a heterozygous *FLT3*-ITD PDX sample, antibody-treatment alone already resulted in very efficient eradication of AML cells, whereby no conclusion about synergistic or additive effects could be drawn. A synergism was shown for a heterozygous *FLT3*-ITD positive primary AML patient sample, harbouring a high ITD mutational load. Competitive lysis experiments of untreated and Quizartinib pre-treated *FLT3*-ITD homozygous MV4-11 cells confirmed a preferential killing of pre-treated cells with increased surface FLT3. In line with previous reports [463], any modulatory effect of 50nM Quizartinib on T-cell reactivity and function could furthermore be excluded. To finally provide evidence that the increase in fully glycosylated FLT3 mediates the benefit and to exclude any complementary mechanisms governing this synergism, a TCMC assay using Quizartinib with a CD33xCD3 antibody against MV4-11 cells should be performed. TCMC assays investigating the efficacy of the BiTE antibodies CD33xCD3 and FLT3xCD3 in eradicating AML blasts show faster lysis of AML cells highly expressing the target antigen compared to AML cells with a low target antigen expression. This indicates a target antigen-expression dependency of antibody efficacy [114, 356]. In line with previous reports [353], a FLT3-expression-specific cell lysis by the FLT3xCD3 antibody was demonstrated by an antibody serial dilution. TCMC efficacy thus depends on sufficient antigen expression and available antibody. Our and other studies provided evidence that the FLT3 surface increase *in vitro* seems to be influenced by the pretreatment *FLT3*-ITD mRNA level. Nevertheless, assessment of the native FLT3 surface expression remains essential in AML patients to determine the potency of the FLT3-antibody treatment without adding TKIs, since neither the *FLT3*-genotype nor the pretreatment *FLT3* mRNA level predict for the FLT3 surface expression per se [181, 356]. AML cases harbouring a LOH are expected to demonstrate little native FLT3 surface expression, due to their intracellular

retained localization profile of FLT3-D835Y and ITD mutants *in vitro*. Retention results in decelerated trafficking along the biosynthetic route, whereby any TKI-mediated acceleration would be beneficial with regards to surface antigen presentation. [207, 208, 213, 214] Since in our study the effect of enhanced TCMC was not consistently augmented in dependence of the TKI-mediated surface increase, further confirmation is required to link the synergy to the increase in antigen presentation. Additional experiments are required to investigate whether early or late FLT3 surface increase influences the therapeutic benefit by the TKI, when combined with the FLT3xCD3 antibody. This requires larger sample sizes of primary AML cells compared to our proof-of-principle study. Subsequently, *FLT3*-TKD and especially *FLT3*-ITD-TKD positive samples should be investigated to examine if dual targeting overcomes TKI-resistance mechanisms. Similarly, AML cells with upregulated immune checkpoint mediators that predictably govern resistance to targeted immunotherapy should be investigated. The proposed experiments should evaluate if the accelerated AML cell eradication, induced by combining TKIs with FLT3xCD3 antibodies, is sufficient for preventing long-term resistance to single agent treatment.

For FLT3-WT AML cells, TCMC was not significantly improved by addition of Quizartinib in our study, as exemplified by HL60. Since HL60 expresses only little FLT3, further FLT3-WT expressing AML cell lines, PDX samples and following primary AML patient samples should be investigated to assess any *FLT3*-genotype specific pattern of this drug combination. Hence, cells with a higher FLT3 surface expression per se might result in a sufficient TCMC by single treatment with an anti-FLT3 antibody. Hence, a potential advantage of adding Quizartinib might only be seen in FLT3-WT cells responding to TKI treatment, due to other concomitant alterations, as for example Kasumi-1 or EOL-1. Therefore, the potential efficacy of TKI treatment towards clinical responses might be assessed beforehand. This should confirm AML blasts vulnerability towards FLT3-targeted treatment and exclude any confounder mediating resistance as for example a *KRAS* mutation like in PL-21. To assess and monitor the inhibition of FLT3 activity plasma inhibitory activity (PIA) assays are used [288, 289, 312, 452]. Determination of the serum FL levels might further be informative. Investigating normal HSCs is of clinical relevance too. In normal HSCs neither single agent nor the combination should mediate any severe off-leukemia cytotoxicity.

Since Quizartinib sensitized *FLT3*-ITD positive AML cells towards FLT3xCD3 therapy, investigations with other TKIs should be performed to show whether TKIs mediate a synergism with FLT3xCD3 antibody cytotoxicity in general. This is of special interest hence TKIs are generally capable of impairing T-cell function through inhibition of various signalling pathways. For the TKIs Dasatinib, Nilotinib and Sunitinib this has already been shown. They impair T-cells already at low nanomolar concentrations. Sorafenib inhibits the proliferation and activation of primary human T-cells *in vitro* and lead to immunosuppression *in vivo* at concentrations similar to those used in patients. [464] Clinically relevant doses of Quizartinib and Midostaurin (up to 50 nM), in contrast, do not impair HD T-cell proliferation, reactivity or function. [463, 465, 466] This was also confirmed by our experiment. Of note, higher doses of Midostaurin (100 nM) reduce the proliferation of T-cells, which is not the case for Quizartinib [463]. Experiments adding 1000 nM Midostaurin to a bispecific FLT3xCD3 BiTE antibody thus show reduced TCMC, due to a decrease in CD3/CD28-mediated T-cell proliferation. Hence, BiTE activity is reduced, because

proper cytotoxic T-cell function is impeded [356]. These experiments should therefore be repeated with a Midostaurin dose adjusted to clinically relevant concentrations, since higher TKI doses seem to make a difference. Importantly, the combination of Midostaurin and a bispecific FLT3xCD3 BiTE antibody has been tested in an autologous system, investigating the primary AML samples without adding HD T-cells. With regards to the condition in the clinical setting of AML, T-cell efficacy would thus be better mimicked. In an autologous system, the effector to target ratio (E:T) is not fixed but merely influenced by the number of residual T-cells in the patient sample [356]. Hence, not only the TKI concentration might be problematic. Testing Quizartinib combined with the FLT3xCD3 antibody in further primary AML patient samples in an autologous system might be essential to gain insights of the efficacy of the cytotoxic T-cells in the AML patient. This may give a better estimate about the efficiency of T-cell mediated AML cell killing in combination with the TKI's performance *in vivo*. Moreover, investigations on the applicability of other TKIs should follow - with special focus on their immunomodulatory effect on cytotoxic T-cells, based on T-cell propagation and function. Modulation of T-cell efficacy may also be relevant if expanding our findings to a combination with FLT3-primed CAR T-cells.

Initial experiments testing this combination have been performed recently. Interestingly, FLT3-primed CAR T-cells (BV10-scFv-IgG4hinge-CD28-CD3 $\zeta$ -EGFRt) showed a synergism in cytotoxicity when combined with 10 to 50 nM Midostaurin against MOLM-13 cells engrafted in mice. In line with our hypothesis, a preferential killing of Midostaurin resistant MOLM-13 cells (with higher FLT3 surface levels) demonstrated a higher cytotoxic response compared to Midostaurin native MOLM-13 cells. [362] Similarly, FLT3-ITD positive AML cells treated with 10 nM Crenolanib show increased the surface FLT3 expression and consecutively enhanced the recognition by FLT3-CAR T-cells *in vitro* and *in vivo*. [365] FLT3 expression on normal HSC and FLT3-WT AML cells remained unaltered upon Midostaurin or Crenolanib treatment. Mice treated with the combination of Midostaurin or Crenolanib plus FLT3-primed CAR T-cells showed superior engraftment and expansion of FLT3-primed CAR T-cells and a higher overall response rate than mice receiving FLT3-CAR T-cells alone. Achievement of complete remission of AML from PB, BM and spleen was observed in the combination arm. Since BV10-scFv-IgG4hinge-CD28-CD3 $\zeta$ -EGFRt has been shown to recognize normal HSCs *in vitro* and *in vivo* and interferes with normal hematopoiesis in colony formation assays *in vitro*, its clinical applicability, however, remains uncertain. Adoptive therapy with FLT3-CAR T-cells may be thus limited to the initial reduction of leukemic burden, requiring subsequent CAR T-cell depletion and allogeneic HSCT to reconstitute the hematopoietic system. [362, 365] Nonetheless, performance of other FLT3-primed CAR T-cells in combination with TKIs might be more constructive and have to be evaluated. Furthermore, the combination of TKIs with monoclonal antibodies carrying a cytotoxic load should be tested, since their cytotoxic efficacy does not rely on immune cells.

With regards to the *in vivo* efficacy of combining TKIs with FLT3-directed immunotherapy, microenvironmental factors should not be neglected - especially with regards to LSCs eradication. Particularly important is the chemo- and TKI protection governed by bone marrow stromal cells (BMSCs). *In vitro* and *in vivo* xenograft experiments demonstrate that BMSCs protect FLT3-ITD positive AML cells by highly expressing cytochrome P450 (CYP) enzymes, including CYP3A4. CYP3A4 is responsible for hepatic inactivation of chemotherapeutic drugs and

TKIs, including Quizartinib, Sorafenib and Gilteritinib. [467, 468] Through a combination of direct cell-to-cell contact and soluble factors, BMSCs activate protective anti-apoptotic pathways in AML blasts. Sustained cytokine-activation of ERK signalling is thereby essential in mediating the protective effect. FL furthermore augments the protection by increasing FLT3 phosphorylation and thus the requirement of higher drug doses for proper inhibition – TKI and perhaps also FLT3 antibody. [352, 469] Although our *in vitro* TCMC assays were performed using MS-5 feeder cells, a resistance might only be visible after a longer treatment period.

Another protective effect in AML cells is reached by binding to the BM extracellular matrix (ECM) through integrins. Integrins are transmembrane heterodimers, serving as cell-to-cell adhesion molecules to assist in the cell-to-cell contact as well as in attachment of cells to the ECM [470]. Osteopontin-mediated activation of integrin  $\alpha\beta3$  induces  $\beta$ -catenin signalling in *FLT3*-ITD positive AML cells through PI3K pathway activation, enforcing transcription of *MYC* and *CCND1*, thereby promoting TKI resistance. [221, 471]

In the BM and HSC niche, microenvironmental hypoxia (low oxygen partial pressure) also leads to cell cycle arrest of AML blasts and inhibition of apoptosis by inducing the expression of the X-linked inhibitor of apoptosis protein (XIAP) [472]. Of note, in some patients hypoxia is capable of downregulating FLT3 expression in AML blasts, independent of the *FLT3* mutational state. The hypoxia-mediated FLT3 downregulation is proteasome-dependent and mediated by PI3K signalling. [473] This questions how effective the TKI-mediated FLT3 surface increase and thus induced antigen presentation for FLT3-targeted immunotherapy in a large cohort of AML patients will be. With regards to immune evasion, hypoxia-induced autophagy furthermore attenuates TCMC by upregulating miR-210 and subsequent silencing of protein tyrosine phosphatase non-receptor type 1 (PTPN1) and hypoxia inducible factor (HIF)-1 $\alpha$ -dependent activation of STAT3 in target cells, demonstrated by experiments using non-small cell lung carcinoma cells [458, 474]. Consistently, overexpression of miR-210 as well as HIF-1  $\alpha$  is associated with a poor prognosis in AML [475, 476]. PTPN1 has just recently been discovered to act as a tumor suppressor in the myeloid lineage cells, with deficiency in PTPN1 being sufficient to drive AML in mice [477]. The generation of NOX-generated ROS by increased surface FLT3 as described above might additionally enforce autophagy in AML blasts. Hypoxia induced HIF-2 $\alpha$ -dependent upregulation of Tec family kinase BMX is also known to mediate chemotherapeutic and TKI resistance by sustained STAT5 and AKT signalling [478]. Thus, AML blasts might not only evade chemotherapy but also FLT3-targeted therapy due to hypoxic conditions.

Regarding the *in vivo* immunogenicity, a pivotal role can be attributed to regulatory T ( $T_{reg}$ ) cells.  $T_{reg}$  cells are a subset of CD4<sup>+</sup> T-cells with a suppressive function on cytotoxic T-cells to sustain self-tolerance. In AML patients, they are frequently present at higher concentrations driving immune-surveillance of leukemic blasts. Essential for their development are Forkhead-Box-Protein P3 (FOXP3), IL-2 and TGF- $\beta$  signals. Modulation of these factors impacts on immunogenicity. [479-482] Of note, IL-2 cytokine release is influenced by the FLT3 antibody type and concentration. Increasing concentrations of the FLT3xCD3 antibody (FLT3 clone 4G8) leads to increased IL-2 releases, compared to other constructs based on different FLT3 clones. [353] This means that certain FLT3xCD3 clones might impede TCMC by increasing the IL-2

concentration, thereby enhancing T<sub>reg</sub> development and function and thus suppressing cytotoxic T-cell activity. This may influence the applicability of different FLT3 antibody constructs in AML immunotherapy. Importantly, TKIs might impact on FOXP3 depending on their target specificity. FOXP3 phosphorylation and subsequent proteasomal degradation can be induced by PIM kinases. [480-482] Inhibition of PIM kinases (either directly or indirectly) might thus be counterproductive with regards to TCMC. Since the target profile of Midostaurin includes PIM kinases [483], its applicability with FLT3-directed immunotherapy is further questionable. However, recent *in vitro* investigations revealed that upon Midostaurin treatment a significant reduction of the T<sub>reg</sub> population (CD4<sup>+</sup>/CD25<sup>+</sup> T-cells) is observed in healthy and AML patient PB samples. Midostaurin also reduced *FOXP3* mRNA expression. Sorafenib modestly decreased T<sub>reg</sub> cell number, while Tandutinib and Quizartinib did not affect the T<sub>reg</sub> cell population. In contrast, total lymphocytes, CD3<sup>+</sup>, CD4<sup>+</sup> and CD8<sup>+</sup> T-cell populations in the PB were not affected by these TKIs. [484] The inhibitory strength of different TKIs on FOXP3 should receive further attention. Different TKIs might be applied depending on their therapy intend. During graft transplantation, FOXP3 activation would be beneficial, hence enhancing the immunosuppressive activity of T<sub>reg</sub> cells. [480, 482] Thus, as bridging therapy towards HSCT TKIs are likely of added value. Conversely, during anti-cancer immunotherapy T<sub>reg</sub> cell activity should be down-regulated to improve T-cell mediated cytotoxicity [482, 485]. Since BM progenitors that seed the thymus are FLT3 positive and early thymic T-cell progenitors express FLT3 [486], the influence of the TKIs on T-cell population in the thymus might be differently affected. Furthermore, decreased expression of CD99 induced by Midostaurin [450], might hinder the TCR/CD3-dependent cellular activation of T-cells, involving CD99 engagement. [487, 488] Additionally, FL impacts on T<sub>reg</sub> propagation. FL-mediated DC expansion can induce proliferation of T<sub>reg</sub> cells and suppression of anti-tumor immune responses. [486] Systemic immunogenicity is therefore difficult to monitor *in vitro*. With regards to *in vivo* efficacy of our combinatorial approach combining TKIs with FLT3-directed immunotherapy, any immune-modulatory impact of the TKIs should be noted and further evaluated. Based on the reviewed literature, Quizartinib seems to be the most promising agent for a combination with FLT3-directed immunotherapy. Since Tandutinib interferes differently with activated FLT3 compared to first- and second-generation TKIs, its exploitability in FLT3-directed immunotherapy requires evaluation.

Considering all these resistance mediating mechanisms (Figure 18), it remains essential to investigate if any combination therapy is capable of cooperatively surpassing all these probable limitations. Estimations about any drug-interfering mechanism enabling persistence of leukemia or causing severe side effects should be examined beforehand. Although clinical trials assessing TKIs, FLT3-directed antibodies or CAR T-cells as single agent might provide an informative basis with regards to off-leukemia cytotoxicity, combined drug interactions or interferences might only be seen *in vivo*. Thus mimicking the conditions in patients best possible is essential - especially with regards to T-cell propagation and function. Subsequent pre-clinical xenograft experiments investigating any TCMC effects are limited and cumbersome. However, immune responses might be monitored using SCID (severe combined immunodeficiency) or RAG-1<sup>-/-</sup> (recombination activating gene 1 deficient) humanized mice, since they lack B- and T-cells, whereof a human immune system can be implanted using human BM or enriched T-cells

populations. [489, 490] These experiments should evaluate if the combination can be applied safely. Thereafter, first in-human trials might be initiated to investigate if this combination leads to a sustained PB and BM remission rate, including the complete eradication of LSCs and avoidance of resistance mechanisms. Based on data from clinical trials treating refractory solid tumours [491], a safe application of combining these types of agents in humans is feasible. This applies to the combination of the TKI Gefitinib with the monoclonal EGFR antibody Cetuximab in patients with refractory non-small cell lung cancer. Also the combination of the TKI Lapatinib with the monoclonal human epidermal growth factor receptor 2 (HER2) antibody Trastuzumab (Herceptin) is safe. [491, 492] With regards to systemic toxicity and therapeutic efficacy, the target definitely matters. Single agent approval is however prerequisite prior application of the combination in humans. The treatment intensity will furthermore determine its applicability (e.g. if applicable in medically unfit patients). Meanwhile other combinations might be applied, like the combination of Midostaurin with chemotherapy. Besides our approach, researchers have also been investigating the combination of TKIs with other drugs for their intent in clinical applications to overcome therapy-resistance.

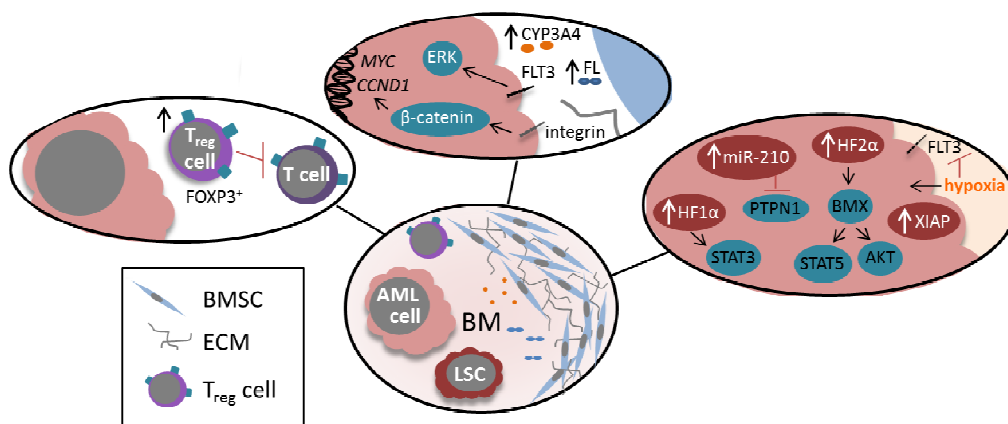


**Figure 18: Mechanisms governing AML cells and LSCs therapy-resistance and immune-surveillance.**

In the bone marrow (BM) the bone marrow stromal cells (BMSCs), the extracellular matrix (ECM) as well as hypoxic conditions provide a tumor-supportive microenvironment against TKIs and chemotherapy. In addition regulatory immune-suppressive mechanisms are activated upon certain treatment periods, reversing immunotherapeutic anti-tumor effects. This mechanism occurs naturally and is designated to control inflammation and to maintain immune tolerance. [467, 469, 471-474, 480]

### 5.3.4 Other TKI drug combinations to evade therapy-resistance

In contrast to the combination of TKIs with FLT3-targeted immunotherapy, which intends to exploit the TKI-mediated increase in FLT3 surface expression, researchers also investigated if inhibition of *N*-glycosylation in combination with TKIs acts synergistically. Interestingly, the combination of TKIs, including Quizartinib, Midostaurin, Crenolanib and Lestauritinib, with agents blocking protein *N*-glycosylation, such as tunicamycin, fluvastatin or 2-DG, enhanced the TKI-mediated cytotoxicity in *FLT3*-ITD positive AML cell lines and primary AML cells. *FLT3*-WT expressing normal and AML cells remained unaffected. The synergistic cytotoxicity governed by inhibition of *N*-glycosylation is thereby mediated by the intracellular retention of *FLT3*-ITD



preventing AKT and ERK signalling activation. NOX-generated ROS induction as well as FL induced resistance is inhibited by cytosolic FLT3 retention. Fluvastatin also reduces the expression of immature and mature FLT3 in primary AML patient samples. With regards to any clinical applicability, fluvastatin is a widely prescribed cholesterol-lowering drug well tolerated in patients. [493, 494]

Other approaches interfere with FLT3 protein stability and signalling. Addition of the PIM inhibitor LGB321 or Quercetagenin to TKIs resulted in increased cytotoxicity against *FLT3*-ITD mutated AML cell lines and primary AML patient samples, probably since abrogating its support in *MYC* transcription. [217, 495, 496] However, a clinical trial using a dual PIM/FLT3 inhibitor (SEL24), with promising anti-leukemic efficacy *in vitro* and *in vivo* in AML xenografts, is on hold at the moment due to severe adverse events [497, 498]. This might be attributed to the role of PIM kinases in modulating T<sub>reg</sub> cell propagation and function via FOXP3 [482]. The proteasome inhibitor Bortezomib in contrast induced an autophagy-mediated early degradation of FLT3-ITD but not FLT3-WT in AML cells. The combination of Sorafenib and Bortezomib for AML patients with a high *FLT3*-ITD burden is under investigation in a clinical trial. [497, 499] Other studies aim to interfere with cyclin-dependent kinases (CDK) 4 and 6, which are involved in cell cycle regulation [500]. CDK6 directly activates the transcription of *FLT3* and *PIM* kinases [501]. Compared to single agent TKI treatment with Quizartinib or Sorafenib, the dual CDK4/6 inhibitor AMG925 conferred only a slight effect on tumor burden, induced by *FLT3*-ITD positive MOLM-13 cells. Nonetheless, AMG925 might govern advantage against TKI-resistant cells with additional *FLT3*-TKD-PM [500, 502]. In contrast, combination of the dual CDK4/6 inhibitor Palbociclib with different TKIs against *FLT3*-ITD positive AML cells showed a synergistic effect in impairing the *FLT3*-dependent cell growth *in vitro* and leukemogenesis *in vivo*. [501] Important in this context is the capacity of FLT3 to phosphorylate p27. Phosphorylated p27 loses its inhibitory function on CDKs and thus enables cell proliferation. Accordingly, inhibition of FLT3 activity by TKIs reduced p27 phosphorylation in FLT3-WT AML patient samples. In contrast, in some *FLT3*-ITD positive AML patient samples, Quizartinib treatment led to increased phosphorylation of p27, induced by other tyrosine kinases. This was circumvented by treatment with the multipotent TKI Dasatinib. [503]

Hence, many pathways and mediators are involved in TKI resistance; there exist a lot of potential targets and possible drug combinations [352]. Amongst them the ERK/MAPK signalling is highly reactivated in TKI-resistant *FLT3*-mutant AML cells [447, 455, 504]. Therefore, researchers investigated many agents to target both FLT3 and ERK/MAPK signalling mediators. Combination of Sorafenib with a low-dose MEK inhibitor (PD0325901) for example synergistically decreased AML cell proliferation and resulted in significant reduction of PB and BM blasts in AML xenografts [447]. Similarly, a novel dual MEK/FLT3 inhibitor (E6201) exerted cytotoxicity against TKI-resistant AML cells; even under hypoxic conditions and during co-culture with mesenchymal stem cells [505]. Another example is the inhibitor TP-0903, which inhibits both FLT3 and AXL. AXL is an upstream RTK of ERK/MAPK signalling, found to be highly phosphorylated in Quizartinib and Midostaurin resistant AML cells. [506, 507] The TKI Gilteritinib is a promising dual FLT3/AXL inhibitor, currently investigated in clinical trials [307, 322, 426]. FLT3 and JAK inhibitors in combination are further capable of overriding the BM stromal-mediated TKI resistance [508].

Hence, multipotent TKIs might be of a higher value with regards to avoiding TKI resistance than more FLT3-specific TKIs – although implicating more side effects and a lower pharmacologic property.

Several other studies and clinical trials investigated the use of TKIs with hypomethylating agents (e.g. Azacytidine and Decitabine) to enhance the eradication of LSCs [497]. LSCs frequently display a resistance pattern against TKIs with epigenetic gene mutations, resulting in altered gene expression. Tumor-suppressor genes (e.g. SHP-1, a negative regulator of the AKT/STAT pathway) or genes responsible for hematopoietic differentiation (e.g. GATA2) are genetically silenced, while the expression of stem and progenitor cell markers (e.g. SOCS) is increased. Commonly, co-occurring mutations in *IDH1/2*, *TET2* and *DNMT3A* in AML cells modulate this epigenetic pattern. [461, 509-512] Therefore, hypomethylating agents are thought to sensitize AML cells towards TKI treatment by demethylating silenced genes. In addition, hypomethylating agents only minimally increase plasma FL concentrations, which might bypass FL-mediated resistance, as seen in conventional chemotherapy [513, 514] Crenolanib in combination with Azacytidine abrogates the stromal protection of niche cells, reducing the clonogenic capacity of *FLT3*-ITD positive LSCs *in vitro* and impairing engraftment of *FLT3*-ITD positive PDX cells *in vivo* [515]. *In vitro* experiments combining Quizartinib or Sorafenib with Azacytidine or Decitabine against *FLT3*-ITD positive AML cell lines and primary AML patient samples show a synergistic cytotoxicity, based on anti-leukemic effects mediated by induction of apoptosis and differentiation. Of note, simultaneous treatment was most effective. Adding Azacytidine or Decitabine after TKI treatment was antagonistic in primary patient samples. [514] A pre-clinical study using Gilteritinib in combination with Azacytidine against *FLT3*-ITD positive MV4-11 cells *in vitro* and *in vivo* showed superior anti-leukemic efficacy compared to single agent treatment [427]. In clinical trials, Sorafenib plus Azacytidine showed effectiveness in patients with relapsed and refractory *FLT3*-mutated AML [513]. Similarly, Midostaurin plus Azacytidine was safe and tolerable in AML patients. AML patients harboring a *FLT3* mutation, who were not exposed to TKIs before and not previously transplanted, benefitted the most. In contrast, rates for AML patients without a *FLT3*-mutation were comparable to Azacytidine treatment alone. [497, 516, 517] Combination of Quizartinib and Azacytidine was highly active amongst AML patients with a *FLT3*-ITD mutation [428].

Whether the combinatorial approach of our study or of those others mentioned is beneficial with respect to anti-leukemic efficiency, tolerability and clinical outcome is open for further investigations.

## 6 Conclusion

Taken together, within this doctoral work research on *FLT3*-mutated AML was performed. The applicability of HTAS for *FLT3*-ITD detection in standard routine was investigated. Although the performance of NGS-based *FLT3*-ITD detection methods has been investigated already for several patient samples [249, 259, 281, 282], this study assessed its accuracy and benefit over routine diagnostic tools in a large cohort of *FLT3*-ITD positive patients. This work demonstrated HTAS to be accurate and highly sensitive, capturing a high ITD clonal heterogeneity in comparison to standard routine and to other available *FLT3*-ITD detection methods. After applying optimized bioinformatic algorithms, HTAS might provide a highly reliable tool with high sensitivity of prognostic value. Since novel diagnostic techniques reveal a lot of different *FLT3* mutations [229], the identification of gain-of-function mutations that may be targetable remains essential. Therefore, a patient derived recurrent *FLT3* mutation was investigated on its oncogenic impact in mediating AML relapse. FLT3-p.Q569Vfs\*2 displayed a truncation prior the JMD thus lacking essential residues for receptor autophosphorylation. Cells expressing both FLT3-p.Q569Vfs\*2 and FLT3-WT, demonstrated a dominant-negative effect of FLT3-p.Q569Vfs\*2 on FLT3-WT. This highlights the importance of assessing the biological impact of novel *FLT3* mutations, since conclusions across truncated receptors with different protein structures are not possible plus not all resistance-specific mutations drive relapse and are targetable by TKIs. Furthermore, the cellular response upon TKI treatment was investigated systematically, in cells harbouring different *FLT3* genotypes, since this has not been performed before in great detail. A TKI-driven restoration of the surface localization of intracellular retrained FLT3-mutants based on *N*-linked glycosylation was encountered. The FLT3 surface increase correlated inversely with proliferation and was dependent on the pretreatment *FLT3*-ITD mRNA level. This *FLT3*-mutant specific response provided a rational for combining TKIs with FLT3-directed immunotherapy. Proof-of-principle experiments adding AC220 to a bispecific FLT3xCD3 antibody confirmed a synergistic effect against *FLT3*-ITD positive AML cells. Thus, this was the first study to investigate the TKI-mediated FLT3 surface expression increase systematically and to exploit this mechanism for a combination with FLT3-directed immunotherapy to evade single-agent therapy-resistance. Besides combining TKIs with FLT3-directed antibodies, this approach might further be used for FLT3-primed CAR T-cell therapy. However, ongoing research is essential to confirm our proof-of-principle with other TKIs as well as to investigate the immunological implications of this combination *in vitro* and *in vivo*. Although further research is still required to translate these approaches into clinical practice, this doctoral work provided several interesting findings with clinical relevance for the diagnosis, risk stratification and therapy of *FLT3*-mutated AML.

## 7 Annex

### 7.1 References

1. Torre LA, Bray F, Siegel RL, Ferlay J, Lortet-Tieulent J and Jemal A. Global cancer statistics, 2012. *CA Cancer J Clin.* 2015; 65(2):87-108.
2. Barnes BB, J.; Buttmann-Schweiger, N.; Fiebig, J.; Jordan, S.; Kraywinkel, K.; Niemann, H.; Nowossadeck, E.; Poethko-Mueller, C.; Pruetz, F.; Rattay, P.; Schoenfeld, I.; Starker, A.; Wienecke, A.; Wolf, U.; Castell, S.; Deleré, Y.; Grabow, D.; Kaatsch, P.; Multmeier, J.; Spix, C.; Tenckhoff, B. Bericht zum Krebsgeschehen in Deutschland 2016. Robert Koch-Institut, Gesellschaft der epidemiologischen Krebsregister in Deutschland eV, Berlin. 2016.
3. Ferlay J, Steliarova-Foucher E, Lortet-Tieulent J, Rosso S, Coebergh JW, Comber H, Forman D and Bray F. Cancer incidence and mortality patterns in Europe: estimates for 40 countries in 2012. *Eur J Cancer.* 2013; 49(6):1374-1403.
4. Udensi UK and Tchounwou PB. Dual effect of oxidative stress on leukemia cancer induction and treatment. *J Exp Clin Cancer Res.* 2014; 33:106.
5. Deschler B and Lubbert M. Acute myeloid leukemia: epidemiology and etiology. *Cancer.* 2006; 107(9):2099-2107.
6. Hehlmann R, Hochhaus A, Baccarani M and European L. Chronic myeloid leukaemia. *Lancet.* 2007; 370(9584):342-350.
7. Estey EHFHKHM. Hematologic Malignancies: Acute Leukemias. Springer, Berlin, Heidelberg 2008.
8. De Kouchkovsky I and Abdul-Hay M. 'Acute myeloid leukemia: a comprehensive review and 2016 update'. *Blood Cancer J.* 2016; 6(7):e441.
9. Whitman SP, Ruppert AS, Radmacher MD, Mrozek K, Paschka P, Langer C, Baldus CD, Wen J, Racke F, Powell BL, Kolitz JE, Larson RA, Caligiuri MA, Marcucci G and Bloomfield CD. FLT3 D835/I836 mutations are associated with poor disease-free survival and a distinct gene-expression signature among younger adults with de novo cytogenetically normal acute myeloid leukemia lacking FLT3 internal tandem duplications. *Blood.* 2008; 111(3):1552-1559.
10. Whitman SP, Maharry K, Radmacher MD, Becker H, Mrozek K, Margeson D, Holland KB, Wu YZ, Schwind S, Metzeler KH, Wen J, Baer MR, Powell BL, Carter TH, Kolitz JE, Wetzler M, et al. FLT3 internal tandem duplication associates with adverse outcome and gene- and microRNA-expression signatures in patients 60 years of age or older with primary cytogenetically normal acute myeloid leukemia: a Cancer and Leukemia Group B study. *Blood.* 2010; 116(18):3622-3626.
11. Thiede C, Steudel C, Mohr B, Schaich M, Schakel U, Platzbecker U, Wermke M, Bornhauser M, Ritter M, Neubauer A, Ehninger G and Illmer T. Analysis of FLT3-activating mutations in 979 patients with acute myelogenous leukemia: association with FAB subtypes and identification of subgroups with poor prognosis. *Blood.* 2002; 99(12):4326-4335.
12. Levis M. FLT3 mutations in acute myeloid leukemia: what is the best approach in 2013? *Hematology Am Soc Hematol Educ Program.* 2013; 2013:220-226.
13. Chen Y, Pan Y, Guo Y, Zhao W, Ho WT, Wang J, Xu M, Yang FC and Zhao ZJ. Tyrosine kinase inhibitors targeting FLT3 in the treatment of acute myeloid leukemia. *Stem Cell Investig.* 2017; 4:48.
14. Puumala SE, Ross JA, Aplenc R and Spector LG. Epidemiology of childhood acute myeloid leukemia. *Pediatr Blood Cancer.* 2013; 60(5):728-733.
15. Siegel RL, Miller KD and Jemal A. Cancer statistics, 2016. *CA Cancer J Clin.* 2016; 66(1):7-30.
16. Bowen DT. Etiology of acute myeloid leukemia in the elderly. *Semin Hematol.* 2006; 43(2):82-88.

17. Leone G, Mele L, Pulsoni A, Equitani F and Pagano L. The incidence of secondary leukemias. *Haematologica*. 1999; 84(10):937-945.
18. Byrd JC, Edenfield WJ, Shields DJ and Dawson NA. Extramedullary myeloid cell tumors in acute nonlymphocytic leukemia: a clinical review. *J Clin Oncol*. 1995; 13(7):1800-1816.
19. Ratnam KV, Khor CJ and Su WP. Leukemia cutis. *Dermatol Clin*. 1994; 12(2):419-431.
20. Schoch C, Kern W, Schnittger S, Hiddemann W and Haferlach T. Karyotype is an independent prognostic parameter in therapy-related acute myeloid leukemia (t-AML): an analysis of 93 patients with t-AML in comparison to 1091 patients with de novo AML. *Leukemia*. 2004; 18(1):120-125.
21. Seita J and Weissman IL. Hematopoietic stem cell: self-renewal versus differentiation. *Wiley Interdiscip Rev Syst Biol Med*. 2010; 2(6):640-653.
22. Siveen KS, Uddin S and Mohammad RM. Targeting acute myeloid leukemia stem cell signaling by natural products. *Mol Cancer*. 2017; 16(1):13.
23. Steffen B, Muller-Tidow C, Schwable J, Berdel WE and Serve H. The molecular pathogenesis of acute myeloid leukemia. *Crit Rev Oncol Hematol*. 2005; 56(2):195-221.
24. Lowenberg B, Downing JR and Burnett A. Acute myeloid leukemia. *N Engl J Med*. 1999; 341(14):1051-1062.
25. Tan BT, Park CY, Ailles LE and Weissman IL. The cancer stem cell hypothesis: a work in progress. *Lab Invest*. 2006; 86(12):1203-1207.
26. Uribealago I and Di Croce L. Dynamics of epigenetic modifications in leukemia. *Brief Funct Genomics*. 2011; 10(1):18-29.
27. Kronke J, Bullinger L, Teleanu V, Tschurtz F, Gaidzik VI, Kuhn MW, Rucker FG, Holzmann K, Paschka P, Kapp-Schworer S, Spath D, Kindler T, Schittenhelm M, Krauter J, Ganser A, Gohring G, et al. Clonal evolution in relapsed NPM1-mutated acute myeloid leukemia. *Blood*. 2013; 122(1):100-108.
28. Kampen KR. The discovery and early understanding of leukemia. *Leuk Res*. 2012; 36(1):6-13.
29. Grimwade D, Ivey A and Huntly BJ. Molecular landscape of acute myeloid leukemia in younger adults and its clinical relevance. *Blood*. 2016; 127(1):29-41.
30. Graubert TA, Brunner AM and Fathi AT. New molecular abnormalities and clonal architecture in AML: from reciprocal translocations to whole-genome sequencing. *Am Soc Clin Oncol Educ Book*. 2014:e334-340.
31. Cancer Genome Atlas Research N, Ley TJ, Miller C, Ding L, Raphael BJ, Mungall AJ, Robertson A, Hoadley K, Triche TJ, Jr., Laird PW, Baty JD, Fulton LL, Fulton R, Heath SE, Kalicki-Veizer J, Kandoth C, et al. Genomic and epigenomic landscapes of adult de novo acute myeloid leukemia. *N Engl J Med*. 2013; 368(22):2059-2074.
32. Shlush LI, Mitchell A, Heisler L, Abelson S, Ng SWK, Trotman-Grant A, Medeiros JF, Rao-Bhatia A, Jaciw-Zurakowsky I, Marke R, McLeod JL, Doedens M, Bader G, Voisin V, Xu C, McPherson JD, et al. Tracing the origins of relapse in acute myeloid leukaemia to stem cells. *Nature*. 2017; 547(7661):104-108.
33. Thiede C. Mutant DNMT3A: teaming up to transform. *Blood*. 2012; 119(24):5615-5617.
34. Cruikshank ML, M.; Wijermans, P.; Huls, G.;. Clinical Results of Hypomethylating Agents in AML Treatment. *J Clin Med*. 2015.
35. Larsson CA, Cote G and Quintas-Cardama A. The changing mutational landscape of acute myeloid leukemia and myelodysplastic syndrome. *Mol Cancer Res*. 2013; 11(8):815-827.
36. Meyer SC and Levine RL. Translational implications of somatic genomics in acute myeloid leukaemia. *Lancet Oncol*. 2014; 15(9):e382-394.
37. Chen SJ, Shen Y and Chen Z. A panoramic view of acute myeloid leukemia. *Nat Genet*. 2013; 45(6):586-587.
38. Dohner H, Estey EH, Amadori S, Appelbaum FR, Buchner T, Burnett AK, Dombret H, Fenaux P, Grimwade D, Larson RA, Lo-Coco F, Naoe T, Niederwieser D, Ossenkoppele GJ, Sanz MA, Sierra J, et al. Diagnosis and management of acute myeloid leukemia in adults: recommendations from an international expert panel, on behalf of the European LeukemiaNet. *Blood*. 2010; 115(3):453-474.

39. Bennett JM, Catovsky D, Daniel MT, Flandrin G, Galton DA, Gralnick HR and Sultan C. Proposed revised criteria for the classification of acute myeloid leukemia. A report of the French-American-British Cooperative Group. *Ann Intern Med.* 1985; 103(4):620-625.
40. Bennett JM, Catovsky D, Daniel MT, Flandrin G, Galton DA, Gralnick HR and Sultan C. Proposals for the classification of the acute leukaemias. French-American-British (FAB) co-operative group. *Br J Haematol.* 1976; 33(4):451-458.
41. Ladines-Castro WB-I, G.; Luna-Pérez, M.A.; Santoyo-Sánchez, A.; Collazo-Jaloma, J.; Mendoza-García, E.; Ramos-Peñafiel, C.O. Morphology of leukaemias. *Revista Médica del Hospital General de México - Masson Doyma México SA.* 2015; Volume 79(Issue 2):Pages 107-113.
42. Corey SJ, Locker J, Oliveri DR, Shekhter-Levin S, Redner RL, PENCHANSKY L and GOLLIN SM. A non-classical translocation involving 17q12 (retinoic acid receptor alpha) in acute promyelocytic leukemia (APML) with atypical features. *Leukemia.* 1994; 8(8):1350-1353.
43. Collins SJ. The role of retinoids and retinoic acid receptors in normal hematopoiesis. *Leukemia.* 2002; 16(10):1896-1905.
44. Grignani F, Ferrucci PF, Testa U, Talamo G, Fagioli M, Alcalay M, Mencarelli A, Grignani F, Peschle C, Nicoletti I and et al. The acute promyelocytic leukemia-specific PML-RAR alpha fusion protein inhibits differentiation and promotes survival of myeloid precursor cells. *Cell.* 1993; 74(3):423-431.
45. Rose DH, T.; Schnittger, S.; Perglerová, K.; Kern, W.; Haferlach, C. Specific Patterns of Molecular Mutations Determine the Morphologic Differentiation Stages in Acute Myeloid Leukemia (AML). *Blood - American Society of Hematology.* 2014; vol. 124 (no. 21):2388.
46. Haferlach C, Rieder H, Lillington DM, Dastugue N, Hagemeijer A, Harbott J, Stilgenbauer S, Knuutila S, Johansson B and Fonatsch C. Proposals for standardized protocols for cytogenetic analyses of acute leukemias, chronic lymphocytic leukemia, chronic myeloid leukemia, chronic myeloproliferative disorders, and myelodysplastic syndromes. *Genes Chromosomes Cancer.* 2007; 46(5):494-499.
47. Zech L. Chromosome banding methods. *Acta Histochem Suppl.* 1979; 20:121-125.
48. Cremer T, Landegent J, Bruckner A, Scholl HP, Schardin M, Hager HD, Devilee P, Pearson P and van der Ploeg M. Detection of chromosome aberrations in the human interphase nucleus by visualization of specific target DNAs with radioactive and non-radioactive in situ hybridization techniques: diagnosis of trisomy 18 with probe L1.84. *Hum Genet.* 1986; 74(4):346-352.
49. Bayani J and Squire J. Multi-color FISH techniques. *Curr Protoc Cell Biol.* 2004; Chapter 22:Unit 22 25.
50. Dohner H, Estey E, Grimwade D, Amadori S, Appelbaum FR, Buchner T, Dombret H, Ebert BL, Fenaux P, Larson RA, Levine RL, Lo-Coco F, Naoe T, Niederwieser D, Ossenkoppele GJ, Sanz M, et al. Diagnosis and management of AML in adults: 2017 ELN recommendations from an international expert panel. *Blood.* 2017; 129(4):424-447.
51. Erber WNS-S, M.; Yuan, C.M.; Harrison, C.J.; Schwab, C.; Mills, K. Diagnostic techniques in hematologic malignancies. Cambridge University Press, New York 2010.
52. Grimwade D, Walker H, Harrison G, Oliver F, Chatters S, Harrison CJ, Wheatley K, Burnett AK, Goldstone AH and Medical Research Council Adult Leukemia Working P. The predictive value of hierarchical cytogenetic classification in older adults with acute myeloid leukemia (AML): analysis of 1065 patients entered into the United Kingdom Medical Research Council AML11 trial. *Blood.* 2001; 98(5):1312-1320.
53. Schnittger S, Schoch C, Dugas M, Kern W, Staib P, Wuchter C, Löffler H, Sauerland CM, Serve H, Buchner T, Haferlach T and Hiddemann W. Analysis of FLT3 length mutations in 1003 patients with acute myeloid leukemia: correlation to cytogenetics, FAB subtype, and prognosis in the AMLCG study and usefulness as a marker for the detection of minimal residual disease. *Blood.* 2002; 100(1):59-66.
54. Alcalay M, Meani N, Gelmetti V, Fantozzi A, Fagioli M, Orleth A, Riganelli D, Sebastiani C, Cappelli E, Casciari C, Scieurpi MT, Mariano AR, Minardi SP, Luzi L, Muller H, Di Fiore PP, et al. Acute myeloid leukemia fusion proteins deregulate genes involved in stem cell maintenance and DNA repair. *J Clin Invest.* 2003; 112(11):1751-1761.

55. Schessl C, Rawat VP, Cusan M, Deshpande A, Kohl TM, Rosten PM, Spiekermann K, Humphries RK, Schnittger S, Kern W, Hiddemann W, Quintanilla-Martinez L, Bohlander SK, Feuring-Buske M and Buske C. The AML1-ETO fusion gene and the FLT3 length mutation collaborate in inducing acute leukemia in mice. *J Clin Invest.* 2005; 115(8):2159-2168.
56. Schoch C, Haferlach T, Haase D, Fonatsch C, Löffler H, Schlegelberger B, Staib P, Sauerland MC, Heinecke A, Buchner T, Hiddemann W and German AMLCSG. Patients with de novo acute myeloid leukaemia and complex karyotype aberrations show a poor prognosis despite intensive treatment: a study of 90 patients. *Br J Haematol.* 2001; 112(1):118-126.
57. Schoch C, Kern W, Kohlmann A, Hiddemann W, Schnittger S and Haferlach T. Acute myeloid leukemia with a complex aberrant karyotype is a distinct biological entity characterized by genomic imbalances and a specific gene expression profile. *Genes Chromosomes Cancer.* 2005; 43(3):227-238.
58. Dastugue N, Payen C, Lafage-Pochitaloff M, Bernard P, Leroux D, Huguet-Rigal F, Stoppa AM, Marit G, Molina L, Michallet M and et al. Prognostic significance of karyotype in de novo adult acute myeloid leukemia. The BGMT group. *Leukemia.* 1995; 9(9):1491-1498.
59. Rowley JD and Testa JR. Chromosome abnormalities in malignant hematologic diseases. *Adv Cancer Res.* 1982; 36:103-148.
60. Rowley JD. Chromosome abnormalities in human acute nonlymphocytic leukemia: relationship to age, sex, and exposure to mutagens. *Natl Cancer Inst Monogr.* 1982; 60:17-23.
61. Dimartino JF and Cleary ML. MLL rearrangements in haematological malignancies: lessons from clinical and biological studies. *Br J Haematol.* 1999; 106(3):614-626.
62. Forrest DL, Nevill TJ, Horsman DE, Brockington DA, Fung HC, Toze CL, Conneally EA, Hogge DE, Sutherland HJ, Nantel SH, Shepherd JD and Barnett MJ. Bone marrow transplantation for adults with acute leukaemia and 11q23 chromosomal abnormalities. *Br J Haematol.* 1998; 103(3):630-638.
63. Secker-Walker LM, Moorman AV, Bain BJ and Mehta AB. Secondary acute leukemia and myelodysplastic syndrome with 11q23 abnormalities. EU Concerted Action 11q23 Workshop. *Leukemia.* 1998; 12(5):840-844.
64. Vardiman JW, Thiele J, Arber DA, Brunning RD, Borowitz MJ, Porwit A, Harris NL, Le Beau MM, Hellstrom-Lindberg E, Tefferi A and Bloomfield CD. The 2008 revision of the World Health Organization (WHO) classification of myeloid neoplasms and acute leukemia: rationale and important changes. *Blood.* 2009; 114(5):937-951.
65. Vardiman JW, Harris NL and Brunning RD. The World Health Organization (WHO) classification of the myeloid neoplasms. *Blood.* 2002; 100(7):2292-2302.
66. Swerdlow SHC, E.; Harris, N.L.; Jaffe, E.S.; Pileri, S.A.; Stein, H.; and Thiele JV, J.W. . WHO Classification of Tumours of Haematopoietic and Lymphoid Tissue. World Health Organization. 2008.
67. Bennett JM, Catovsky D, Daniel MT, Flandrin G, Galton DA, Gralnick HR and Sultan C. Proposal for the recognition of minimally differentiated acute myeloid leukaemia (AML-MO). *Br J Haematol.* 1991; 78(3):325-329.
68. Malvezzi M, Carioli G, Bertuccio P, Rosso T, Boffetta P, Levi F, La Vecchia C and Negri E. European cancer mortality predictions for the year 2016 with focus on leukaemias. *Ann Oncol.* 2016; 27(4):725-731.
69. Dores GM, Devesa SS, Curtis RE, Linet MS and Morton LM. Acute leukemia incidence and patient survival among children and adults in the United States, 2001-2007. *Blood.* 2012; 119(1):34-43.
70. Grimwade D, Hills RK, Moorman AV, Walker H, Chatters S, Goldstone AH, Wheatley K, Harrison CJ, Burnett AK and National Cancer Research Institute Adult Leukaemia Working G. Refinement of cytogenetic classification in acute myeloid leukemia: determination of prognostic significance of rare recurring chromosomal abnormalities among 5876 younger adult patients treated in the United Kingdom Medical Research Council trials. *Blood.* 2010; 116(3):354-365.
71. Grimwade D, Walker H, Oliver F, Wheatley K, Harrison C, Harrison G, Rees J, Hann I, Stevens R, Burnett A and Goldstone A. The importance of diagnostic cytogenetics on outcome in AML:

analysis of 1,612 patients entered into the MRC AML 10 trial. The Medical Research Council Adult and Children's Leukaemia Working Parties. *Blood*. 1998; 92(7):2322-2333.

72. Marcucci G, Mrozek K, Ruppert AS, Archer KJ, Pettenati MJ, Heerema NA, Carroll AJ, Koduru PR, Kolitz JE, Sterling LJ, Edwards CG, Anastasi J, Larson RA and Bloomfield CD. Abnormal cytogenetics at date of morphologic complete remission predicts short overall and disease-free survival, and higher relapse rate in adult acute myeloid leukemia: results from cancer and leukemia group B study 8461. *J Clin Oncol*. 2004; 22(12):2410-2418.

73. Kadia TM, Jain P, Ravandi F, Garcia-Manero G, Andreef M, Takahashi K, Borthakur G, Jabbour E, Konopleva M, Daver NG, Dinardo C, Pierce S, Kanagal-Shamanna R, Patel K, Estrov Z, Cortes J, et al. TP53 mutations in newly diagnosed acute myeloid leukemia: Clinicomolecular characteristics, response to therapy, and outcomes. *Cancer*. 2016.

74. Breems DA, Van Putten WL, De Greef GE, Van Zelderen-Bhola SL, Gerssen-Schoorl KB, Mellink CH, Nieuwint A, Jotterand M, Hagemeijer A, Beverloo HB and Lowenberg B. Monosomal karyotype in acute myeloid leukemia: a better indicator of poor prognosis than a complex karyotype. *J Clin Oncol*. 2008; 26(29):4791-4797.

75. Medeiros BC, Othus M, Fang M, Roulston D and Appelbaum FR. Prognostic impact of monosomal karyotype in young adult and elderly acute myeloid leukemia: the Southwest Oncology Group (SWOG) experience. *Blood*. 2010; 116(13):2224-2228.

76. Estey E. Acute myeloid leukemia: 2016 Update on risk-stratification and management. *Am J Hematol*. 2016; 91(8):824-846.

77. Godley LA and Larson RA. Therapy-related myeloid leukemia. *Semin Oncol*. 2008; 35(4):418-429.

78. Weinberg OK, Seetharam M, Ren L, Seo K, Ma L, Merker JD, Gotlib J, Zehnder JL and Arber DA. Clinical characterization of acute myeloid leukemia with myelodysplasia-related changes as defined by the 2008 WHO classification system. *Blood*. 2009; 113(9):1906-1908.

79. Kayser S, Dohner K, Krauter J, Kohne CH, Horst HA, Held G, von Lilienfeld-Toal M, Wilhelm S, Kundgen A, Gotze K, Rummel M, Nachbaur D, Schlegelberger B, Gohring G, Spath D, Morlok C, et al. The impact of therapy-related acute myeloid leukemia (AML) on outcome in 2853 adult patients with newly diagnosed AML. *Blood*. 2011; 117(7):2137-2145.

80. Cruz NM, Mencia-Trinchant N, Hassane DC and Guzman ML. Minimal residual disease in acute myelogenous leukemia. *Int J Lab Hematol*. 2017; 39 Suppl 1:53-60.

81. Burnett A, Wetzler M and Lowenberg B. Therapeutic advances in acute myeloid leukemia. *J Clin Oncol*. 2011; 29(5):487-494.

82. Estey E. Acute myeloid leukemia and myelodysplastic syndromes in older patients. *J Clin Oncol*. 2007; 25(14):1908-1915.

83. Zafar SY, Currow D and Abernethy AP. Defining best supportive care. *J Clin Oncol*. 2008; 26(31):5139-5140.

84. Lichtenegger FS, Krupka C, Kohnke T and Subklewe M. Immunotherapy for Acute Myeloid Leukemia. *Semin Hematol*. 2015; 52(3):207-214.

85. Lee JH, Joo YD, Kim H, Bae SH, Kim MK, Zang DY, Lee JL, Lee GW, Lee JH, Park JH, Kim DY, Lee WS, Ryoo HM, Hyun MS, Kim HJ, Min YJ, et al. A randomized trial comparing standard versus high-dose daunorubicin induction in patients with acute myeloid leukemia. *Blood*. 2011; 118(14):3832-3841.

86. Burnett AK, Milligan D, Prentice AG, Goldstone AH, McMullin MF, Hills RK and Wheatley K. A comparison of low-dose cytarabine and hydroxyurea with or without all-trans retinoic acid for acute myeloid leukemia and high-risk myelodysplastic syndrome in patients not considered fit for intensive treatment. *Cancer*. 2007; 109(6):1114-1124.

87. Lengfelder E, Hofmann WK and Nowak D. Impact of arsenic trioxide in the treatment of acute promyelocytic leukemia. *Leukemia*. 2012; 26(3):433-442.

88. Grimwade D, Biondi A, Mozziconacci MJ, Hagemeijer A, Berger R, Neat M, Howe K, Dastugue N, Jansen J, Radford-Weiss I, Lo Coco F, Lessard M, Hernandez JM, Delabesse E, Head D, Liso V, et al. Characterization of acute promyelocytic leukemia cases lacking the classic t(15;17): results of the



- European Working Party. Groupe Francais de Cytogenetique Hematologique, Groupe de Francais d'Hematologie Cellulaire, UK Cancer Cytogenetics Group and BIOMED 1 European Community-Concerted Action "Molecular Cytogenetic Diagnosis in Haematological Malignancies". *Blood*. 2000; 96(4):1297-1308.
89. Proytcheva MAB, B.J.; Chaleff, S.; Chang, K.; Choi, J.K.; Jaffe, R.; Jennings, L.; Jhang, J.; Kratz, A.; Leuer, K.C.; Lorsbach, R.B.; Onciu, M.; Perkins, S.L.; Pope, E.; Sheehan, A.M.; Shelat, S.G.; Taylor, G.; Thomas, A.E.; Han van Krieven, J.; Wang, S.A.; Zota, V. *Diagnostic pediatric hematopathology*. Cambridge University Press. 2011.
  90. Estey E, Levine RL and Lowenberg B. Current challenges in clinical development of "targeted therapies": the case of acute myeloid leukemia. *Blood*. 2015; 125(16):2461-2466.
  91. Kern W, Haferlach T, Schoch C, Löffler H, Gassmann W, Heinecke A, Sauerland MC, Berdel W, Buchner T and Hiddemann W. Early blast clearance by remission induction therapy is a major independent prognostic factor for both achievement of complete remission and long-term outcome in acute myeloid leukemia: data from the German AML Cooperative Group (AMLCG) 1992 Trial. *Blood*. 2003; 101(1):64-70.
  92. Levis M. Midostaurin approved for FLT3-mutated AML. *Blood*. 2017; 129(26):3403-3406.
  93. Stone RM, Mandrekar SJ, Sanford BL, Laumann K, Geyer S, Bloomfield CD, Thiede C, Prior TW, Dohner K, Marcucci G, Lo-Coco F, Klisovic RB, Wei A, Sierra J, Sanz MA, Brandwein JM, et al. Midostaurin plus Chemotherapy for Acute Myeloid Leukemia with a FLT3 Mutation. *N Engl J Med*. 2017; 377(5):454-464.
  94. Rollig C, Bornhauser M, Thiede C, Taube F, Kramer M, Mohr B, Aulitzky W, Bodenstein H, Tischler HJ, Stuhlmann R, Schuler U, Stolzel F, von Bonin M, Wandt H, Schafer-Eckart K, Schaich M, et al. Long-term prognosis of acute myeloid leukemia according to the new genetic risk classification of the European LeukemiaNet recommendations: evaluation of the proposed reporting system. *J Clin Oncol*. 2011; 29(20):2758-2765.
  95. Mrozek K, Marcucci G, Nicolet D, Maharry KS, Becker H, Whitman SP, Metzeler KH, Schwind S, Wu YZ, Kohlschmidt J, Pettenati MJ, Heerema NA, Block AW, Patil SR, Baer MR, Kolitz JE, et al. Prognostic significance of the European LeukemiaNet standardized system for reporting cytogenetic and molecular alterations in adults with acute myeloid leukemia. *J Clin Oncol*. 2012; 30(36):4515-4523.
  96. Rashidi A, Walter RB, Tallman MS, Appelbaum FR and DiPersio JF. Maintenance therapy in acute myeloid leukemia: an evidence-based review of randomized trials. *Blood*. 2016; 128(6):763-773.
  97. Stelljes M, Krug U, Beelen DW, Braess J, Sauerland MC, Heinecke A, Ligges S, Sauer T, Tschanter P, Thoennissen GB, Berning B, Kolb HJ, Reichle A, Holler E, Schwerdtfeger R, Arnold R, et al. Allogeneic transplantation versus chemotherapy as postremission therapy for acute myeloid leukemia: a prospective matched pairs analysis. *J Clin Oncol*. 2014; 32(4):288-296.
  98. Edenfield WJ and Gore SD. Stage-specific application of allogeneic and autologous marrow transplantation in the management of acute myeloid leukemia. *Semin Oncol*. 1999; 26(1):21-34.
  99. de Lima M, Anagnostopoulos A, Munsell M, Shahjahan M, Ueno N, Ippoliti C, Andersson BS, Gajewski J, Couriel D, Cortes J, Donato M, Neumann J, Champlin R and Giral S. Nonablative versus reduced-intensity conditioning regimens in the treatment of acute myeloid leukemia and high-risk myelodysplastic syndrome: dose is relevant for long-term disease control after allogeneic hematopoietic stem cell transplantation. *Blood*. 2004; 104(3):865-872.
  100. Zittoun RA, Mandelli F, Willemze R, de Witte T, Labar B, Resegotti L, Leoni F, Damasio E, Visani G, Papa G and et al. Autologous or allogeneic bone marrow transplantation compared with intensive chemotherapy in acute myelogenous leukemia. European Organization for Research and Treatment of Cancer (EORTC) and the Gruppo Italiano Malattie Ematologiche Maligne dell'Adulto (GIMEMA) Leukemia Cooperative Groups. *N Engl J Med*. 1995; 332(4):217-223.
  101. Mawad R, Lionberger JM and Pagel JM. Strategies to reduce relapse after allogeneic hematopoietic cell transplantation in acute myeloid leukemia. *Curr Hematol Malig Rep*. 2013; 8(2):132-140.

102. Lane SW, Scadden DT and Gilliland DG. The leukemic stem cell niche: current concepts and therapeutic opportunities. *Blood*. 2009; 114(6):1150-1157.
103. Konopleva MY and Jordan CT. Leukemia stem cells and microenvironment: biology and therapeutic targeting. *J Clin Oncol*. 2011; 29(5):591-599.
104. Tabe Y and Konopleva M. Advances in understanding the leukaemia microenvironment. *Br J Haematol*. 2014; 164(6):767-778.
105. Schepers K, Campbell TB and Passegue E. Normal and leukemic stem cell niches: insights and therapeutic opportunities. *Cell Stem Cell*. 2015; 16(3):254-267.
106. Hackl H, Astanina K and Wieser R. Molecular and genetic alterations associated with therapy resistance and relapse of acute myeloid leukemia. *J Hematol Oncol*. 2017; 10(1):51.
107. Patel C, Stenke L, Varma S, Lindberg ML, Bjorkholm M, Sjoberg J, Viktorsson K, Lewensohn R, Landgren O, Gottesman MM and Gillet JP. Multidrug resistance in relapsed acute myeloid leukemia: evidence of biological heterogeneity. *Cancer*. 2013; 119(16):3076-3083.
108. Menzin J, Lang K, Earle CC, Kerney D and Mallick R. The outcomes and costs of acute myeloid leukemia among the elderly. *Arch Intern Med*. 2002; 162(14):1597-1603.
109. Leith CP, Kopecky KJ, Godwin J, McConnell T, Slovak ML, Chen IM, Head DR, Appelbaum FR and Willman CL. Acute myeloid leukemia in the elderly: assessment of multidrug resistance (MDR1) and cytogenetics distinguishes biologic subgroups with remarkably distinct responses to standard chemotherapy. A Southwest Oncology Group study. *Blood*. 1997; 89(9):3323-3329.
110. Walter RB and Estey EH. Management of older or unfit patients with acute myeloid leukemia. *Leukemia*. 2015; 29(4):770-775.
111. Pulte D, Gondos A and Brenner H. Improvements in survival of adults diagnosed with acute myeloblastic leukemia in the early 21st century. *Haematologica*. 2008; 93(4):594-600.
112. Deschler B, de Witte T, Mertelsmann R and Lubbert M. Treatment decision-making for older patients with high-risk myelodysplastic syndrome or acute myeloid leukemia: problems and approaches. *Haematologica*. 2006; 91(11):1513-1522.
113. Hills RK, Castaigne S, Appelbaum FR, Delaunay J, Petersdorf S, Othus M, Estey EH, Dombret H, Chevret S, Ifrah N, Cahn JY, Recher C, Chilton L, Moorman AV and Burnett AK. Addition of gemtuzumab ozogamicin to induction chemotherapy in adult patients with acute myeloid leukaemia: a meta-analysis of individual patient data from randomised controlled trials. *Lancet Oncol*. 2014; 15(9):986-996.
114. Krupka C, Kufer P, Kischel R, Zugmaier G, Bogeholz J, Kohnke T, Lichtenegger FS, Schneider S, Metzeler KH, Fiegl M, Spiekermann K, Baeuerle PA, Hiddemann W, Riethmuller G and Subklewe M. CD33 target validation and sustained depletion of AML blasts in long-term cultures by the bispecific T-cell-engaging antibody AMG 330. *Blood*. 2014; 123(3):356-365.
115. Brown P, Meshinchi S, Levis M, Alonzo TA, Gerbing R, Lange B, Arceci R and Small D. Pediatric AML primary samples with FLT3/ITD mutations are preferentially killed by FLT3 inhibition. *Blood*. 2004; 104(6):1841-1849.
116. Gilliland DG and Griffin JD. The roles of FLT3 in hematopoiesis and leukemia. *Blood*. 2002; 100(5):1532-1542.
117. Blume-Jensen P and Hunter T. Oncogenic kinase signalling. *Nature*. 2001; 411(6835):355-365.
118. Agnes F, Shamoon B, Dina C, Rosnet O, Birnbaum D and Galibert F. Genomic structure of the downstream part of the human FLT3 gene: exon/intron structure conservation among genes encoding receptor tyrosine kinases (RTK) of subclass III. *Gene*. 1994; 145(2):283-288.
119. Robinson DR, Wu YM and Lin SF. The protein tyrosine kinase family of the human genome. *Oncogene*. 2000; 19(49):5548-5557.
120. Reilly JT. Receptor tyrosine kinases in normal and malignant haematopoiesis. *Blood Rev*. 2003; 17(4):241-248.
121. Carow CE, Kim E, Hawkins AL, Webb HD, Griffin CA, Jabs EW, Civin CI and Small D. Localization of the human stem cell tyrosine kinase-1 gene (FLT3) to 13q12-->q13. *Cytogenet Cell Genet*. 1995; 70(3-4):255-257.

122. Abu-Duhier FM, Goodeve AC, Wilson GA, Care RS, Peake IR and Reilly JT. Genomic structure of human FLT3: implications for mutational analysis. *Br J Haematol.* 2001; 113(4):1076-1077.
123. Rosnet O, Buhring HJ, Marchetto S, Rappold I, Lavagna C, Sainty D, Arnoulet C, Chabannon C, Kanz L, Hannum C and Birnbaum D. Human FLT3/FLK2 receptor tyrosine kinase is expressed at the surface of normal and malignant hematopoietic cells. *Leukemia.* 1996; 10(2):238-248.
124. Lyman SD, James L, Zappone J, Sleath PR, Beckmann MP and Bird T. Characterization of the protein encoded by the flt3 (flk2) receptor-like tyrosine kinase gene. *Oncogene.* 1993; 8(4):815-822.
125. Reilly JT. FLT3 and its role in the pathogenesis of acute myeloid leukaemia. *Leuk Lymphoma.* 2003; 44(1):1-7.
126. Lemmon MA and Schlessinger J. Cell signaling by receptor tyrosine kinases. *Cell.* 2010; 141(7):1117-1134.
127. Hanks SK, Quinn AM and Hunter T. The protein kinase family: conserved features and deduced phylogeny of the catalytic domains. *Science.* 1988; 241(4861):42-52.
128. Spinner NBC, L. K.; Neitzel, H.; Möckel, M.; Siegmund, B.; Dietel, M.; Suttorp N. *Harrisons Innere Medizin ABW Wissenschaftsverlagsgesellschaft; Thieme Verlagsgruppe.* 2016; 19. Auflage(83e Chromosomenaberrationen).
129. Shaughnessy J, Tian E, Sawyer J, Bumm K, Landes R, Badros A, Morris C, Tricot G, Epstein J and Barlogie B. High incidence of chromosome 13 deletion in multiple myeloma detected by multiprobe interphase FISH. *Blood.* 2000; 96(4):1505-1511.
130. Whitman SP, Archer KJ, Feng L, Baldus C, Becknell B, Carlson BD, Carroll AJ, Mrozek K, Vardiman JW, George SL, Kolitz JE, Larson RA, Bloomfield CD and Caligiuri MA. Absence of the wild-type allele predicts poor prognosis in adult de novo acute myeloid leukemia with normal cytogenetics and the internal tandem duplication of FLT3: a cancer and leukemia group B study. *Cancer Res.* 2001; 61(19):7233-7239.
131. Opatz S, Polzer H, Herold T, Konstandin NP, Ksienzyk B, Zellmeier E, Vosberg S, Graf A, Krebs S, Blum H, Hopfner KP, Kakadia PM, Schneider S, Dufour A, Braess J, Sauerland MC, et al. Exome sequencing identifies recurring FLT3 N676K mutations in core-binding factor leukemia. *Blood.* 2013; 122(10):1761-1769.
132. Kikushige Y, Yoshimoto G, Miyamoto T, Iino T, Mori Y, Iwasaki H, Niino H, Takenaka K, Nagafuji K, Harada M, Ishikawa F and Akashi K. Human Flt3 is expressed at the hematopoietic stem cell and the granulocyte/macrophage progenitor stages to maintain cell survival. *J Immunol.* 2008; 180(11):7358-7367.
133. Matthews W, Jordan CT, Wiegand GW, Pardoll D and Lemischka IR. A receptor tyrosine kinase specific to hematopoietic stem and progenitor cell-enriched populations. *Cell.* 1991; 65(7):1143-1152.
134. Harada S, Kimura T, Fujiki H, Nakagawa H, Ueda Y, Itoh T, Yamagishi H and Sonoda Y. Flt3 ligand promotes myeloid dendritic cell differentiation of human hematopoietic progenitor cells: possible application for cancer immunotherapy. *Int J Oncol.* 2007; 30(6):1461-1468.
135. Heiss E, Masson K, Sundberg C, Pedersen M, Sun J, Bengtsson S and Ronnstrand L. Identification of Y589 and Y599 in the juxtamembrane domain of Flt3 as ligand-induced autophosphorylation sites involved in binding of Src family kinases and the protein tyrosine phosphatase SHP2. *Blood.* 2006; 108(5):1542-1550.
136. Chen L, Mao H, Zhang J, Chu J, Devine S, Caligiuri MA and Yu J. Targeting FLT3 by chimeric antigen receptor T cells for the treatment of acute myeloid leukemia. *Leukemia.* 2017; 31(8):1830-1834.
137. Volpe G, Walton DS, Del Pozzo W, Garcia P, Dasse E, O'Neill LP, Griffiths M, Frampton J and Dumon S. C/EBPalpha and MYB regulate FLT3 expression in AML. *Leukemia.* 2013; 27(7):1487-1496.
138. Stirewalt DL and Radich JP. The role of FLT3 in haematopoietic malignancies. *Nat Rev Cancer.* 2003; 3(9):650-665.
139. Maroc N, Rottapel R, Rosnet O, Marchetto S, Lavezzi C, Mannoni P, Birnbaum D and Dubreuil P. Biochemical characterization and analysis of the transforming potential of the FLT3/FLK2 receptor tyrosine kinase. *Oncogene.* 1993; 8(4):909-918.

140. Christensen JL and Weissman IL. Flk-2 is a marker in hematopoietic stem cell differentiation: a simple method to isolate long-term stem cells. *Proc Natl Acad Sci U S A*. 2001; 98(25):14541-14546.
141. McKenna HJ, Stocking KL, Miller RE, Brasel K, De Smedt T, Maraskovsky E, Maliszewski CR, Lynch DH, Smith J, Pulendran B, Roux ER, Teepe M, Lyman SD and Peschon JJ. Mice lacking flt3 ligand have deficient hematopoiesis affecting hematopoietic progenitor cells, dendritic cells, and natural killer cells. *Blood*. 2000; 95(11):3489-3497.
142. Adolfsson J, Borge OJ, Bryder D, Theilgaard-Monch K, Astrand-Grundstrom I, Sitnicka E, Sasaki Y and Jacobsen SE. Upregulation of Flt3 expression within the bone marrow Lin(-)Sca1(+)c-kit(+) stem cell compartment is accompanied by loss of self-renewal capacity. *Immunity*. 2001; 15(4):659-669.
143. Griffith J, Black J, Faerman C, Swenson L, Wynn M, Lu F, Lippke J and Saxena K. The structural basis for autoinhibition of FLT3 by the juxtamembrane domain. *Mol Cell*. 2004; 13(2):169-178.
144. Reilly JT. Class III receptor tyrosine kinases: role in leukaemogenesis. *Br J Haematol*. 2002; 116(4):744-757.
145. Levis M and Small D. FLT3: ITDoes matter in leukemia. *Leukemia*. 2003; 17(9):1738-1752.
146. Heldin CH. Dimerization of cell surface receptors in signal transduction. *Cell*. 1995; 80(2):213-223.
147. Kazi JU, Chougule RA, Li T, Su X, Moharram SA, Rupar K, Marhall A, Gazi M, Sun J, Zhao H and Ronnstrand L. Tyrosine 842 in the activation loop is required for full transformation by the oncogenic mutant FLT3-ITD. *Cell Mol Life Sci*. 2017; 74(14):2679-2688.
148. Rosnet O, Buhning HJ, deLapeyriere O, Beslu N, Lavagna C, Marchetto S, Rappold I, Drexler HG, Birg F, Rottapel R, Hannum C, Dubreuil P and Birnbaum D. Expression and signal transduction of the FLT3 tyrosine kinase receptor. *Acta Haematol*. 1996; 95(3-4):218-223.
149. Kindler T, Breitenbuecher F, Kasper S, Estey E, Giles F, Feldman E, Ehninger G, Schiller G, Klimek V, Nimer SD, Gratwohl A, Choudhary CR, Mueller-Tidow C, Serve H, Gschaidmeier H, Cohen PS, et al. Identification of a novel activating mutation (Y842C) within the activation loop of FLT3 in patients with acute myeloid leukemia (AML). *Blood*. 2005; 105(1):335-340.
150. Ullrich A and Schlessinger J. Signal transduction by receptors with tyrosine kinase activity. *Cell*. 1990; 61(2):203-212.
151. Turner AM, Lin NL, Issarachai S, Lyman SD and Broudy VC. FLT3 receptor expression on the surface of normal and malignant human hematopoietic cells. *Blood*. 1996; 88(9):3383-3390.
152. Masson K, Liu T, Khan R, Sun J and Ronnstrand L. A role of Gab2 association in Flt3 ITD mediated Stat5 phosphorylation and cell survival. *Br J Haematol*. 2009; 146(2):193-202.
153. Zhang S and Broxmeyer HE. Flt3 ligand induces tyrosine phosphorylation of gab1 and gab2 and their association with shp-2, grb2, and PI3 kinase. *Biochem Biophys Res Commun*. 2000; 277(1):195-199.
154. Swords R, Freeman C and Giles F. Targeting the FMS-like tyrosine kinase 3 in acute myeloid leukemia. *Leukemia*. 2012; 26(10):2176-2185.
155. Grafone T, Palmisano M, Nicci C and Storti S. An overview on the role of FLT3-tyrosine kinase receptor in acute myeloid leukemia: biology and treatment. *Oncol Rev*. 2012; 6(1):e8.
156. Matrone A, Valerio L, Pieruzzi L, Giani C, Cappagli V, Lorusso L, Agate L, Puleo L, Viola D, Bottici V, Del Re M, Molinaro E, Danesi R and Elisei R. Protein kinase inhibitors for the treatment of advanced and progressive radiorefractory thyroid tumors: From the clinical trials to the real life. *Best Pract Res Clin Endocrinol Metab*. 2017; 31(3):319-334.
157. Reindl C, Bagrintseva K, Vempati S, Schnittger S, Ellwart JW, Wenig K, Hopfner KP, Hiddemann W and Spiekermann K. Point mutations in the juxtamembrane domain of FLT3 define a new class of activating mutations in AML. *Blood*. 2006; 107(9):3700-3707.
158. Kiyoi H. Flt3 Inhibitors: Recent Advances and Problems for Clinical Application. *Nagoya J Med Sci*. 2015; 77(1-2):7-17.
159. Lagunas-Rangel FA and Chavez-Valencia V. FLT3-ITD and its current role in acute myeloid leukaemia. *Med Oncol*. 2017; 34(6):114.
160. Kayser S, Schlenk RF, Londono MC, Breitenbuecher F, Wittke K, Du J, Groner S, Spath D, Krauter J, Ganser A, Dohner H, Fischer T, Dohner K and German-Austrian AMLSG. Insertion of FLT3

internal tandem duplication in the tyrosine kinase domain-1 is associated with resistance to chemotherapy and inferior outcome. *Blood*. 2009; 114(12):2386-2392.

161. Chan PM, Ilangumaran S, La Rose J, Chakrabartty A and Rottapel R. Autoinhibition of the kit receptor tyrosine kinase by the cytosolic juxtamembrane region. *Mol Cell Biol*. 2003; 23(9):3067-3078.
162. Swaminathan G and Tsygankov AY. The Cbl family proteins: ring leaders in regulation of cell signaling. *J Cell Physiol*. 2006; 209(1):21-43.
163. Schmidt MH and Dikic I. The Cbl interactome and its functions. *Nat Rev Mol Cell Biol*. 2005; 6(12):907-918.
164. Thien CB and Langdon WY. Cbl: many adaptations to regulate protein tyrosine kinases. *Nat Rev Mol Cell Biol*. 2001; 2(4):294-307.
165. Ryan PE, Davies GC, Nau MM and Lipkowitz S. Regulating the regulator: negative regulation of Cbl ubiquitin ligases. *Trends Biochem Sci*. 2006; 31(2):79-88.
166. Mohapatra B, Ahmad G, Nadeau S, Zutshi N, An W, Scheffe S, Dong L, Feng D, Goetz B, Arya P, Bailey TA, Palermo N, Borgstahl GE, Natarajan A, Raja SM, Naramura M, et al. Protein tyrosine kinase regulation by ubiquitination: critical roles of Cbl-family ubiquitin ligases. *Biochim Biophys Acta*. 2013; 1833(1):122-139.
167. Oshikawa G, Nagao T, Wu N, Kurosu T and Miura O. c-Cbl and Cbl-b ligases mediate 17-allylaminodemethoxygeldanamycin-induced degradation of autophosphorylated Flt3 kinase with internal tandem duplication through the ubiquitin proteasome pathway. *J Biol Chem*. 2011; 286(35):30263-30273.
168. Robinson LJX, J. . Proteosomal Degradation of Flt3 Is Stimulated by Leukemia-Associated Flt3 Mutations. *Blood*. 2004; 104(11):2574.
169. Kottaridis PD, Gale RE and Linch DC. Flt3 mutations and leukaemia. *Br J Haematol*. 2003; 122(4):523-538.
170. Gupta R, Knight CL and Bain BJ. Receptor tyrosine kinase mutations in myeloid neoplasms. *Br J Haematol*. 2002; 117(3):489-508.
171. Kelly LM, Liu Q, Kutok JL, Williams IR, Boulton CL and Gilliland DG. FLT3 internal tandem duplication mutations associated with human acute myeloid leukemias induce myeloproliferative disease in a murine bone marrow transplant model. *Blood*. 2002; 99(1):310-318.
172. Lee BH, Tothova Z, Levine RL, Anderson K, Buza-Vidas N, Cullen DE, McDowell EP, Adelsperger J, Frohling S, Huntly BJ, Beran M, Jacobsen SE and Gilliland DG. FLT3 mutations confer enhanced proliferation and survival properties to multipotent progenitors in a murine model of chronic myelomonocytic leukemia. *Cancer Cell*. 2007; 12(4):367-380.
173. Drexler HG. Expression of FLT3 receptor and response to FLT3 ligand by leukemic cells. *Leukemia*. 1996; 10(4):588-599.
174. Carow CE, Levenstein M, Kaufmann SH, Chen J, Amin S, Rockwell P, Witte L, Borowitz MJ, Civin CI and Small D. Expression of the hematopoietic growth factor receptor FLT3 (STK-1/Flk2) in human leukemias. *Blood*. 1996; 87(3):1089-1096.
175. Kuchenbauer F, Kern W, Schoch C, Kohlmann A, Hiddemann W, Haferlach T and Schnittger S. Detailed analysis of FLT3 expression levels in acute myeloid leukemia. *Haematologica*. 2005; 90(12):1617-1625.
176. Wang GG, Pasillas MP and Kamps MP. Persistent transactivation by meis1 replaces hox function in myeloid leukemogenesis models: evidence for co-occupancy of meis1-pbx and hox-pbx complexes on promoters of leukemia-associated genes. *Mol Cell Biol*. 2006; 26(10):3902-3916.
177. Ozeki K, Kiyoi H, Hirose Y, Iwai M, Ninomiya M, Kadera Y, Miyawaki S, Kuriyama K, Shimazaki C, Akiyama H, Nishimura M, Motoji T, Shinagawa K, Takeshita A, Ueda R, Ohno R, et al. Biologic and clinical significance of the FLT3 transcript level in acute myeloid leukemia. *Blood*. 2004; 103(5):1901-1908.
178. Zheng R, Levis M, Piloto O, Brown P, Baldwin BR, Gorin NC, Beran M, Zhu Z, Ludwig D, Hicklin D, Witte L, Li Y and Small D. FLT3 ligand causes autocrine signaling in acute myeloid leukemia cells. *Blood*. 2004; 103(1):267-274.

179. Kiyoi H and Naoe T. FLT3 in human hematologic malignancies. *Leuk Lymphoma*. 2002; 43(8):1541-1547.
180. Zheng R, Bailey E, Nguyen B, Yang X, Piloto O, Levis M and Small D. Further activation of FLT3 mutants by FLT3 ligand. *Oncogene*. 2011; 30(38):4004-4014.
181. Tarlock K, Alonzo TA, Loken MR, Gerbing RB, Ries RE, Aplenc R, Sung L, Raimondi SC, Hirsch BA, Kahwash SB, McKenney A, Kolb EA, Gamis AS and Meshinchi S. Disease Characteristics and Prognostic Implications of Cell-Surface FLT3 Receptor (CD135) Expression in Pediatric Acute Myeloid Leukemia: A Report from the Children's Oncology Group. *Clin Cancer Res*. 2017; 23(14):3649-3656.
182. Goldstein RH, A.; Koppikar, P.; Archibeque, I.; Frank, B.; Balazs, M.; Dahlhoff, C.; Raum, T.; Li, C.-M.; Wahl, J.; Rock, D.; Thomas, O.; Karbowski, C.; Krupka, C.; Subklewe, M.; Coxon, A.; Chapman-Arvedson T. Evaluation of a FLT3 Bite® for Acute Myeloid Leukemia Blood. 2017; 130(Suppl 1):1354.
183. Cheng J, Qu L, Wang J, Cheng L and Wang Y. High expression of FLT3 is a risk factor in leukemia. *Mol Med Rep*. 2018; 17(2):2885-2892.
184. Vempati S, Reindl C, Kaza SK, Kern R, Malamoussi T, Dugas M, Mellert G, Schnittger S, Hiddemann W and Spiekermann K. Arginine 595 is duplicated in patients with acute leukemias carrying internal tandem duplications of FLT3 and modulates its transforming potential. *Blood*. 2007; 110(2):686-694.
185. Mrozek K, Marcucci G, Paschka P, Whitman SP and Bloomfield CD. Clinical relevance of mutations and gene-expression changes in adult acute myeloid leukemia with normal cytogenetics: are we ready for a prognostically prioritized molecular classification? *Blood*. 2007; 109(2):431-448.
186. Andreeff M. (2015). *Targeted Therapy of Acute Myeloid Leukemia*: Springer-Verlag New York 2015).
187. Kavanagh S, Murphy T, Law A, Yehudai D, Ho JM, Chan S and Schimmer AD. Emerging therapies for acute myeloid leukemia: translating biology into the clinic. *JCI Insight*. 2017; 2(18).
188. Deeb KK, Smonskey MT, DeFedericis H, Deeb G, Sait SN, Wetzler M, Wang ES and Starostik P. Deletion and deletion/insertion mutations in the juxtamembrane domain of the FLT3 gene in adult acute myeloid leukemia. *Leuk Res Rep*. 2014; 3(2):86-89.
189. Kottaridis PD, Gale RE, Frew ME, Harrison G, Langabeer SE, Belton AA, Walker H, Wheatley K, Bowen DT, Burnett AK, Goldstone AH and Linch DC. The presence of a FLT3 internal tandem duplication in patients with acute myeloid leukemia (AML) adds important prognostic information to cytogenetic risk group and response to the first cycle of chemotherapy: analysis of 854 patients from the United Kingdom Medical Research Council AML 10 and 12 trials. *Blood*. 2001; 98(6):1752-1759.
190. Nakao M, Yokota S, Iwai T, Kaneko H, Horiike S, Kashima K, Sonoda Y, Fujimoto T and Misawa S. Internal tandem duplication of the *flt3* gene found in acute myeloid leukemia. *Leukemia*. 1996; 10(12):1911-1918.
191. Welch JS, Ley TJ, Link DC, Miller CA, Larson DE, Koboldt DC, Wartman LD, Lamprecht TL, Liu F, Xia J, Kandoth C, Fulton RS, McLellan MD, Dooling DJ, Wallis JW, Chen K, et al. The origin and evolution of mutations in acute myeloid leukemia. *Cell*. 2012; 150(2):264-278.
192. Jan M, Snyder TM, Corces-Zimmerman MR, Vyas P, Weissman IL, Quake SR and Majeti R. Clonal evolution of preleukemic hematopoietic stem cells precedes human acute myeloid leukemia. *Sci Transl Med*. 2012; 4(149):149ra118.
193. Schnittger S, Bacher U, Haferlach C, Alpermann T, Kern W and Haferlach T. Diversity of the juxtamembrane and TKD1 mutations (exons 13-15) in the FLT3 gene with regards to mutant load, sequence, length, localization, and correlation with biological data. *Genes Chromosomes Cancer*. 2012; 51(10):910-924.
194. Stirewalt DL, Kopecky KJ, Meshinchi S, Engel JH, Pogossova-Agadjanyan EL, Linsley J, Slovak ML, Willman CL and Radich JP. Size of FLT3 internal tandem duplication has prognostic significance in patients with acute myeloid leukemia. *Blood*. 2006; 107(9):3724-3726.
195. Schnittger S, Schoch C, Kern W, Hiddemann W and Haferlach T. FLT3 length mutations as marker for follow-up studies in acute myeloid leukaemia. *Acta Haematol*. 2004; 112(1-2):68-78.

196. Breitenbuecher F, Schnittger S, Grundler R, Markova B, Carius B, Brecht A, Duyster J, Haferlach T, Huber C and Fischer T. Identification of a novel type of ITD mutations located in nonjuxtamembrane domains of the FLT3 tyrosine kinase receptor. *Blood*. 2009; 113(17):4074-4077.
197. Abu-Duhier FM, Goodeve AC, Wilson GA, Gari MA, Peake IR, Rees DC, Vandenbergh EA, Winship PR and Reilly JT. FLT3 internal tandem duplication mutations in adult acute myeloid leukaemia define a high-risk group. *Br J Haematol*. 2000; 111(1):190-195.
198. Spiekermann K, Bagrintseva K, Schoch C, Haferlach T, Hiddemann W and Schnittger S. A new and recurrent activating length mutation in exon 20 of the FLT3 gene in acute myeloid leukemia. *Blood*. 2002; 100(9):3423-3425.
199. Stirewalt DL, Meshinchi S, Kussick SJ, Sheets KM, Pogossova-Agadjanyan E, Willman CL and Radich JP. Novel FLT3 point mutations within exon 14 found in patients with acute myeloid leukaemia. *Br J Haematol*. 2004; 124(4):481-484.
200. Yamamoto Y, Kiyoi H, Nakano Y, Suzuki R, Kidera Y, Miyawaki S, Asou N, Kuriyama K, Yagasaki F, Shimazaki C, Akiyama H, Saito K, Nishimura M, Motoji T, Shinagawa K, Takeshita A, et al. Activating mutation of D835 within the activation loop of FLT3 in human hematologic malignancies. *Blood*. 2001; 97(8):2434-2439.
201. Abu-Duhier FM, Goodeve AC, Wilson GA, Care RS, Peake IR and Reilly JT. Identification of novel FLT-3 Asp835 mutations in adult acute myeloid leukaemia. *Br J Haematol*. 2001; 113(4):983-988.
202. Bacher U, Haferlach C, Kern W, Haferlach T and Schnittger S. Prognostic relevance of FLT3-TKD mutations in AML: the combination matters--an analysis of 3082 patients. *Blood*. 2008; 111(5):2527-2537.
203. Chatain NR, J.; Rossetti, G.; Perera, R.C.; Carloni, P.; Haferlach, T.; Brummendorf, T.H.; Schnittger, S. and Koschmieder, S. Novel Deletion Mutants in the Juxtamembrane Domain of Fms-like Tyrosine Kinase 3 (FLT3) Induce Transformation By Release from Autoinhibition in AML. *Blood*. 2014; 124(21):885.
204. Choudhary C, Muller-Tidow C, Berdel WE and Serve H. Signal transduction of oncogenic Flt3. *Int J Hematol*. 2005; 82(2):93-99.
205. Choudhary C, Brandts C, Schwable J, Tickenbrock L, Sargin B, Ueker A, Bohmer FD, Berdel WE, Muller-Tidow C and Serve H. Activation mechanisms of STAT5 by oncogenic Flt3-ITD. *Blood*. 2007; 110(1):370-374.
206. Choudhary C, Schwable J, Brandts C, Tickenbrock L, Sargin B, Kindler T, Fischer T, Berdel WE, Muller-Tidow C and Serve H. AML-associated Flt3 kinase domain mutations show signal transduction differences compared with Flt3 ITD mutations. *Blood*. 2005; 106(1):265-273.
207. Choudhary C, Olsen JV, Brandts C, Cox J, Reddy PN, Bohmer FD, Gerke V, Schmidt-Arras DE, Berdel WE, Muller-Tidow C, Mann M and Serve H. Mislocalized activation of oncogenic RTKs switches downstream signaling outcomes. *Mol Cell*. 2009; 36(2):326-339.
208. Schmidt-Arras D, Bohmer SA, Koch S, Muller JP, Blei L, Cornils H, Bauer R, Korasikha S, Thiede C and Bohmer FD. Anchoring of FLT3 in the endoplasmic reticulum alters signaling quality. *Blood*. 2009; 113(15):3568-3576.
209. Rocnik JL, Okabe R, Yu JC, Lee BH, Giese N, Schenkein DP and Gilliland DG. Roles of tyrosine 589 and 591 in STAT5 activation and transformation mediated by FLT3-ITD. *Blood*. 2006; 108(4):1339-1345.
210. Spiekermann K, Bagrintseva K, Schwab R, Schmieja K and Hiddemann W. Overexpression and constitutive activation of FLT3 induces STAT5 activation in primary acute myeloid leukemia blast cells. *Clin Cancer Res*. 2003; 9(6):2140-2150.
211. Badar T, Patel KP, Thompson PA, DiNardo C, Takahashi K, Cabrero M, Borthakur G, Cortes J, Konopleva M, Kadia T, Bohannon Z, Pierce S, Jabbour EJ, Ravandi F, Daver N, Luthra R, et al. Detectable FLT3-ITD or RAS mutation at the time of transformation from MDS to AML predicts for very poor outcomes. *Leuk Res*. 2015; 39(12):1367-1374.
212. Weisberg E, Sattler M, Ray A and Griffin JD. Drug resistance in mutant FLT3-positive AML. *Oncogene*. 2010; 29(37):5120-5134.

213. Chan PM. Differential signaling of Flt3 activating mutations in acute myeloid leukemia: a working model. *Protein Cell*. 2011; 2(2):108-115.
214. Koch S, Jacobi A, Ryser M, Ehninger G and Thiede C. Abnormal localization and accumulation of FLT3-ITD, a mutant receptor tyrosine kinase involved in leukemogenesis. *Cells Tissues Organs*. 2008; 188(1-2):225-235.
215. Cauchy P, James SR, Zacarias-Cabeza J, Ptasinska A, Imperato MR, Assi SA, Piper J, Canestraro M, Hoogenkamp M, Raghavan M, Loke J, Akiki S, Clokie SJ, Richards SJ, Westhead DR, Griffiths MJ, et al. Chronic FLT3-ITD Signaling in Acute Myeloid Leukemia Is Connected to a Specific Chromatin Signature. *Cell Rep*. 2015; 12(5):821-836.
216. Sallmyr A, Fan J, Datta K, Kim KT, Grosu D, Shapiro P, Small D and Rassool F. Internal tandem duplication of FLT3 (FLT3/ITD) induces increased ROS production, DNA damage, and misrepair: implications for poor prognosis in AML. *Blood*. 2008; 111(6):3173-3182.
217. Natarajan K, Xie Y, Burcu M, Linn DE, Qiu Y and Baer MR. Pim-1 kinase phosphorylates and stabilizes 130 kDa FLT3 and promotes aberrant STAT5 signaling in acute myeloid leukemia with FLT3 internal tandem duplication. *PLoS One*. 2013; 8(9):e74653.
218. Hayakawa F, Towatari M, Kiyoi H, Tanimoto M, Kitamura T, Saito H and Naoe T. Tandem-duplicated Flt3 constitutively activates STAT5 and MAP kinase and introduces autonomous cell growth in IL-3-dependent cell lines. *Oncogene*. 2000; 19(5):624-631.
219. Coffey PJ, Koenderman L and de Groot RP. The role of STATs in myeloid differentiation and leukemia. *Oncogene*. 2000; 19(21):2511-2522.
220. Kiyoi H, Ohno R, Ueda R, Saito H and Naoe T. Mechanism of constitutive activation of FLT3 with internal tandem duplication in the juxtamembrane domain. *Oncogene*. 2002; 21(16):2555-2563.
221. Tickenbrock L, Schwable J, Wiedehage M, Steffen B, Sargin B, Choudhary C, Brandts C, Berdel WE, Muller-Tidow C and Serve H. Flt3 tandem duplication mutations cooperate with Wnt signaling in leukemic signal transduction. *Blood*. 2005; 105(9):3699-3706.
222. Hirade TA, M.; Onishi, C.; Yamaguchi, S.; Fukud, S. Flt3/ITD Confers Resistance to FLT3 Inhibitor AC220 By up-Regulating Runx1. *Blood*. 2014; 124(21):2223.
223. Hirade T, Abe M, Onishi C, Taketani T, Yamaguchi S and Fukuda S. Internal tandem duplication of FLT3 deregulates proliferation and differentiation and confers resistance to the FLT3 inhibitor AC220 by Up-regulating RUNX1 expression in hematopoietic cells. *Int J Hematol*. 2016; 103(1):95-106.
224. Goyama S, Schibler J, Cunningham L, Zhang Y, Rao Y, Nishimoto N, Nakagawa M, Olsson A, Wunderlich M, Link KA, Mizukawa B, Grimes HL, Kurokawa M, Liu PP, Huang G and Mulloy JC. Transcription factor RUNX1 promotes survival of acute myeloid leukemia cells. *J Clin Invest*. 2013; 123(9):3876-3888.
225. Gerloff D, Grundler R, Wurm AA, Brauer-Hartmann D, Katzerke C, Hartmann JU, Madan V, Muller-Tidow C, Duyster J, Tenen DG, Niederwieser D and Behre G. NF-kappaB/STAT5/miR-155 network targets PU.1 in FLT3-ITD-driven acute myeloid leukemia. *Leukemia*. 2015; 29(3):535-547.
226. Radomska HS, Alberich-Jorda M, Will B, Gonzalez D, Delwel R and Tenen DG. Targeting CDK1 promotes FLT3-activated acute myeloid leukemia differentiation through C/EBPalpha. *J Clin Invest*. 2012; 122(8):2955-2966.
227. Janke H, Pastore F, Schumacher D, Herold T, Hopfner KP, Schneider S, Berdel WE, Buchner T, Woermann BJ, Subklewe M, Bohlander SK, Hiddemann W, Spiekermann K and Polzer H. Activating FLT3 mutants show distinct gain-of-function phenotypes in vitro and a characteristic signaling pathway profile associated with prognosis in acute myeloid leukemia. *PLoS One*. 2014; 9(3):e89560.
228. Hou P, Wu C, Wang Y, Qi R, Bhavanasi D, Zuo Z, Dos Santos C, Chen S, Chen Y, Zheng H, Wang H, Perl A, Guo D and Huang J. A Genome-Wide CRISPR Screen Identifies Genes Critical for Resistance to FLT3 Inhibitor AC220. *Cancer Res*. 2017; 77(16):4402-4413.
229. Frohling S, Scholl C, Levine RL, Loriaux M, Boggon TJ, Bernard OA, Berger R, Dohner H, Dohner K, Ebert BL, Teckie S, Golub TR, Jiang J, Schittenhelm MM, Lee BH, Griffin JD, et al. Identification of driver and passenger mutations of FLT3 by high-throughput DNA sequence analysis and functional assessment of candidate alleles. *Cancer Cell*. 2007; 12(6):501-513.



230. Moore MA. Converging pathways in leukemogenesis and stem cell self-renewal. *Exp Hematol*. 2005; 33(7):719-737.
231. Chung KY, Morrone G, Schuringa JJ, Wong B, Dorn DC and Moore MA. Enforced expression of an Flt3 internal tandem duplication in human CD34+ cells confers properties of self-renewal and enhanced erythropoiesis. *Blood*. 2005; 105(1):77-84.
232. Li L, Piloto O, Nguyen HB, Greenberg K, Takamiya K, Racke F, Huso D and Small D. Knock-in of an internal tandem duplication mutation into murine FLT3 confers myeloproliferative disease in a mouse model. *Blood*. 2008; 111(7):3849-3858.
233. Frohling S, Schlenk RF, Breitnick J, Benner A, Kreitmeier S, Tobis K, Dohner H, Dohner K and leukemia AMLSGUAm. Prognostic significance of activating FLT3 mutations in younger adults (16 to 60 years) with acute myeloid leukemia and normal cytogenetics: a study of the AML Study Group Ulm. *Blood*. 2002; 100(13):4372-4380.
234. Poitras JL, Heiser D, Li L, Nguyen B, Nagai K, Duffield AS, Gamper C and Small D. Dnmt3a deletion cooperates with the Flt3/ITD mutation to drive leukemogenesis in a murine model. *Oncotarget*. 2016; 7(43):69124-69135.
235. Rombouts EJ, Pavic B, Lowenberg B and Ploemacher RE. Relation between CXCR-4 expression, Flt3 mutations, and unfavorable prognosis of adult acute myeloid leukemia. *Blood*. 2004; 104(2):550-557.
236. Levis M. CXCR-4: homing in on Flt3. *Blood*. 2004; 104(2):303-304.
237. Schneider F, Hoster E, Unterhalt M, Schneider S, Dufour A, Benthaus T, Mellert G, Zellmeier E, Kakadia PM, Bohlander SK, Feuring-Buske M, Buske C, Braess J, Heinecke A, Sauerland MC, Berdel WE, et al. The FLT3ITD mRNA level has a high prognostic impact in NPM1 mutated, but not in NPM1 unmutated, AML with a normal karyotype. *Blood*. 2012; 119(19):4383-4386.
238. Best DHS, J.J.; Coleman, W.B.; Tsongalis, G.J. . Molecular and translational medicine - molecular genetics and personalized medicine. Springer New York. 2012.
239. Kim Y, Lee GD, Park J, Yoon JH, Kim HJ, Min WS and Kim M. Quantitative fragment analysis of FLT3-ITD efficiently identifying poor prognostic group with high mutant allele burden or long ITD length. *Blood Cancer J*. 2015; 5:e336.
240. Murphy KM, Levis M, Hafez MJ, Geiger T, Cooper LC, Smith BD, Small D and Berg KD. Detection of FLT3 internal tandem duplication and D835 mutations by a multiplex polymerase chain reaction and capillary electrophoresis assay. *J Mol Diagn*. 2003; 5(2):96-102.
241. Mills KI, Gilkes AF, Walsh V, Sweeney M and Gale R. Rapid and sensitive detection of internal tandem duplication and activating loop mutations of FLT3. *Br J Haematol*. 2005; 130(2):203-208.
242. Levis M, Murphy KM, Pham R, Kim KT, Stine A, Li L, McNiece I, Smith BD and Small D. Internal tandem duplications of the FLT3 gene are present in leukemia stem cells. *Blood*. 2005; 106(2):673-680.
243. Schlenk RF, Dohner K, Krauter J, Frohling S, Corbacioglu A, Bullinger L, Habdank M, Spath D, Morgan M, Benner A, Schlegelberger B, Heil G, Ganser A, Dohner H and German-Austrian Acute Myeloid Leukemia Study G. Mutations and treatment outcome in cytogenetically normal acute myeloid leukemia. *N Engl J Med*. 2008; 358(18):1909-1918.
244. Brunet S, Labopin M, Esteve J, Cornelissen J, Socie G, Iori AP, Verdonck LF, Volin L, Gratwohl A, Sierra J, Mohty M and Rocha V. Impact of FLT3 internal tandem duplication on the outcome of related and unrelated hematopoietic transplantation for adult acute myeloid leukemia in first remission: a retrospective analysis. *J Clin Oncol*. 2012; 30(7):735-741.
245. Zwaan CM, Meshinchi S, Radich JP, Veerman AJ, Huismans DR, Munske L, Podleschny M, Hahlen K, Pieters R, Zimmermann M, Reinhardt D, Harbott J, Creutzig U, Kaspers GJ and Griesinger F. FLT3 internal tandem duplication in 234 children with acute myeloid leukemia: prognostic significance and relation to cellular drug resistance. *Blood*. 2003; 102(7):2387-2394.
246. Bullinger L, Dohner K, Kranz R, Stirner C, Frohling S, Scholl C, Kim YH, Schlenk RF, Tibshirani R, Dohner H and Pollack JR. An FLT3 gene-expression signature predicts clinical outcome in normal karyotype AML. *Blood*. 2008; 111(9):4490-4495.

247. Iwai T, Yokota S, Nakao M, Okamoto T, Taniwaki M, Onodera N, Watanabe A, Kikuta A, Tanaka A, Asami K, Sekine I, Mugishima H, Nishimura Y, Koizumi S, Horikoshi Y, Mimaya J, et al. Internal tandem duplication of the FLT3 gene and clinical evaluation in childhood acute myeloid leukemia. The Children's Cancer and Leukemia Study Group, Japan. *Leukemia*. 1999; 13(1):38-43.
248. Rombouts WJ, Blokland I, Lowenberg B and Ploemacher RE. Biological characteristics and prognosis of adult acute myeloid leukemia with internal tandem duplications in the Flt3 gene. *Leukemia*. 2000; 14(4):675-683.
249. Thol F, Kolking B, Damm F, Reinhardt K, Klusmann JH, Reinhardt D, von Neuhoff N, Brugman MH, Schlegelberger B, Suerbaum S, Krauter J, Ganzer A and Heuser M. Next-generation sequencing for minimal residual disease monitoring in acute myeloid leukemia patients with FLT3-ITD or NPM1 mutations. *Genes Chromosomes Cancer*. 2012; 51(7):689-695.
250. Schlenk RF, Kayser S, Bullinger L, Kobbe G, Casper J, Ringhoffer M, Held G, Brossart P, Lubbert M, Salih HR, Kindler T, Horst HA, Wulf G, Nachbaur D, Gotze K, Lamparter A, et al. Differential impact of allelic ratio and insertion site in FLT3-ITD-positive AML with respect to allogeneic transplantation. *Blood*. 2014; 124(23):3441-3449.
251. Arriba-Tutusaus P, Mack TS, Bullinger L, Schnoder TM, Polanetzki A, Weinert S, Ballaschk A, Wang Z, Deshpande AJ, Armstrong SA, Dohner K, Fischer T and Heidel FH. Impact of FLT3-ITD location on sensitivity to TKI-therapy in vitro and in vivo. *Leukemia*. 2016; 30(5):1220-1225.
252. Breitenbuecher F, Markova B, Kasper S, Carius B, Stauder T, Bohmer FD, Masson K, Ronnstrand L, Huber C, Kindler T and Fischer T. A novel molecular mechanism of primary resistance to FLT3-kinase inhibitors in AML. *Blood*. 2009; 113(17):4063-4073.
253. Heidel F, Solem FK, Breitenbuecher F, Lipka DB, Kasper S, Thiede MH, Brandts C, Serve H, Roesel J, Giles F, Feldman E, Ehninger G, Schiller GJ, Nimer S, Stone RM, Wang Y, et al. Clinical resistance to the kinase inhibitor PKC412 in acute myeloid leukemia by mutation of Asn-676 in the FLT3 tyrosine kinase domain. *Blood*. 2006; 107(1):293-300.
254. Blau O, Berenstein R, Sindram A and Blau IW. Molecular analysis of different FLT3-ITD mutations in acute myeloid leukemia. *Leuk Lymphoma*. 2013; 54(1):145-152.
255. Kusec R, Jaksic O, Ostojic S, Kardum-Skelin I, Vrhovac R and Jaksic B. More on prognostic significance of FLT3/ITD size in acute myeloid leukemia (AML). *Blood*. 2006; 108(1):405-406; author reply 406.
256. Ponziani V, Gianfaldoni G, Mannelli F, Leoni F, Ciolli S, Guglielmelli P, Antonioli E, Longo G, Bosi A and Vannucchi AM. The size of duplication does not add to the prognostic significance of FLT3 internal tandem duplication in acute myeloid leukemia patients. *Leukemia*. 2006; 20(11):2074-2076.
257. Gale RE, Green C, Allen C, Mead AJ, Burnett AK, Hills RK, Linch DC and Medical Research Council Adult Leukaemia Working P. The impact of FLT3 internal tandem duplication mutant level, number, size, and interaction with NPM1 mutations in a large cohort of young adult patients with acute myeloid leukemia. *Blood*. 2008; 111(5):2776-2784.
258. Mead AJ, Linch DC, Hills RK, Wheatley K, Burnett AK and Gale RE. FLT3 tyrosine kinase domain mutations are biologically distinct from and have a significantly more favorable prognosis than FLT3 internal tandem duplications in patients with acute myeloid leukemia. *Blood*. 2007; 110(4):1262-1270.
259. Zuffa E, Franchini E, Papayannidis C, Baldazzi C, Simonetti G, Testoni N, Abbenante MC, Paolini S, Sartor C, Parisi S, Marconi G, Cattina F, Bochicchio MT, Venturi C, Ottaviani E, Cavo M, et al. Revealing very small FLT3 ITD mutated clones by ultra-deep sequencing analysis has important clinical implications in AML patients. *Oncotarget*. 2015; 6(31):31284-31294.
260. Chen Y and Fu L. Mechanisms of acquired resistance to tyrosine kinase inhibitors. *Acta Pharmaceutica Sinica B*. 2011; 1(4):197-207.
261. Grunwald MR and Levis MJ. FLT3 inhibitors for acute myeloid leukemia: a review of their efficacy and mechanisms of resistance. *Int J Hematol*. 2013; 97(6):683-694.
262. Moreno I, Martin G, Bolufer P, Barragan E, Rueda E, Roman J, Fernandez P, Leon P, Mena A, Cervera J, Torres A and Sanz MA. Incidence and prognostic value of FLT3 internal tandem duplication and D835 mutations in acute myeloid leukemia. *Haematologica*. 2003; 88(1):19-24.

263. Smith CC, Lin K, Stecula A, Sali A and Shah NP. FLT3 D835 mutations confer differential resistance to type II FLT3 inhibitors. *Leukemia*. 2015; 29(12):2390-2392.
264. Daver N, Cortes J, Ravandi F, Patel KP, Burger JA, Konopleva M and Kantarjian H. Secondary mutations as mediators of resistance to targeted therapy in leukemia. *Blood*. 2015; 125(21):3236-3245.
265. Baker SD, Zimmerman EI, Wang YD, Orwick S, Zatechka DS, Buaboonnam J, Neale GA, Olsen SR, Enemark EJ, Shurtleff S, Rubnitz JE, Mullighan CG and Inaba H. Emergence of polyclonal FLT3 tyrosine kinase domain mutations during sequential therapy with sorafenib and sunitinib in FLT3-ITD-positive acute myeloid leukemia. *Clin Cancer Res*. 2013; 19(20):5758-5768.
266. Williams AB, Nguyen B, Li L, Brown P, Levis M, Leahy D and Small D. Mutations of FLT3/ITD confer resistance to multiple tyrosine kinase inhibitors. *Leukemia*. 2013; 27(1):48-55.
267. Chu SH and Small D. Mechanisms of resistance to FLT3 inhibitors. *Drug Resist Updat*. 2009; 12(1-2):8-16.
268. Ommen HB. Monitoring minimal residual disease in acute myeloid leukaemia: a review of the current evolving strategies. *Ther Adv Hematol*. 2016; 7(1):3-16.
269. Cloos J, Goemans BF, Hess CJ, van Oostveen JW, Waisfisz Q, Corthals S, de Lange D, Boeckx N, Hahlen K, Reinhardt D, Creutzig U, Schuurhuis GJ, Zwaan Ch M and Kaspers GJ. Stability and prognostic influence of FLT3 mutations in paired initial and relapsed AML samples. *Leukemia*. 2006; 20(7):1217-1220.
270. Abdelhamid E, Preudhomme C, Helevaut N, Nibourel O, Gardin C, Rousselot P, Castaigne S, Gruson B, Berthon C, Soua Z and Renneville A. Minimal residual disease monitoring based on FLT3 internal tandem duplication in adult acute myeloid leukemia. *Leuk Res*. 2012; 36(3):316-323.
271. Shih LY, Huang CF, Wu JH, Lin TL, Dunn P, Wang PN, Kuo MC, Lai CL and Hsu HC. Internal tandem duplication of FLT3 in relapsed acute myeloid leukemia: a comparative analysis of bone marrow samples from 108 adult patients at diagnosis and relapse. *Blood*. 2002; 100(7):2387-2392.
272. Bachas C, Schuurhuis GJ, Hollink IH, Kwidama ZJ, Goemans BF, Zwaan CM, van den Heuvel-Eibrink MM, de Bont ES, Reinhardt D, Creutzig U, de Haas V, Assaraf YG, Kaspers GJ and Cloos J. High-frequency type I/II mutational shifts between diagnosis and relapse are associated with outcome in pediatric AML: implications for personalized medicine. *Blood*. 2010; 116(15):2752-2758.
273. Tiesmeier J, Muller-Tidow C, Westermann A, Czwalińska A, Hoffmann M, Krauter J, Heil G, Ganser A, Serve H and Verbeek W. Evolution of FLT3-ITD and D835 activating point mutations in relapsing acute myeloid leukemia and response to salvage therapy. *Leuk Res*. 2004; 28(10):1069-1074.
274. Welch JS. Mutation position within evolutionary subclonal architecture in AML. *Semin Hematol*. 2014; 51(4):273-281.
275. Garg M, Nagata Y, Kanojia D, Mayakonda A, Yoshida K, Haridas Keloth S, Zang ZJ, Okuno Y, Shiraishi Y, Chiba K, Tanaka H, Miyano S, Ding LW, Alpermann T, Sun QY, Lin DC, et al. Profiling of somatic mutations in acute myeloid leukemia with FLT3-ITD at diagnosis and relapse. *Blood*. 2015; 126(22):2491-2501.
276. Del Principe MI, Buccisano F, Maurillo L, Sconocchia G, Cefalo M, Consalvo MI, Sarlo C, Conti C, De Santis G, De Bellis E, Di Veroli A, Palomba P, Attrotto C, Zizzari A, Paterno G, Voso MT, et al. Minimal Residual Disease in Acute Myeloid Leukemia of Adults: Determination, Prognostic Impact and Clinical Applications. *Mediterr J Hematol Infect Dis*. 2016; 8(1):e2016052.
277. Bachas C, Schuurhuis GJ, Zwaan CM, van den Heuvel-Eibrink MM, den Boer ML, de Bont ES, Kwidama ZJ, Reinhardt D, Creutzig U, de Haas V, Kaspers GJ and Cloos J. Gene expression profiles associated with pediatric relapsed AML. *PLoS One*. 2015; 10(4):e0121730.
278. Ottone T, Zaza S, Divona M, Hasan SK, Lavorgna S, Laterza S, Cicconi L, Panetta P, Di Giandomenico J, Cittadini M, Ciardi C, Montefusco E, Franchi A, Annino L, Venditti A, Amadori S, et al. Identification of emerging FLT3 ITD-positive clones during clinical remission and kinetics of disease relapse in acute myeloid leukaemia with mutated nucleophosmin. *Br J Haematol*. 2013; 161(4):533-540.

279. Lin MT, Tseng LH, Beierl K, Hsieh A, Thiess M, Chase N, Stafford A, Levis MJ, Eshleman JR and Gocke CD. Tandem duplication PCR: an ultrasensitive assay for the detection of internal tandem duplications of the FLT3 gene. *Diagn Mol Pathol*. 2013; 22(3):149-155.
280. Beierl K, Tseng LH, Beierl R, Haley L, Gocke CD, Eshleman JR and Lin MT. Detection of minor clones with internal tandem duplication mutations of FLT3 gene in acute myeloid leukemia using delta-PCR. *Diagn Mol Pathol*. 2013; 22(1):1-9.
281. Bibault JE, Figeac M, Helevaut N, Rodriguez C, Quief S, Sebda S, Renneville A, Nibourel O, Rousselot P, Gruson B, Dombret H, Castaigne S and Preudhomme C. Next-generation sequencing of FLT3 internal tandem duplications for minimal residual disease monitoring in acute myeloid leukemia. *Oncotarget*. 2015; 6(26):22812-22821.
282. Spencer DH, Abel HJ, Lockwood CM, Payton JE, Szankasi P, Kelley TW, Kulkarni S, Pfeifer JD and Duncavage EJ. Detection of FLT3 internal tandem duplication in targeted, short-read-length, next-generation sequencing data. *J Mol Diagn*. 2013; 15(1):81-93.
283. Hourigan CS and Karp JE. Minimal residual disease in acute myeloid leukaemia. *Nat Rev Clin Oncol*. 2013; 10(8):460-471.
284. Luthra R, Patel KP, Reddy NG, Haghshenas V, Routbort MJ, Harmon MA, Barkoh BA, Kanagal-Shamanna R, Ravandi F, Cortes JE, Kantarjian HM, Medeiros LJ and Singh RR. Next-generation sequencing-based multigene mutational screening for acute myeloid leukemia using MiSeq: applicability for diagnostics and disease monitoring. *Haematologica*. 2014; 99(3):465-473.
285. Ilyas AM, Ahmad S, Faheem M, Naseer MI, Kumosani TA, Al-Qahtani MH, Gari M and Ahmed F. Next generation sequencing of acute myeloid leukemia: influencing prognosis. *BMC Genomics*. 2015; 16 Suppl 1:S5.
286. Grimwade D and Freeman SD. Defining minimal residual disease in acute myeloid leukemia: which platforms are ready for "prime time"? *Hematology Am Soc Hematol Educ Program*. 2014; 2014(1):222-233.
287. Altman JKP, A.E.; Cortes, J.E.; Smith, C.C.; Litzow, M.R.; Hill, J.E.; Larson, R.A.; Liu, C.; Ritchie, E.K.; Strickland, S.A.; Wang, E.S.; Neubauer, A.; Martinelli, G.; Bahceci, E.; Levis, M.J. Deep molecular response to gilteritinib to improve survival in FLT3 mutation-positive relapsed/refractory acute myeloid leukemia. *Journal of Clinical Oncology* 2017; 35(no. 15\_suppl ):7003.
288. Levis M, Brown P, Smith BD, Stine A, Pham R, Stone R, Deangelo D, Galinsky I, Giles F, Estey E, Kantarjian H, Cohen P, Wang Y, Roesel J, Karp JE and Small D. Plasma inhibitory activity (PIA): a pharmacodynamic assay reveals insights into the basis for cytotoxic response to FLT3 inhibitors. *Blood*. 2006; 108(10):3477-3483.
289. Knapper S, Burnett AK, Littlewood T, Kell WJ, Agrawal S, Chopra R, Clark R, Levis MJ and Small D. A phase 2 trial of the FLT3 inhibitor lestaurtinib (CEP701) as first-line treatment for older patients with acute myeloid leukemia not considered fit for intensive chemotherapy. *Blood*. 2006; 108(10):3262-3270.
290. Brown P and Small D. FLT3 inhibitors: a paradigm for the development of targeted therapeutics for paediatric cancer. *Eur J Cancer*. 2004; 40(5):707-721, discussion 722-704.
291. Zarrinkar PP, Gunawardane RN, Cramer MD, Gardner MF, Brigham D, Belli B, Karaman MW, Pratz KW, Pallares G, Chao Q, Sprankle KG, Patel HK, Levis M, Armstrong RC, James J and Bhagwat SS. AC220 is a uniquely potent and selective inhibitor of FLT3 for the treatment of acute myeloid leukemia (AML). *Blood*. 2009; 114(14):2984-2992.
292. Klaeger S, Heinzlmeir S, Wilhelm M, Polzer H, Vick B, Koenig PA, Reinecke M, Ruprecht B, Petzoldt S, Meng C, Zecha J, Reiter K, Qiao H, Helm D, Koch H, Schoof M, et al. The target landscape of clinical kinase drugs. *Science*. 2017; 358(6367).
293. Levis M, Pham R, Smith BD and Small D. In vitro studies of a FLT3 inhibitor combined with chemotherapy: sequence of administration is important to achieve synergistic cytotoxic effects. *Blood*. 2004; 104(4):1145-1150.
294. DeAngelo DJ, Stone RM, Heaney ML, Nimer SD, Paquette RL, Klisovic RB, Caligiuri MA, Cooper MR, Lecerf JM, Karol MD, Sheng S, Holford N, Curtin PT, Druker BJ and Heinrich MC. Phase 1 clinical results with tandutinib (MLN518), a novel FLT3 antagonist, in patients with acute myelogenous

- leukemia or high-risk myelodysplastic syndrome: safety, pharmacokinetics, and pharmacodynamics. *Blood*. 2006; 108(12):3674-3681.
295. Zhang W, Konopleva M, Shi YX, McQueen T, Harris D, Ling X, Estrov Z, Quintas-Cardama A, Small D, Cortes J and Andreeff M. Mutant FLT3: a direct target of sorafenib in acute myelogenous leukemia. *J Natl Cancer Inst*. 2008; 100(3):184-198.
  296. Inaba H, Rubnitz JE, Coustan-Smith E, Li L, Furmanski BD, Mascara GP, Heym KM, Christensen R, Onciu M, Shurtleff SA, Pounds SB, Pui CH, Ribeiro RC, Campana D and Baker SD. Phase I pharmacokinetic and pharmacodynamic study of the multikinase inhibitor sorafenib in combination with clofarabine and cytarabine in pediatric relapsed/refractory leukemia. *J Clin Oncol*. 2011; 29(24):3293-3300.
  297. Widemann BC, Kim A, Fox E, Baruchel S, Adamson PC, Ingle AM, Glade Bender J, Burke M, Weigel B, Stempak D, Balis FM and Blaney SM. A phase I trial and pharmacokinetic study of sorafenib in children with refractory solid tumors or leukemias: a Children's Oncology Group Phase I Consortium report. *Clin Cancer Res*. 2012; 18(21):6011-6022.
  298. Kufareva I and Abagyan R. Type-II kinase inhibitor docking, screening, and profiling using modified structures of active kinase states. *J Med Chem*. 2008; 51(24):7921-7932.
  299. Krause DS and Van Etten RA. Tyrosine kinases as targets for cancer therapy. *N Engl J Med*. 2005; 353(2):172-187.
  300. Garuti L, Roberti M and Bottegoni G. Non-ATP competitive protein kinase inhibitors. *Curr Med Chem*. 2010; 17(25):2804-2821.
  301. Grundler R, Thiede C, Miething C, Steudel C, Peschel C and Duyster J. Sensitivity toward tyrosine kinase inhibitors varies between different activating mutations of the FLT3 receptor. *Blood*. 2003; 102(2):646-651.
  302. Clark JJ, Cools J, Curley DP, Yu JC, Lokker NA, Giese NA and Gilliland DG. Variable sensitivity of FLT3 activation loop mutations to the small molecule tyrosine kinase inhibitor MLN518. *Blood*. 2004; 104(9):2867-2872.
  303. Kampa-Schittenhelm KM, Heinrich MC, Akmut F, Dohner H, Dohner K and Schittenhelm MM. Quizartinib (AC220) is a potent second generation class III tyrosine kinase inhibitor that displays a distinct inhibition profile against mutant-FLT3, -PDGFRA and -KIT isoforms. *Mol Cancer*. 2013; 12:19.
  304. Spiekermann K, Dirschinger RJ, Schwab R, Bagrintseva K, Faber F, Buske C, Schnittger S, Kelly LM, Gilliland DG and Hiddemann W. The protein tyrosine kinase inhibitor SU5614 inhibits FLT3 and induces growth arrest and apoptosis in AML-derived cell lines expressing a constitutively activated FLT3. *Blood*. 2003; 101(4):1494-1504.
  305. Tse KF, Allebach J, Levis M, Smith BD, Bohmer FD and Small D. Inhibition of the transforming activity of FLT3 internal tandem duplication mutants from AML patients by a tyrosine kinase inhibitor. *Leukemia*. 2002; 16(10):2027-2036.
  306. Smith CC, Wang Q, Chin CS, Salerno S, Damon LE, Levis MJ, Perl AE, Travers KJ, Wang S, Hunt JP, Zarrinkar PP, Schadt EE, Kasarskis A, Kuriyan J and Shah NP. Validation of ITD mutations in FLT3 as a therapeutic target in human acute myeloid leukaemia. *Nature*. 2012; 485(7397):260-263.
  307. Lee LY, Hernandez D, Rajkhowa T, Smith SC, Raman JR, Nguyen B, Small D and Levis M. Preclinical studies of gilteritinib, a next-generation FLT3 inhibitor. *Blood*. 2017; 129(2):257-260.
  308. Al-Hussaini M and DiPersio JF. Small molecule inhibitors in acute myeloid leukemia: from the bench to the clinic. *Expert Rev Hematol*. 2014; 7(4):439-464.
  309. Stone RM, DeAngelo DJ, Klimek V, Galinsky I, Estey E, Nimer SD, Grandin W, Lebwohl D, Wang Y, Cohen P, Fox EA, Neuberg D, Clark J, Gilliland DG and Griffin JD. Patients with acute myeloid leukemia and an activating mutation in FLT3 respond to a small-molecule FLT3 tyrosine kinase inhibitor, PKC412. *Blood*. 2005; 105(1):54-60.
  310. Fischer T, Stone RM, Deangelo DJ, Galinsky I, Estey E, Lanza C, Fox E, Ehninger G, Feldman EJ, Schiller GJ, Klimek VM, Nimer SD, Gilliland DG, Dutreix C, Huntsman-Labed A, Virkus J, et al. Phase IIB trial of oral Midostaurin (PKC412), the FMS-like tyrosine kinase 3 receptor (FLT3) and multi-targeted kinase inhibitor, in patients with acute myeloid leukemia and high-risk myelodysplastic syndrome with either wild-type or mutated FLT3. *J Clin Oncol*. 2010; 28(28):4339-4345.

311. Propper DJ, McDonald AC, Man A, Thavasu P, Balkwill F, Braybrooke JP, Caponigro F, Graf P, Dutreix C, Blackie R, Kaye SB, Ganesan TS, Talbot DC, Harris AL and Twelves C. Phase I and pharmacokinetic study of PKC412, an inhibitor of protein kinase C. *J Clin Oncol*. 2001; 19(5):1485-1492.
312. Knapper S, Russell N, Gilkes A, Hills RK, Gale RE, Cavenagh JD, Jones G, Kjeldsen L, Grunwald MR, Thomas I, Konig H, Levis MJ and Burnett AK. A randomized assessment of adding the kinase inhibitor lestaurtinib to first-line chemotherapy for FLT3-mutated AML. *Blood*. 2017; 129(9):1143-1154.
313. Metzelder S, Wang Y, Wollmer E, Wanzel M, Teichler S, Chaturvedi A, Eilers M, Enghofer E, Neubauer A and Burchert A. Compassionate use of sorafenib in FLT3-ITD-positive acute myeloid leukemia: sustained regression before and after allogeneic stem cell transplantation. *Blood*. 2009; 113(26):6567-6571.
314. Metzelder SK, Schroeder T, Finck A, Scholl S, Fey M, Gotze K, Linn YC, Kroger M, Reiter A, Salih HR, Heinicke T, Stuhlmann R, Muller L, Giagounidis A, Meyer RG, Brugger W, et al. High activity of sorafenib in FLT3-ITD-positive acute myeloid leukemia synergizes with allo-immune effects to induce sustained responses. *Leukemia*. 2012; 26(11):2353-2359.
315. Cortes JE, Kantarjian H, Foran JM, Ghirdaladze D, Zodelava M, Borthakur G, Gammon G, Trone D, Armstrong RC, James J and Levis M. Phase I study of quizartinib administered daily to patients with relapsed or refractory acute myeloid leukemia irrespective of FMS-like tyrosine kinase 3-internal tandem duplication status. *J Clin Oncol*. 2013; 31(29):3681-3687.
316. Schiller GJT, M.S.; Goldberg, S.L.; Perl, A.E.; Marie, J.-P.; Martinelli, G.; Larson, R.A.; Russell, N.; Trone, D.; Gammon, G.; Levis, M.J.; Cortes, J.E. Final results of a randomized phase 2 study showing the clinical benefit of quizartinib (AC220) in patients with FLT3-ITD positive relapsed or refractory acute myeloid leukemia. . *Journal of Clinical Oncology*. 2014; 32(15\_suppl ): 7100.
317. Cortes JEP, A.E.; Dombret, H.; Kayser, S.; Steffen, B.; Rousselot, P.; Martinelli, G.; Estey, E.H.; Burnett, A.K.; Gammon, G.; Trone, D.; Leo, E.; Levis, M.J. Final Results of a Phase 2 Open-Label, Monotherapy Efficacy and Safety Study of Quizartinib (AC220) in Patients  $\geq 60$  Years of Age with FLT3 ITD Positive or Negative Relapsed/Refractory Acute Myeloid Leukemia. *Blood*. 2012; 120(21):48.
318. Cortes JEP, A.E.; Dombret, H.; Dohner, H.; Steffen, B.; Rousselot, P.H.; Martinelli, G.; Estey, E.; Shah, N.P.; Burnett, A.K.; Gammon, G.; Trone, D.; Levis, M.J. Response rate and bridging to hematopoietic stem cell transplantation (HSCT) with quizartinib (AC220) in patients with FLT3-ITD positive or negative relapsed/refractory AML after second-line chemotherapy or previous bone marrow transplant. . *Journal of Clinical Oncology*. 2013; 31(15):7012.
319. Levis MJP, A.E.; Dombret, H.; Dohner, H.; Steffen, B.; Rousselot, P.; Martinelli, G.; Estey, E.H.; Burnett, A.K.; Gammon, G.; Trone, D.; Leo, E.; Cortes, J.E. . Final Results of a Phase 2 Open-Label, Monotherapy Efficacy and Safety Study of Quizartinib (AC220) in Patients with FLT3-ITD Positive or Negative Relapsed/Refractory Acute Myeloid Leukemia After Second-Line Chemotherapy or Hematopoietic Stem Cell Transplantation. *Blood*. 2012; 120(21):673.
320. Cortes JEP, A.E.; Smith, C.C.; Kovacsics, T.; Dombret, H.; Dohner, H.; Steffen, B.; Pigneux, A.; Rousselot, P.; Krauter, J.; Martinelli, G.; Estey, E.H.; Burnett, A.K.; Ho, A.D.; Ifrah, N.; de Witt, T.; Corringham, R.; James, J.; Lilienfeld, D.; Leo, E.; Gammon, G.; Levis, M.J. A Phase II Open-Label, Ac220 Monotherapy Efficacy Study In Patients with Refractory/Relapsed Flt3-ItD Positive Acute Myeloid Leukemia: Updated Interim Results. *Blood*. 2011; 118(21):2576.
321. Levis MJP, A.E.; Altman, J.K.; Cortes, J.E.; Ritchie, E.K.; Larson, R.A.; Smith, C.C.; Wang, E.S.; Strickland, S.A.; Baer, M.R.; Litzow, M.R.; Claxton, D.; Schiller, G.J.; Ustun, C.; Liu, C.; Gill, S.; Sargent, B.; Bahceci, E. Results of a first-in-human, phase I/II trial of ASP2215, a selective, potent inhibitor of FLT3/Axl in patients with relapsed or refractory (R/R) acute myeloid leukemia (AML). . *Journal of Clinical Oncology*. 2015; 33(15\_suppl):7003.
322. Perl AE, Altman JK, Cortes J, Smith C, Litzow M, Baer MR, Claxton D, Erba HP, Gill S, Goldberg S, Jurcic JG, Larson RA, Liu C, Ritchie E, Schiller G, Spira AI, et al. Selective inhibition of FLT3 by gilteritinib in relapsed or refractory acute myeloid leukaemia: a multicentre, first-in-human, open-label, phase 1-2 study. *Lancet Oncol*. 2017; 18(8):1061-1075.

323. Levis MJP, A.E.; Altman, J.K.; Cortes, J.E.; Smith, C.C.; Baer, M.R.; Claxton, D.F.; Jurcic, J.G.; Ritchie, E.K.; Strickland, S.A.; Tibes, R.; Hill, J.; Liu S.; Bahceci, E. Evaluation of the Impact of Minimal Residual Disease, FLT3 Allelic Ratio, and FLT3 Mutation Status on Overall Survival in FLT3 Mutation-Positive Patients with Relapsed/Refractory (R/R) Acute Myeloid Leukemia (AML) in the Chrysalis Phase 1/2 Study. *Blood*. 2017; 130(Suppl 1):2705.
324. McMahon CMC, J.; Rea, B.; Sargent, R.L.; Morrisette, J.J.D.; Lieberman, D.B.; Watt, C.; Schwartz, G.W.; Faryabi, R.B.; Ferng, T.T.; Shah, N.P.; Smith, C.C.; Carroll, M.; Perl, A.E. Mechanisms of Acquired Resistance to Gilteritinib Therapy in Relapsed and Refractory FLT3-Mutated Acute Myeloid Leukemia *Blood*. 2017:295.
325. DeAngelo DJS, R.M.; Heaney, M.L.; Nimer, S.D.; Paquette, R.; Bruner-Klisovic, R.; Caligiuri, M.A.; Cooper, M.R.; LeCerf, J.-M.; Iyer, G.; Heinrich, M.C.; Druker, B.J. Phase II Evaluation of the Tyrosine Kinase Inhibitor MLN518 in Patients with Acute Myeloid Leukemia (AML) Bearing a FLT3 Internal Tandem Duplication (ITD) Mutation. *Blood*. 2004; 104(11):1792.
326. Schittenhelm MM, Kampa KM, Yee KW and Heinrich MC. The FLT3 inhibitor tandutinib (formerly MLN518) has sequence-independent synergistic effects with cytarabine and daunorubicin. *Cell Cycle*. 2009; 8(16):2621-2630.
327. von Bubnoff N, Engh RA, Aberg E, Sanger J, Peschel C and Duyster J. FMS-like tyrosine kinase 3-internal tandem duplication tyrosine kinase inhibitors display a nonoverlapping profile of resistance mutations in vitro. *Cancer Res*. 2009; 69(7):3032-3041.
328. Man CH, Fung TK, Ho C, Han HH, Chow HC, Ma AC, Choi WW, Lok S, Cheung AM, Eaves C, Kwong YL and Leung AY. Sorafenib treatment of FLT3-ITD(+) acute myeloid leukemia: favorable initial outcome and mechanisms of subsequent nonresponsiveness associated with the emergence of a D835 mutation. *Blood*. 2012; 119(22):5133-5143.
329. Parmar A, Marz S, Rushton S, Holzwarth C, Lind K, Kayser S, Dohner K, Peschel C, Oostendorp RA and Gotze KS. Stromal niche cells protect early leukemic FLT3-ITD+ progenitor cells against first-generation FLT3 tyrosine kinase inhibitors. *Cancer Res*. 2011; 71(13):4696-4706.
330. Cools J, Mentens N, Furet P, Fabbro D, Clark JJ, Griffin JD, Marynen P and Gilliland DG. Prediction of resistance to small molecule FLT3 inhibitors: implications for molecularly targeted therapy of acute leukemia. *Cancer Res*. 2004; 64(18):6385-6389.
331. Smith CC, Zhang C, Lin KC, Lasater EA, Zhang Y, Massi E, Damon LE, Pendleton M, Bashir A, Sebra R, Perl A, Kasarskis A, Shellooe R, Tsang G, Carias H, Powell B, et al. Characterizing and Overriding the Structural Mechanism of the Quizartinib-Resistant FLT3 "Gatekeeper" F691L Mutation with PLX3397. *Cancer Discov*. 2015; 5(6):668-679.
332. Stone RM, Fischer T, Paquette R, Schiller G, Schiffer CA, Ehninger G, Cortes J, Kantarjian HM, DeAngelo DJ, Huntsman-Labed A, Dutreix C, del Corral A and Giles F. Phase IB study of the FLT3 kinase inhibitor midostaurin with chemotherapy in younger newly diagnosed adult patients with acute myeloid leukemia. *Leukemia*. 2012; 26(9):2061-2068.
333. Stone RMF, T.; Paquette, R.; Schiller, G.; Schiffer, C.A.; Ehninger, G.; Cortes, J.; Kantarjian, H.M.; DeAngelo, D.J.; Huntsman-Labed, A.; Dutreix, C.; Rai, S.; Giles F. A Phase 1b Study of Midostaurin (PKC412) in Combination with Daunorubicin and Cytarabine Induction and High-Dose Cytarabine Consolidation in Patients Under Age 61 with Newly Diagnosed De Novo Acute Myeloid Leukemia: Overall Survival of Patients Whose Blasts Have FLT3 Mutations Is Similar to Those with Wild-Type FLT3. *Blood*. 2009; 114(22):634.
334. Stone RMD, H.; Ehninger, G.; Villeneuve, M.; Teasdale, T.; Virkus, J.D.; Bressler, L.R.; Seiler, M.M.; Marcucci, G.; Larson, R.A. CALGB 10603 (RATIFY): A randomized phase III study of induction (daunorubicin/cytarabine) and consolidation (high-dose cytarabine) chemotherapy combined with midostaurin or placebo in treatment-naïve patients with FLT3 mutated AML. . *Journal of Clinical Oncology*. 2011; 29(15\_suppl):TPS199.
335. Ravandi F, Cortes JE, Jones D, Faderl S, Garcia-Manero G, Konopleva MY, O'Brien S, Estrov Z, Borthakur G, Thomas D, Pierce SR, Brandt M, Byrd A, Bekele BN, Pratz K, Luthra R, et al. Phase I/II study of combination therapy with sorafenib, idarubicin, and cytarabine in younger patients with acute myeloid leukemia. *J Clin Oncol*. 2010; 28(11):1856-1862.

336. Gallogly MM and Lazarus HM. Midostaurin: an emerging treatment for acute myeloid leukemia patients. *J Blood Med*. 2016; 7:73-83.
337. Rollig C, Serve H, Huttmann A, Noppeney R, Muller-Tidow C, Krug U, Baldus CD, Brandts CH, Kunzmann V, Einsele H, Kramer A, Schafer-Eckart K, Neubauer A, Burchert A, Giagounidis A, Krause SW, et al. Addition of sorafenib versus placebo to standard therapy in patients aged 60 years or younger with newly diagnosed acute myeloid leukaemia (SORAML): a multicentre, phase 2, randomised controlled trial. *Lancet Oncol*. 2015; 16(16):1691-1699.
338. Levis M, Ravandi F, Wang ES, Baer MR, Perl A, Coutre S, Erba H, Stuart RK, Baccarani M, Cripe LD, Tallman MS, Meloni G, Godley LA, Langston AA, Amadori S, Lewis ID, et al. Results from a randomized trial of salvage chemotherapy followed by lestaurtinib for patients with FLT3 mutant AML in first relapse. *Blood*. 2011; 117(12):3294-3301.
339. Serve H, Krug U, Wagner R, Sauerland MC, Heinecke A, Brunnberg U, Schaich M, Ottmann O, Duyster J, Wandt H, Fischer T, Giagounidis A, Neubauer A, Reichle A, Aulitzky W, Noppeney R, et al. Sorafenib in combination with intensive chemotherapy in elderly patients with acute myeloid leukemia: results from a randomized, placebo-controlled trial. *J Clin Oncol*. 2013; 31(25):3110-3118.
340. Giri S, Hamdeh S, Bhatt VR and Schwarz JK. Sorafenib in Relapsed AML With FMS-Like Receptor Tyrosine Kinase-3 Internal Tandem Duplication Mutation. *J Natl Compr Canc Netw*. 2015; 13(5):508-514.
341. Fiedler W, Kayser S, Kebenko M, Janning M, Krauter J, Schittenhelm M, Gotze K, Weber D, Gohring G, Teleanu V, Thol F, Heuser M, Dohner K, Ganser A, Dohner H and Schlenk RF. A phase I/II study of sunitinib and intensive chemotherapy in patients over 60 years of age with acute myeloid leukaemia and activating FLT3 mutations. *Br J Haematol*. 2015; 169(5):694-700.
342. Perl AEC, J.E.; Strickland, S.A.; Ritchie, E.K.; Neubauer, A.; Martinelli, G.; Naoe, T.; Pigneux, A.; Rousselot, P.H.; Röllig, C.; Baer, M.R.; Larson, R.A.; James, A.J.; Chen, C.; Shu, L.; Hasabou, N.; Bahceci, E. An open-label, randomized phase III study of gilteritinib versus salvage chemotherapy in relapsed or refractory FLT3 mutation-positive acute myeloid leukemia. *Journal of Clinical Oncology*. 2017; 35(15\_suppl):TPS7067.
343. Rasko JEJ and Hughes TP. First Approved Kinase Inhibitor for AML. *Cell*. 2017; 171(5):981.
344. Hoseini SS and Cheung NK. Acute myeloid leukemia targets for bispecific antibodies. *Blood Cancer J*. 2017; 7(4):e552.
345. Li Y and Zhu Z. FLT3 antibody-based therapeutics for leukemia therapy. *Int J Hematol*. 2005; 82(2):108-114.
346. Gasiorowski RE, Clark GJ, Bradstock K and Hart DN. Antibody therapy for acute myeloid leukaemia. *Br J Haematol*. 2014; 164(4):481-495.
347. Williams B, Atkins A, Zhang H, Lu D, Jimenez X, Li H, Wang MN, Ludwig D, Balderes P, Witte L, Li Y and Zhu Z. Cell-based selection of internalizing fully human antagonistic antibodies directed against FLT3 for suppression of leukemia cell growth. *Leukemia*. 2005; 19(8):1432-1438.
348. Li Y, Li H, Wang MN, Lu D, Bassi R, Wu Y, Zhang H, Balderes P, Ludwig DL, Pytowski B, Kussie P, Piloto O, Small D, Bohlen P, Witte L, Zhu Z, et al. Suppression of leukemia expressing wild-type or ITD-mutant FLT3 receptor by a fully human anti-FLT3 neutralizing antibody. *Blood*. 2004; 104(4):1137-1144.
349. Yamamoto Y, Tsuzuki S, Akahori Y, Ukai Y, Sumitomo M, Murayama Y, Yamamoto K, Inaguma Y, Tokuda M, Abe A, Akatsuka Y, Emi N and Kurosawa Y. Isolation of human mAbs that directly modulate FMS-related tyrosine kinase 3 signaling. *Cancer Sci*. 2012; 103(2):350-359.
350. Piloto O, Nguyen B, Huso D, Kim KT, Li Y, Witte L, Hicklin DJ, Brown P and Small D. IMC-EB10, an anti-FLT3 monoclonal antibody, prolongs survival and reduces nonobese diabetic/severe combined immunodeficient engraftment of some acute lymphoblastic leukemia cell lines and primary leukemic samples. *Cancer Res*. 2006; 66(9):4843-4851.
351. Youssoufian H, Rowinsky EK, Tonra J and Li Y. Targeting FMS-related tyrosine kinase receptor 3 with the human immunoglobulin G1 monoclonal antibody IMC-EB10. *Cancer*. 2010; 116(4 Suppl):1013-1017.



352. Hospital MA, Green AS, Maciel TT, Moura IC, Leung AY, Bouscary D and Tamburini J. FLT3 inhibitors: clinical potential in acute myeloid leukemia. *Onco Targets Ther.* 2017; 10:607-615.
353. Durben M, Schmiedel D, Hofmann M, Vogt F, Nubling T, Pyz E, Buhning HJ, Rammensee HG, Salih HR, Grosse-Hovest L and Jung G. Characterization of a bispecific FLT3 X CD3 antibody in an improved, recombinant format for the treatment of leukemia. *Mol Ther.* 2015; 23(4):648-655.
354. Hofmann M, Grosse-Hovest L, Nubling T, Pyz E, Bamberg ML, Aulwurm S, Buhning HJ, Schwartz K, Haen SP, Schilbach K, Rammensee HG, Salih HR and Jung G. Generation, selection and preclinical characterization of an Fc-optimized FLT3 antibody for the treatment of myeloid leukemia. *Leukemia.* 2012; 26(6):1228-1237.
355. Sanford DB, W.G.; Ravandi, F.; Klisovic, R.B.; Borthakur, G.; Walker, A.R.; Garcia-Manero, G.; Marcucci, G.; Wierda, W.G.; Whitman, S.P.; Kantarjian, H.M.; Cortes J.E. Efficacy and safety of an anti-FLT3 antibody (LY3012218) in patients with relapsed acute myeloid leukemia. *Journal of Clinical Oncology.* 2015; 33(15):7059.
356. Lindl BK, C.; Chapman-Arvedson, T.; Kischel, R.; Kufer, P.; Haubner, S.; Lichtenegger, F.S.; Koehnke, T.; Metzeler, K.H.; Konstandin, N.; Spiekermann, K.; Hiddemann W.; Subklewe M. Midostaurin Reduces Bite® Mediated Cytotoxicity Against Acute Myeloid Leukemia. *Blood.* 2017; 130(Suppl 1):2656.
357. Rudra-Ganguly NL, C.; Virata, C.; Leavitt, M.; Jin, L.; Mendelsohn, B.; Snyder, J.; Aviña, H.; Zhang, C.; Russell, D.L.; Mattie, M.; Yang, P.; Randhawa, B.; Liu, G.; Malik, F.; Vest, M.; Abad, J.D.; Kemball, C.C.; Hubert, R.; Karki, S.; Anand, B.; An, Z.; Grant, J.; Dick, J.E.; Doñate, F.; Morrison, K.; Challita-Eid, P.; Joseph, I.B.; Pereira, D.S.; Stover, D.R. AGS62P1, a Novel Anti-FLT3 Antibody Drug Conjugate, Employing Site Specific Conjugation, Demonstrates Preclinical Anti-Tumor Efficacy in AML Tumor and Patient Derived Xenografts. *Blood.* 2015; 126(23):3806.
358. Bouchard H, Viskov C and Garcia-Echeverria C. Antibody-drug conjugates-a new wave of cancer drugs. *Bioorg Med Chem Lett.* 2014; 24(23):5357-5363.
359. Diamantis N and Banerji U. Antibody-drug conjugates--an emerging class of cancer treatment. *Br J Cancer.* 2016; 114(4):362-367.
360. Grosso DA, Hess RC and Weiss MA. Immunotherapy in acute myeloid leukemia. *Cancer.* 2015; 121(16):2689-2704.
361. Rudnick SI and Adams GP. Affinity and avidity in antibody-based tumor targeting. *Cancer Biother Radiopharm.* 2009; 24(2):155-161.
362. Jetani HG-C, I.; Nerreter, T.; Rydzek, J.; Thomas, S.; Herr, W.; Sierra, J.; Bönig, H.; Einsele, H.; Hudecek M. CAR T Cells Targeting FLT3 on AML Confer Potent Anti-Leukemic Activity and Act Synergistically with the FLT3 Inhibitor Midostaurin *Blood.* 2017; 130(Suppl 1):1351.
363. Jackson HJ, Rafiq S and Brentjens RJ. Driving CAR T-cells forward. *Nat Rev Clin Oncol.* 2016; 13(6):370-383.
364. Whilding LM and Maher J. CAR T-cell immunotherapy: The path from the by-road to the freeway? *Mol Oncol.* 2015; 9(10):1994-2018.
365. Jetani H, Garcia-Cadenas I, Nerreter T, Thomas S, Rydzek J, Meijide JB, Bonig H, Herr W, Sierra J, Einsele H and Hudecek M. CAR T-cells targeting FLT3 have potent activity against FLT3(-)ITD(+) AML and act synergistically with the FLT3-inhibitor crenolanib. *Leukemia.* 2018; 32(5):1168-1179.
366. Lim WA and June CH. The Principles of Engineering Immune Cells to Treat Cancer. *Cell.* 2017; 168(4):724-740.
367. Wander SA, Levis MJ and Fathi AT. The evolving role of FLT3 inhibitors in acute myeloid leukemia: quizartinib and beyond. *Ther Adv Hematol.* 2014; 5(3):65-77.
368. Levis M. FLT3 dancing on the stem cell. *J Exp Med.* 2017; 214(7):1857-1859.
369. Pratz KW, Sato T, Murphy KM, Stine A, Rajkhowa T and Levis M. FLT3-mutant allelic burden and clinical status are predictive of response to FLT3 inhibitors in AML. *Blood.* 2010; 115(7):1425-1432.
370. Iwasaki Y, Nishiuchi R, Aoe M, Takahashi T, Watanabe H, Tokorotani C, Kikkawa K and Shimada A. Positive Minimal Residual Disease of FLT3-ITD before Hematopoietic Stem Cell

Transplantation Resulted in a Poor Prognosis of an Acute Myeloid Leukemia. *Acta Med Okayama*. 2017; 71(1):79-83.

371. Au CH, Wa A, Ho DN, Chan TL and Ma ES. Clinical evaluation of panel testing by next-generation sequencing (NGS) for gene mutations in myeloid neoplasms. *Diagn Pathol*. 2016; 11:11.
372. Bolli N, Manes N, McKerrell T, Chi J, Park N, Gundem G, Quail MA, Sathiseelan V, Herman B, Crawley C, Craig JI, Conte N, Grove C, Papaemmanuil E, Campbell PJ, Varela I, et al. Characterization of gene mutations and copy number changes in acute myeloid leukemia using a rapid target enrichment protocol. *Haematologica*. 2015; 100(2):214-222.
373. Meshinchi S, Alonzo TA, Stirewalt DL, Zwaan M, Zimmerman M, Reinhardt D, Kaspers GJ, Heerema NA, Gerbing R, Lange BJ and Radich JP. Clinical implications of FLT3 mutations in pediatric AML. *Blood*. 2006; 108(12):3654-3661.
374. Smith CCP, A.E.; Altman, J.K.; Carson, A.; Cortes, J.E.; Stenzel, T.T.; Hill, J.; Lu, Q.; Bahceci E.; Levis, M.J. Comparative Assessment of FLT3 Variant Allele Frequency By Capillary Electrophoresis and Next-Generation Sequencing in FLT3mut+ patients with Relapsed/Refractory (R/R) Acute Myeloid Leukemia (AML) Who Received Gilteritinib Therapy. *Blood*. 2017; 130(Suppl 1):1411.
375. Shin JK, D.; Hong, Y.; Koh, Y.; Yun, H.; Shin, D.-Y.; Yoon, S.-S.; Kim, I.; Lee J.; Kim, B.-S. Improved Sensitivity in Detection of FMS-like Tyrosine Kinase Internal Tandem Duplication of a Method Using Next-Generation Sequencing Data. *Blood*. 2016; 128(22):2844.
376. Ye K, Schulz MH, Long Q, Apweiler R and Ning Z. Pindel: a pattern growth approach to detect break points of large deletions and medium sized insertions from paired-end short reads. *Bioinformatics*. 2009; 25(21):2865-2871.
377. Roloff GW, Lai C, Hourigan CS and Dillon LW. Technical Advances in the Measurement of Residual Disease in Acute Myeloid Leukemia. *J Clin Med*. 2017; 6(9).
378. Endrullat C, Glokler J, Franke P and Frohme M. Standardization and quality management in next-generation sequencing. *Appl Transl Genom*. 2016; 10:2-9.
379. Aziz N, Zhao Q, Bry L, Driscoll DK, Funke B, Gibson JS, Grody WW, Hegde MR, Hoeltge GA, Leonard DG, Merker JD, Nagarajan R, Palicki LA, Robetorye RS, Schrijver I, Weck KE, et al. College of American Pathologists' laboratory standards for next-generation sequencing clinical tests. *Arch Pathol Lab Med*. 2015; 139(4):481-493.
380. Gargis AS, Kalman L, Berry MW, Bick DP, Dimmock DP, Hambuch T, Lu F, Lyon E, Voelkerding KV, Zehnbauser BA, Agarwala R, Bennett SF, Chen B, Chin EL, Compton JG, Das S, et al. Assuring the quality of next-generation sequencing in clinical laboratory practice. *Nat Biotechnol*. 2012; 30(11):1033-1036.
381. Nollet FM, B. Challenges and pitfalls of next generation sequencing in molecular haematology. *Belgian Journal of Hematology*. 2016; 7(2):63-68.
382. Patel NM, Michelini VV, Snell JM, Balu S, Hoyle AP, Parker JS, Hayward MC, Eberhard DA, Salazar AH, McNeillie P, Xu J, Huettner CS, Koyama T, Utro F, Rhrissorakrai K, Norel R, et al. Enhancing Next-Generation Sequencing-Guided Cancer Care Through Cognitive Computing. *Oncologist*. 2018; 23(2):179-185.
383. Tojo A. Clinical sequencing in leukemia with the assistance of artificial intelligence. *Rinsho Ketsueki*. 2017; 58(10):1913-1917.
384. Hughes MDZ, R.; Miller K.L.; Meshinchi S. Augmentation of sensitivity of FLT3/ITD assay allows detection of minimal residual disease in stem cell transplantation recipients – correlation with flow cytometry MRD assessment. *Blood*. 2010; 116(21):1717.
385. Levis MJ, Perl AE, Altman JK, Gocke CD, Bahceci E, Hill J, Liu C, Xie Z, Carson AR, McClain V, Stenzel TT and Miller JE. A next-generation sequencing-based assay for minimal residual disease assessment in AML patients with FLT3-ITD mutations. *Blood Adv*. 2018; 2(8):825-831.
386. Metzeler KH, Herold T, Rothenberg-Thurley M, Amler S, Sauerland MC, Gorlich D, Schneider S, Konstandin NP, Dufour A, Braundl K, Ksienzyk B, Zellmeier E, Hartmann L, Greif PA, Fiegl M, Subklewe M, et al. Spectrum and prognostic relevance of driver gene mutations in acute myeloid leukemia. *Blood*. 2016; 128(5):686-698.

387. Papaemmanuil E, Gerstung M, Malcovati L, Tauro S, Gundem G, Van Loo P, Yoon CJ, Ellis P, Wedge DC, Pellagatti A, Shlien A, Groves MJ, Forbes SA, Raine K, Hinton J, Mudie LJ, et al. Clinical and biological implications of driver mutations in myelodysplastic syndromes. *Blood*. 2013; 122(22):3616-3627; quiz 3699.
388. Schulz WLD, T.JS.; Rinder, J.; Tormey, C.A.; Torres, R.; Smith, B.R.; Hager, K.M.; Howe, J.G.; Siddon, A.J. Impact of Molecular Clonality on Survival in Acute Myeloid Leukemia. *Blood*. 2015; 126(23):3385.
389. Borthakur G, Kantarjian H, Patel KP, Ravandi F, Qiao W, Faderl S, Kadia T, Luthra R, Pierce S and Cortes JE. Impact of numerical variation in FMS-like tyrosine kinase receptor 3 internal tandem duplications on clinical outcome in normal karyotype acute myelogenous leukemia. *Cancer*. 2012; 118(23):5819-5822.
390. Bhatt PK and Abdel-Wahab O. Refining the prognostic importance of the diversity of FLT3 internal tandem duplications. *Leuk Lymphoma*. 2013; 54(1):3-4.
391. Fischer M, Schnetzke U, Spies-Weisschart B, Walther M, Fleischmann M, Hilgendorf I, Hochhaus A and Scholl S. Impact of FLT3-ITD diversity on response to induction chemotherapy in patients with acute myeloid leukemia. *Haematologica*. 2017; 102(4):e129-e131.
392. Cucchi DGJ, Denys B, Kaspers G, Janssen J, Ossenkoppele G, de Haas V, Zwaan CM, van den Heuvel-Eibrink MM, Philippe J, Csikos T, Kwidama Z, de Moerloose B, de Bont E, Lissenberg-Witte BI, Zweegman S, Verwer F, et al. RNA-based FLT3-ITD allelic ratio is associated with outcome and ex vivo response to FLT3 inhibitors in pediatric AML. *Blood*. 2018.
393. Gorin NC, Labopin M, Meloni G, Pigneux A, Esteve J, Mohamad M, Acute Leukemia Working Party of the European Group for B and Marrow T. Impact of FLT3 ITD/NPM1 mutation status in adult patients with acute myelocytic leukemia autografted in first remission. *Haematologica*. 2013; 98(2):e12-14.
394. Canaani JL, M.; Huang, X. J.; Arcese, W.; Ciceri, F.; Blaise, D.; Irrera, G.; Corral, L. L.; Bruno, B.; Santarone, S.; van Lint, M. T.; Vitek, A.; Esteve, J.; Mohty M.; Nagler, A. Haploidentical Stem Cell Transplantation Attenuates the Prognostic Impact of FLT3-ITD in Acute Myeloid Leukemia. *Blood*. 2017; 130(Suppl 1):4584.
395. Canaani J, Labopin M, Huang XJ, Arcese W, Ciceri F, Blaise D, Irrera G, Corral LL, Bruno B, Santarone S, Van Lint MT, Vitek A, Esteve J, Mohty M and Nagler A. T-cell replete haploidentical stem cell transplantation attenuates the prognostic impact of FLT3-ITD in acute myeloid leukemia: A report from the Acute Leukemia Working Party of the European Society for Blood and Marrow Transplantation. *Am J Hematol*. 2018.
396. Jourdan E, Boissel N, Chevret S, Delabesse E, Renneville A, Cornillet P, Blanchet O, Cayuela JM, Recher C, Raffoux E, Delaunay J, Pigneux A, Bulabois CE, Berthon C, Pautas C, Vey N, et al. Prospective evaluation of gene mutations and minimal residual disease in patients with core binding factor acute myeloid leukemia. *Blood*. 2013; 121(12):2213-2223.
397. Chou WC, Hou HA, Liu CY, Chen CY, Lin LI, Huang YN, Chao YC, Hsu CA, Huang CF and Tien HF. Sensitive measurement of quantity dynamics of FLT3 internal tandem duplication at early time points provides prognostic information. *Ann Oncol*. 2011; 22(3):696-704.
398. Parkin B, Londono-Joshi A, Kang Q, Tewari M, Rhim AD and Malek SN. Ultrasensitive mutation detection identifies rare residual cells causing acute myelogenous leukemia relapse. *J Clin Invest*. 2017; 127(9):3484-3495.
399. Lin MT, Tseng LH, Dudley JC, Riel S, Tsai H, Zheng G, Pratz KW, Levis MJ and Gocke CD. A Novel Tandem Duplication Assay to Detect Minimal Residual Disease in FLT3/ITD AML. *Mol Diagn Ther*. 2015; 19(6):409-417.
400. Whale AS, Huggett JF and Tzonev S. Fundamentals of multiplexing with digital PCR. *Biomol Detect Quantif*. 2016; 10:15-23.
401. Patnaik MM. The importance of FLT3 mutational analysis in acute myeloid leukemia. *Leuk Lymphoma*. 2017:1-14.
402. Hubmann M, Kohnke T, Hoster E, Schneider S, Dufour A, Zellmeier E, Fiegl M, Braess J, Bohlander SK, Subklewe M, Sauerland MC, Berdel WE, Buchner T, Wormann B, Hiddemann W and

Spiekermann K. Molecular response assessment by quantitative real-time polymerase chain reaction after induction therapy in NPM1-mutated patients identifies those at high risk of relapse.

Haematologica. 2014; 99(8):1317-1325.

403. Liu Y, He P, Liu F, Shi L, Zhu H, Zhao J, Wang Y, Cheng X and Zhang M. Prognostic significance of NPM1 mutations in acute myeloid leukemia: A meta-analysis. *Mol Clin Oncol*. 2014; 2(2):275-281.

404. Boddu P, Kantarjian H, Borthakur G, Kadia T, Daver N, Pierce S, Andreeff M, Ravandi F, Cortes J and Kornblau SM. Co-occurrence of FLT3-TKD and NPM1 mutations defines a highly favorable prognostic AML group. *Blood Adv*. 2017; 1(19):1546-1550.

405. Chatain N, Perera RC, Rossetti G, Rossa J, Carloni P, Schemionek M, Haferlach T, Brummendorf TH, Schnittger S and Koschmieder S. Rare FLT3 deletion mutants may provide additional treatment options to patients with AML: an approach to individualized medicine. *Leukemia*. 2015; 29(12):2434-2438.

406. Vempati S, Reindl C, Wolf U, Kern R, Petropoulos K, Naidu VM, Buske C, Hiddemann W, Kohl TM and Spiekermann K. Transformation by oncogenic mutants and ligand-dependent activation of FLT3 wild-type requires the tyrosine residues 589 and 591. *Clin Cancer Res*. 2008; 14(14):4437-4445.

407. Basu A, Raghunath M, Bishayee S and Das M. Inhibition of tyrosine kinase activity of the epidermal growth factor (EGF) receptor by a truncated receptor form that binds to EGF: role for interreceptor interaction in kinase regulation. *Mol Cell Biol*. 1989; 9(2):671-677.

408. Kashles O, Yarden Y, Fischer R, Ullrich A and Schlessinger J. A dominant negative mutation suppresses the function of normal epidermal growth factor receptors by heterodimerization. *Mol Cell Biol*. 1991; 11(3):1454-1463.

409. Hug N, Longman D and Caceres JF. Mechanism and regulation of the nonsense-mediated decay pathway. *Nucleic Acids Res*. 2016; 44(4):1483-1495.

410. Schweingruber C, Rufener SC, Zund D, Yamashita A and Muhlemann O. Nonsense-mediated mRNA decay - mechanisms of substrate mRNA recognition and degradation in mammalian cells. *Biochim Biophys Acta*. 2013; 1829(6-7):612-623.

411. Anczukow O, Ware MD, Buisson M, Zetoune AB, Stoppa-Lyonnet D, Sinilnikova OM and Mazoyer S. Does the nonsense-mediated mRNA decay mechanism prevent the synthesis of truncated BRCA1, CHK2, and p53 proteins? *Hum Mutat*. 2008; 29(1):65-73.

412. Bhuvanagiri M, Lewis J, Putzker K, Becker JP, Leicht S, Krijgsveld J, Batra R, Turnwald B, Jovanovic B, Hauer C, Sieber J, Hentze MW and Kulozik AE. 5-azacytidine inhibits nonsense-mediated decay in a MYC-dependent fashion. *EMBO Mol Med*. 2014; 6(12):1593-1609.

413. van de Geijn GJ, Gits J, Aarts LH, Heijmans-Antonissen C and Touw IP. G-CSF receptor truncations found in SCN/AML relieve SOCS3-controlled inhibition of STAT5 but leave suppression of STAT3 intact. *Blood*. 2004; 104(3):667-674.

414. Lopez AF, Hercus TR, Ekert P, Littler DR, Guthridge M, Thomas D, Ramshaw HS, Stomski F, Perugini M, D'Andrea R, Grimbaldston M and Parker MW. Molecular basis of cytokine receptor activation. *IUBMB Life*. 2010; 62(7):509-518.

415. Liongue C and Ward AC. Granulocyte colony-stimulating factor receptor mutations in myeloid malignancy. *Front Oncol*. 2014; 4:93.

416. Meyer J, Rhein M, Schiedlmeier B, Kustikova O, Rudolph C, Kamino K, Neumann T, Yang M, Wahlers A, Fehse B, Reuther GW, Schlegelberger B, Ganser A, Baum C and Li Z. Remarkable leukemogenic potency and quality of a constitutively active neurotrophin receptor, deltaTrkA. *Leukemia*. 2007; 21(10):2171-2180.

417. Reuther GW, Lambert QT, Caligiuri MA and Der CJ. Identification and characterization of an activating TrkA deletion mutation in acute myeloid leukemia. *Mol Cell Biol*. 2000; 20(23):8655-8666.

418. Tacconelli A, Farina AR, Cappabianca L, Gulino A and Mackay AR. Alternative TrkAIII splicing: a potential regulated tumor-promoting switch and therapeutic target in neuroblastoma. *Future Oncol*. 2005; 1(5):689-698.

419. Stone RM, Manley PW, Larson RA and Capdeville R. Midostaurin: its odyssey from discovery to approval for treating acute myeloid leukemia and advanced systemic mastocytosis. *Blood Adv*. 2018; 2(4):444-453.

420. Stone RM, Mandrekar S, Sanford BL, Geyer S, Bloomfield CD, Dohner K, Thiede C, Marcucci G, Lo-Coco F, Klisovic RB, Wei A, Sierra J, Sanz MA, Brandwein JM, de Witte T, Niederwieser D, et al. (2015). The Multi-Kinase Inhibitor Midostaurin (M) Prolongs Survival Compared with Placebo (P) in Combination with Daunorubicin (D)/Cytarabine (C) Induction (ind), High-Dose C Consolidation (consol), and As Maintenance (maint) Therapy in Newly Diagnosed Acute Myeloid Leukemia (AML) Patients (pts) Age 18-60 with FLT3 Mutations (mut): An International Prospective Randomized (rand) P-Controlled Double-Blind Trial (CALGB 10603/RATIFY [Alliance]). 57th ASH Annual Meeting. (Orlando, FL: Blood), pp. 6.
421. Watanabe-Smith KR, M.; Bucy, T.; Tyner, J.W.; Borate, U. Factors Predicting Response and Resistance to Midostaurin in FLT3 Positive and FLT3 Negative AML in 483 Primary AML Patient Samples. *Blood*. 2017; 130(Suppl 1):296.
422. Chen F, Ishikawa Y, Akashi A, Naoe T and Kiyoi H. Co-expression of wild-type FLT3 attenuates the inhibitory effect of FLT3 inhibitor on FLT3 mutated leukemia cells. *Oncotarget*. 2016; 7(30):47018-47032.
423. Davis MI, Hunt JP, Herrgard S, Ciceri P, Wodicka LM, Pallares G, Hocker M, Treiber DK and Zarrinkar PP. Comprehensive analysis of kinase inhibitor selectivity. *Nat Biotechnol*. 2011; 29(11):1046-1051.
424. Nguyen B, Williams AB, Young DJ, Ma H, Li L, Levis M, Brown P and Small D. FLT3 activating mutations display differential sensitivity to multiple tyrosine kinase inhibitors. *Oncotarget*. 2017; 8(7):10931-10944.
425. Stone RM, Larson RA and Dohner H. Midostaurin in FLT3-Mutated Acute Myeloid Leukemia. *N Engl J Med*. 2017; 377(19):1903.
426. Mori M, Kaneko N, Ueno Y, Yamada M, Tanaka R, Saito R, Shimada I, Mori K and Kuromitsu S. Gilteritinib, a FLT3/AXL inhibitor, shows antileukemic activity in mouse models of FLT3 mutated acute myeloid leukemia. *Invest New Drugs*. 2017; 35(5):556-565.
427. Ueno YM, M.; Kamiyama, Y.; Kaneko, N.; Isshiki E.; Takeuchi, M. Gilteritinib (ASP2215), a Novel FLT3/AXL Inhibitor: Preclinical Evaluation in Combination with Azacitidine in Acute Myeloid Leukemia. 128. 2016; 22(2830).
428. Swaminathan MK, H.M.; Daver, N.; Borthakur, G.; Ohanian, M.; Kadia, T.; DiNardo, C.D.; Jain, N.; Estrov, Z.; Ferrajoli, A.; Garcia-Manero, G.; Konopleva, M.; Andreeff, M.; Pemmaraju, N.; Jabbour, E. J.; Wierda, W.G.; Ravandi, F.; Pinsoy M.R.; Cortes, J.E. The Combination of Quizartinib with Azacitidine or Low Dose Cytarabine Is Highly Active in Patients (Pts) with FLT3-ITD Mutated Myeloid Leukemias: Interim Report of a Phase I/II Trial. *Blood*. 2017; 130(Suppl 1):723.
429. Pemmaraju N, Kantarjian H, Andreeff M, Cortes J and Ravandi F. Investigational FMS-like tyrosine kinase 3 inhibitors in treatment of acute myeloid leukemia. *Expert Opin Investig Drugs*. 2014; 23(7):943-954.
430. Smith CC, Viny AD, Massi ES, Kandoth C, Socci ND, Hsu H, West B, Bollag G, Taylor BS, Levine RL and Shah NP. (2015). Recurrent Mutations in CCND3 Confer Clinical Resistance to FLT3 Inhibitors. 57th ASH Annual Meeting. (Orlando, FL: Blood), pp. 677.
431. Zhang H, Watanabe-Smith KM, Bottomly D, Wilmot B, McWeeney SK, Kantarjian HM, Ho J, Davis J, Pond B, Borthakur G, Ramachandran A, Cortes JE, Collins R and Tyner JW. (2015). Exome Sequencing Informs Mechanisms of Clinical Resistance to the FLT3-D835 Inhibitor Crenolanib. 57th ASH Annual Meeting. (Orlando, FL: Blood), pp. 2468.
432. Li L, Osdal T, Ho Y, Chun S, McDonald T, Agarwal P, Lin A, Chu S, Qi J, Li L, Hsieh YT, Dos Santos C, Yuan H, Ha TQ, Popa M, Hovland R, et al. SIRT1 activation by a c-MYC oncogenic network promotes the maintenance and drug resistance of human FLT3-ITD acute myeloid leukemia stem cells. *Cell Stem Cell*. 2014; 15(4):431-446.
433. Hemann MT, Bric A, Teruya-Feldstein J, Herbst A, Nilsson JA, Cordon-Cardo C, Cleveland JL, Tansey WP and Lowe SW. Evasion of the p53 tumour surveillance network by tumour-derived MYC mutants. *Nature*. 2005; 436(7052):807-811.

434. Jiang X, Huang H, Li Z, Li Y, Wang X, Gurbuxani S, Chen P, He C, You D, Zhang S, Wang J, Arnovitz S, Elkahouloun A, Price C, Hong GM, Ren H, et al. Blockade of miR-150 maturation by MLL-fusion/MYC/LIN-28 is required for MLL-associated leukemia. *Cancer Cell*. 2012; 22(4):524-535.
435. He Y, Jiang X and Chen J. The role of miR-150 in normal and malignant hematopoiesis. *Oncogene*. 2014; 33(30):3887-3893.
436. Staffas A, Arabanian LS, Wei SY, Jansson A, Stahlman S, Johansson P, Fogelstrand L, Cammenga J, Kuchenbauer F and Palmqvist L. Upregulation of Flt3 is a passive event in Hoxa9/Meis1-induced acute myeloid leukemia in mice. *Oncogene*. 2017; 36(11):1516-1524.
437. Wang GG, Pasillas MP and Kamps MP. Meis1 programs transcription of FLT3 and cancer stem cell character, using a mechanism that requires interaction with Pbx and a novel function of the Meis1 C-terminus. *Blood*. 2005; 106(1):254-264.
438. Jin G, Yamazaki Y, Takuwa M, Takahara T, Kaneko K, Kuwata T, Miyata S and Nakamura T. Trib1 and Evi1 cooperate with Hoxa and Meis1 in myeloid leukemogenesis. *Blood*. 2007; 109(9):3998-4005.
439. Kuo YH, Qi J and Cook GJ. Regain control of p53: Targeting leukemia stem cells by isoform-specific HDAC inhibition. *Exp Hematol*. 2016; 44(5):315-321.
440. Kim KT, Baird K, Davis S, Piloto O, Levis M, Li L, Chen P, Meltzer P and Small D. Constitutive Fms-like tyrosine kinase 3 activation results in specific changes in gene expression in myeloid leukaemic cells. *Br J Haematol*. 2007; 138(5):603-615.
441. Lisovsky M, Braun SE, Ge Y, Takahira H, Lu L, Savchenko VG, Lyman SD and Broxmeyer HE. Flt3-ligand production by human bone marrow stromal cells. *Leukemia*. 1996; 10(6):1012-1018.
442. Weisberg E, Ray A, Nelson E, Adamia S, Barrett R, Sattler M, Zhang C, Daley JF, Frank D, Fox E and Griffin JD. Reversible resistance induced by FLT3 inhibition: a novel resistance mechanism in mutant FLT3-expressing cells. *PLoS One*. 2011; 6(9):e25351.
443. Weisberg E, Boulton C, Kelly LM, Manley P, Fabbro D, Meyer T, Gilliland DG and Griffin JD. Inhibition of mutant FLT3 receptors in leukemia cells by the small molecule tyrosine kinase inhibitor PKC412. *Cancer Cell*. 2002; 1(5):433-443.
444. Schmidt-Arras DE, Bohmer A, Markova B, Choudhary C, Serve H and Bohmer FD. Tyrosine phosphorylation regulates maturation of receptor tyrosine kinases. *Mol Cell Biol*. 2005; 25(9):3690-3703.
445. Levis M, Allebach J, Tse KF, Zheng R, Baldwin BR, Smith BD, Jones-Bolin S, Ruggeri B, Dionne C and Small D. A FLT3-targeted tyrosine kinase inhibitor is cytotoxic to leukemia cells in vitro and in vivo. *Blood*. 2002; 99(11):3885-3891.
446. Scheijen B, Ngo HT, Kang H and Griffin JD. FLT3 receptors with internal tandem duplications promote cell viability and proliferation by signaling through Foxo proteins. *Oncogene*. 2004; 23(19):3338-3349.
447. Bruner JK, Ma HS, Li L, Qin ACR, Rudek MA, Jones RJ, Levis MJ, Pratz KW, Pratilas CA and Small D. Adaptation to TKI Treatment Reactivates ERK Signaling in Tyrosine Kinase-Driven Leukemias and Other Malignancies. *Cancer Res*. 2017; 77(20):5554-5563.
448. Lee HS, Qi Y and Im W. Effects of N-glycosylation on protein conformation and dynamics: Protein Data Bank analysis and molecular dynamics simulation study. *Sci Rep*. 2015; 5:8926.
449. Minami Y, Kiyoi H, Yamamoto Y, Yamamoto K, Ueda R, Saito H and Naoe T. Selective apoptosis of tandemly duplicated FLT3-transformed leukemia cells by Hsp90 inhibitors. *Leukemia*. 2002; 16(8):1535-1540.
450. Vaikari VPW, S.; Zhang, T.; Kartman, S.; Abdi, M.; Metzeler, K.H.; Akhtari M.; Alachkar, H. Interaction between FLT3 and CD99 in Acute Myeloid Leukemia. *Blood*. 2017; 130(Suppl 1):3786.
451. Kindler T, Lipka DB and Fischer T. FLT3 as a therapeutic target in AML: still challenging after all these years. *Blood*. 2010; 116(24):5089-5102.
452. Sato T, Yang X, Knapper S, White P, Smith BD, Galkin S, Small D, Burnett A and Levis M. FLT3 ligand impedes the efficacy of FLT3 inhibitors in vitro and in vivo. *Blood*. 2011; 117(12):3286-3293.
453. Fiskus W, Sharma S, Qi J, Shah B, Devaraj SG, Leveque C, Portier BP, Iyer S, Bradner JE and Bhalla KN. BET protein antagonist JQ1 is synergistically lethal with FLT3 tyrosine kinase inhibitor (TKI)

- and overcomes resistance to FLT3-TKI in AML cells expressing FLT-ITD. *Mol Cancer Ther.* 2014; 13(10):2315-2327.
454. Levis M. FLT3/ITD AML and the law of unintended consequences. *Blood.* 2011; 117(26):6987-6990.
  455. Piloto O, Wright M, Brown P, Kim KT, Levis M and Small D. Prolonged exposure to FLT3 inhibitors leads to resistance via activation of parallel signaling pathways. *Blood.* 2007; 109(4):1643-1652.
  456. Moloney JN, Stanicka J and Cotter TG. Subcellular localization of the FLT3-ITD oncogene plays a significant role in the production of NOX- and p22(phox)-derived reactive oxygen species in acute myeloid leukemia. *Leuk Res.* 2017; 52:34-42.
  457. Trachootham D, Alexandre J and Huang P. Targeting cancer cells by ROS-mediated mechanisms: a radical therapeutic approach? *Nat Rev Drug Discov.* 2009; 8(7):579-591.
  458. Noman MZ, Janji B, Berchem G, Mami-Chouaib F and Chouaib S. Hypoxia-induced autophagy: a new player in cancer immunotherapy? *Autophagy.* 2012; 8(4):704-706.
  459. Wolfert MA and Boons GJ. Adaptive immune activation: glycosylation does matter. *Nat Chem Biol.* 2013; 9(12):776-784.
  460. Pratz KW and Levis M. How I treat FLT3-mutated AML. *Blood.* 2017; 129(5):565-571.
  461. Sykes SM, Kokkaliaris KD, Milsom MD, Levine RL and Majeti R. Clonal evolution of preleukemic hematopoietic stem cells in acute myeloid leukemia. *Exp Hematol.* 2015; 43(12):989-992.
  462. Krupka C, Kufer P, Kischel R, Zugmaier G, Lichtenegger FS, Kohnke T, Vick B, Jeremias I, Metzeler KH, Altmann T, Schneider S, Fiegl M, Spiekermann K, Bauerle PA, Hiddemann W, Riethmuller G, et al. Blockade of the PD-1/PD-L1 axis augments lysis of AML cells by the CD33/CD3 BiTE antibody construct AMG 330: reversing a T-cell-induced immune escape mechanism. *Leukemia.* 2016; 30(2):484-491.
  463. Wolleschak D, Mack TS, Perner F, Frey S, Schnoder TM, Wagner MC, Hoding C, Pils MC, Parkner A, Kliche S, Schraven B, Hebel K, Brunner-Weinzierl M, Ranjan S, Isermann B, Lipka DB, et al. Clinically relevant doses of FLT3-kinase inhibitors quizartinib and midostaurin do not impair T-cell reactivity and function. *Haematologica.* 2014; 99(6):e90-93.
  464. Zhao W, Gu YH, Song R, Qu BQ and Xu Q. Sorafenib inhibits activation of human peripheral blood T cells by targeting LCK phosphorylation. *Leukemia.* 2008; 22(6):1226-1233.
  465. Kreutzman A, Porkka K and Mustjoki S. Immunomodulatory Effects of Tyrosine Kinase Inhibitors. *International Trends in Immunity.* 2013; 1(3):17-28.
  466. Gu Y, Zhao W, Meng F, Qu B, Zhu X, Sun Y, Shu Y and Xu Q. Sunitinib impairs the proliferation and function of human peripheral T cell and prevents T-cell-mediated immune response in mice. *Clin Immunol.* 2010; 135(1):55-62.
  467. Chang Y-TH, D.; Ghiaur, G.; Levis, M.J.; Jones, R.J. Bone Marrow Stroma Protects FLT3 Acute Myeloid Leukemia (AML) through CYP3A4-Mediated Drug Metabolization of FLT3 Tyrosine Kinase Inhibitors (TKIs). *Blood.* 2017; 130(Suppl 1):2519.
  468. Alonso S, Su M, Jones JW, Ganguly S, Kane MA, Jones RJ and Ghiaur G. Human bone marrow niche chemoprotection mediated by cytochrome P450 enzymes. *Oncotarget.* 2015; 6(17):14905-14912.
  469. Yang X, Sexauer A and Levis M. Bone marrow stroma-mediated resistance to FLT3 inhibitors in FLT3-ITD AML is mediated by persistent activation of extracellular regulated kinase. *Br J Haematol.* 2014; 164(1):61-72.
  470. Alberts BJ, A.; Lewis, J.; Raff, M.; Roberts, K.; Walter, P. *Molecular Biology of the Cell.* Garland Science Verlag - Taylor and Francis Group. 2002; 4th edition(Part V. Cells in Their Social Context - Chapter 19. Cell Junctions, Cell Adhesion, and the Extracellular Matrix).
  471. Yi H, Zeng D, Shen Z, Liao J, Wang X, Liu Y, Zhang X and Kong P. Integrin alphavbeta3 enhances beta-catenin signaling in acute myeloid leukemia harboring Fms-like tyrosine kinase-3 internal tandem duplication mutations: implications for microenvironment influence on sorafenib sensitivity. *Oncotarget.* 2016; 7(26):40387-40397.

472. Drolle H, Wagner M, Vasold J, Kutt A, Deniffel C, Sotlar K, Sironi S, Herold T, Rieger C and Fiegl M. Hypoxia regulates proliferation of acute myeloid leukemia and sensitivity against chemotherapy. *Leuk Res.* 2015; 39(7):779-785.
473. Sironi S, Wagner M, Kuett A, Drolle H, Polzer H, Spiekermann K, Rieger C and Fiegl M. Microenvironmental hypoxia regulates FLT3 expression and biology in AML. *Sci Rep.* 2015; 5:17550.
474. Noman MZ, Buart S, Romero P, Ketari S, Janji B, Mari B, Mami-Chouaib F and Chouaib S. Hypoxia-inducible miR-210 regulates the susceptibility of tumor cells to lysis by cytotoxic T cells. *Cancer Res.* 2012; 72(18):4629-4641.
475. Tang X, Chen L, Yan X, Li Y, Xiong Y and Zhou X. Overexpression of miR-210 is Associated with Poor Prognosis of Acute Myeloid Leukemia. *Med Sci Monit.* 2015; 21:3427-3433.
476. Deeb G, Vaughan MM, McInnis I, Ford LA, Sait SN, Starostik P, Wetzler M, Mashtare T and Wang ES. Hypoxia-inducible factor-1alpha protein expression is associated with poor survival in normal karyotype adult acute myeloid leukemia. *Leuk Res.* 2011; 35(5):579-584.
477. Le Sommer S, Morrice N, Pesaresi M, Thompson D, Vickers MA, Murray GI, Mody N, Neel BG, Bence KK, Wilson HM and Delibegovic M. Deficiency in Protein Tyrosine Phosphatase PTP1B Shortens Lifespan and Leads to Development of Acute Leukemia. *Cancer Res.* 2018; 78(1):75-87.
478. van Oosterwijk JG, Buelow DR, Drenberg CD, Vasilyeva A, Li L, Shi L, Wang YD, Finkelstein D, Shurtleff SA, Janke LJ, Pounds S, Rubnitz JE, Inaba H, Pabla N and Baker SD. Hypoxia-induced upregulation of BMX kinase mediates therapeutic resistance in acute myeloid leukemia. *J Clin Invest.* 2018; 128(1):369-380.
479. Tursynbay Y, Zhang J, Li Z, Tokay T, Zhumadilov Z, Wu D and Xie Y. Pim-1 kinase as cancer drug target: An update. *Biomed Rep.* 2016; 4(2):140-146.
480. Hori S, Nomura T and Sakaguchi S. Control of regulatory T cell development by the transcription factor Foxp3. *Science.* 2003; 299(5609):1057-1061.
481. Nie J, Li YY, Zheng SG, Tsun A and Li B. FOXP3(+) Treg Cells and Gender Bias in Autoimmune Diseases. *Front Immunol.* 2015; 6:493.
482. Li Z, Lin F, Zhuo C, Deng G, Chen Z, Yin S, Gao Z, Piccioni M, Tsun A, Cai S, Zheng SG, Zhang Y and Li B. PIM1 kinase phosphorylates the human transcription factor FOXP3 at serine 422 to negatively regulate its activity under inflammation. *J Biol Chem.* 2014; 289(39):26872-26881.
483. Peter B, Winter GE, Blatt K, Bennett KL, Stefanzi G, Rix U, Eisenwort G, Hadzijusufovic E, Gridling M, Dutreix C, Hoermann G, Schwaab J, Radia D, Roesel J, Manley PW, Reiter A, et al. Target interaction profiling of midostaurin and its metabolites in neoplastic mast cells predicts distinct effects on activation and growth. *Leukemia.* 2016; 30(2):464-472.
484. Gutierrez LZ, T.; Jang, M.; Akhtari, M.; Alachkar, H. Midostaurin Reduces Regulatory T Cell Population in Healthy and Acute Myeloid Leukemia Cells. *Blood.* 2017; 130(Suppl 1):2621.
485. Ha TY. The role of regulatory T cells in cancer. *Immune Netw.* 2009; 9(6):209-235.
486. Tsapogas P, Mooney CJ, Brown G and Rolink A. The Cytokine Flt3-Ligand in Normal and Malignant Hematopoiesis. *Int J Mol Sci.* 2017; 18(6).
487. Choi EY, Park WS, Jung KC, Kim SH, Kim YY, Lee WJ and Park SH. Engagement of CD99 induces up-regulation of TCR and MHC class I and II molecules on the surface of human thymocytes. *J Immunol.* 1998; 161(2):749-754.
488. Waclavicek M, Majdic O, Stulnig T, Berger M, Sunder-Plassmann R, Zlabinger GJ, Baumruker T, Stockl J, Ebner C, Knapp W and Pickl WF. CD99 engagement on human peripheral blood T cells results in TCR/CD3-dependent cellular activation and allows for Th1-restricted cytokine production. *J Immunol.* 1998; 161(9):4671-4678.
489. Grimm HB, U. Xenotransplantation -- Grundlagen - Chancen - Risiken Schattauer Verlag GmbH. 2003; (Kapitel 5.2: T-Zell-vermittelte Immunantwort gegen xenogene porcine antigenpräsentierende Zellen):161-167.
490. Budhu S, Wolchok J and Merghoub T. The importance of animal models in tumor immunity and immunotherapy. *Curr Opin Genet Dev.* 2014; 24:46-51.
491. Weiner LMS, R.; Wang S. Antibodies and cancer therapy: versatile platforms for cancer immunotherapy. *Nat Rev Immunol.* 2010; 10(5):317-327.



492. Ramalingam S, Forster J, Naret C, Evans T, Sulecki M, Lu H, Teegarden P, Weber MR and Belani CP. Dual inhibition of the epidermal growth factor receptor with cetuximab, an IgG1 monoclonal antibody, and gefitinib, a tyrosine kinase inhibitor, in patients with refractory non-small cell lung cancer (NSCLC): a phase I study. *J Thorac Oncol.* 2008; 3(3):258-264.
493. Williams AB, Li L, Nguyen B, Brown P, Levis M and Small D. Fluvastatin inhibits FLT3 glycosylation in human and murine cells and prolongs survival of mice with FLT3/ITD leukemia. *Blood.* 2012; 120(15):3069-3079.
494. Tsitsipatis D, Jayavelu AK, Muller JP, Bauer R, Schmidt-Arras D, Mahboobi S, Schnoder TM, Heidel F and Bohmer FD. Synergistic killing of FLT3ITD-positive AML cells by combined inhibition of tyrosine-kinase activity and N-glycosylation. *Oncotarget.* 2017; 8(16):26613-26624.
495. Zhang Y, Wang Z, Li X and Magnuson NS. Pim kinase-dependent inhibition of c-Myc degradation. *Oncogene.* 2008; 27(35):4809-4819.
496. Green AS, Maciel TT, Hospital MA, Yin C, Mazed F, Townsend EC, Pilorge S, Lambert M, Paubelle E, Jacquell A, Zylbersztejn F, Decroocq J, Poulain L, Sujobert P, Jacque N, Adam K, et al. Pim kinases modulate resistance to FLT3 tyrosine kinase inhibitors in FLT3-ITD acute myeloid leukemia. *Sci Adv.* 2015; 1(8):e1500221.
497. Assi R and Ravandi F. FLT3 inhibitors in acute myeloid leukemia: Choosing the best when the optimal does not exist. *Am J Hematol.* 2018; 93(4):553-563.
498. Czardybon W, Windak R, Golas A, Galezowski M, Sabiniarz A, Dolata I, Salwinska M, Guzik P, Zawadzka M, Gabor-Worwa E, Winnik B, Zurawska M, Kolasinska E, Wincza E, Bugaj M, Danielewicz M, et al. A novel, dual pan-PIM/FLT3 inhibitor SEL24 exhibits broad therapeutic potential in acute myeloid leukemia. *Oncotarget.* 2018; 9(24):16917-16931.
499. Larrue C, Saland E, Boutzen H, Vergez F, David M, Joffre C, Hospital MA, Tamburini J, Delabesse E, Manenti S, Sarry JE and Recher C. Proteasome inhibitors induce FLT3-ITD degradation through autophagy in AML cells. *Blood.* 2016; 127(7):882-892.
500. Zhang Y, Hsu CP, Lu JF, Kuchimanchi M, Sun YN, Ma J, Xu G, Zhang Y, Xu Y, Weidner M, Huard J and D'Argenio DZ. FLT3 and CDK4/6 inhibitors: signaling mechanisms and tumor burden in subcutaneous and orthotopic mouse models of acute myeloid leukemia. *J Pharmacokinet Pharmacodyn.* 2014; 41(6):675-691.
501. Uras IZ, Walter GJ, Scheicher R, Bellutti F, Prchal-Murphy M, Tigan AS, Valent P, Heidel FH, Kubicek S, Scholl C, Frohling S and Sexl V. Palbociclib treatment of FLT3-ITD+ AML cells uncovers a kinase-dependent transcriptional regulation of FLT3 and PIM1 by CDK6. *Blood.* 2016; 127(23):2890-2902.
502. Li C, Liu L, Liang L, Xia Z, Li Z, Wang X, McGee LR, Newhall K, Sinclair A, Kamb A, Wickramasinghe D and Dai K. AMG 925 is a dual FLT3/CDK4 inhibitor with the potential to overcome FLT3 inhibitor resistance in acute myeloid leukemia. *Mol Cancer Ther.* 2015; 14(2):375-383.
503. Peschel I, Podmirseg SR, Taschler M, Duyster J, Gotze KS, Sill H, Nachbaur D, Jakel H and Hengst L. FLT3 and FLT3-ITD phosphorylate and inactivate the cyclin-dependent kinase inhibitor p27(Kip1) in acute myeloid leukemia. *Haematologica.* 2017; 102(8):1378-1389.
504. Lindblad O, Cordero E, Puissant A, Macaulay L, Ramos A, Kabir NN, Sun J, Vallon-Christersson J, Haraldsson K, Hemann MT, Borg A, Levander F, Stegmaier K, Pietras K, Ronnstrand L and Kazi JU. Aberrant activation of the PI3K/mTOR pathway promotes resistance to sorafenib in AML. *Oncogene.* 2016; 35(39):5119-5131.
505. Zhang W, Borthakur G, Gao C, Chen Y, Mu H, Ruvolo VR, Nomoto K, Zhao N, Konopleva M and Andreeff M. The Dual MEK/FLT3 Inhibitor E6201 Exerts Cytotoxic Activity against Acute Myeloid Leukemia Cells Harboring Resistance-Confering FLT3 Mutations. *Cancer Res.* 2016; 76(6):1528-1537.
506. Park IK, Mundy-Bosse B, Whitman SP, Zhang X, Warner SL, Bearss DJ, Blum W, Marcucci G and Caligiuri MA. Receptor tyrosine kinase Axl is required for resistance of leukemic cells to FLT3-targeted therapy in acute myeloid leukemia. *Leukemia.* 2015; 29(12):2382-2389.
507. Jeon JYP, I.-K.; Buelow, D.R.; Whatcott, C.; Warner, S.L.; Blum W.; Baker, S. TP-0903, a Novel Axl Inhibitor with Activity in Drug Resistant FLT3-ITD+ AML through a Mechanism That Includes FLT3 Inhibition. *Blood.* 2017; 130(Suppl 1):2522.

508. Weisberg E, Liu Q, Nelson E, Kung AL, Christie AL, Bronson R, Sattler M, Sanda T, Zhao Z, Hur W, Mitsiades C, Smith R, Daley JF, Stone R, Galinsky I, Griffin JD, et al. Using combination therapy to override stromal-mediated chemoresistance in mutant FLT3-positive AML: synergism between FLT3 inhibitors, dasatinib/multi-targeted inhibitors and JAK inhibitors. *Leukemia*. 2012; 26(10):2233-2244.
509. Al-Jamal HA, Mat Jusoh SA, Hassan R and Johan MF. Enhancing SHP-1 expression with 5-azacytidine may inhibit STAT3 activation and confer sensitivity in lestaurtinib (CEP-701)-resistant FLT3-ITD positive acute myeloid leukemia. *BMC Cancer*. 2015; 15:869.
510. Zhou J, Bi C, Janakakumara JV, Liu SC, Chng WJ, Tay KG, Poon LF, Xie Z, Palaniyandi S, Yu H, Glaser KB, Albert DH, Davidsen SK and Chen CS. Enhanced activation of STAT pathways and overexpression of survivin confer resistance to FLT3 inhibitors and could be therapeutic targets in AML. *Blood*. 2009; 113(17):4052-4062.
511. Figueroa ME, Abdel-Wahab O, Lu C, Ward PS, Patel J, Shih A, Li Y, Bhagwat N, Vasanthakumar A, Fernandez HF, Tallman MS, Sun Z, Wolniak K, Peeters JK, Liu W, Choe SE, et al. Leukemic IDH1 and IDH2 mutations result in a hypermethylation phenotype, disrupt TET2 function, and impair hematopoietic differentiation. *Cancer Cell*. 2010; 18(6):553-567.
512. Metzeler KH, Walker A, Geyer S, Garzon R, Klisovic RB, Bloomfield CD, Blum W and Marcucci G. DNMT3A mutations and response to the hypomethylating agent decitabine in acute myeloid leukemia. *Leukemia*. 2012; 26(5):1106-1107.
513. Ravandi F, Alattar ML, Grunwald MR, Rudek MA, Rajkhowa T, Richie MA, Pierce S, Daver N, Garcia-Manero G, Faderl S, Nazha A, Konopleva M, Borthakur G, Burger J, Kadia T, Deltasala S, et al. Phase 2 study of azacytidine plus sorafenib in patients with acute myeloid leukemia and FLT-3 internal tandem duplication mutation. *Blood*. 2013; 121(23):4655-4662.
514. Chang E, Ganguly S, Rajkhowa T, Gocke CD, Levis M and Konig H. The combination of FLT3 and DNA methyltransferase inhibition is synergistically cytotoxic to FLT3/ITD acute myeloid leukemia cells. *Leukemia*. 2016; 30(5):1025-1032.
515. Garz AK, Wolf S, Grath S, Gaidzik V, Habringer S, Vick B, Rudelius M, Ziegenhain C, Herold S, Weickert MT, Smets M, Peschel C, Oostendorp RAJ, Bultmann S, Jeremias I, Thiede C, et al. Azacitidine combined with the selective FLT3 kinase inhibitor crenolanib disrupts stromal protection and inhibits expansion of residual leukemia-initiating cells in FLT3-ITD AML with concurrent epigenetic mutations. *Oncotarget*. 2017; 8(65):108738-108759.
516. Strati P, Kantarjian H, Ravandi F, Nazha A, Borthakur G, Daver N, Kadia T, Estrov Z, Garcia-Manero G, Konopleva M, Rajkhowa T, Durand M, Andreeff M, Levis M and Cortes J. Phase I/II trial of the combination of midostaurin (PKC412) and 5-azacytidine for patients with acute myeloid leukemia and myelodysplastic syndrome. *Am J Hematol*. 2015; 90(4):276-281.
517. Cooper BW, Kindwall-Keller TL, Craig MD, Creger RJ, Hamadani M, Tse WW and Lazarus HM. A phase I study of midostaurin and azacitidine in relapsed and elderly AML patients. *Clin Lymphoma Myeloma Leuk*. 2015; 15(7):428-432 e422.

## 7.2 Abbreviations

ABL1	Abelson murine leukemia viral oncogene homolog 1
ADC	antibody drug conjugate
AI	artificial intelligence
ALL	acute lymphoid leukemia
AML	acute myeloid leukemia
ARaC, ATRA	all-trans-retinoic acid
ATK	serine/threonine-kinase or protein kinase B
ATO	arsentrioxid
ATP	adenine-triphosphate
BiTE	bispecific T-cell engager
BM	bone marrow
BMSCs	bone marrow stromal cells
C	cytosine
CAR	chimeric antigen receptor
Cas9	CRISPR-associated protein 9 nuclease
CBF	core-binding factor
CBFB-MYH11	core-binding factor beta subunit - myosin heavy chain 11
CBL	casitas B-lineage lymphoma
CD33	cluster of differentiation 33
CDK	cyclin-dependent kinases
CEBPA	CCAAT-enhancer-binding protein alpha
CFC	colony forming cell
CLL	chronic lymphoid leukemia
CLP	common lymphoid progenitor
CML	chronic myeloid leukemia
CMP	common myeloid progenitor
CN	cytogenetically normal
CR	complete remission
CRISPR	clustered regularly interspaced short palindromic repeats
CSF1R	colony-stimulating factor 1 receptor
CSF3R	colony-stimulating factor 3 receptor
2-DG	2-deoxy-D-glucose
DCs	dendritic cells
ddPCR	digital droplet PCR
DNMT3A	DNA-methyltransferase
E:T	effector to target ratio
ECM	extracellular matrix
EGFR	epidermal growth factor receptor
ELN	European Leukemia Net
ENT1	equilibrative nucleoside transporter 1
ERK	extracellular signal-regulated kinase
FAB	French-American-British
FISH	fluorescent in-situ hybridization
FL	FLT3 ligand

FLK2	fetal liver kinase 2
FLT3	FMS-related tyrosine kinase receptor 3
FMS	fibroblast-macrophage stimulating factor
FOXC1	forkhead box 1
FOXP3	forkhead-box-protein P3
HD	healthy donor
HER2	epidermal growth factor receptor 2
HIF	hypoxia inducible factor
HSC	hematopoietic stem cell
HSCT	hematopoietic stem cell transplantation
HSP 90	heat shock protein 90
HTAS	high-throughput amplicon sequencing
IDH1/2	isocitrat-dehydrogenase 1 and 2
Ig1-5	immunoglobulin-like globes
IL-2	interleukin 2
INF- $\gamma$	interferon gamma
INV	inversion
ITD	internal tandem duplication
JAK2	Janus kinase 2
JMD	juxtamembrane domain
KIT	proto-oncogene receptor tyrosine kinase
KMT2A	lysine methyltransferase 2A
LSC	leukemic stem cell
MDS	myelodysplastic syndrome
miR	micro RNA
MLL	mixed-lineage leukemia
MPP	multipotent progenitor
MRC	Medical Research Council
MRD	minimal residual disease
mTOR	mammalian target of rapamycin
NDM	nonsense-mediated mRNA decay
NF $\kappa$ B	nuclear factor kappa B
NGS	next generation sequencing
NK-cells	natural killer cells
NOX	NADPH oxidase
NPM1	nucelophosmin 1
OS	overall survival
PB	peripheral blood
PDGFR	platelet-derived growth factor receptor
PDX	patient-derived xenograft
pFLT3	phosphorylated FLT3
PI3K	phosphoinoside-3-kinase
PML-RARA	Promyelocytic leukemia - retinoic acid receptor alpha
PMs	point mutations
PTB	phosphotyrosine binding
PTD	partial tandem duplication
PTPN1	protein tyrosine phosphatase non-receptor type 1

---

RAG-1 <sup>-/-</sup>	recombination activating gene 1 deficient
RAS	V-Ki-ras2 Kirsten rat sarcoma viral oncogene homolog
RFS	relapse-free survival
ROS	reactive oxygen species
RQ-PCR	real-time quantitative RT-PCR
RTK	receptor tyrosine kinase
RUNX1-RUNX1T1	runt-related transcription factor 1 - RUNX1 translocation partner 1
s-AML	secondary related AML
SCFR	stem cell growth factor receptor
scFv	single chain variable fragment
SCID	severe combined immunodeficiency
SCN	severe congenital neutropenia
SH2	Src-homology 2
SHP2	Src-homology 2 domain-containing phosphatase 2
SOCS	suppressors of cytokine signalling
SPRY3	sprouty RTK signalling antagonist 3
STAT5	signal transducer and activator of transcription 5
STK1	stem cell kinase 1
t-AML	therapy-related AML
TCMC	T-cell mediated cytotoxicity
TKD	tyrosine kinase domains
TKI	tyrosine kinase inhibitor
TM	transmembrane domain
TP53	tumor protein p53
T <sub>reg</sub>	regulatory T-cells
UMIs	unique molecular indexes
VAFs	variant allele frequencies
WBC	white blood cell
WES	whole-exome sequencing
WHO	world health organization
Wnt	Wingless-type
WT	wild-type
XIAP	X-linked inhibitor of apoptosis protein

## 7.3 Contribution

### *Declaration of contributions to “Clonal heterogeneity of FLT3-ITD detected by high throughput amplicon sequencing correlates with adverse prognosis in acute myeloid leukemia”*

This project was conceived by Philipp A. Greif, Max Hubmann and Karsten Spiekermann. The study cohort was defined by Max Hubmann, Karsten Spiekermann and Egor Harin. Together with Philipp A. Greif, I performed the experimental study design and the project management.

The *FLT3*-amplicon and library preparation of all analysed samples for the high-throughput amplicon sequencing (HTAS) was performed by me with the technical assistance of Kathrin Bräundl and Bianka Ksienzyk. The bioinformatic workflow for *FLT3*-ITD data analysis was established by Sebastian Vosberg, Aarif Mohamed Nazeer Batcha and Sebastian Schaaf. Together with Egor Harin I ran the *FLT3*-ITD workflow for all sequenced samples to generate *FLT3*-ITD sequencing data Pindel output files. I evaluated the raw sequencing data and defined the cut-off for the variant allele frequency in an empirical manner. Furthermore, I analysed and assessed the sensitivity of HTAS by serial dilution of cDNA derived from the *FLT3*-ITD positive cell line MOLM-13 in cDNA derived from the *FLT3*-WT cell line HL60. For validating ITD subclones of selected samples data from targeted *FLT3* sequencing analysis was obtained, that had been generated by Tobias Herold, Klaus Metzeler, Maja Rothenberg-Thurley and Hanna Janke (part of Supplementary Table S1 and S5). Genomic DNA and cDNA sample preparation, *FLT3*-ITD fragment analysis as well as Sanger sequencing was performed by Bianka Ksienzyk and by routine diagnostics at the laboratory of leukemia diagnostics at the university hospital of the LMU Munich, respectively.

Statistical analysis of the clinical data regarding RFS and OS was performed by Egor Harin and Max Hubmann with my contribution towards parameter selection, resulting in Figure 6, Supplementary Figure S1, S3, S4 and S11 as well as the data for Table 1 and 2, Supplementary Table S2, S3 and S6. I performed the statistical analysis for the methodological comparison of the ITD detection, resulting in Figure 4, 5, 7 and 8 as well as Supplementary Figure S2, S5, S6, S7, S8 and S9. Furthermore, I prepared Figure 1, 2 and 3, Table 2, Supplementary Table S1, S4, S5, S7 and S8 as well as Supplementary Figure S10. All tables and figures were edited and assembled for the manuscript by me. Together with Philipp A. Greif and Sebastian Vosberg I interpreted the data. I wrote the first draft of the manuscript (except for the method section “Patient samples” and “Statistical Analysis”, which was written by Max Hubmann and Egor Harin and only edited by me). Philipp A. Greif, Sebastian Vosberg, Max Hubmann, Klaus H. Metzeler, Stephanie Schneider and Stefan K. Bohlander proof-read the manuscript and provided intellectual input. Together with Philipp A. Greif and Max Hubmann, I revised and finalized the manuscript.

*Declaration of contributions to “The new and recurrent FLT3 juxtamembrane deletion mutation shows a dominant negative effect on the wild-type FLT3 receptor”*

For this project I established and performed the immunofluorescent staining and subsequent data analysis, resulting in figure 1e. Moreover, I prepared the figure and wrote the corresponding method section “Immunofluorescent staining”. Furthermore I proofread the manuscript and assisted during the revision process.

*Declaration of contributions to “Tyrosine kinase inhibition increases the cell surface localization of FLT3-ITD and enhances FLT3-directed immunotherapy of acute myeloid leukemia”*

Under the supervision of Philipp A. Greif, Karsten Spiekermann and Heinrich Leonhardt I conceived this project and performed the project management. I designed the experimental set-up for all experiments, except for figure 6, showing flow cytometry from diagnostic routine for disease monitoring of patients under TKI treatment at the University Hospital Tübingen and figure 7 b and c and supplementary figure 7, showing experiments designed by Christina Krupka and Marion Subklewe.

I performed the vast majority of experiments, except for proliferation assays and RT-PCR assay\*, which were performed by Harald Polzer (resulting in the data presented in figure 2c and 3c, supplementary figures S2e, S3c and S5f and Ic(50) values presented in supplementary table S1 and S2), the TCMC assays which were performed by Christina Krupka (resulting in the data presented in figure 7b and c, supplementary figure S7 and supplementary table S4), the Western blot\* resulting in supplementary figure S5i, which was performed by Belay Tizazu and the mutational profiling of AML cell lines and PDX samples, which was performed by Maja Rothenberg-Thurley (resulting in the mutation profiles presented in table 1 and supplementary table S3). The fragment analysis data (resulting in the data presented in supplementary figure S4 and S5g) was compiled with technical assistance of Gudrun Mellert and Jutta Sturm, whereas I generated the input cDNA samples. Patient data presented in this publication (presented in figure 6, supplementary table S3 and S5 as well as supplementary figure S6) were obtained from diagnostic routine and assembled by myself. PDX samples for the assays were provided by Binje Vick and Irmela Jeremias. With technical assistance of Andreas Maiser I optimized the immunofluorescent staining protocol for the hematopoietic suspension cells, leading to the data presented in supplementary figure S1b. I performed the statistical analysis throughout this work.

Furthermore, I wrote the first draft of the manuscript (except for the method draft for the supplementary method section “quantitative real-time RT-PCR”, which was written by Harald Polzer) and prepared most figures and tables, except for the graphs displaying the proliferation and RT-PCR data (figure 2c and 3c, supplementary figures S2e, S3c and S5f), fragment analysis images (supplementary figure S4, S5g and S6), flow cytometry plots displayed in figure 6a, 7b and c, supplementary figure S7) and the line graphs shown in supplementary figure S7a and b,

which I only assembled. Philipp Greif, Karsten Spiekermann, Marion Subklewe, Christina Krupka and Harald Polzer proof-read the manuscript and provided intellectual input. Together with Philipp Greif I revised and finalized the manuscript.

\*I generated the samples that were analysed (cDNA and whole cell lysates, respectively)

## 7.4 Acknowledgements

In this way I would like to thank all the people who supported me during the progress of the projects I have been working on during my doctoral thesis.

First of all I would like to thank my supervisor PD. Dr. Philipp A. Greif for the opportunity to work at the experimental leukemia and lymphoma research laboratory at the Department of Internal Medicine 3 of the University Hospital of the LMU. I have learned a lot of skills within his group during my doctoral thesis. Furthermore I would like to thank my doctoral father Prof. Dr. Heinrich Leonhardt for his support and supervision. I also want to thank Prof. Dr. Elfriede Nößner for being part of the TAC committee, supporting the projects providing intellectual input. I am very grateful to the biomedical assistants Andreas Maiser, Bianka Ksienzyk, Belay Tizazu and Kathrin Bräundl for their professional technical advices and assistance whenever needed. Many thanks as well to the whole team of the Laboratory for Leukemia Diagnostics. I would like to thank Dr. Christina Krupka, Prof. Dr. Marion Subklewe, Dr. Binje Vick, Prof. Dr. Irmela Jeremias, Prof. Dr. Florian Heidel, Prof. Dr. Gundram Jung as well as Prof. Dr. Karsten Spiekermann for their effort making these cooperative projects possible. Furthermore I want to express my gratitude to my laboratory and former graduate student colleagues for their help, great working atmosphere and scientific as well as motivating input. Special thanks to Dr. Harald Polzer, Dr. Deepak Bavaria, Dr. Sebastian Vosberg and Georg Leuboldt for the scientific communication and assistance. Thanks to the German Cancer Center (DKFZ) and German Special Research Department (SFB) for their financial support to realize this project (SFB Project Number1243). Last but not least I want to thank my parents, my grandparents and my whole family - especially my husband for their support and encouragement. I am deeply grateful to have you all in my life.



## 7.5 Curriculum vitae

### Katrin Susanne Schranz, M.Sc. (née Reiter)

Experimental Leukemia and Lymphoma Research (ELLF)  
 Department of Internal Medicine III, University Hospital  
 Ludwig-Maximilians-Universität (LMU) Munich  
 Max-Lebsche-Platz 30  
 D-81377 Munich

**Date of birth:** April 16, 1988 – Salzburg (Austria)

**Major Research Interest:** Molecular biology and translational cancer research.

### Scientific Education:

- |                   |  |
|-------------------|--|
| 02.2013 – 06.2018 | <p><b>Doctoral Candidate (Biology)</b> at the Ludwig-Maximilians-Universität (LMU) Munich, Germany</p> <p><i>Doctoral Thesis</i> at the Deutsches Krebsforschungszentrum (DKFZ), the partner site Munich, Laboratory for Experimental Leukemia and Lymphoma Research (ELLF), University Hospital at the LMU Munich, Germany</p> <p><i>HELENA Graduate School</i> participation at the Helmholtz Center Munich, Germany</p> |
| 10.2010 – 01.2013 | <p><b>Master of Science (Genetics)</b> at the Paris Lodron University of Salzburg (PLUS), Austria</p> <p><i>Master Thesis</i> at the Salzburger Landeskliniken (SALK) at the Department of Pathology, Laboratory for Immunohistochemistry and Molecular Biology, Salzburg, Austria</p>   |
| 10.2007 – 07.2010 | <p><b>Bachelor of Science (Genetics)</b> at the Paris Lodron University of Salzburg (PLUS), Austria</p>  |

### Publications:

1. **Schranz K**, Hubmann M, Harin E, Vosberg S, Herold T, Metzeler KH, Rothenberg-Thurley M, Janke H, Bräundl K, Ksienzyk B, Batcha AMN, Schaaf S, Schneider S, Bohlander SK, Görlich D, Berdel WE, Wörmann BJ, Braess J, Krebs S, Hiddemann W, Mansmann U, Spiekermann K, Greif PA. **Clonal heterogeneity of FLT3-ITD detected by high-throughput amplicon sequencing correlates with adverse prognosis in acute myeloid leukemia.** *Oncotarget* 2018 (9).
2. **Reiter K**, Polzer H, Krupka C, Maiser A, Vick B, Rothenberg-Thurley M, Metzeler KH, Dörfel D, Salih HR, Jung G, Nößner E, Jeremias I, Hiddemann W, Leonhardt H, Spiekermann K, Subklewe M, Greif PA. **Tyrosine kinase inhibition increases the cell surface localization of FLT3-ITD and enhances FLT3-directed immunotherapy of acute myeloid leukemia.** *Leukemia* 2018, 32(2).

3. Klaeger S, Heinzlmeir S, Wilhelm M, Polzer H, Vick B, Koenig PA, Reinecke M, Ruprecht B, Petzoldt S, Meng C, Zecha J, **Reiter K**, Qiao H, Helm D, Koch H, Schoof M, Canevari G, Casale E, Depaolini SR, Feuchtinger A, Wu Z, Schmidt T, Rueckert L, Becker W, Huenges J, Garz AK, Gohlke BO, Zolg DP, Kayser G, Vooder T, Preissner R, Hahne H, Tönisson N, Kramer K, Götze K, Bassermann F, Schlegl J, Ehrlich HC, Aiche S, Walch A, Greif PA, Schneider S, Felder ER, Ruland J, Médard G, Jeremias I, Spiekermann K, Kuster B. **The target landscape of clinical kinase drugs.** Science 2017, 358(6367).
4. Sandhöfer N, Bauer J, **Reiter K**, Dufour A, Rothenberg M, Konstandin NP, Zellmeier E, Tizazu B, Greif PA, Metzeler KH, Hiddemann W, Polzer H, Spiekermann K. **The new and recurrent FLT3 juxtamembrane deletion mutation shows a dominant negative effect on the wild-type FLT3 receptor.** Scientific Reports 2016 (6).
5. Hartmann L, Dutta S, Opatz S, Vosberg S, **Reiter K**, Leubolt G, Metzeler KH, Herold T, Bamopoulos SA, Bräundl K, Zellmeier E, Ksienzyk B, Konstandin NP, Schneider S, Hopfner KP, Graf A, Krebs S, Blum H, Middeke JM, Stölzel F, Thiede C, Wolf S, Bohlander SK, Preiss C, Chen-Wichmann L, Wichmann C, Sauerland MC, Büchner T, Berdel WE, Wörmann BJ, Braess J, Hiddemann W, Spiekermann K, Greif PA. **ZBTB7A mutations in acute myeloid leukemia with t(8;21) translocation.** Nature Communications 2016 (7).
6. Weinberger EE, Isakovic A, Scheiblhofer S, Ramsauer C, **Reiter K**, Hauser-Kronberger C, Thalhamer J, Weiss R. **The influence of antigen targeting to sub-cellular compartments on the anti-allergic potential of a DNA vaccine.** Vaccine 2013, 31(51).

#### Peer-reviewed Conference Abstracts:

1. **Reiter K**, Hubmann M, Harin E, Vosberg S, Bräundl K, Ksienzyk B, Schneider S, Dufour AM, Zellmeier E, Bohlander KS, Sauerland C, Berdel WE, Wörmann BJ, Büchner T, Braess J, Hiddemann W, Spiekermann K, Greif PA. **Comparison of FLT3-ITD Detection by High-Throughput Amplicon Sequencing to Routine Diagnostics – a Retrospective Analysis of AMLCG Study Patients.** Blood 2016, 128(22) – Abstract #1682 (58<sup>th</sup> Annual Meeting and Exposition of the American Society of Hematology)
2. **Reiter K**, Polzer H, Krupka C, Vick B, Maiser A, Subklewe M, Jeremias I, Leonhardt H, Spiekermann K, Greif PA. **Tyrosin kinase inhibition restores the membrane localization of FLT3-ITD.** Blood 2015, 126(23) – Abstract #1274 (57<sup>th</sup> Annual Meeting and Exposition of the American Society of Hematology)